UC Irvine
UC Irvine Electronic Theses and Dissertations

Title

Lithium 4,4'-Di-Tert-Butylbiphenylide: Characterization, Use in Spirocyclic Synthesis and Applications in Flow Reactors

Permalink

https://escholarship.org/uc/item/4zp5z2qm

Author

Hill, Richard

Publication Date

2016

Copyright Information

Peer reviewed|Thesis/dissertation

UNIVERSITY OF CALIFORNIA,
IRVINE

Lithium 4,4'-Di-*Tert*-Butylbiphenylide: Characterization, Use in Spirocyclic Synthesis and
Applications in Flow Reactors

DISSERTATION

Submitted in partial satisfaction of the requirements
for the degree of

DOCTOR OF PHILOSOPHY

in Chemistry

by

Richard R. Hill

Dissertation Committee:
Professor Scott D. Rychnovsky, Chair
Professor Kenneth J. Shea
Professor Zhibin Guan

2016

DEDICATION

To my parents:

Richard A. Hill

and

Melissa C. Hill

TABLE OF CONTENTS

Page

LIST OF GRAPHS

Page

LIST OF FIGURES

LIST OF SCHEMES

LIST OF TABLES

LIST OF ABBREVIATIONS

Å	Angstrom(s)
Ac	Acyl
Ar	Aryl
BPR	Back pressure regulator
Bn	Benzyl
Bz	Benzoyl
Bp	Boiling point
BF$_3$•Et$_2$O	Boron trifluoride diethyl etherate
Boc	*tert*-butoxycarbonyl
Bu	Butyl
CI	Chemical ionization
Cy	Cyclohexyl
DAST	Diethylaminosulfur trifluoride
dr	Diastereomeric ratio
DMF	N,N-Dimethylformamide
DMSO	Dimethyl sulfoxide
DMPU	1,3-dimethyl-3,4,5,6-tetrahydro-2(*1H*)-pyrimidinone
DBB	4,4'-di-*tert*-butylbiphenyl
EI	Electron Impact
ee	Enantiomeric excess

er	Enantiomeric ratio
Et	Ethyl
Equiv	Equivalent
FCC	Flash column chromatography
GCMS	Gas chromatography-mass spectrometry
GR	Gas remover
Hz	Hertz
HMPA	Hexamethylphosphoramide
HOMO	Highest occupied molecular orbital
HPLC	High Performance Liquid Chromatography
HRMS	High resolution mass spectrometry
IR	Infared spectrometry
i	iso
iPr	isopropyl
ID	Internal diameter
J	Coupling constant
KDBB	Potassium 4,4'- di-*tert*-butylbiphenylide
LDA	Lithium diisopropylamide
LDMAN	Lithium 1-(dimethylamino)-naphthalenide
LiDBB	Lithium 4,4'- di-*tert*-butylbiphenylide
LiN	Lithium naphthalenide
LiTMP	Lithium tetramethylpiperidide
MHz	Megahertz

Me	Methyl
μ	Micro
m	Milli
Min	Minute(s)
M	Molar
NBS	N-Bromosuccinimide
NMI	N-Methylimidazole
NMO	N-Methylmorpholine N-oxide
NMR	Nuclear magnetic resonance
p-TSA	p-Toluenesulfonic acid
ppm	Parts per million
PFA	Perfluoroalkoxy alkane
Ph	Phenyl
PEEK	Polyether ether ketone
PDMS	Poly dimethylsiloxane
PTFE	Polytetrafluoroethylene
PPTs	Pyridinium p-Toluenesulfonate
Quant	Quantitative yield
R_t	Residence time
RT	Room temperature
s	Sec
Sec	Second(s)
t	*Tert*

TBS	*Tert*-butyldimethylsilyl
TBDPS	*Tert*-butyldiphenylsilyl
THF	Tetrahydrofuran
THP	Tetrahydropyran
TMEDA	N,N,N',N'-tetramethylethylenediamine
TBAF	Tetra-n-butylammonium fluoride
TLC	Thin layer chromatography
Ts	4-Toluenesulfonyl
TFA	Trifluoroacetic acid
Tf	Triflyl
TIPS	Triisopropylsilyl
TMS	Trimethylsilyl
VCAM-1	Vascular cell adhesion molecule-1

ACKNOWLEDGMENTS

When I came to UCI I was unsure if I would be able to complete the degree I had been accepted for. I hoped I would be able to find the way through the task itself. While this was mostly true, completing the Ph.D. by myself would have been impossible from a physical and emotional standpoint. Just as it takes a village to raise a child, so too are a multitude of people required to produce a Ph.D. graduate. I hope I can give proper credit to those who helped me complete this work and kept me sane through the more trying periods.

Leading the lab is the most influential person toward my degree, Scott D. Rychnovsky. I was originally drawn to Scott's work through a chemistry class taught by Javier Read de Alaniz at UCSB. Scott was kind enough to meet with me before I even joined UCI and I was struck by his humility and deep understanding of organic reactions. As our fearless leader, Scott has a goldilocks approach to research: enough input to aid the direction and outcome, but never in a heavy-handed way. Thank you Scott for allowing me to join your lab and investigate areas of my research tangential the original scope. I will have fond memories of our discussions, chemically related or not.

After joining the Rychnovsky lab, the group served as much more than just a gathering of like-minded individuals; it was a home with people who cared and aided one another. To this end, thank you to all of the lab members who helped me become the scientist I am today. Much of my on-the-job training was from Tony Burke; thank you for your patience and involvement while I learned the basics of organic research. Eventually I migrated to room 3004 and found myself influenced by Nick Sizemore and Matt Perry.

Nick, you were awesome and always kept the bay lively. Matt, you were one of hardest working people I have had the opportunity to work with. I'm honored I was able to publish on spirocyclic methodology with you. I was able to pass on what I learned from you and the rest of the lab to my undergraduate Kimberly Hilby. Kimberly, thank you for your help in flow reactor optimization and synthesis of starting materials. I hope you find a graduate school that fits you and your goals in life. Additionally, many thanks to Sarah Block, Jacob Deforest, Eric Novitsky, and Greg Suryn for your thoughtful corrections of my thesis chapters. This tome would be lacking if not for your input.

To my closest friend in the lab, Renzo Samame you were so much more than a colleague. You were there when I needed to bounce ideas off someone and when I needed to talk about deeper topics. I enjoyed two firsts with you and your wife Katrina: dyeing Easter Eggs and a trip to Raging Waters. Thank you for all of the wonderful memories and for only moving a few times. Congratulation to you and Katrina on the birth of your son, Kealan. I know he will be raised in a loving and thoughtful family. I wish the three of you the best in your endeavors.

Lastly I need to thank my friends: Afshin Anoushiravani, Alex Jabbari, Jim Surmeli and Adam and Steph Swanson. Thank you for your friendship and adventures over the years. Afshin, I know you'll become a fantastic surgeon. Hang in there and give them hell. Alex, good luck with finishing with your master's in BME and where ever life takes you next. Jim, keep up the swanky legal work. Adam/Steph, I'm so glad I met you two at UCSB and was a groomsman at your wedding.

CURRICULUM VITAE

Richard R. Hill

Education

University of California, Irvine CA   Sept. 2010–Feb. 2016
Ph.D. in Organic Chemistry 2016
Dissertation: "Lithium 4,4'-Di-*Tert*-Butylbiphenylide: Characterization, Use in Spirocyclic Synthesis and Applications in Flow Reactors"
Advisor: Professor Scott D. Rychnovsky

University of California, Santa Barbara CA   Sept. 2006-2010
B.S in Chemistry; Dean's list

Research Experience

University of California, Irvine, Graduate Researcher   Feb. 2010–Feb. 2016
- Developed a titration method for Lithium 4,4'-Di-*tert*-butylbiphenylide (LiDBB)
- Investigated the formation of LiDBB and tracked degradation products
- Expanded double alkylation and reductive cyclization methodology
- Built and tested several flow reactors to quickly make and use unstable intermediates
- Experienced with HPLC and chiral gas chromatography upkeep and set-up

Fjord Venture, Laguna Hills CA. Biomedical Engineering Internship
- Supervisor: Troy Bremer Ph.D, Director,   June–Sept. 2009, June–Sept. 2010
  Metonom Health
- Role: Evaluated oxygen absorbing complexes with desired binding affinities
- Development of an implantable continuous glucose monitoring devise (USP: US20140163345 A1)

California Institute of Technology   June–Sept 2008
- Supervisor: Morteza Gharib Ph.D., Vice Provost and Hans W. Liepmann Professor of Aeronautics and Professor of Bioinspired Engineering
- Applied biomedical engineering developing an impedance pump based on a unicameral embryonic zebrafish heart
- Studied flow conditions in simulated capillaries utilizing specialty solutions
- Employed high-speed video to characterize pump flow as a function of amplitude

Teaching Experience

University of California, Irvine, Undergraduate Mentor

- Trained in organic laboratory and analytical techniques
- Directed research on spirocycle synthesis in flow reactors
- Provided guidance for research applications

University of California, Irvine, *Undergraduate Instructor*
 General Chemistry labs: I, II, and III
 Organic Chemistry lecture: I, II, and III
 Organic Chemistry labs: I, II, and III
 Advanced Organic Synthesis Lab

Publications

1. Perry, M.; Hill R.; Rychnovsky, S. "Trianion Synthon Approach to Spirocyclic Heterocycles," *Org. Lett.* **2013**, *15*, 2226–2229

2. Hill, R.; Perry, M.; Leong, J.; Rychnovsky, S. "Stereochemical Outcomes in Reductive Cyclizations to Form Spirocyclic Heterocycles" *Org. Lett.* **2015**, *17*, 3268–3271

Awards

- Graduate Teaching Award   June 2014
- The Merk Index Award   June 2010
- Dean's Honor Roll (UCSB)   July 2009
- Nation Society of Collegiate Scholars member   2006-Present

ABSTRACT OF THE DISSERTATION

Lithium 4,4'-Di-*Tert*-Butylbiphenylide: Characterization, Use in Spirocyclic Synthesis and Applications in Flow Reactors

By

Richard R. Hill

Doctor of Philosophy in Chemistry

University of California, Irvine, 2016

Professor Scott D. Rychnovsky, Chair

The first part of the dissertation describes the characterization of lithium 4,4'-di-*tert*-butylbiphenylide (LiDBB). The rates of formation and degradation of LiDBB were investigated and decomposition products identified. Stored LiDBB was found to give equivalent yields of a [4.5] spirocycle over 16 weeks.

The second part of the dissertation details the preparation of substituted spiropyrrolidines and spiropiperidines by double alkylation of α-aminonitriles, followed by stereoselective reductive lithiation and cyclization. In all cases, cyclization occurred with high diastereoselectivity.

The third part of the dissertation investigated the use of LiDBB in flow reactors. Direct ring opening of an epoxide, instead of its thiophenyl derivative, was examined. Non-cryogenic flow conditions substantially increased the yield of spiropyrrolidines and a spiropiperidine. A substituted [4.5] spirocycle also was formed in higher yield and diastereoselectivity as compared to batch conditions.

Chapter 1

Characteristics, Preparation and Stereoselectivity of α-Aminoorganolithiums

Abstract

Generation of α-aminoorganolithium reagents by permutational interconversion and reductive insertion methods are described herein. The stereochemical outcome of these intermediates and synthetic use is detailed, with emphasis on lithiated pyrrolidine and piperidine derivatives. Reductive lithiation, a sub-class of reductive insertion, is highlighted due to the nature of the work presented in the following chapters.

Introduction

Organolithium reagents are among the most ubiquitous reagents in any synthetic laboratory. Their use in preparing more complex lithiated intermediates makes them the focus of numerous books and review articles.[1,2] The reactivity of the reagents is highly affected by their substitution, and α-aminoorganolithiums are no exception to this. These compounds, first described in the literature in 1965, have been heavily studied for their synthetic utility.[3,4] Nitrogen's effect on these lithium carbanions is found in their structure and reactivity relationships seen below.

Two basic types of α-aminoorganolithium reagents are described in the literature. Those bearing only alkyl groups are considered unstabilized (**1.1**), while those with an amide-like functional group are described as stabilized (**1.2, Figure 1.1**).[5] The stabilization provided by inclusion of a carbonyl, imine, or thiocarbonyl causes the nitrogen's lone-pair to be delocalized into the adjacent pi-system (**1.3**). Additionally, the heteroatom on this pi-

system can coordinate to the lithium, producing a chelate. The net effect produces a favorable dipole arrangement, which results in a more stable organolithium.

Figure 1.1. Unstabilized and stabilized α-aminoorganolithiums

1.1	**1.2**	**1.3**
Unstabilized	Dipole Stabilized	Coordinative stabilized
R_1 = Alkyl	X = O, NR_1, S	X = O, NR_1, S
R_2 = Alkyl	Z = H, alkyl, XR_1	Z = H, alkyl, XR_1
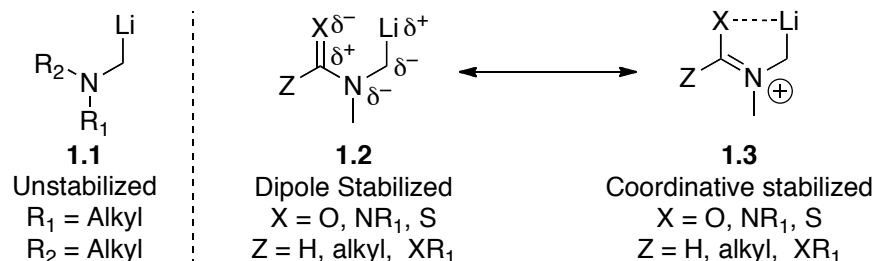
Work by Schleyer *et. al.* revealed evidence for the conformational preferences of aminomethanide **1.4** and (aminomethyl)lithium **1.6** (**Figure 1.2**).[6] Computations showed that eclipsing of the nitrogen and carbon lone pairs (**1.4**) is disfavored by 10.2 kcal/mol and instead, the staggered orientation (**1.5**) is preferred. However this effect was found to reverse when an alkyllithium was used instead of the naked carbanion. The bridging lithium and syn conformation in compound **1.7** was calculated to be 14.3 kcal/mol lower in energy than the staggered orientation of **1.6**. These results point to self-stabilization of α-aminoorganolithiums bearing no formally stabilizing group.

Figure 1.2. Conformational preference of α-aminoorganocarbanion and organolithium

1.4	**1.5**	**1.6**	**1.7**
Eclipsed	Staggered	Staggered	Bridged
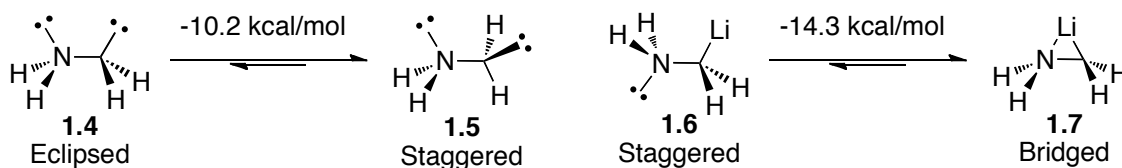
Crystal and solution structures of α-aminoorganolithiums have shed further light on the predictions of Schleyer. When dimer **1.8** was crystallized from TMEDA, the unstabilized lithiated structure possessed the bridging lithium that computational calculations had predicted (**Figure 1.3**).[7] Further evidence for such cyclic lithium species

was determined via ^{13}C and [6]Li based NMR techniques.[8] The coupling of ^{13}C and [6]Li in compound **1.9** shows a monomeric structure with the same bridging lithium observed in **1.8**. By contrast, stabilized α-aminoorganolithiums do not show this effect. Instead, the crystal structure of **1.10** revealed coordination of the lithium to the carbonyl as expected from the stabilized structures **1.2** and **1.3** (**Figure 1.2**).[7] The closely related **1.11** was determined in an analogous way to **1.9** (**Figure 1.3**).[9] The equivalent coordination observed in crystal and solution phase show the validity of such techniques in determining the structure of these reactive species.

Figure 1.3. Crystal and solution structures of α-aminoorganolithiums
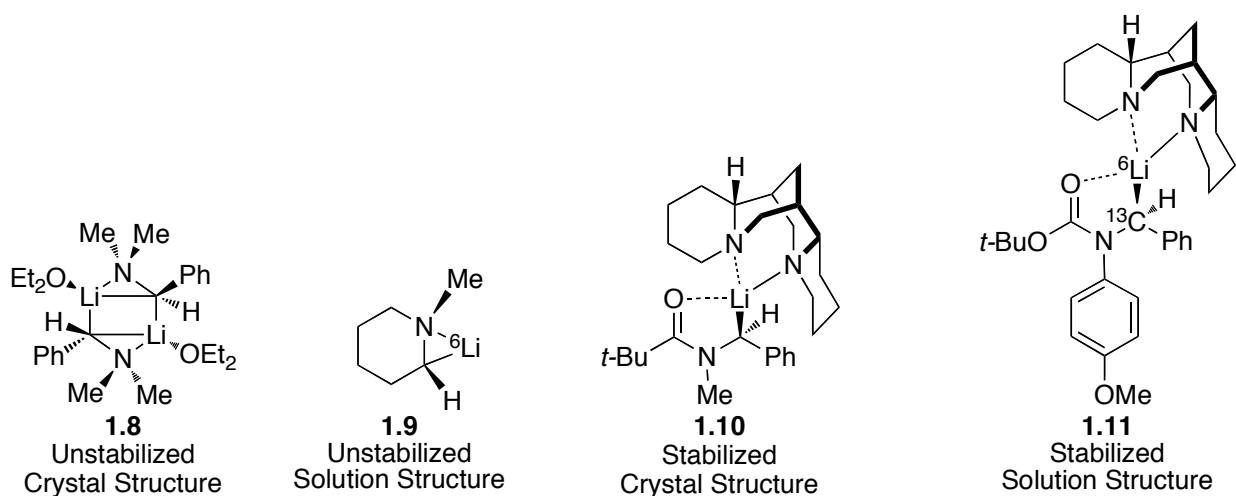
The conformational stability of α-aminoorganolithiums has been discussed at length in the literature. Isonitrile **1.12** retained its chirality up to –52 °C unlike its nitrile analog (**Figure 1.4**).[10] Unstabilized pyrrolidine **1.13** and piperidine **1.14** were found to be the most resistant to racemization of the examples in **Figure 1.4**.[11] By comparison, the pyrrolidines **1.15** and **1.16** lost optical activity at –60 °C and –78 °C, respectively. The acyclic case **1.17** required –95 °C to maintain its conformation. It would appear that cyclic α-aminoorganolithiums are inherently more unstable than their cyclic counterparts.[12]

3

TMEDA has non-obvious effects on the temperature of racemization. The conformational stability of compounds **1.13** and **1.14** was not affected by TMEDA, but its addition did prevent decomposition of the organolithium. Compound **1.15** had improved resistance to racemization with the addition of TMEDA. Protected pyrrolidine **1.16** showed higher retention of configuration without TMEDA. [13] Unstabilized compounds **1.13** and **1.14** are believed to possess a higher barrier to inversion due to a bridging lithium as seen in **1.9** (**Figure 1.3**). Cyclopropane **1.12** would appear to have a degree of this bridging due to its thermal stability being between the unstabilized and stabilized aminoorganolithiums (**Figure 1.4**). The stabilized **1.16** is believed to have a lower configurational stability due to a "conducted tour" mechanism.[14] Gawley proposed that dissociation of the lithium from **1.18** would produce carbanion **1.19**. This anion could invert, giving **1.20** and subsequent association of the lithium would return the epimeric product **1.21**.

Figure 1.4. Configurational stability of α-aminoorganolithiums and conducted tour

1.12	1.13	1.14	1.18	1.19
≤–52 °C	≤–40 °C	≤–40 °C	R = H or –(CH₂)₃–	
THF	THF/TMEDA	THF/TMEDA		

1.15	1.16	1.17	1.21	1.20
≤–60 °C	–78 °C	–95 °C		
THF/TMEDA	Et₂O	THF		
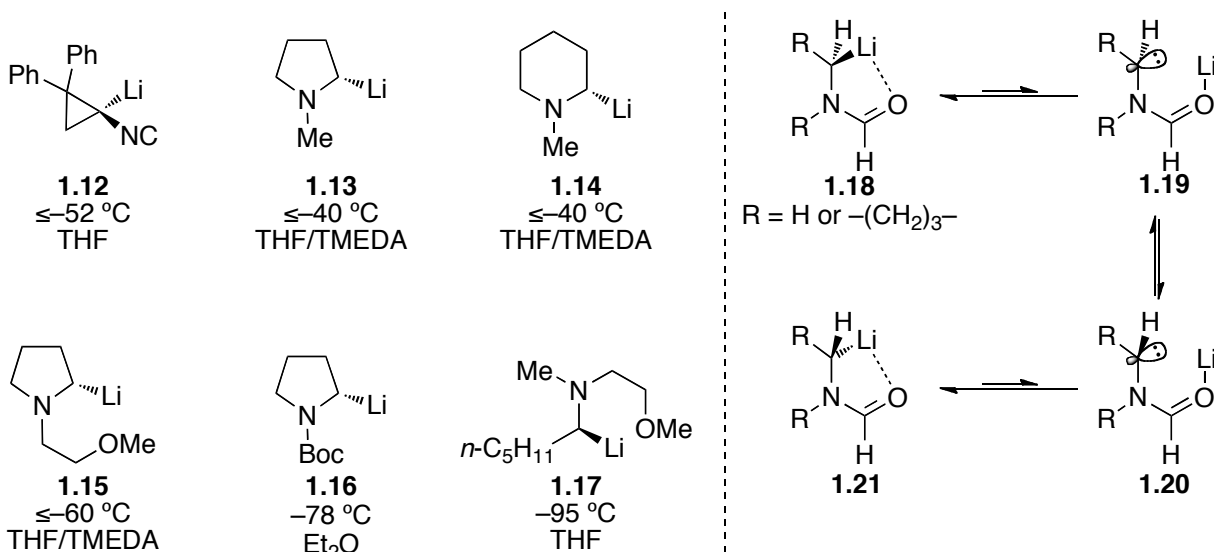
Reaction mechanisms of organolithium reagents

The description of bimolecular electrophilic substitution or S_E2 was published by Ingold in 1953.[15] However, Gawley found this term lacking and suggested that such descriptors should include the stereochemical course of the reaction.[16] This led to the modified terms $S_E2_{ret,}$ and S_E2_{inv} for bimolecular electrophilic substitutions with retention or inversion of configuration, respectively. The possible reaction mechanisms for this substitution are presented in **Scheme 1.1**. In the first reaction, the major lobe of alkyllithium **1.22** reacts with the σ^* orbital of the C–X bond of the electrophile, leading to transition state **1.24.** This S_E2_{ret} reaction yields product **1.25** with retention of the organolithium center (eq 1).[17] Alternatively, the minor lobe of alkyllithium **1.22** could attack the σ^* orbital of the C–X bond, leading to transition state **1.27.** This is reminiscent of the S_N2 transition-state and in the case of S_E2_{inv}, the organolithium reacts with net inversion of its center, as seen in product **1.28**. Equation 3 shows a single-electron transfer from **1.22** to the electrophile, leading to scrambling of stereochemistry on both the electrophile and nucleophile. Radical recombination yields the products **1.25** and **1.28**. A fourth but symmetry forbidden reaction is the S_Ei, where coordination of the lithium and halide would afford **1.25** (eq 4). In cases where the reaction is intramolecular, SE_{ret} and SE_{inv} have been used to describe the stereochemical course of the reaction.[18]

Scheme 1.1. Reaction mechanisms of organolithiums
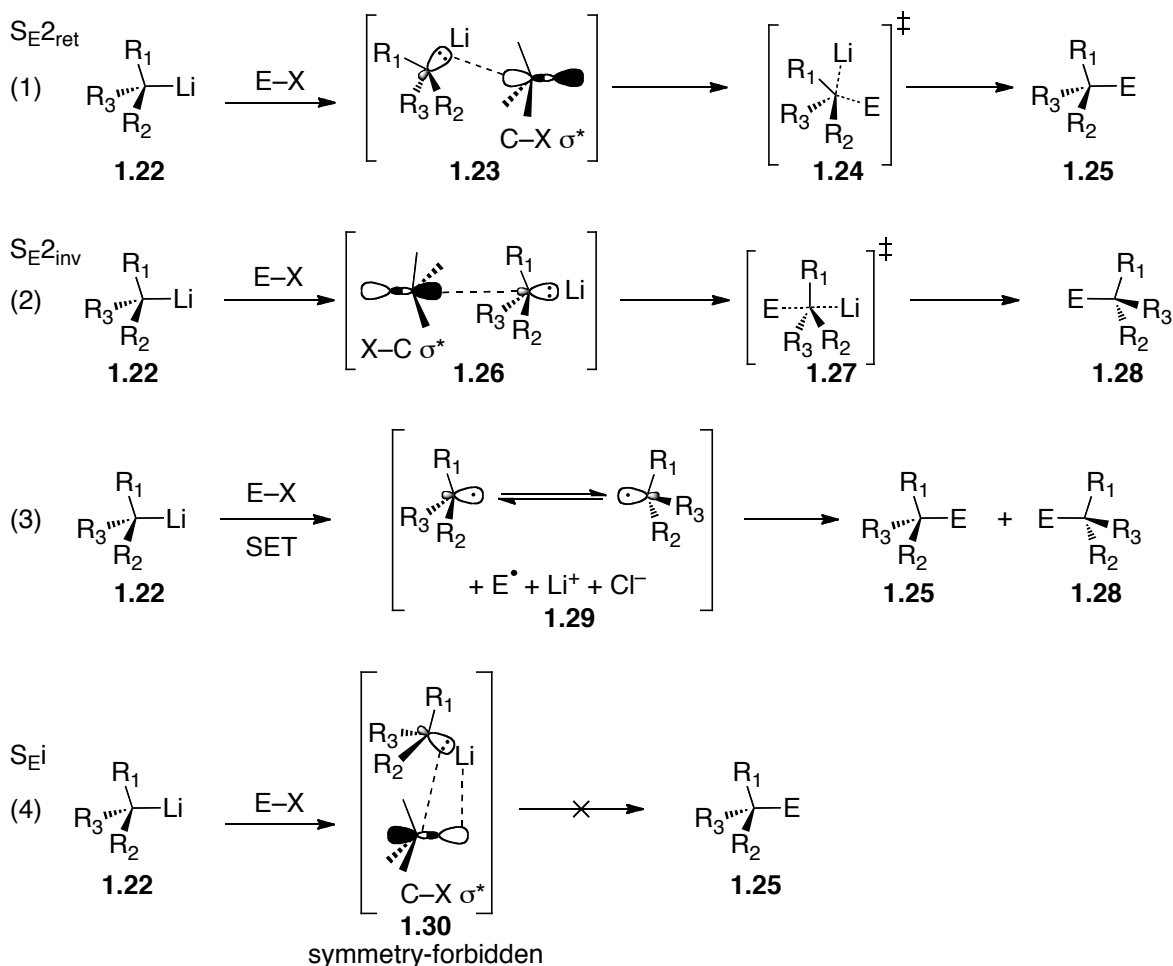
The stereochemical outcome of reactions with unstabilized 2-lithio-piperidine **1.14** (**Scheme 1.2**) followed equations 1-3 in **Scheme 1.1**, depending on the electrophile used.[19] When CO_2, t-BuCOCl, or Bu_3SnCl was reacted with **1.14**, the products (**1.31–1.33**) were formed with retention of configuration at the alkyllithium center. Use of unactivated alkylbromides returned inverted piperidines **1.36** and **1.37** with respect to the lithiated carbon. Activated electrophiles, such as benzophenone and benzyl bromide, yielded racemic piperidines **1.34** and **1.35**

6

Scheme 1.2. Stereochemical course of various electrophiles on **1.14**
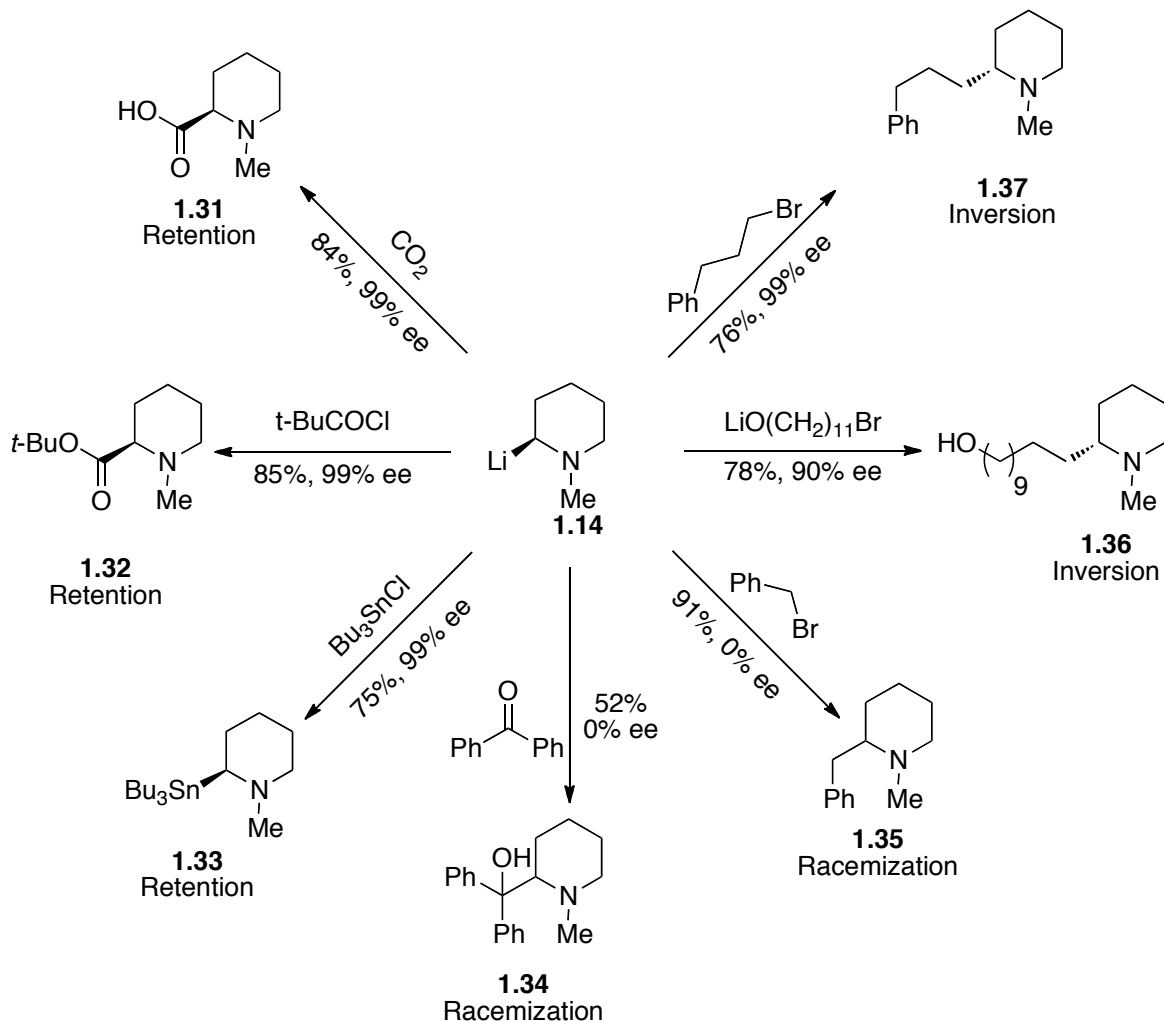
Using the stabilized lithiate **1.38**, Beak discovered a similar pattern of reactivity to that of **Scheme 1.3**.[20] When **1.38** was reacted with CO_2 or $ClCO_2Me$, the reaction occurred with retention of configuration (entries 1, 2). Inversion of the tertiary lithium occurred with CO_2, Me_3SnCl or allyl triflate (entries 1–3).

Scheme 1.3. Inversion and retention reactions of stabilized an α-aminoorganolithium
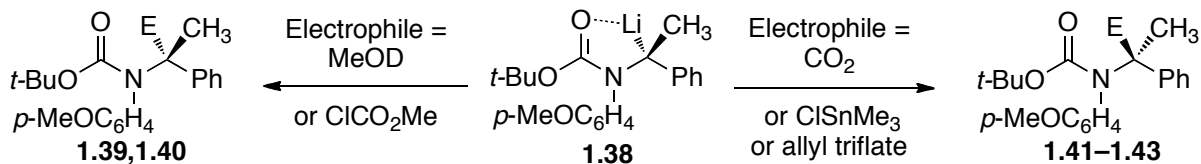
Entry	er of **1.38**	Electrophile	E	Product (yield, er)
1	97:3	MeOD	D	**1.39** (80%, 97:3)
2	97:3	ClCO$_2$Me	CO$_2$Me	**1.40** (61%, 95:5)
3	99:1	CO$_2$	CO$_2$H	**1.41** (84%, 70:30)
4	99:1	ClSnMe$_3$	SnMe$_3$	**1.42** (75%, 99:1)
5	99:1	Allyl triflate	allyl	**1.43** (96%, 98:2)

Gawley and Beak reached similar conclusions for the rational behind the S$_E$2$_{ret}$ or S$_E$2$_{inv}$ mechanism for alkyllithiums **1.14** and **1.38** (**Scheme 1.2** and **1.3**, respectively).[21] Retentive reactions occurred with electrophiles that would pre-coordinate with the alkyllithium as seen in **1.44** and **1.46** (**Figure 1.5**). Non-coordinating electrophiles were thought to react though **1.45** and **1.47**, leading to inversion of the carbon center. It should be noted that CO$_2$ and trialkylstannyl chlorides reacted with opposite preference in these reactions.

Figure 1.5. Electrophile approach for S$_E$2$_{ret}$ or S$_E$2$_{inv}$ mechanisms for **1.14** and **1.38**
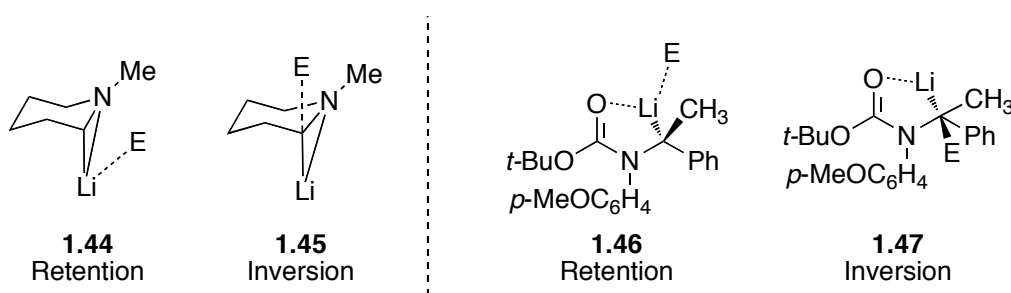
Generation of α-aminoorganolithiums

Two methods for the generation of organolithium reagents are described by Schlosser.[22] The first is known as permutational interconversion (eq 1) and is the most widely known (**Scheme 1.4**). Permutational interconversion encompasses deprotonation (eq 2), lithium-halogen exchange (eq 3) and transmetallation (eq 4). Deprotonation allows direct access to organolithium reagents; however, without an acidifying/directing group (e.g.: nitroso or carbonyl) this method is hampered by the high pK_a of C–H bonds and the regioselectivity of deprotonation. Fortunately, deprotonation with butyl lithium reagents leads to evaporation of butane, driving the reaction forward. Lithium-halogen exchange gives far greater regioselectivity over the lithiation event. This method, reported by Gilman[23] and Wittig[24], allows for rapid preparation of organolithiums in an equilibrium process favoring the more stable alkyllithium.[25] The last sub-class of permutational interconversion is transmetallation. This method, like lithium-halogen exchange, is reversible and favors the most stable alkyllithium.

Scheme 1.4. Formation of alkyllithiums by permutational interconversion
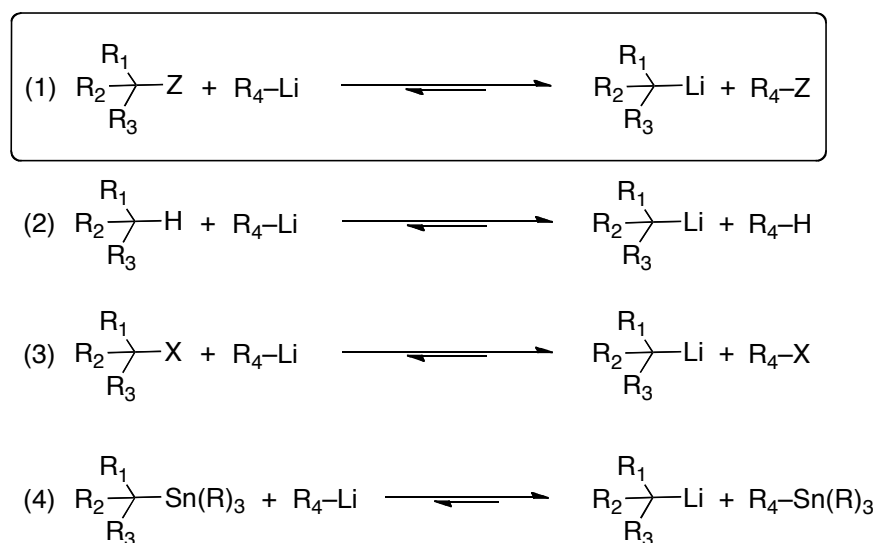
Reductive insertion is the second general method for the generation of organolithium reagents.[22] This method inserts a metal into the C–Z bond in equation 1, leading to the organometallic reagent (**Scheme 1.5**). The commercially available *tert- sec-* and *n*-butyl lithium reagents are made this way by sequential single-electron reductions of alkyl chlorides with two equivalents of lithium metal (eq 2).[26] Reductive lithiation is the last and most recently developed of these methods (eq 3). By reducing arenes, such as naphthalene and biphenyl with lithium metal, these aromatic compounds are transformed into powerful single-electron reductants. The use of dissolving metal conditions (e.g Li^0/NH_3) also falls into this category.

Scheme 1.5. Formation of alkyllithiums by reductive insertion

$$(1) \quad R_2\overset{R_1}{\underset{R_3}{\diagup}}Z + 2\,M^0 \;\rightleftharpoons\; R_2\overset{R_1}{\underset{R_3}{\diagup}}M + M\!-\!Z$$

$$(2) \quad R_2\overset{R_1}{\underset{R_3}{\diagup}}X + 2\,Li^0 \;\rightleftharpoons\; R_2\overset{R_1}{\underset{R_3}{\diagup}}Li + Li\!-\!X$$

$$(3) \quad R_2\overset{R_1}{\underset{R_3}{\diagup}}Z + 2\,Li^+[Ar]^{\cdot\ominus} \;\rightleftharpoons\; R_2\overset{R_1}{\underset{R_3}{\diagup}}Li + Li\!-\!Z + Ar$$
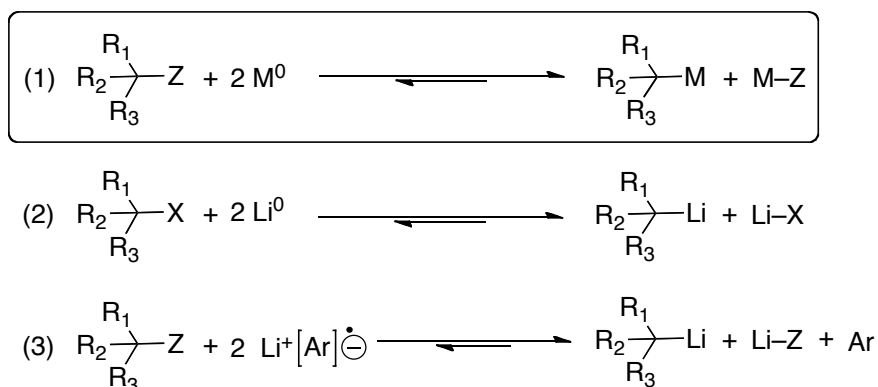
Preparation by deprotonation

Generation of α-aminoorganolithiums by deprotonation was first reported by Peterson in 1965.[27] Since then, no general method for the direct lithiation of unactivated tertiary amines has been developed.[28] A workaround was developed by Kessar using BF_3 and *s*-BuLi.[29] Other Lewis acids have also been successfully employed in a similar strategy.[30] The most general approach for deprotonation alpha to a nitrogen is through the use of polar directing groups such as nitroso,[31] formamide,[32] amide,[33] carbamate,[34] urea,[35]

or thioimidate.[36] These electron-withdrawing groups allow for deprotonation under milder conditions.

The acidifying effect of N–nitrosamines led to investigations into their synthetic utility. Fraser described the lithiation and alkylation of nitrosamine **1.48** (**Scheme 1.6**).[37] This led to the axially substituted **1.49**. Repeating the sequence with **1.49**, yielded di-axial product **1.50**. The unusual stereochemistry from these alkylations is believed to be due to delocalization of the anion across the planar C–N–N–O pi-system of structures **1.51** and **1.52**. Alkylation leading to compound **1.49** proceeding though the lower energy, chair-like transition state **1.53**. To form the equatorially substituted **1.55**, the compound would have to react through a ≥2.7 kcal/mol higher energy twist-boat-like transition state (**1.54**). It should be noted that nitrosamines are believed to be both carcinogenic and mutagenic.[38] A one-pot, N–nitrosation/lithiation/alkylation/denitrosation procedure was developed by Seebach to avoid exposure to these substrates.[39] Alkylation of N-nitroso piperidines allowed access to 2,6-diaxially substituted piperidines in great overall yield.

Scheme 1.6. Alkylation of N–nitroso piperidines
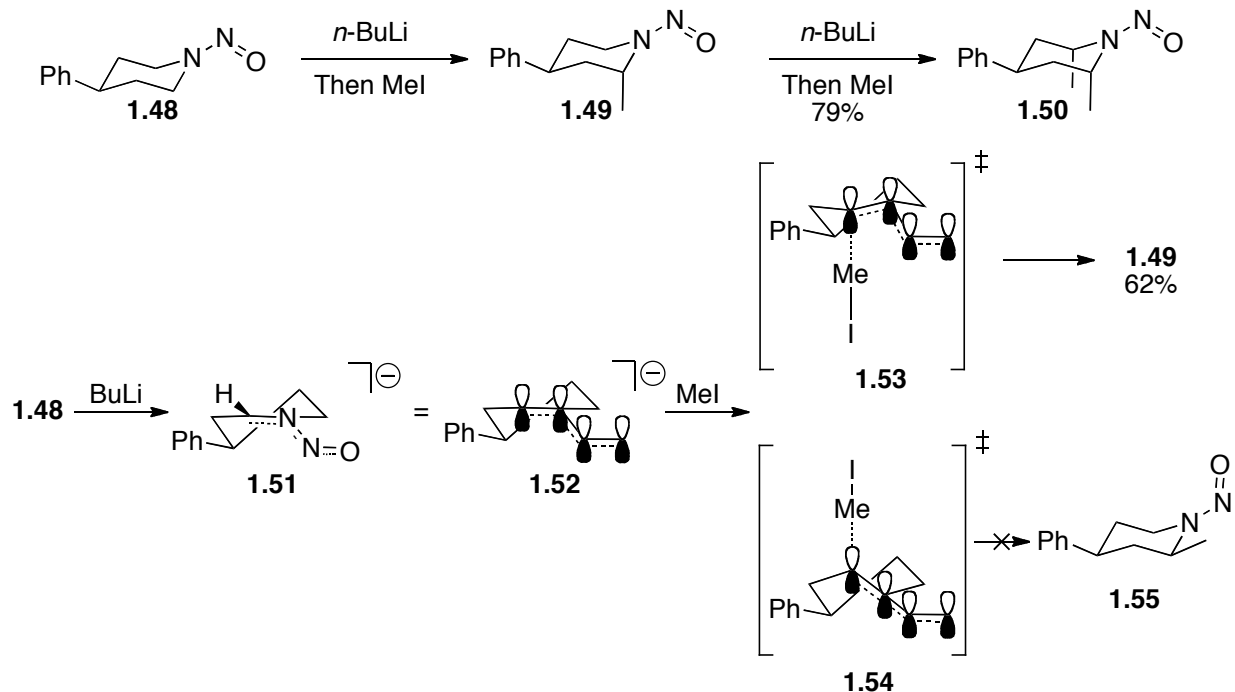
In contrast to the 2,6-diaxial alkylation products obtained through the use of nitrosamines, N–Boc piperidines react to form 2,6-trans products.[40] Deprotonation of compound **1.56** leads to equatorial anion **1.57** (**Scheme 1.7**). The axial alkyllithium was not formed since calculations indicate an unfavorable HOMO–HOMO interaction between the C–Li and nitrogen lone pairs (ca. 17 kcal/mol).[41] Alkylation then proceeds via the equatorial alkyllithium. When structure **1.58** is alkylated, an $A^{1,3}$ strain develops due to Boc resonance structures. This would cause a ring-flip to place the methyl group axial; however, doing so would also place the phenyl group axial. Instead, Beak suggests a twist-boat-like conformation to keep the phenyl group equatorial and methyl group axial thus avoiding the $A^{1,3}$ strain.[40] This results in equatorial methylation and a 2,6-trans relationship between the newly added substituents.

Scheme 1.7. Trans-dialkylation of Boc protected piperidine
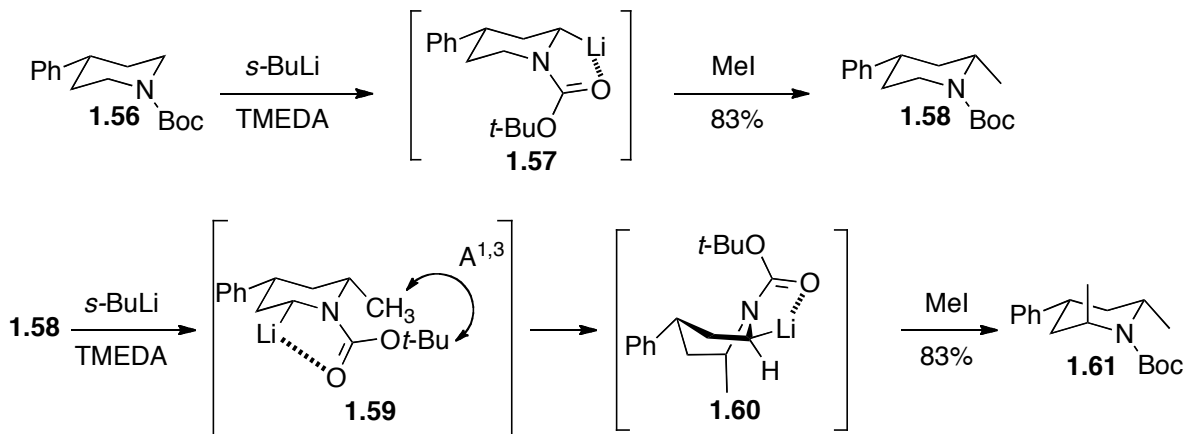
Access to 2,6-diequitorial piperidines was described by Meyers in 1984.[42] Subjecting compound **1.62** to *t*–BuLi, led to intermediate **1.63** (**Scheme 1.8**). Axial lithiation is believed to not occur for the same reasons as the above Boc case. Alkylation to give equatorial **1.64** occurred in great yield. Upon secondary lithiation, intermediate **1.65** was formed. The N–*t*–butylformamide group is smaller than the Boc group and $A^{1,3}$ strain is absent. Therefore, direct alkylation of **1.65** in a chair conformation takes place, leading to the 2,6-diequitorial piperidine **1.66**.

Scheme 1.8. Cis-dialkylation of N-formamidinyl piperidines
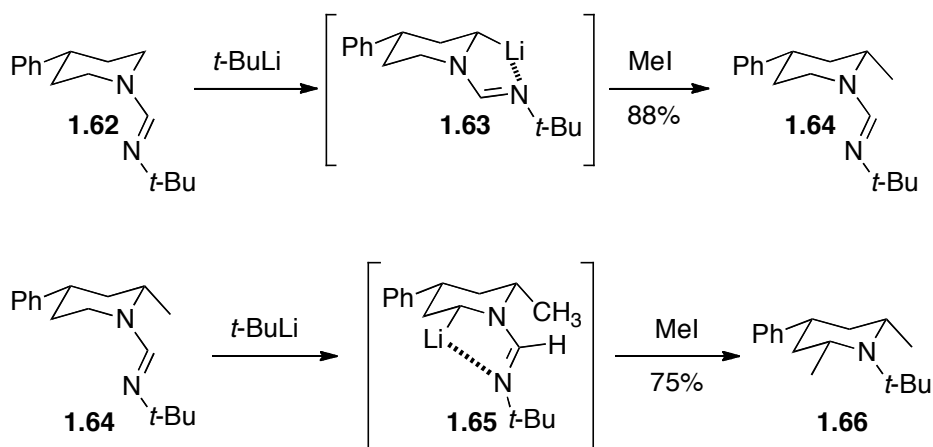
Kotomori and co-workers recently reported on the stereochemical behavior of lithiated 2-cyanopiperidines.[43] Entries 1-4 show retention or inversion product ratios that are electrophile dependent (**Scheme 1.9**). The authors believe that deprotonation of **1.67** gives the urea stabilized lithiate **1.68**. When more reactive electrophiles were used (entries 1, 2), alkylation occurs with retention. Less reactive electrophiles (entries 3, 4) provide enough time for isomerization of the metallated nitrile to the N-lithiated keteniminate **1.71**. Alkylation would occur from both faces of the keteniminate; however, the axial methyl group blocks one side of the ring, leading to net inversion of the nitrile center.

Scheme 1.9. Alkylation of a tertiary α-aminonitrile

Entry	Electrophile	Product	Yield (%), Ret:Inv
1	2-ClC₆H₄COCl	**1.69**	91, 89:11
2	C₆H₅COCl	**1.70**	83, 74:26
3	4-MeOC₆H₄COCl	**1.72**	93, 48:52
4	MeI	**1.73**	75, 1:99
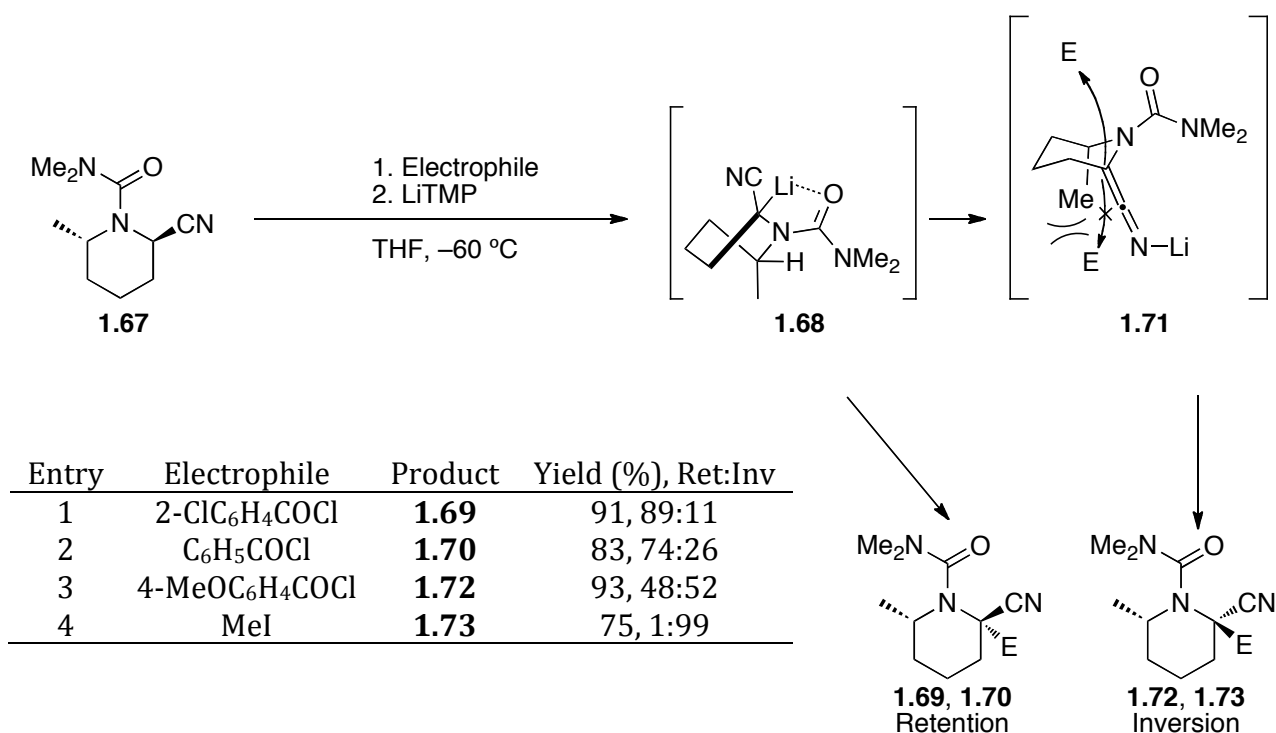
Preparation by lithium-halogen exchange

Formation of α-aminoorganolithiums by lithium-halogen exchange is practically absent in the literature. This is likely due to the inherent instability of α–aminohalogens.

Compound **1.74** was found to decompose within hours of isolation despite the use of a Boc protecting group (**Scheme 1.10**).[44] Azeridine **1.75** appears to be more resistant to decomposition and lithium-halogen exchange was successfully implemented to provide lithiate **1.76**. Addition into 3-pentanone gave the product **1.77** in excellent yield as a single diastereomer.

Scheme 1.10. Stability and lithium-halogen exchange of α-aminoorganohalides
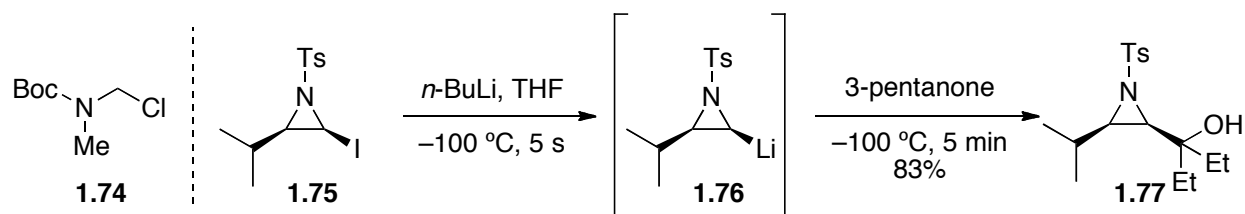
The third permutational interconversion method for generating α-aminoorganolithiums is by transmetallation. Tin is by far the most used metal for this reaction and the method was initially reported by Peterson as an alternative to low yielding deprotonation reactions.[45] Alkyllithiums formed this way are believed to fully retain the stereochemical information of the organotin precursor.[46] This method is considered a general way to obtain α-aminoorganolithiums; however, some compounds fail to transmetallate due to the unfavorable thermodynamics of the reaction.[47,48]

Scheme 1.11. Cyclization to (+)-pseudoheliotridane
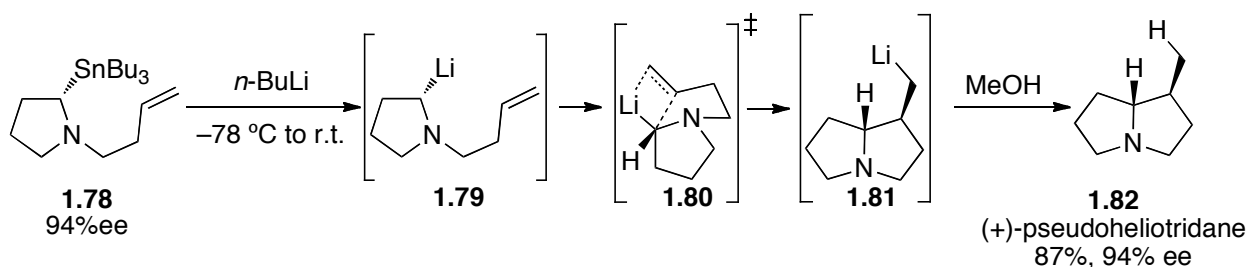
The transmetallation of pyrrolidine **1.78** to lithiate **1.79** was described by Coldham as a way to access substituted pyrrolizidines (**Scheme 1.11**).[49] This reaction is believed to occur through four-membered transition-state **1.80**, with overall retention of configuration. The resulting alkyllithium **1.81** was quenched with methanol to give the natural product (+)-pseudoheliotridane (**1.82**) with no loss of optical purity despite the cyclization occurring at 0 °C.

Scheme 1.12. Anionic [2,3] rearrangement of pyrrolidium bromides

1.83 R = H, 94% ee
1.84 R = Me, 94% ee

1.85 R = H
1.86 R = Me

1.87 R = H, 67%, 88% ee
1.88 R = Me, 71%, 94% ee
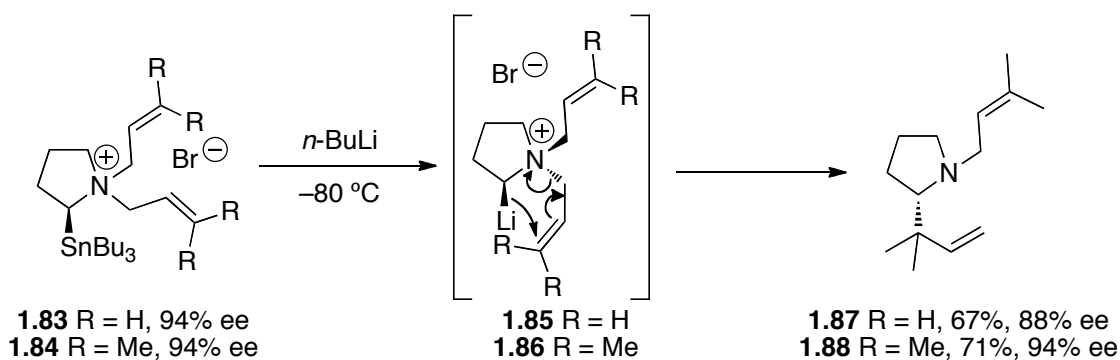
Anionic [2,3] rearrangement of α-stannyl pyrrolidiums was reported by Gawley in 1995.[50] Both **1.83** and **1.84** could be transmetallated and reacted in excellent yield and ee (**Scheme 1.12**). Surprisingly, the more substituted **1.84** was obtained in higher yield and ee than **1.83**. Both of the cyclizations occurred with inversion of the C–Li bond. Use of tertiary amines in the sequence returned rearranged products in low ee due to racemization of the organolithium intermediate.

Pearson was the first to report a stabilized α-aminoorganolithium prepared by tin-lithium exchange.[51] Substrates **1.89** and **1.92** were reacted with *n*-BuLi to give **1.90** and **1.91** with retention (**Scheme 1.13**). However, in the case of **1.91**, the unfavorable steric clashing from the syn methyl and phenyl groups caused isomerization to **1.90**. Trapping of the lithiate gave product **1.93** with a 1:1 dr with respect to the formed alcohol.

Scheme 1.13. Steric bias of oxazolidinone bearing α-aminoorganolithiums
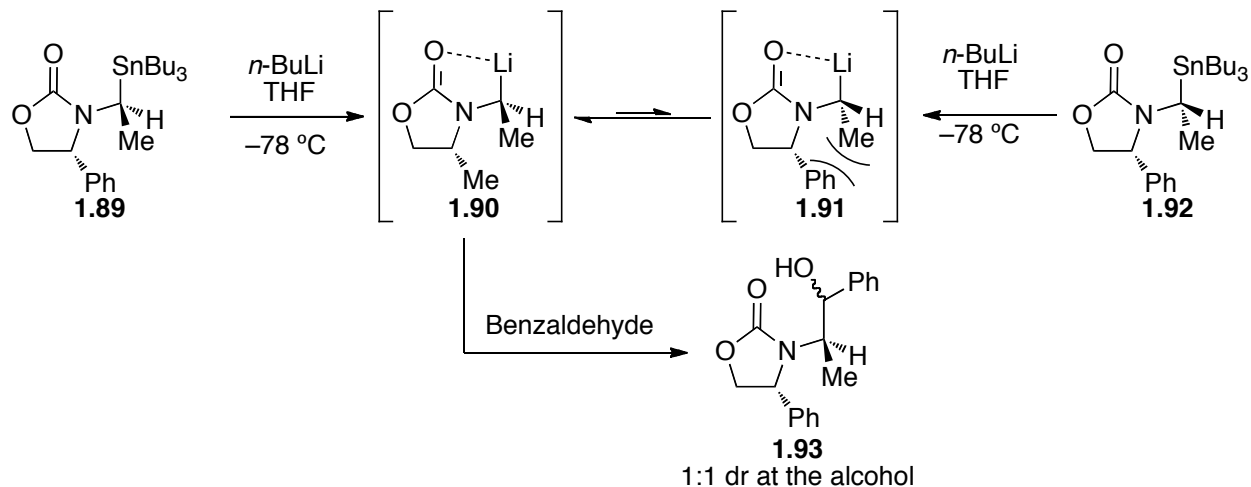
Preparation by radical arene reduction

The last general method for synthesis of alkyllithium reagents is by reductive lithiation. Whether the process is stepwise or concerted depends on the nature of the reducible Z group in **1.94** (**Scheme 1.14**). In either case, an electron is transferred into the LUMO of this group. If the LUMO is a low energy π* or empty d-orbital, the process is likely stepwise.[4] After addition of an electron, intermediate **1.95** is formed, before expulsion of the reduced Z⁻ and formation of radical **1.96**. If the LUMO is too high to be accessible, then a concerted process takes over. Here, addition of an electron to **1.94** directly leads to radical **1.96**. Once this radical is generated by either pathway, another radical is added to the SOMO of **1.96** to give the anion **1.97**.

Scheme 1.14. General mechanism of reductive lithiation

Figure 1.6. Common aromatic radical carriers

1.98
lithium
naphthalenide (LiN)

1.99
lithium 1-(dimethylamino)-
naphthalenide (LDMAN)

1.100
lithium 4,4'-di-*tert*-
butylbiphenylide
(LiDBB or Freeman's Reagent)
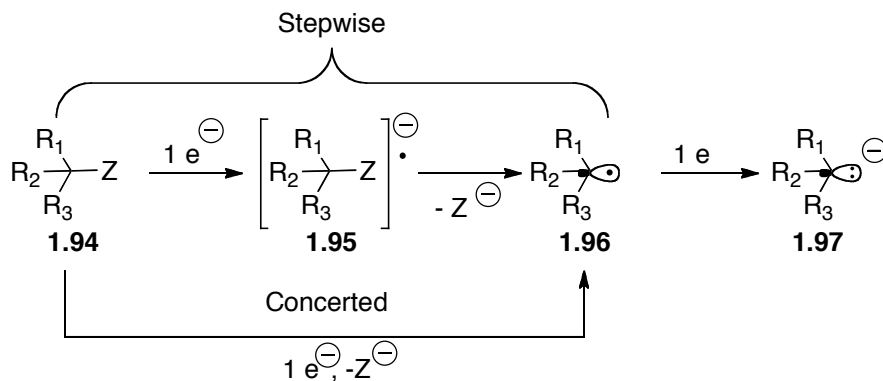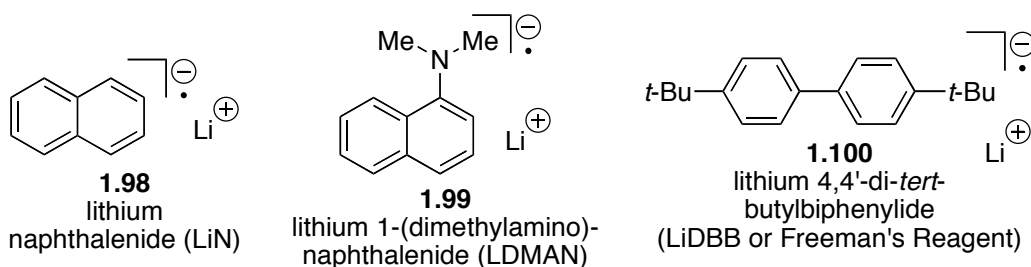
The first description of a lithium based aromatic radical carrier was by Screttas in 1972.[52,53] Using lithium naphthalenide (LiN, **1.98**, **Figure 1.6**), halobenzenes **1.101** and **1.102** were reduced and carboxylated to give benzoic acid in excellent yield (**Scheme 1.15**). While LiN is an efficient reagent for the reduction of alkyl and aryl halides, some drawbacks were identified.[54] Radical intermediates from the reduction were found to couple with LiN, leading to **1.106** (**Scheme 1.16**, eq 1). Alternatively, over-reduction of LiN to **1.107** can occur and the dianion can react with an electrophile before its reduction. This is of particular concern when sodium is used in place of lithium.[55]

Scheme 1.15. Reductive lithiation of halobenzenes

1.101 X = Cl
1.102 X = F

1.103

1.104
85% from **1.101**
91% from **1.102**
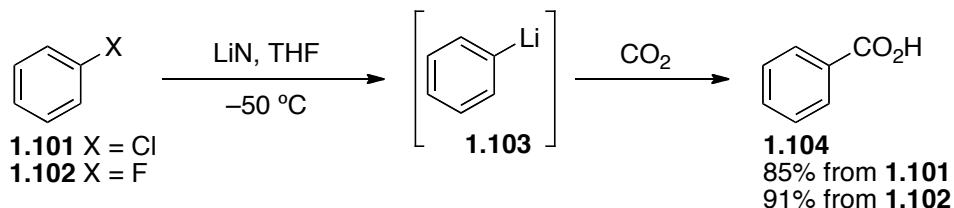
Scheme 1.16. Decomposition pathways for LiN

(1)

1.98

1.105

+ LiX + R·

1.106 H   R

(2)

1.98

1.107

1.106 H   R

1.108 H   R
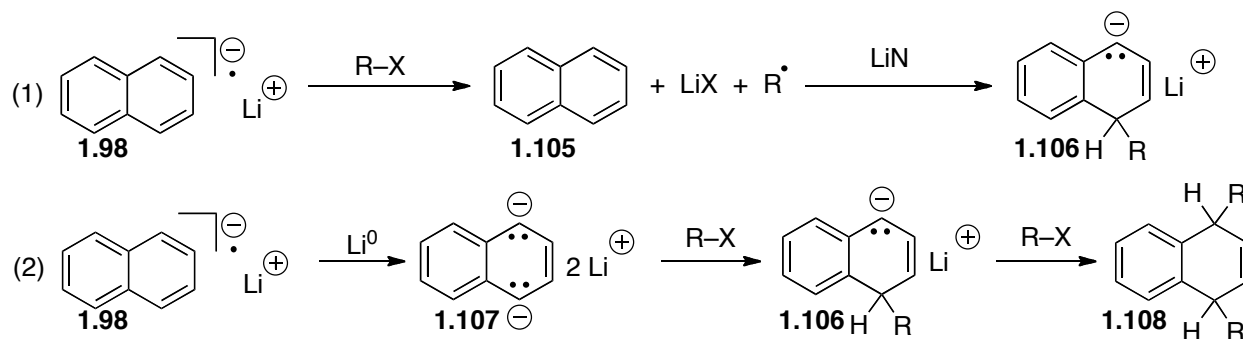
The use of LiN in organic synthesis has an additional drawback; after work-up, a large quantity of naphthalene is isolated in the crude reaction mixture. Co-elution during chromatography is possible if the desired product is sufficiently non-polar. To avoid this problem, Cohen described the generation of LDMAN (**Figure 1.6**).[56] This reductive lithiation reagent can be removed during work-up with the addition of dilute acid. The nitrogen that allows for water solubility is also the cause of LDMAN's decomposition above –45 °C.[57] Cohen theorized that LDMAN could disproportionate into **1.109** and dianon **1.110** (**Scheme 1.17**). While this is expected to be an unfavorable equilibrium (favoring **1.99**), elimination of **1.112** makes the more stable **1.111**, providing a driving force for the overall reaction.

Scheme 1.17. Decomposition pathway for LDMAN
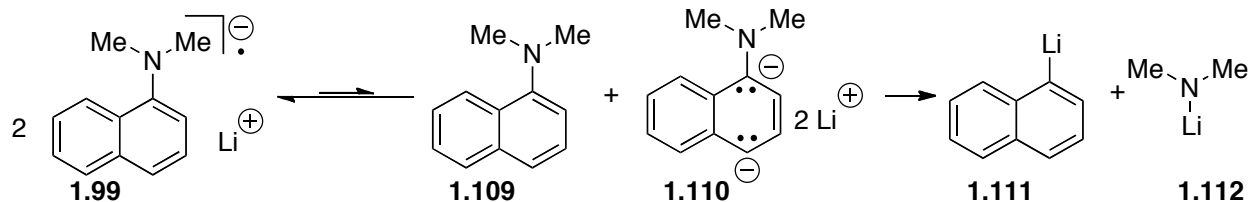
A third reductively lithiating arene, LiDBB, was described by Freeman (**Figure 1.6**, **1.100**).[58] This reagent incorporates *tert*-butyl groups to shield the aromatic core of the molecule from undesired alkylations, which can occur at distances of ≤2.0 Å. Since electron transfer can occur as far away as 7-9 Å, the steric bulk of the *tert*-butyl groups has no impact on the reductive ability of the reagent. In fact, LiDBB was found to give higher yielding reductions of alkyl chlorides than LiN.[59] This is partially due to the higher reducing power of LiDBB vs. LiN .[60]

The first report of an α-aminoorganolithium, prepared by dissolving metal conditions, was by Welvart.[61] Reduction lithiation of the nitrile afforded the corresponding organolithium intermediate, that was immediately protonated in situ to give a 3:1 ratio of compounds **1.114** and **1.115** (**Scheme 1.18**).

Scheme 1.18. Early example of reductive decyanation on an α-aminonitrile
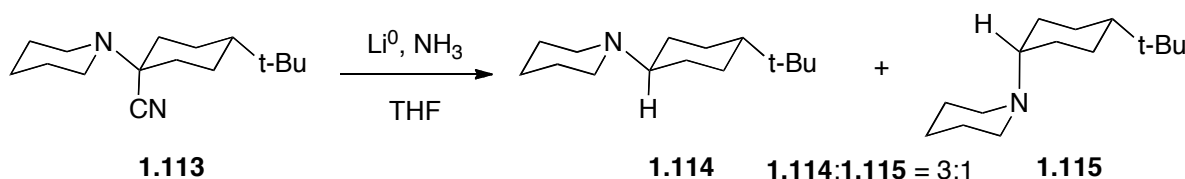
Spirocyclization of aminonitrile **1.116** was reported by Husson in 1994 (**Scheme 1.19**).[62] Reduction of the nitrile to the corresponding unstabilized α-aminoorganolithium **1.117** with LiDBB led to cyclization onto the nearby alkyl chloride in good yield given the

high reactivity of the lithium intermediate. The synthesis also revealed a preference for the reduction of the nitrile over the chloride.

Scheme 1.19. Spiroannulation by reductive decyanation
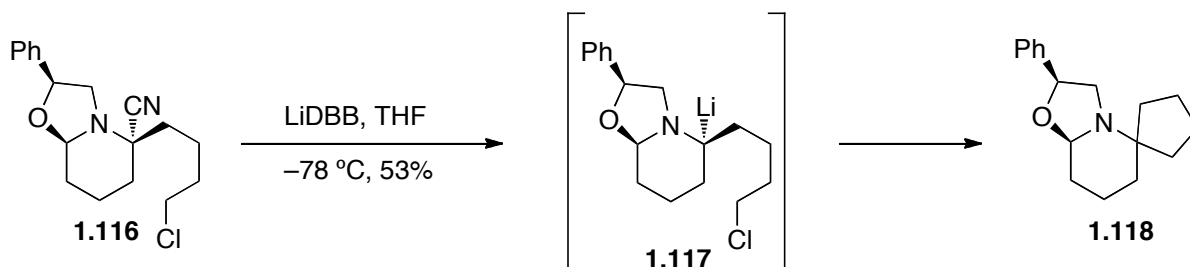
The difference in reactivity between stabilized and unstabilized α-aminoorganolithiums was demonstrated by Rychnovsky and Bahde. [63] Reductive decyanation of **1.119** produced the corresponding alkyllithium, which then cyclized onto the nearby alkene (**Scheme 1.20**). The lithiated intermediate **1.120** was quenched with methanol to afford spirocycle **1.121** in great yield and excellent stereoselectivity. Attempts to repeat this process with the homologated **1.122** returned none of the desired spirocycle **1.124** (eq 2). Only the decyanated product **1.123** was found. It is believed that the entropic cost of the transition state leading to **1.124** is inaccessible at temperatures that prevented decomposition of the reductively lithiated intermediate.[64] The N-Boc-piperidine **1.125** also failed to cyclize to spirocycle **1.126** (eq 3). This was attributed to the stability of Boc- Li coordination, leading to a less reactive intermediate than in the N-Benzyl case (eq 1).

Scheme 1.20. Reductive spiroannulation by carbolithation

(1) 1.119 → LiDBB, THF, −78 ºC → [1.120] → MeOH, 67%, 95:5 dr → 1.121

(2) 1.122 → 1. LiDBB, THF −78 to −40 ºC; 2. MeOH → 1.123; 1.124 not observed

(3) 1.125 → 1. LiDBB, THF −78 to −40 ºC; 2. MeOH, 83% → 1.126; 1.127 not observed
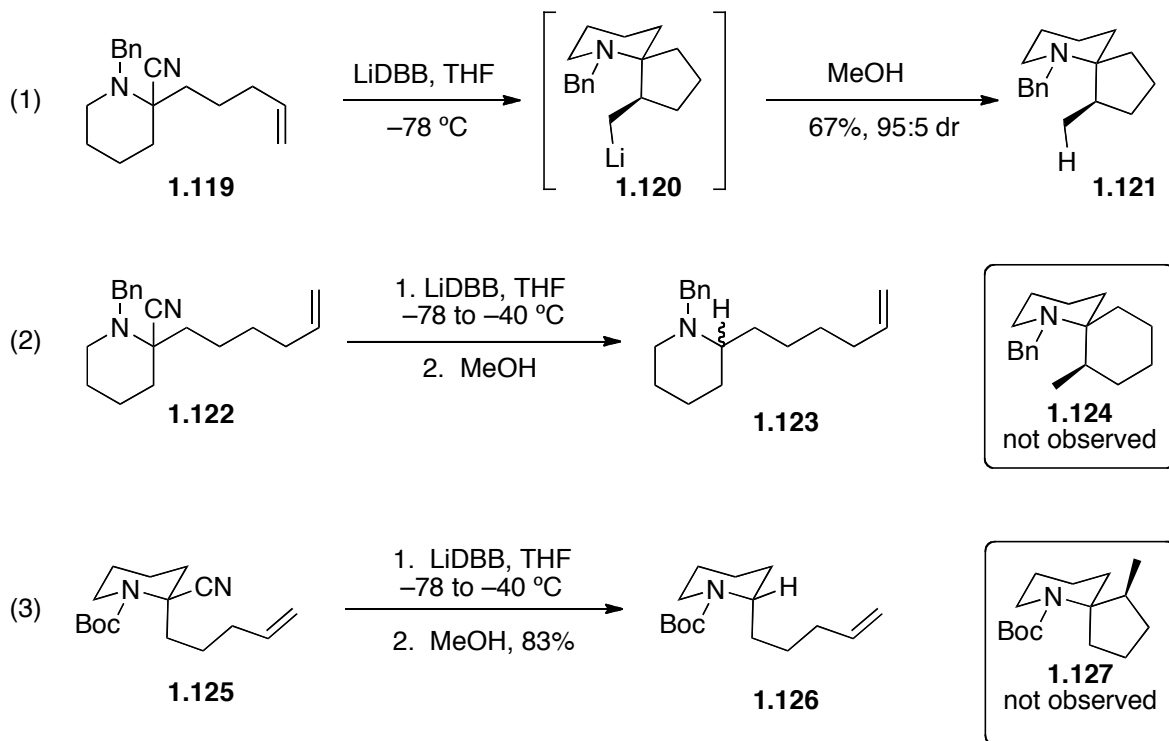
Conclusions

The unique reactivity of α-aminoorganolithiums has driven much research on the subject over the last 50 years. Studies have highlighted their utility in natural product synthesis as well as for stereoselective carbon-carbon bond formations. Continuing research on the subject will provide insight into the varying modes of reactivity and synthetic approaches available through these useful reagents.

[1] Books: (a) Rappoport, Z.; Marek, I. *The Chemistry of Organolithium Compounds*; Wiley: Chichester, West Sussex, England, 2004. (b) Clayden, J. *Organolithiums: Selectivity for Synthesis*; Pergamon: Amsterdam, 2002. (c) Alpatova, N. M. *Organolithium Compounds, Solvated Electrons*; Springer-Verlag: Berlin, 1987. (d) Alpatova, N. M. *Organolithium Compounds, Solvated Electrons*; Springer-Verlag: Berlin, 1987.

[2] Review Articles: (a) Beak, P.; Meyers, A. *Acc. Chem. Res.* **1986**, *19*, 356–363. (b) Yus, M. Arene-Catalyzed Lithiation. *Chem. Soc. Rev.* **1996**, *25*, 155–161. (c) Capriati, V.; Perna, F. M.; Salomone, A. *Dalton Trans*, **2014**, *43*, 14204–14210.

[3] (a) Beak, P.; Zajdel, W. Reitz, D. *Chem. Rev.* **1984**, *84*, 471–523. (b) Katritzky, A.; Qi, M. *Tetrahedron* **1998**, *54*, 2647–2668

[4] Perry, M.; Rychnovsky, S. *Nat. Prod. Rep.* **2015**, *32*, 517–533.

[5] Beak, P.; Reitz, D.; *Chem. Rev.* **1978**, *78*, 275–316.

[6] Schleyer, P.; Clark, T.; Kos, A.; Spitznagel, G.; Rohde, C.; Arad, D.; Houk, K.; Rondan, N. *J. Am. Chem. Soc.* **1984**, *106*, 6467–6475.

[7] Boche, G.; Marsch, M.; Harbach, J.; Harms, K.; Ledig, B.; Schubert, F.; Lohrenz, J.; Ahlbrecht, H. *Chem. Ber.* **1993**, *126*, 1887–1894.

[8] Low. E.; Gawley, R. *J. Am Chem. Soc.* **2000**, *122*, 9562–9563.

[9] Reich, H. *Chem. Rev.* **2013**, *113*, 7130–7178.

[10] Walborsky, H.; Periasamy, M. *J. Am. Chem. Soc.* **1974**, *96*, 3711–3712.

[11] Gawley, R.; Zhang, Q. *Tetrahedron* **1994**, *50*, 6077–6088.

[12] Gawley, R. α-Amino Organolithium Compounds. In The Chemistry of Organolithium Compounds; Wiley: Chichester, West Sussex, England, 2004; Vol. 2, pp. 1005–1006.

[13] Ashweek, N.; Brant, P.; Coldham, I, Dufour, S.; Gawley R.; Haeffnew, F.; Klein, R.; Sanchez-Jimenez, G. *J. Am. Chem. Soc.* **2004**, *127,* 449–457.

[14] Haeffnew, F.; Chong, J.; Park, S.; Gawley, R. *Org. Lett.* **2002**, *4*, 2101–2014.

[15] Ingold, C. K. *Structure and Mechanism in Organic Chemistry;* Comell University: Ithaca, NY, 1953.

[16] Gawley, R. *Tetrahedron Lett.* **1999**, 4297–4300.

[17] Gawley, R.; Low, E.; Zhang, Q.; Harris, R. *J. Am Chem. Soc.* **2000***, 122,* 3344–3350.

[18] (a) Perry, M.; Morin, M.; Slafer, B.; Wolckenhauer, S.; Rychnovsky, S. *J. Am. Chem. Soc.* **2010**, *132*, 9591–9593. (b) Perry, M.; Morin, M.; Slafer, B.; Wolckenhauer, S.; Rychnovsky, S. *J. Org.Chem.* **2012**, *77*, 3390–3340.

[19] Gawley, R.; Zhang, Q. *J. Org. Chem.* **1995***, 60*, 5763–5769.

[20] (a) Kerrick, S.; Beak, P. *J. Am. Chem. Soc.* **1993***, 113*, 9708–9710. (b) Beak, P.; Kerrick, S.; Wu, S.; Chu, J. *J. Am. Chem. Soc.* **1994***, 116*, 3231–3239. (c) Park, Y.; Boys, M.; Beak, P. *J. Am. Chem. Soc.* **1996***, 118*, 3757–3758.

[21] (a) Gawley, R.; Low, E.; Zhang, Q.; Harris, R. *J. Am. Chem. Soc.* **2000***, 122*, 3344–3350. (b) Faibish, N.; Park, Y.; Lee, S.; Beak, P. *J. Am. Chem. Soc.* **1997**, *119*, 11561–11571.

[22] Schlosser, M. *Organometallics In Synthesis: A Manual*; Wiley-Blackwell: Hoboken, 2011; pp. 1–351.

[23] Gilman, H.; Langham, W.; Jacoby, A. *J. Am. Chem. Soc.* **1939***, 61*, 106–109.

[24] Wittig, G.; Pockels, U.; Dröge, H. *Ber. Deutsch. Chem. Ges.* **1938***, 71*, 1903.

[25] Jones, R.; Gilman, H. *Chem. Rev.* **1954***, 54*, 835–890.

[26] Wakefield, B. *Organolithium Methods*, Academic Press, London, 1988.

[27] Peterson, D.; Hays, H.; *J. Org. Chem.* **1965***, 30*, 1939–1942.

[28] Seebach, D.; Enders D. *Angew. Chem. Int. Ed.* **1975**, *14*, 15–32.

[29] Kessar, S.; Singh, P.; Vohra, R.; Kaur, N.; Singh, K. *J. Chem. Soc., Chem. Commun.* **1991,** 568–570.

[30] Kessar, S.; Singh, P. *Chem. Rev.* **1997,** *97*, 721–737.

[31] Keefer, L.; Fodor, C. *J. Am. Chem. Soc.* **1970**, *92,* 5747–5748.

[32] Shawe, T.; Meyers, A. *J. Org. Chem.* **1991**, *56,* 2751–2755.

[33] Seebach, D.; Wykypiel, W.; Lubosch, W.; Kalinowski, H. *Helv. Chim. Acta* **1978**, *61,* 3100–3102.

[34] Beak, P.; Lee, W. *J. Org. Chem.* **1990**, *55*, 2578–2580.

[35] Clayden, J.; Dufour, J.; Grainger, D.; Helliwell, M. *J. Am. Chem. Soc.* **2007***, 129*, 7488–7489.

[36] Hirai, K.; Matsuda, H.; Kishida, Y. *Tetrahedron Lett.* **1971**, 4359–4362.

[37] Fraser, G.; Grindley, T.; Passannanti, S.; *Can. J. Chem.* **1975**, *53*, 2473–2480.

[38] National Toxicology Program, *Report on Carsinogens*, National Institute of Heath, 2011, vol. 12, pp 302–303.

[39] Seebach, D.; Wykypiel, W. *Synthesis*, **1979**, 423–424.

[40] Beak, P.; Lee, W. *J. Org. Chem.* **1993**, *53*, 1109–1117.

[41] Bach, R.; Braden, M.; Wolber, G. *J. Org. Chem.* **1983**, *48*, 1509–1514.

[42] Meyers, A.; Milot, G. *J. Am. Chem. Soc.* **1993**, *115,* 6652–6660.

[43] Kotomori, Y.; Sasaki, M.; Kawahata, M.; Yamaguchi, K.; Takeda, K. *J. Org. Chem.* **2015**, *80*, 11013–11020.

[44] Samame, R. Chemistry Department, UCI, Irvine, CA. Personal communication, January 2016.

[45](a) Peterson, D.; *J. Organomet. Chem.* **1970**, *21*, P63–P64. (b) Peterson, D. *J. Am. Chem. Soc.* **1971**, *93*, 4027–4031.

[46] (a) Still, W.; Sreekumar, C. *J. Am. Chem. Soc.* **1980**, *102*, 1201–1202. (b) Sawyer, J.; Kucerovy, A.; Macdonald, T.; McGarvey, G.; *J. Am Chem. Soc.* **1988**, *110*, 842–853

[47] Failure of Tin-lithium exchange in acyclic cases: (a) Tsunoda, T.; Fujiwara, K.; Yamamoto, Y.; Ito, S. *Tetrahedron Lett.* **1991,** *32,* 1975–1978. (b) Burchat, A. F.; Chong, J. M.; Park, S. B. *Tetrahedron Lett.* **1993,** *34,* 51-54. (c) Santiago, M; Low, E.; Chambournier, G.; Gawley, R. E. *J. Org. Chem.* **2003,** *68,* 8480-8484.

[48] Failure of Tin-lithium exchange in a cyclic case: Klein, R.; Gawley, R. E. *J. Am. Chem. Soc.* **2007,***129,* 4126-4127.

[49] Coldham, I.; Hufton, R.; Snowden, D. *J. Am. Chem. Soc.* **1996**, *118*, 5322–5323.

[50] Gawley, R.; Zhang, Q.; Campagna, S. *J. Am. Chem. Soc.* **1995,** *117*, 11817–11818.

[51] Pearson, W.; Lindbeck, A. *J. Org. Chem.* **1980**, *54*, 5651–5654.

[52] Screttas, C. *J. Chem. Soc., Chem. Commun.* **1972**, 752–753.

[53] Sodium naphthalenide and potassium naphthalenide were described before lithium naphthalenide. See reference 51 for additional information

[54] Holy, N. *Chem. Rev.* **1974**, *74*, 234–274.

[55] Freeman, P.; Hutchinson, L. *J. Org. Chem.* **1980**, *45*, 1924–1930.

[56] Cohen, T.; Matz, J. *Synth. Commun.,* **1980**, *10*, 311–317.

[57] Yang, A.; Butela, H.; Deng, K.; Doubleday, M.; Cohen, T. *Tetrahedron* **2006,** *62,* 6526-6535.

[58] Freeman, P.; Hutchinson, L. *Tetrahedron Lett.* **1976**, *22*, 1849–1852.

[59] Freeman, P.; Hutchinson, L. *J. Org. Chem.* **1980**, *45*, 1924–1930.

[60] 4,4'-di-*tert*-butylbiphenyl has a reductive potential of –2.14 eV vs. SCE, while Naphthalene has a reductive potential of –1.98eV vs. SCE. See Reference 4 for additional information.

[61] Fabre, C.; Welvart, Z. *C. R. Acad. Sci. Ser.* **1970***, 270*, 1887–1890.

[62] Ribeiro, C.; de Melo, S.; Bonin, M.; Quirion, J.; Husson,H. *Tetrahedron Lett.* **1994***, 35*, 7227–7230.

[63] Bahde, R.; Rychnovsky, S. *Org. Lett.* **2008**, *10,* 4017-4020.

[64] Ashweek, N.; Coldham, I.; Snowden, D.; Vennall, G. *Chem.-Eur, J.* **2002,** *8,* 195-207.

Chapter 2

LiDBB Formation and Decomposition Rates and Storage

Abstract

Characterization of LiDBB's formation, rate of overall decomposition and storage potential is described herein. The reaction solvent tetrahydrofuran was found to under go decomposition, mainly by retro [2+3], and ethylene, in the presence of LiDBB, formed unanticipated products such as vinyl lithium, and ethylated DBB. Use of LiDBB stored at −25 °C over 16 weeks was found to give equivalent yields of a spirocycle as compared to freshly prepared solutions.

Introduction

The synthetic importance of alkyllithium reagents in organic chemistry cannot be overstated. Organolithium compounds have been studied for nearly 100 years and hundreds of review articles have been written on the subject.[1] The use of these reagents has become indispensable to academic[2] and pharmacological research.[3] Their wide use and incredible utility incentivize additional ways of forming them

One of several ways to form organolithiums is through two sequential single-electron- transfers, commonly known as reductive lithiation. Reduction of alkyl chloride **2.1** with lithium metal yields radical intermediate **2.2** (**Scheme 2.1**).[4] After a second single-electron transfer, alkyllithium **2.3** is formed. One limitation to this method is the higher temperature required to enable reductive chemistry at the lithium surface.[5] These reaction conditions also require the use of extremely inert solvents such as hexane or pentane. This

requirement further diminishes synthetic utility due to the reduced solubility of more complicated substrates. Much research has gone into controlling reductive lithiation to form alkyllithium reagents at lower temperatures, resulting in more precise reactions.[6]

Scheme 2.1. Reductive lithiation of an alkyl chloride
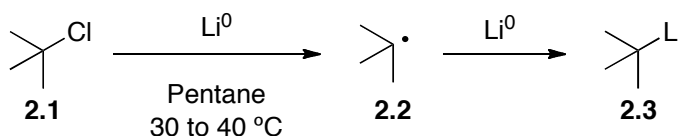
Background

The need for milder conditions to generate alkyllithium reagents has driven research in the area of dissolving metal reductions using aromatic systems. The first lithium based aromatic radical carrier was lithium naphthalenide (LiN, **1.98**, **Figure 1.6**).[7,8] Unfortunately, LiN coupled with other radicals present in solution.[9] Cohen developed another aromatic radical carrier, lithium 1-(dimethylamino)-naphthalenide (LDMAN, **1.99**).[10] This reagent was designed to carry out single-electron reductions, while being water soluble to facilitate its removal upon work-up. While LDMAN addressed the issue of byproduct removal, it is limited by its decomposition to 1-lithionaphthalene above –45 °C.[11] Between the initial reports of LiN and LDMAN, Freeman reported the use of lithium 4,4'-di-*tert*-butylbiphenylide (LiDBB, **1.100**) as a new and more powerful single-electron reductant.[12] This reagent incorporated *tert*-butyl groups to suppress radical coupling seen with LiN and could be formed at 0 °C, unlike LDMAN. While LiDBB was an improvement over other radical carriers, temperatures above 0 °C led to decomposition into unknown byproducts.[13]

Figure 1.6. Common aromatic radical carriers

1.98
lithium
naphthalenide (LiN)

1.99
lithium 1-(dimethylamino)-
naphthalenide (LDMAN)

1.100
lithium 4,4'-di-*tert*-
butylbiphenylide
(LiDBB or Freeman's Reagent)
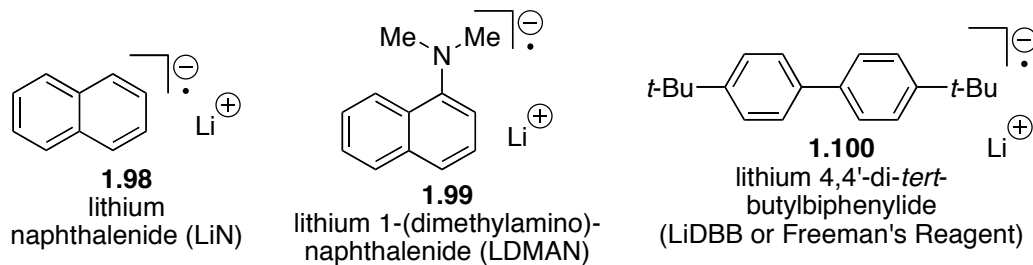
Since the products and rate of LiDBB decomposition were unknown, solutions are prepared fresh over four hours, used once and then discarded. A better understanding of LiDBB and its long-term viability could lead to methods for storing a stock solution rather than requiring hours of preparation before each use. Additionally, a shorter preparation time would save hours of waiting each time the reagent is needed for synthesis. Given these issues, a series of experiments were designed to investigate and expand the value of this reagent.

Titration studies

Initial work on improving LiDBB solutions focused on the time required for LiDBB formation. This meant developing a reliable titration method. Since thioethers are readily cleaved by LiDBB, thioanisole was selected as the titrant.[14] The disappearance of the dark green color of LiDBB was used to follow the titration. Initial testing with a 0.20 M thioanisole solution showed promise (**Scheme 2.2**). Unfortunately, repeated testing showed half the expected molarity of LiDBB solutions (**Table 2.1**, Trial 1). It was postulated that something on the flask surface was reacting with LiDBB, resulting in a lower observed molarity. To mitigate this problem, all titrations were run in the same flask, and the tested LiDBB aliquots removed from the vessel between each titration. This produced a reproducible titer (**Table 2.1**, Trials 1–4). Pre-treating the flask with *n*–BuLi

(**Table 2.2**, Trial 1), gave the correct molarity; however, attempts to run additional titrations in the same flask gave a lower molarity for unknown reasons. Due to the ease of running four titrations in a single flask and excluding the first trial, the method in **Table 2.1** was selected for all future titrations.

Scheme 2.2. Titration of LiDBB
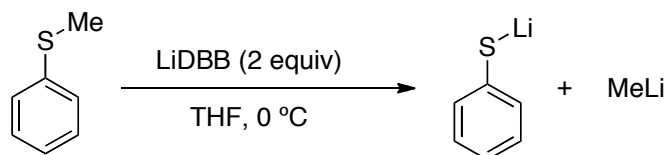
Table 2.1. Sequential titrations of LiDBB   **Table 2.2**. Titrations with pretreatment

Trial	[LiDBB]	Trial	[LiDBB]
1	0.20	1	0.36
2	0.36	2	0.26
3	0.36	3	0.26
4	0.36	4	0.27

0.20 M thioanisole was used as the titrant. [LiDBB] is in Mol/L

0.20 M thioanisole was used as the titrant. [LiDBB] is in Mol/L. Flask pretreated with 2 drops of 2.5 M n-BuLi before titration

Using this titration method, the rate of LiDBB formation was examined at different temperatures and concentrations of 4,4'-di-*tert*-butylbiphenyl (DBB, **2.19**, **Scheme 2.7**). Published conditions for forming a 0.4 M LiDBB solution take 4 hours.[15]   Hourly titrations of a nominal 0.4 M LiDBB solution revealed that 75% of the reagent's full strength is achieved after 1 hour, with a slow rise in molarity over an additional 4 hours to 0.37 M (**Graph 2.1**). Attempts to form a nominal 1.0 M LiDBB solution revealed a much slower formation, providing only 0.22 M LiDBB after one hour. Continuing to follow the reagent's development showed a slow, sigmoidal increase to 0.84 M over 8 hours. Whereas higher

molarity LiDBB would be synthetically useful, the long reaction time required to reach full

molarity negated any added value.

Table 2.3. Defining LiDBB solutions

Solution[a]	[DBB]	[LiDBB][b]	Nominal [LiDBB]
A	0.4	0.36	0.4
B	1.0	0.85	1.0
C	2.0	1.3	2.0
D	3.1	1.0	3.1

[a] Solutions were made from DBB in THF to produce the corresponding molarity shown.
[b] Average of three titrations. To this solution, 10 equivalents of lithium metal were added
at the temperature described. 0.20 M thioanisole was used as the titrant. [LiDBB], [DBB]
are in Mol/L

Due to the long reaction times needed to form LiDBB, it was investigated whether

LiDBB could be formed at room temperature and subsequently cooled to 0 °C after full

molarity was reached.   The standard 0.4 M LiDBB solution (Solution A, **Table 2.3**),

prepared at 20 °C, was found to be 13% higher in molarity after 1 hour than when

prepared at 0 °C (**Graph 2.1**). After two hours, the solution had reached its full molarity

and was ready for use. Solution B was also prepared at 20 °C; after only 40 minutes, this

solution was at 0.76 M. By one hour, the solution reached 99% of its final molarity, with

full experimental molarity after two hours of stirring. Allowing solution B to react for an

additional three hours gave no appreciable increase in molarity. Since both solutions A and

B failed to reach full theoretical molarity, it would appear that a non-linear relationship

exists between the concentration of DBB and the resulting molarity of the LiDBB solution.

Nevertheless, titrations of solutions A and B showed that useable concentrations of the

reagent could be prepared at 20 °C after 2 hours.

Graph 2.1. Rates of LiDBB formation
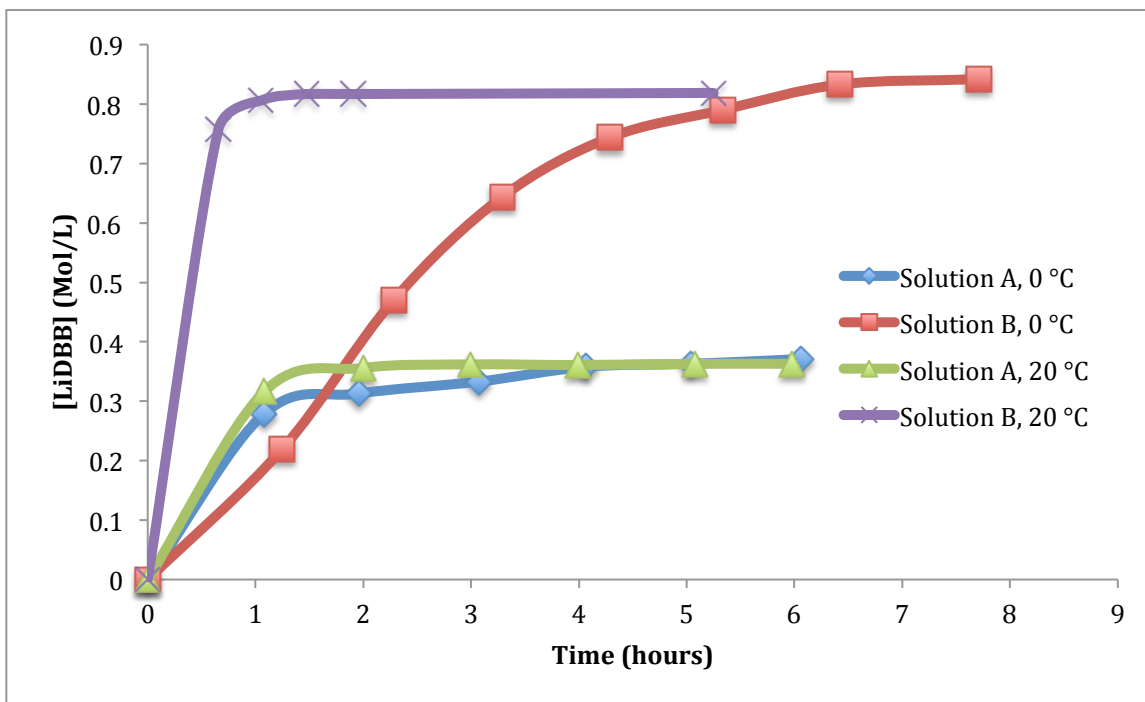
Solutions are defined in **Table 2.3**. Each data point was done in triplicate and averaged

With the success of the higher molarity LiDBB solution B (**Table 2.3**), and the non-linear relationship between DBB and LiDBB concentrations, even higher concentrations were investigated to see if this trend continued. To determine the highest possible LiDBB concentration, a saturated solution of DBB in THF was prepared and found to be 3.1 M. A 2.0 M DBB solution was chosen as the approximate midpoint between the 1.0 M and 3.1 M DBB solutions.   Solutions C and D were prepared at 20 °C and titrated hourly until no further change in molarity was observed. The discrepancy between the molarities of DBB and LiDBB observed with solution B was increased at higher molarities; solution C was found to be 1.3 M and solution D only produced a 1.0 M LiDBB solution. These higher molarity solutions were also significantly more viscous than either the nominal 0.4 M or 1.0 M LiDBB, making titrations difficult. Plotting DBB concentrations versus the resulting

LiDBB molarities fit a curve. From this curve, the theoretical maximum LiDBB concentration was extrapolated to be a 1.27 M solution made from 2.16 M DBB (**Graph 2.2**). Since solutions A and B had ≥90% of the expected LiDBB molarity and were more easily handled at 0 °C, these solutions were selected for further study.

Graph 2.2. Relationship between [DBB] and [LiDBB]
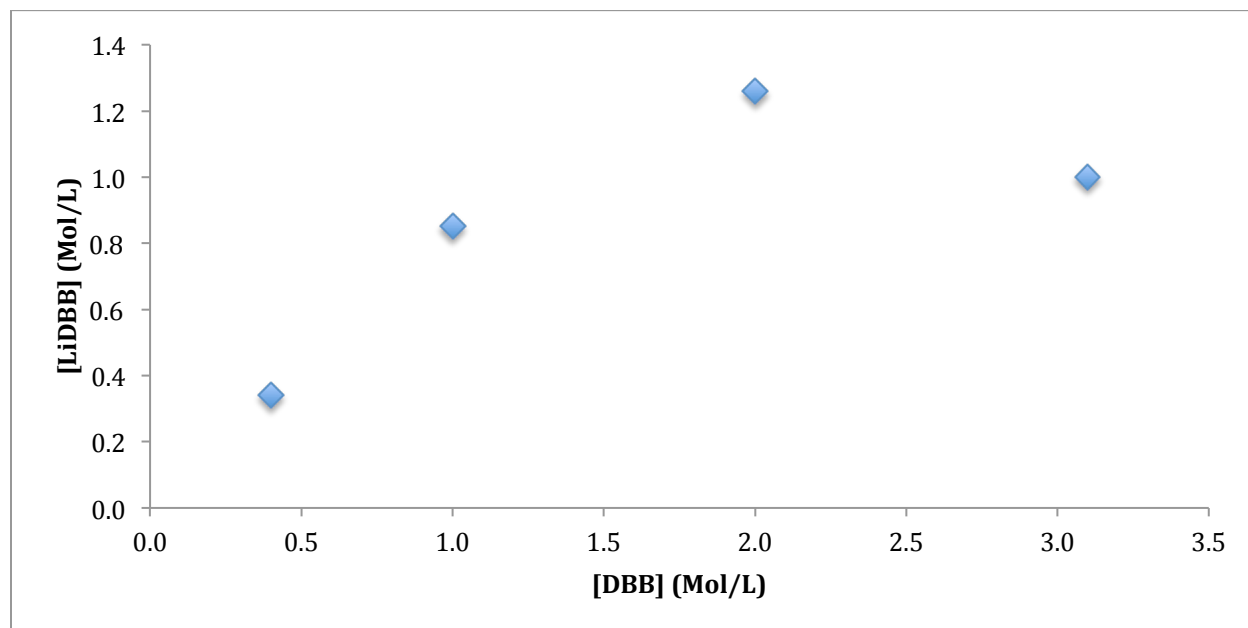
Since LiDBB decomposes above 0 °C, keeping solutions at 20 °C was not feasible. Titrations were done to ensure that solutions cooled to 0 °C after preparation would maintain their full molarity. Solution B (**Table 2.3**) maintain its concentration when prepared at 20 °C and cooled to 0 °C. However further cooling of solution B to –25 °C, to imitate freezer conditions (**Graph 2.3**), produced a 14% drop in molarity. It was hypothesized that the solution became supersaturated at the lower temperature and that some of the LiDBB crashed out of solution. Solution A, prepared at 20 °C, held its molarity when cooled to 0 °C and increased in concentration by 7% after 5 hours at –25 °C (**Graph**

2.4). Because this increase was a result of decreasing temperature, it appears that LiDBB solutions are more resistant to decomposition at –25 °C than at 0 °C. This suggested that a viable stock solution could be stored in the freezer. Before attempting this, it was decided to determine what decomposition products were present and how they were formed.

Graph 2.3. Solution B from 0 °C to –25 °C   **Graph 2.4**. Solution A from 0 °C to –25 °C
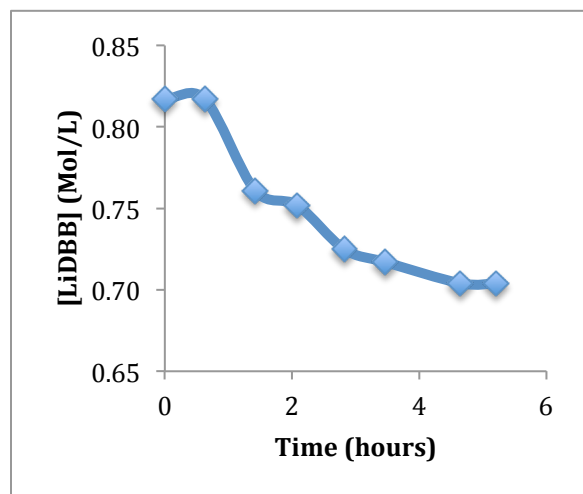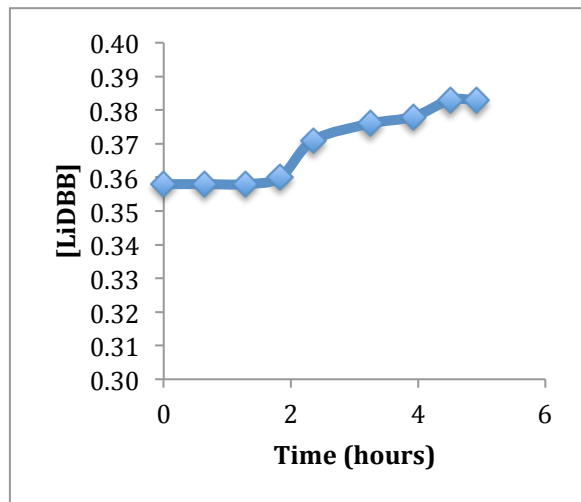
Trapping studies

The success of preparing LiDBB at 20 °C showed that solutions can be made more quickly than reported by Freeman; however, this 2-hour preparation also led to an unknown amount of decomposition.[13] The rates and pathways of this decomposition could not be found in the literature. A more complete understanding of how THF, lithium and DBB react under long-term radical conditions is necessary for developing a practical LiDBB stock solution. Since THF is known to react with alkyllithiums, initial studies focused on the solvent itself.

Scheme 2.3. Known THF ring-opening reactions with organolithium anions and radicals
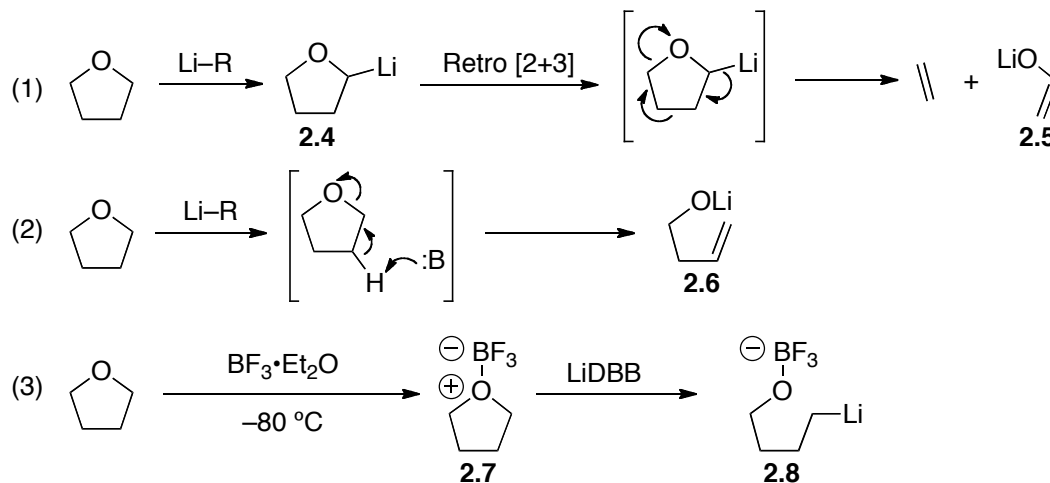
The best-known example of THF degradation is equation 1 (**Scheme 2.3**). Deprotonation of THF gives lithiate **2.4**, which then undergoes a retro [2+3] elimination to give ethylene and lithium enolate **2.5**.[16] Equation 2 shows elimination of the ether, leading to alkoxide **2.6**.[17] Lastly, equation 3 shows THF undergoing ring opening upon activation with BF_3.[18] LiDBB adds an electron into the C-O σ^* orbital of **2.7**, resulting in C–O bond cleavage. A second single-electron transfer forms alkyllithium **2.8**. A series of trapping studies were devised based on these known ring-opening reactions.

Solution A was prepared and kept at 20 °C for two weeks (**Table 2.3**) and this solution was used to analyze LiDBB decomposition products. Attempts to trap these products with benzaldehyde or benzyl bromide led to nothing identifiable by ^{1}H NMR or GCMS. Trapping with TBSCl led to some identifiable compounds; however, analysis was complicated by overlapping GCMS peaks. After screening several silyl chlorides, TBDPSCl was selected as the trapping reagent as all the compounds could be separated by GCMS. The identified compounds are shown in **Scheme 2.4.** Product **2.9** was derived from enolate **2.5,** produced from the retro [2+3] reaction (**Scheme 2.3**, equation 2). Butanol derivative

2.10 was suspected to come from a similar mechanism to equation 3 (**Scheme 2.3**), with lithium acting as the Lewis acid in place of BF$_3$. The source of compounds **2.11** and **2.12** was less apparent and required further examination (**Scheme 2.4**). No other compounds were detected or identified using silyl trapping or ^{1}H NMR analysis of quenched LiDBB samples.

Scheme 2.4. LiDBB decomposition products identified by GCMS
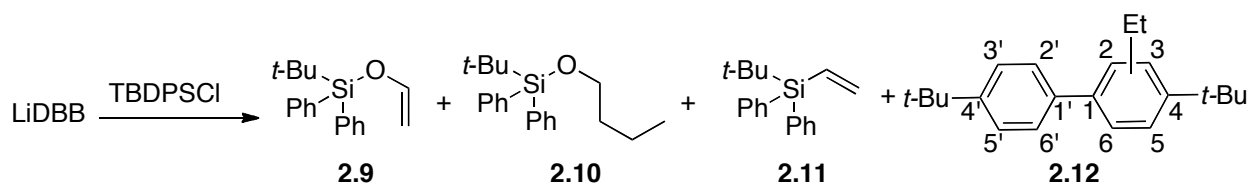
Compounds **2.9–2.12** were identified by high resolution GCMS and authentic standards prepared to confirm their identity (**Scheme 2.5**). Synthesis and assignment of **2.12** can be found in **Schemes 2.6**

Scheme 2.5. Synthesis of authentic samples of **2.9–2.11**
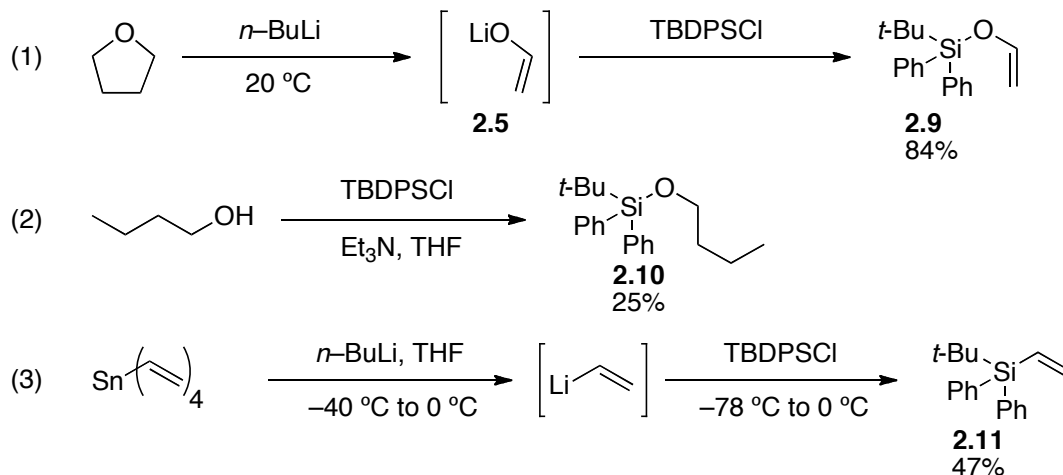
To confirm the identity of compounds **2.9–2.11**, authentic samples were prepared. Enol ether **2.9** was readily made by decomposing THF with *n*–BuLi and trapping enolate **2.5** with TBDPSCl (**Scheme 2.5**, eq 1). Silyl protection of *n*–butanol gave product **2.10**, albeit in low yield (eq 2). Tetravinyltin was transmetalated with *n*–BuLi to give vinyl

lithium, followed by addition of TBDPSCl to this solution to form vinyl silane **2.11** (eq 3). Substrates **2.9–2.11** run on GCMS matched the retention times and splitting pattern observed for the silylated products in **Scheme 2.4**.

The surprising identification of compound **2.11** suggested the presence of vinyl lithium in solution (**Scheme 2.4**). Ethylene has been previously shown to react with lithium metal and biphenyl in dimethoxymethane.[19] This produces 1,2-dilithioethane, which eliminates to yield vinyl lithium and lithium hydride. If the same mechanism was at work here, an aldehyde should react with both products. To test this, a nominal 0.4 M LiDBB solution, made at 20 °C was allowed to stir for 2 days and reacted with aldehyde **2.13**. Small amounts of vinyl adduct **2.14** and alcohol **2.15** were observed, confirming the presence of both vinyl lithium and lithium hydride (**Table 2.4**). Allowing the LiDBB solution to decompose for an additional 12 days and repeating the experiment showed an increase in the amount of both the vinyl and alcohol products **2.14** and **2.15**. To prove ethylene was the source of vinyl lithium, a second LiDBB solution was prepared from 0.4 M DBB under an atmosphere of ethylene gas. After 2 days, the solution was added to aldehyde **2.13**, revealing a dramatic increase in the amount of both products. Vinyl alcohol **2.14** was isolated from the reaction mixture in 29% conversion, with respect to the amount of aldehyde used. These tests provide evidence that ethylene, from the retro [2+3] of THF, eventually becomes vinyl lithium upon exposure to a LiDBB solution.

Table 2.4. Trapping of vinyl lithium with *m*- toluicaldehyde
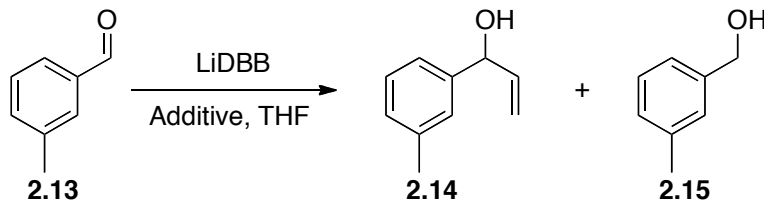
Entry	Age of LiDBB solution	Additive	Conversion to **2.14**[a]	Conversion to **2.15**[a]
1	2 days	None	1%[b]	7%[b]
2	14 days	None	4%[b]	8%[b]
3	2 days	Ethylene gas	29%[c]	22%[b]

Nominal 0.4 M LiDBB solutions used. [a] Conversion was based on the 102 mg of aldehyde added. [b] Yields by ^{1}H NMR with DBB from added LiDBB used an internal standard. [c] Isolated yield

With an understanding of how three out of four decomposition products were formed, attention was turned to the ethyl derivative of DBB (**2.12**, **Scheme 2.6**). To confirm the identity and substitution of the suspected **2.12**, an authentic sample was prepared. The *tert*-butyl groups on DBB should block alkylation at the 3, 5, 3', and 5' positions (**Scheme 2.4**), leaving the 2-ethyl derivative as the most likely identity for compound **2.12**. Synthesis of **2.18** started with Suzuki cross coupling of aryl iodide **2.16** and phenyl boronic acid to yield biphenyl derivative **2.17** (**Scheme 2.6**). Friedel–Crafts alkylation of **2.17** led to a complex reaction mixture. Prep plate separation allowed for a 2% isolated yield of **2.18.** Comparison of compounds **2.18** and **2.12** showed matching retention times and fragmentation patterns by GCMS (**Scheme 2.4**) and confirmed **2.18** to be the last identified decomposition product.

Scheme 2.6. Synthesis of an authentic sample of DBB derivative.
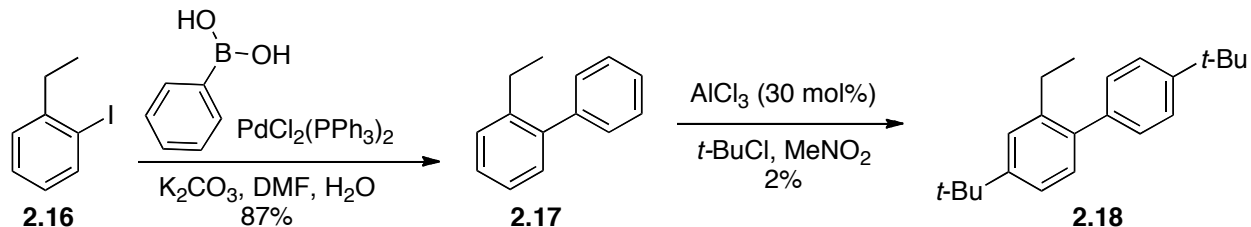
The decomposition of THF leads to two, two-carbon products that could be the source of the ethyl group incorporated into compound **2.18** (**Scheme 2.6**). To test ethylene as the source, two solutions of nominal 0.4 M LiDBB were made at 0 °C, one under argon and the other under ethylene. Three days later, GCMS analysis detected none of compound **2.18**. To determine whether temperature was the missing factor, the two reactions were redone at 20 °C. After three days, again there was no **2.18** observed by GCMS. In a final attempt to find conditions to form **2.18,** the original discovery conditions were reexamined (**Scheme 2.4**). Two solutions of nominal 0.4 M LiDBB were prepared, one at 0 °C and the other at 20 °C (**Table 2.5**). Entry 1 showed no **2.18** after 14 days; however, **2.18** was found in the solution kept at 20 °C (Entry 2). Analysis of entry 2 by ^{1}H NMR showed a 25:1 ratio of DBB:**2.18**, and prolonged stirring increased this ratio to 5:1 (Entry 3). It became clear that decomposition of THF over an extended period of time in an LiDBB solution at 20 °C was responsible for forming **2.18**.

Table 2.5. Conditions for the generation of ethylated DBB

Entry	Age of LiDBB	Temp. (°C)	Ratio DBB:**2.18**
1	14 days	0	100:0[a,b]
2	14 days	20	25:1[b]
3	48 days	20	5:1[b]

[a]by GCMS. [b]by NMR

Given the results from extensively decomposed LiDBB solutions, the following mechanism has been proposed for the formation of **2.18** (**Scheme 2.7**). The pK$_a$ of DBB (**2.19)** is expected to be similar to that of benzene (pK$_a$ = 43); thus deprotonation by the more basic vinyl lithium (pK$_a$ = 44) would provide lithiate **2.20**.[20] This intermediate can react with ethylene as reported by others,[21] and the newly formed alkyllithium **2.21** can then deprotonate THF to give the observed product **2.18**. This propagates the decomposition of THF and the formation of **2.18**, which explains the increase in the amount of product formed over prolonged periods of time.

Scheme 2.7. Possible mechanism for forming compound **2.18**
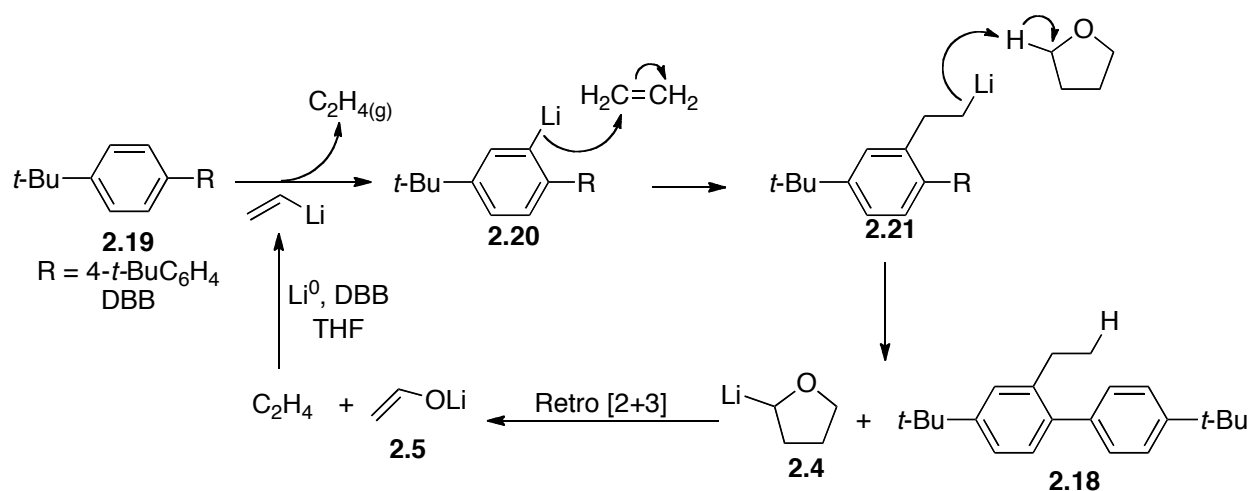
One final test was conducted to confirm that ethylene was indeed the source of the ethyl group added to DBB. Preparing LiDBB in 2-methyltetrahydrofuran **2.22** was expected to show this (**Scheme 2.8**). Deprotonation of **2.22** should give preferential lithiation at the less hindered side, producing alkyllithium **2.23** (eq 1). The retro [2+3] reaction generates propene, which would lead to a propyl derivative of DBB (**2.24**).[22] A small amount of lithiation at the more sterically hindered position of **2.22** is expected to form **2.25**, yielding the previously seen **2.18** (eq 2). A nominal 0.4 M LiDBB solution made

in 2-methyltetrahydrofuran was allowed to degrade at 20 °C for 34 days. Analysis by GCMS

showed a 0.7:0.2:99.1 ratio of **2.24**:**2.18**:**2.19**. The larger quantities of **2.24** showed the

alkene was the source of alkylation leading to products **2.18** and **2.24**.

Scheme 2.8. Decomposition products of LiDBB in 2-methyltetrahydrofuran
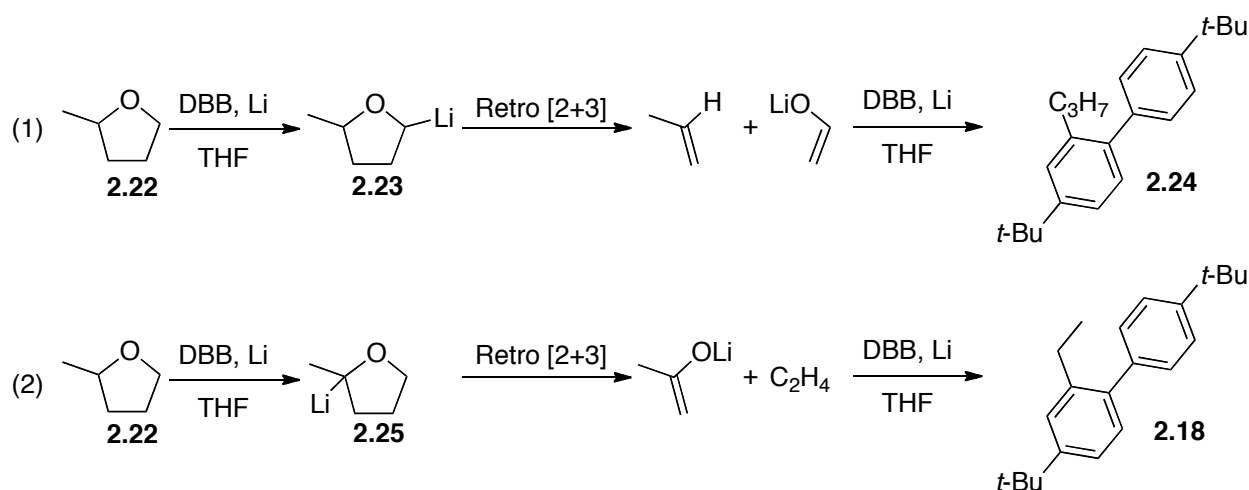
Since product **2.18** alkylated at the 2-position, compound **2.29** was also expected to
alkylate at the same location. GCMS analysis showed a compound with the same m/z as
2.24

Rate studies

With the decomposition products in **Scheme 2.4** identified and their origins

explained, attention was turned to the rates of decomposition of LiDBB solutions.

Determining these rates would allow for practical use of stock solutions. Given that

several pathways were causing reactions with both THF and DBB, it was decided to

simplify the rate study. After LiDBB is generated, any additional oxidation of lithium metal

would reveal the aggregate rates of all decomposition pathways. Solutions A and B (**Table

2.3**) were subjected to atomic absorption spectroscopy to track the concentration of Li$^+$ in

aliquots taken from an LiDBB solution.

Graph 2.5. Concentrations of Li⁺ from LiDBB decomposition
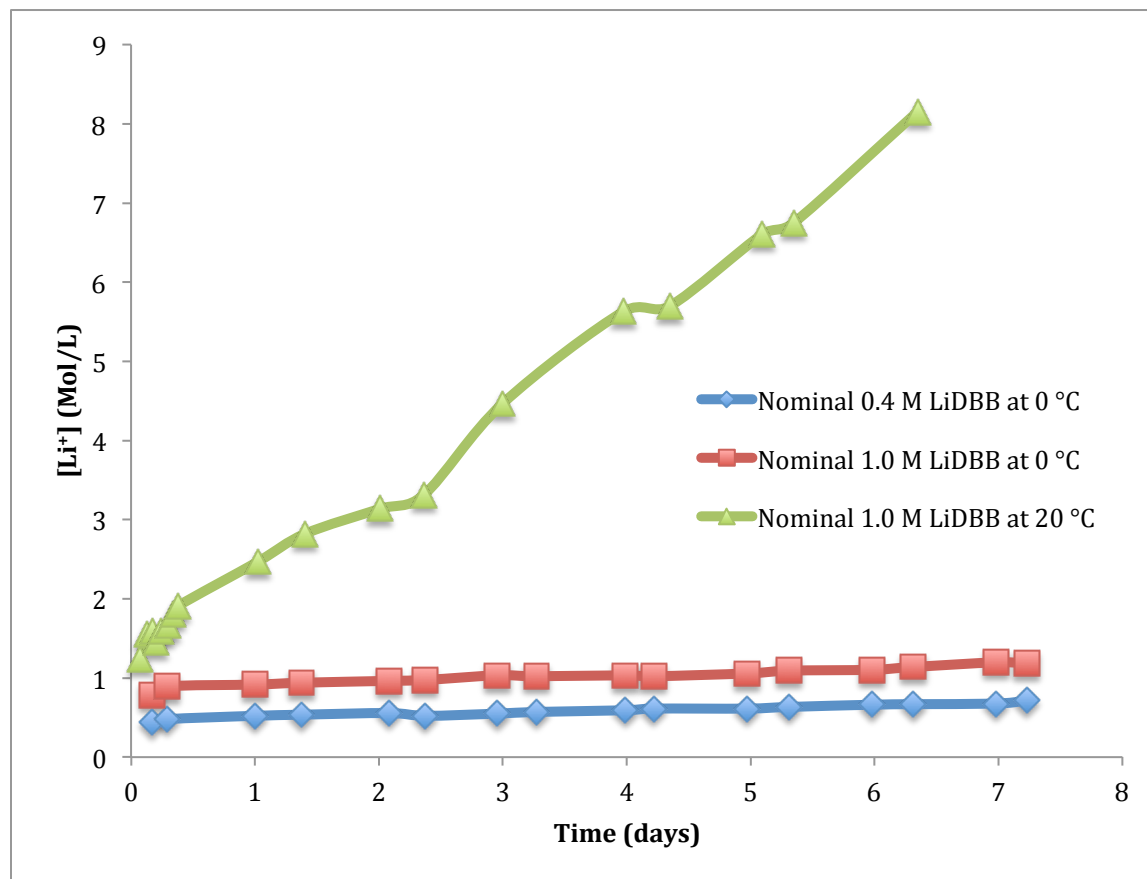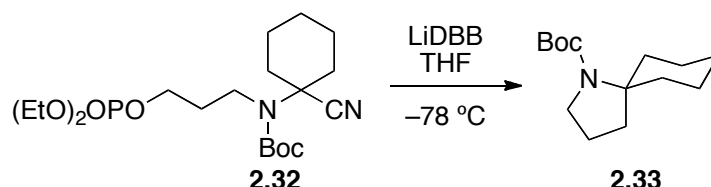
Examining nominal 0.4 M LiDBB at 0 °C showed a slow, but noticeable decomposition of 0.030 equivalents of lithium metal oxidized per day (**Graph 2.5**). Nominal 1.0 M LiDBB at 0 °C showed a 37% faster rate of decomposition, consuming 0.041 equivalents of lithium per day. Over one equivalent of lithium was consumed per day for a nominal 1.0 M LiDBB solution at 20 °C, making it impractical for use. If 0.4 M LiDBB was used as a stock solution, 0.21 equivalents of lithium metal would go on to cause decomposition after one week. Attempts to determine the rate of lithium oxidation for a −25 °C solution of nominal 0.4 M LiDBB were unsuccessful.[23]

Efforts to directly quantify the amount of compounds **2.9–2.11** and determine their rates of formation by quantitative GCMS analysis were inconclusive (**Scheme 2.4**).

43

However larger quantities of **2.9** and **2.11** (in approximately a 1:1 ratio) as compared to **2.10** pointed to THF predominantly decomposing via a retro [2+3] reaction (**Scheme 2.3**, eq 1) over direct ring opening (eq 3). In light of this, a more direct approach to testing decomposition of LiDBB solutions was undertaken.

Since the rate of decomposition of LiDBB was shown to be slow at 0 °C, a solution stored at –25 °C should be even more stable. To get a practical indication of the storage viability, spirocyclization reactions with phosphate **2.32** were run with a stored solution of LiDBB (**Table 2.6**). Solution A was prepared in a Schlenk flask and kept in at –25 °C freezer (**Table 2.3**). Weekly titrations revealed no change of molarity over eight weeks. The yield of spirocycle **2.33** remained constant over 16 weeks, showing a stock solution stored at –25 °C is viable for at least this duration of time.

Table 2.6. Reductive cyclizations with stored LiDBB

Entry	LiDBB Age	Yield (%)
1	5 hours	69
2	1 week	69
3	3 weeks	70[a]
4	8 weeks	66[a]
5	16 weeks	69

[a] A lower initial yield led to the discovery that phosphate **2.32** had decomposed 11% through loss of its Boc group. The yield shown is from an isolated yield and ^{1}H NMR integrations to back calculate the true amount of phosphate **2.32** used

Conclusions

A study of LiDBB revealed many unknown details about its formation and up to now, unknown decomposition. A thioanisole-based titration method was developed to test the molarity of LiDBB solutions. Solutions of nominal 0.4 M LiDBB were ready for use in 4 hours at 0 °C or 2 hours at 20 °C, while nominal 1.0 M LiDBB solutions were ready in 8

hours at 0 °C or 2 hours at 20 °C. Trapping studies confirmed two types of THF ring-opening pathways during decomposition, with generated ethylene causing further decomposition reactions. The rate of lithium oxidation was tracked by atomic absorption spectroscopy and found to be 0.030 equivalents of lithium per day for a nominal 0.4 M LiDBB solution at 0 °C. Similar tests with nominal 1.0 M LiDBB solutions at 0 °C and 20 °C found 0.041 and 1.02 equivalents of lithium per day were consumed, respectively. Lithiation of THF, followed by retro [2+3] was the major decomposition pathway for LiDBB solutions. Lastly, a stock solution kept at –25 °C gave consistent yields over 16 weeks, increasing the synthetic utility of LiDBB-based methodology.

General Experimental and Laboratory Conditions

All glassware was flame- or oven-dried and cooled under argon unless otherwise stated. All reactions and solutions were conducted under argon unless otherwise stated. All reagents were used as received unless otherwise stated. Tetrahydrofuran (THF), dimethylformamide (DMF) and dichloromethane (DCM) were degassed and dried by filtration through activated alumina under vacuum according to the procedure by Grubbs.[24] *n*-BuLi was titrated against *N*-benzylbenzamide according to the procedure by Duhamel and Plaquevent.[25] Thioanisole, and triethylamine (Et$_3$N) were distilled from CaH$_2$. *Tert*-Butyl(chloro)diphenylsilane (TBDPSCl) and nitromethane (NO$_2$Me) were distilled from CaSO$_4$. All reactions involving LiDBB were conducted with glass stirbars. Thin layer chromatography (TLC) was done on Watman (250 μm) 6 Å glass-backed silica gel plates and visualized using potassium permanganate or Dragondorf. Flash column chromatography (FCC) was performed according to the method by Still, Kahn, and Mitra using Fisher reagent silica gel 60 (230-400 mesh).[26]

Instrumentation

All data collected at ambient temperature unless noted. ^{1}H NMR spectra were taken at 500 MHz, calibrated using residual NMR solvent (CDCl$_3$ at 7.26 ppm), and interpreted on the δ scale. ^{13}C NMR spectra were taken at 125 MHz, calibrated using the NMR solvent (CDCl$_3$ at 77.16 ppm), and interpreted on the δ scale with the following abbreviations: s= singlet, d= doublet, t = triplet, q= quartet, dt= doublet of triplets, dd= doublet of doublets, m= multiplet, app= apparent, br= broad. IR taken by thin film. High resolution GCMS was run on an Agilent 7890A using a DB-5ms column (30 m by 0.25 mm, 0.25 μm coating) and

masses detected with a Waters GCT Premier TOF mass spectrometer using chemical ionization (ammonia) as the detection method. Additional GCMS data were collected on a Thermoquest Trace GC 2000 series using a DB-5ms column (30 m by 0.25 mm, 0.25 μm coating) and masses detected with a ThermoFinnegan TraceMS+ mass spectrometer using electron as the detection method. Samples were prepared in DCM or ethyl acetate (0.1–1 mg /mL loading), mixed with a vortex mixer for 30 seconds and submitted for analysis.

LiDBB Formation in THF

LiDBB was prepared fresh before each experiment, example procedure:

LiDBB was prepared by adding 4,4'-di-*tert*-butylbiphenyl (DBB, 1.50 g, 5.64 mmol, 1 equiv), to a 50 mL flask, followed by evacuating and flame-drying. Once the DBB was melted, the flask was backfilled with argon and allowed to cool. An ice bath was applied and lithium wire (0.39 g, 56.4 mmol, 10 equiv) was clipped in under a stream of argon. THF (14 mL) was added and the solution turned green, darkening over for 5 hours at 0 °C. This resulted in a nominal 0.4 M LiDBB solution.

Nominal 1.0 M LiDBB was prepared by the above method by increasing the amount of DBB (3.85 g, 14.5 mmol, 1 equiv) and lithium (1.00 g, 144.5 mmol, 10 equiv) added.

Nominal 2.0 M LiDBB was prepared by the above method by increasing the amount of DBB (7.40 g, 27.8 mmol, 1 equiv) and lithium (1.93 g, 277.8 mmol, 10 equiv) added.

Nominal 3.1 M LiDBB was prepared by the above method by increasing the amount of DBB (11.6 g, 43.5 mmol, 1 equiv) and lithium (3.02 g, 435.4 mmol, 10 equiv) added.

Titrations of Nominal 0.4 M LiDBB

To a 50 mL volumetric flask, thioanisole (1.2 mL, 10.2 mmol) and THF (degassed by freeze-pump-thaw) were added to form a 0.1 M solution. A dry 10 mL flask was evacuated and backfilled with argon 3 times, cooled to 0 °C and 1 mL of the 0.2 M thioanisole solution added. LiDBB was then added dropwise until a persistent dark-green color was observed. The titrated solution was removed and the procedure repeated three times. The first trial was excluded and the average volume added from titrations 2–4 was used to calculate the molarity of the LiDBB.

Titrations of Nominal 1.0, 2.0, 3.1 M LiDBB

Titrations of nominal 1.0, 2.0 and 3.1 M LiDBB followed the same procedure for nominal 0.4 M LiDBB except the molarity of the thioanisole solution was increased to 0.40 M.

Trapping of LiDBB Decomposition Products

A nominal 0.4 M LiDBB solution was prepared at 20 °C and allowed to stir for 14 days. To a dram vial, TBDPSCl (0.2 mL, 0.77 mmol) and LiDBB (0.2 mL) were added and stirred for 2 days. Addition of 1.00 mL of wet DCM and removal of 4 μL of this solution for GC-HRMS analysis led to the identification of **2.9–2.11**, **2.18.**

Trapping Study with *m*-Tolualdehyde.

A nominal 0.4 M LiDBB solution was prepared at 20 °C and allowed to stir for 2 days. *m*-tolualdehyde (0.1 mL, 0.85 mmol) and 0.5 mL of the LiDBB solution were added to a 5 mL flask and allowed to stir for 18 hours. After quenching with $NH_4Cl_{(aq)}$ (2 mL), the reaction

was diluted with DCM (2 mL) and the aqueous layer extracted 3 x 2 mL DCM. The combined organic layers were dried over MgSO$_4$, giving a yellow oil. Using the added DBB as an internal standard, 1-(m-tolyl)prop-2-en-1-ol (**2.14**), and m-tolylmethanol (**2.15**) were quantified from the reaction mixture by ^{1}H NMR. The analytical data matched those previously reported.[27,28] This procedure was repeated with LiDBB stirred for 14 days at 20 °C and with LiDBB prepared under an ethylene atmosphere (2 days at 20 °C). In the latter case, flash column chromatography (2:1 hexanes/Et$_2$O) gave 1-(m-tolyl)prop-2-en-1-ol as a clear oil in 29% conversion (36 mg).

Propyl DBB

LiDBB was prepared by adding 4,4'-di-*tert*-butylbiphenyl (DBB, 1.0 g, 3.75 mmol, 1 equiv), to a 25 mL flask, followed by evacuating and flame-drying. Once the DBB was melted, the flask was backfilled with argon and allowed to cool. Lithium wire (0.26 g, 37.5 mmol, 10 equiv) was clipped in under a stream of argon and 2-methyltetrahydrofuran (9.3 mL) was added. After stirring for 34 days, 1 µL of the solution was analyzed by GCMS. This revealed a ratio of 0.7:0.2:99.1 of **2.24:2.18:2.19**. It was not determined if the substitution was *n*-propyl, or *iso*-propyl.

Atomic Absorption Spectroscopy

Three solutions of LiDBB were prepared: Nominal 0.4 M LiDBB prepared at 0 °C (2.6 g DBB, 0.67 g Li metal, 24 mL THF), nominal 0.4 M LiDBB prepared at 20 °C (2.6 g DBB, 0.67 g Li metal, 24 mL THF), and nominal 1.0 M LiDBB prepared at 0 °C (6.6 g DBB, 1.72 g Li metal, 24 mL THF). Each of these solutions was maintained at their respective temperatures and

a 0.5 mL aliquot removed twice daily. After quenching with 0.05 M $H_2SO_{4(aq)}$ (10 mL), the aliquot was diluted with DCM (10 mL) and the aqueous layer added to a 100 mL volumetric flask. The organic layer was extracted 5 x 10 mL 0.05 M $H_2SO_{4(aq)}$ and the aqueous layers added to the volumetric flask. This was repeated for each aliquot in a separate 100 mL volumetric flask.

Using these volumetric solutions, between 2 and 5 mL was removed and diluted in a 50 mL volumetric flask such that the absorbance from the spectrometer was between 0.000 and 0.120. A calibration curve (see below) was made by diluting a stock 1000 ppm Li^+ solution to 1.00, 1.50, 2.00, 2.50, 3.00, 3.50 ppm using volumetric techniques. This curve was used to calculate the amount of Li^+ for each sample.
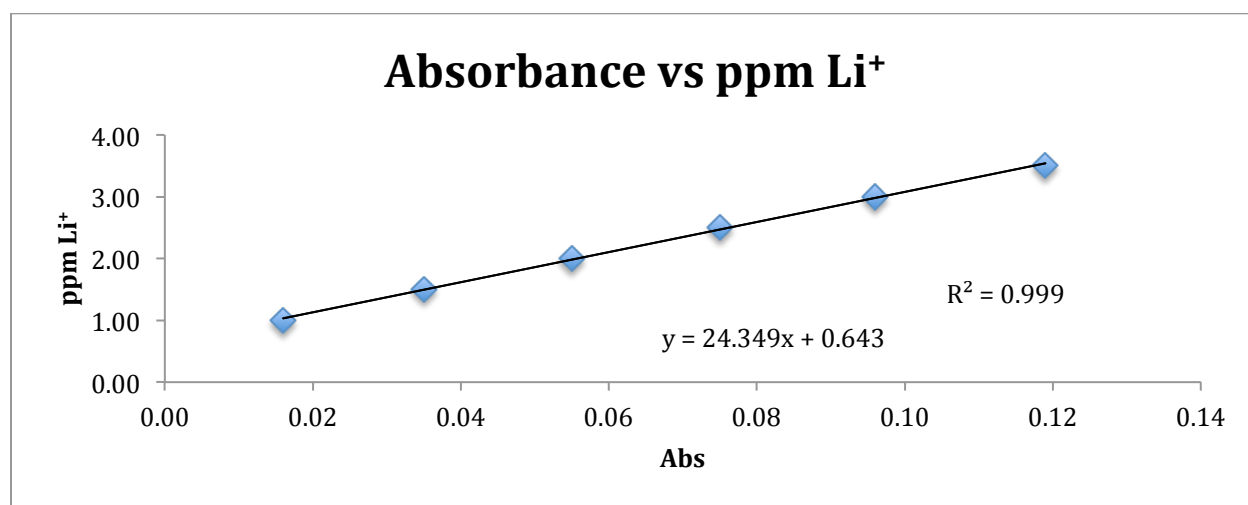
Synthesis of Authentic Standards
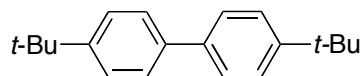
4,4'-di-*tert*-butylbiphenyl (**2.19**) Prepared from biphenyl as described by Tietze *et. al.*[29] The analytical data matched those previously reported.
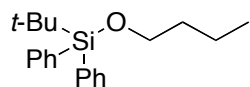
Butoxy(tert-butyl)diphenylsilane (**2.10**) To a solution of *n*-butanol (0.20 mL, 2.2 mmol, 1 equiv) in THF (2.2 mL), Et$_3$N (0.45 mL, 3.3 mmol, 1.5 equiv) and TBDPSCl (0.63 mL, 2.4 mmol, 1.1 equiv) were added. After stirring for 18 hours, the reaction was quenched with a 10% NaHCO$_3$ solution (4 mL), and diluted with ethyl acetate (4 mL). The organic layer was extracted and aqueous layer washed with ethyl acetate (3 x 2 mL) and the combined organic layers were dried with MgSO$_4$ and concentrated *in vacuo*, giving a yellow oil. Flash column chromatography (8:1 Hexanes/DCM) gave butoxy(*tert*-butyl)diphenylsilane in 25% yield (259 mg) as a clear oil. The analytical data matched those previously reported.[30]
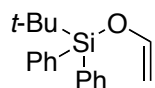
***Tert*-butyldiphenyl(vinyloxy)silane** (**2.9**) Prepared from THF as described by Cohen and Stokes.[31] The analytical data matched those previously reported.[32]
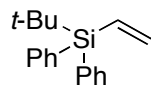
***Tert*-butyldiphenyl(vinyl)silane silane** (**2.11**) Prepared from tetravinyltin as described by Gerstenberger and Konopelski.[33] The analytical data matched those previously reported.

51
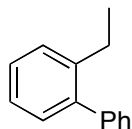
2-ethyl-1,1'-biphenyl (**2.17**) A mixture of DMF (2.8 mL) and H_2O (0.56 mL) was degassed by freeze-pump-thaw, followed by addition of phenyl boronic acid (85 mg, 0.70 mmol, 1 equiv), K_2CO_3 (193 mg, 1.39 mmol, 2 equiv), 1-ethyl-2-iodobenzene (0.1 mL, 0.70 mmol, 1 equiv), and $PdCl_2(Ph_3)_2$ (9.8 mg, 0.014 mmol, 0.02 equiv). The reaction was heated to 60 °C for 18 hours. The solution was diluted with H_2O (5 mL) and pentane (5 mL) and the organic layer extracted.   The aqueous layer was washed with pentane (3 x 3 mL) and the combined organic layers were dried with $MgSO_4$ and concentrated *in vacuo*, giving a yellow oil. Flash column chromatography (100% hexanes) gave 2-ethyl-1,1'-biphenyl in 87% yield (110 mg) as a clear oil. The analytical data matched those previously reported.[34]
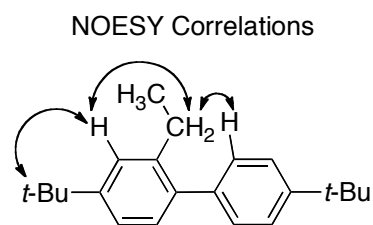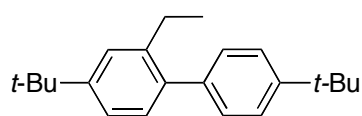
4,4'-di-tert-butyl-2-ethyl-1,1'-biphenyl (**2.18**) To a solution of 2-ethyl-1,1'-biphenyl (0.10 mg, 2.2 mmol, 1 equiv) in $MeNO_2$ (0.6 mL), *tert*-butyl chloride (0.133 mL, 1.21 mmol, 2.2 equiv), followed by $AlCl_3$ (22 mg, 0.16 mmol, 0.3 equiv) were added. After gas evolution stopped (c.a. 5 min), the reaction was poured over crushed ice and diluted with hexanes (3 mL). The hexane layer was extracted and aqueous/NO_2Me layers washed with hexanes (3 x 2 mL) and the combined organic layers were dried with $MgSO_4$ and concentrated *in vacuo*, giving a yellow oil. Preparatory plate chromatography (100% Hexanes) gave 4,4'-di-

tert-butyl-2-ethyl-1,1'-biphenyl in 2% yield (3 mg) as a white solid. Relevant NOSEY correlations shown.

^{1}H NMR (CD$_2$Cl$_2$, 500 MHz) δ 7.49–7.40 (m, 2H), 7.34–7.31 (m, 1H), 7.27–7.22 (m, 3H), 7.13–7.09 (m, 1H), 2.61 (q, *J* = 7.5 Hz, 2H), 1.36 (s, 9H), 1.35 (s, 9H), 1.11 (t, *J* = 7.5 Hz, 3H); ^{13}C NMR (CDCl$_3$, 125 MHz) δ 150.1, 149.4, 139.0; IR (thin film) 3025, 2961, 2887, 1608, 1491 cm^{-1}; HRMS (ESI) calcd for C$_{22}$H$_{30}$NH$_4$ [M+NH$_4$$^+$] 312.2691, found 312.2686

Synthesis of Spirocycle and Precursor
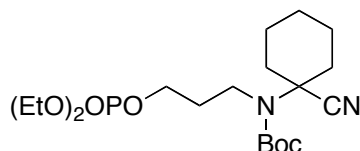
Tert-butyl (1-cyanocyclohexyl)(3-((diethoxyphosphoryl)oxy)propyl)carbamate (**2.32**) Prepared from *tert*-butyl (1-cyanocyclohexyl)(3-hydroxypropyl)carbamate as described by Perry, Hill, and Rychnovsky.[35] The analytical data matched those previously reported.
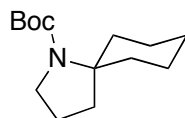
Tert-butyl 1-azaspiro[4.5]decane-1-carboxylate (**2.33**) Prepared from **2.32** as described by Perry, Hill, and Rychnovsky.[35] The analytical data matched those previously reported.

[1] A Scifinder search for reviews on "organolithium" returns 386 review articles. Data retrieved on 12/2/15.

[2] Chinchilla, R.; Nájera, C.; Yus, M. *Tetrahedron* **2005**, *61*, 3139–3176.

[3] Wu, G.; Huang, *Chem. Rev.* **2006**, *106*, 2596–2616.

[4] Wakefield, B. J. *Organolithium Methods;* Academic Press: London, 198; pp 21.

[5] Clayden, J.; *Organolithiums: Selectivity for Synthesis*; Tetrahedron Organic Chemistry Series Vol 23; Elsevier Science: Oxford, UK, 2002; pp 149.

[6] (a) Kennedy, N.; Lu, G.; Liu, P, Cohen, T. *J. Org. Chem.* **2015**, *80*, 8571–8582. (b) Clayden, J.; *Organolithiums: Selectivity for Synthesis*; Tetrahedron Organic Chemistry Series Vol 23; Elsevier Science: Oxford, UK, 2002; pp 149–166. (c) Yus, M. Arene-catalyzed lithiation. In *The Chemistry of Organolithium Compounds*; Rappoport, Z.; Marek, I. Eds.; Wiley: England, 2004; pp 649–742. (d) Azzena, U.; Pisano, L. Reductive Lithiation and Multilithiated Compounds in Synthesis. In *Lithium Compounds in Organic Syntheis* [Online]; Luisi, R.; Capriati, V. Eds.; Wiley, 2014, pp 351–371. URL http://onlinelibrary.wiley.com/doi/ 10.1002/9783527667512.ch12/pdf (Accessed Dec. 12, 2015).

[7] Screttas, C. *J. Chem. Soc., Chem. Commun.* **1972**, 752–753.

[8] Sodium and potassium napthalide were known before Lithium Napthalide: Holy, N. *Chem. Rev*. **1974**, *74*, 243–273.

[9] Clayden, J. *Organolithiums: Selectivity for Synthesis*; Tetrahedron Organic Chemistry Series Vol 23; Elsevier Science: Oxford, UK, 2002; pp 151.

[10] Cohen, T.; Matz, J. *Synth. Commun.* **1980**, *10*, 311–117.

[11] Cohen, T.; Sherbine, J.; Hutchins, R.; Lin, M.-T. *Organometallic Syntheses* **1986**, *3*, 361–371.

[12] Freeman, P.; Hutchinson, L. *Tetrahedron Lett.* **1976**, *22*, 1849–1852.

[13] Freeman, P.; Hutchinson, L. *J. Org. Chem.* **1983**, 48, 4705–4713.

[14] Cohen, T.; Chen, F.; Kulinski, T.; Florio, S.; Capriati, V. *Tetrahedron Lett.* **1995**, *36*, 4459–4462.

[15] Freeman, P.; Hutchinson, L. *J. Org. Chem.* **1980**, *45*, 1924–1930.

[16] Bates, R.; Kroposki, L.; Potter, D. *J. Org. Chem.* **1972**, *37*, 560–562.

[17] Clayden, J.; *Organolithiums: Selectivity for Synthesis*; Tetrahedron Organic Chemistry Series Vol 23; Elsevier Science: Oxford, UK, 2002; pp 6.

[18] Mudryk, B.; Cohen, T. *J. Am. Chem. Soc.* **1991**, *113*, 1866–1867.

[19] Rautenstrauch, V. Angew. Chem. Internat. Ed. **1975**, *14*, 259–260.

[20] Bruice, P. *Organic Chemistry*, 5th ed.; Prentice Hall: New Jersey, 2007; pp A-2.

[21] Krief, A.; Kenda, B.; Barbeaux, P.; Guittet, E. *Tetrahedron* **1994**, *50*, 7177–7192.

[22] It was not determined if the added group was *n*-propyl or *iso*-propyl

[23] The data gave a parabolic curve implying that solubility of lithium salts may have been an issue.

[24] Pangborn, A.; Giardello, M.; Grubbs, R.; Rosen, R.; Timmers, F. *Organometallics* **1996**, *15*, 1518–1520.

[25] Duhamel, L.; Plaquevent, J. *J. Organomet. Chem.* **1993**, *338*, 1–3.

[26] Still, W.; Khan, M.; Mitra, A. *J. Org. Chem.* **1978**, *43*, 2923–2925.

[27] Mojtahedi, M.; Akbarzadeh, E.; Sharifi, R.; Abaee, M. *Org. Lett.* **2007**, *9*, 2791–2793

[28] Brandt, D.; Bellosta, V.; Cossy, J. *Org. Lett.* **2012**, *14*, 5594–5597

[29] Tietze, L.; Hölsken, S.; Adrio, J.; Kinzel, T.; Wegner, C. *Synthesis*, **2004**, *13*, 2236–2239

[30] Cunico, R.; Lewis. B. *J. Org. Chem.* **1980**, *45*, 4797–4798

[31] Cohen, T.; Stokes, S. *Tetrahedron Lett.* **1993***, 34*, 8023–8024

[32] Cuadrado, P.; González-Nogal, A. *Tetrahedron Lett.* **2010**, *41*, 1111-1114.

[33] Gerstenberger, B.; Konopelski, J. **2005**, *70*, 1467–1470

[34] Guan, B.-T.; Xiang, S.-K.; Wang, B.-Q.; Sun, Z.-P.; Wang, Y.; Zhao, K.-Q.; Shi, Z.-J. *J. Am Chem Soc.* **2008**, *130*, 3268–3269

[35] Perry, M.; Hill, R.; Rychnovsky, S. *Org. Lett.* **2013**, *15*, 2226–2229

Chapter 3

Accessing Substituted Azaspirocycles Via Double Alkylation and Reductive Lithiation Methodology

Abstract

The expansion of methodology for accessing azaspirocyclic frameworks is described herein. Substituted spiropyrrolidines and spiropiperidines are crafted via double alkylation of α-aminonitriles, followed by stereoselective reductive lithiation and cyclization. Access to a variety of diastereomerically enriched and synthetically useful spirocycles is detailed below.

Introduction

The prevalence of spirocycles in natural products and pharmaceuticals drugs has led to much research on their synthesis and use.[1,2] The higher potency of spirocycles on biological systems, as compared to acyclic compounds, is due to their challenging molecular architecture.[3] Spirocyclic structures limit the inherent entropy of the molecule, leading to higher binding affinities with a targeted protein.[3,4] In addition, the sp^3 hybridized rings allow for a greater diversity of substrates than with aromatic-based compounds.[3]   Given the need to access spirocycles with a variety of substitution patterns, many methods have been developed for their synthesis.[5,6] It is expected that further research will increase the scope of this underutilized molecular scaffold.

Nitrogen substituted spirocycles display a range of useful pharmacological properties. Halichlorine (**3.1**, **Scheme 3.1**), isolated from the marine sponge *Halichondria*

okadai, blocks production of vascular cell adhesion molecule-1 (VCAM-1).[7] Blocking VCAM-1 has the potential for treating a variety of diseases including coronary artery disease, angina, and atherosclerosis.[8] Spirocycle **3.2** is a very potent pre-clinical drug targeting platelet aggregation as an antithrombotic drug.[9] Structure **3.3** was found while searching for kinase inhibitors as anti-cancer agents.[10] Its ability to target 11 of 24 kinases tested makes it a valuable lead-compound for further studies in selective kinase inhibition. As drug development continues, the inclusion of spirocyclic frameworks should prove to be a valuable feature for increased pharmaceutical potency.

Scheme 3.1. Azaspirocycles with pharmaceutical properties

3.1
halichlorine
Inhibits VCAM-1
$IC_{50} = 17\ \mu M$

3.2
Antithrombotic properties
Antagonist of $P2Y_1$
$IC_{50} = 4.3$ nM

3.3
Inhibits 11 kinases
≥75% at 30 μM
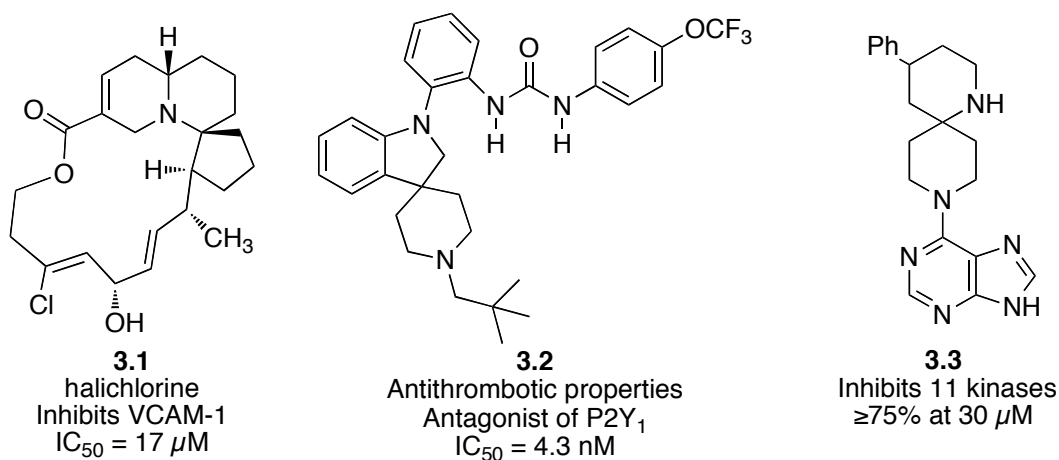
Background

While investigating the total synthesis of cephalotaxine (**3.6**), Husson discovered the selective reduction of α-aminonitriles (**Scheme 3.2**).[11] Compound **3.4** was alkylated with 1-chloro-3-iodopropane to yield cyclization precursor **3.5**. The alkylated product was prepared to test the expected lithium halogen exchange and cyclization onto the nitrile, giving imine **3.8**. Instead, competitive reductive lithiation of the nitrile produced the corresponding tertiary alkyllithium **3.9**, which cyclized onto the pendant alkyl chloride

yielding **3.10** in 57% yield. This first example of reductive lithiation of an α-aminonitrile served as inspiration for the later synthesis of the lepadiformine alkaloids.[12]

Scheme 3.2. Alkylation and selective reductive lithiation of α-aminonitriles
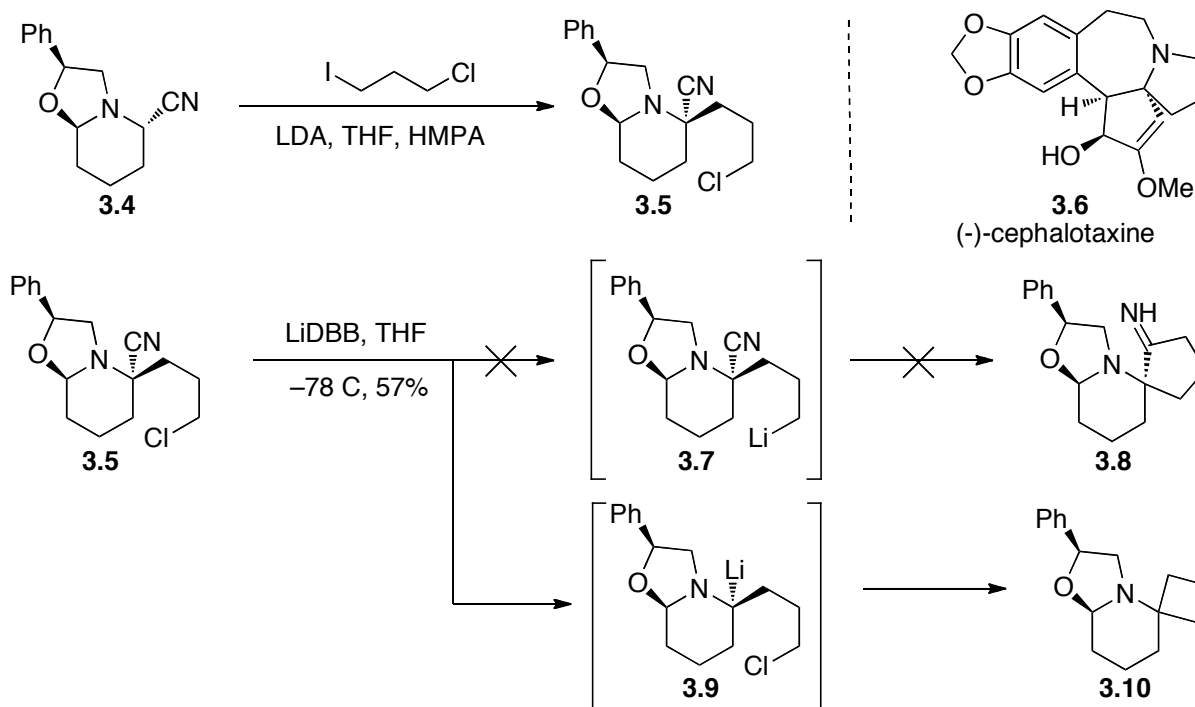
Using Husson's spirocyclization as precedence, Rychnovsky was able to complete the synthesis of the tricyclic marine alkaloid lepadiformine C (**3.16**, **Scheme 3.3**)[13] Starting with α-aminonitrile **3.11,** alkylation with dibromide **3.12** yielded the annulated product **3.13** in 73% yield.[13] Selective deprotection of the TBS ether followed by activation of the alcohol as the phosphate ester gave intermediate **3.14** in 73% and 96% yields, respectively. Previous work had shown that phosphate esters, were the most reliable leaving group, as they do not undergo reductive lithiation under the reaction conditions and can be cyclized with reproducible and consistent yields.[14] Reductive lithiation of nitrile **3.14** and subsequent spirocyclization produced key intermediate **3.15** in excellent yield and diastereoselectivity, despite the radical mechanism. Several synthetic manipulations gave

the natural product (+)-lepadiformine C (**3.16**). Later syntheses would complete the lepadiformine family of alkaloids.[6c]

Scheme 3.3. Key steps of (+)–lepadiformine C synthesis
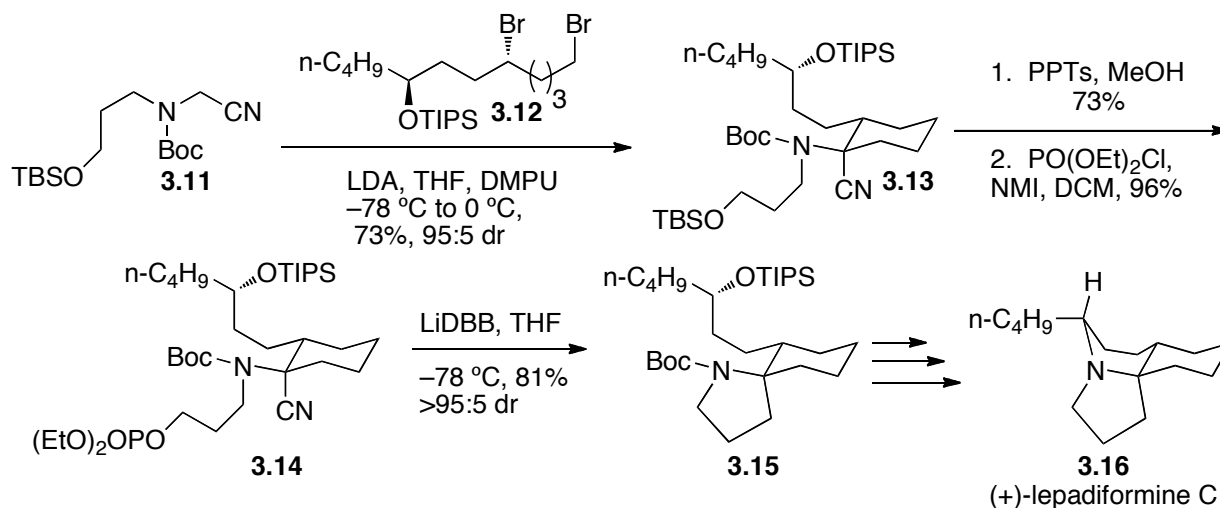
The stereochemical outcome of the reductive cyclization event was of particular interest due to two earlier findings. When compound **3.13** underwent reductive lithiation and protonation at –78 °C, the surprising product **3.20** was isolated (**Scheme 3.4**).[13] The inverted stereochemistry was rationalized by invoking conjugation of the carbon radical in **3.17** with the adjacent nitrogen's lone pairs. This places the Boc and R_1 group in the plane of the radical. A consequence of this is the steric crowding of the R_1 and R_2 groups of intermediate **3.17**. The low inversion barrier of carbon radicals allows for rapid inversion, which followed by a subsequent ring-flip, gives radical **3.18**. Following a second single-electron transfer, alkyllithium **3.19** formed and protonated with retention of stereochemistry, leading to product **3.20**. Due to this isolated product, a double inversion mechanism was proposed in the formation of **3.15** (**Scheme 3.3**). This suggests that an electrophilic substitution reaction with inversion of stereochemistry, with respect to the C–Li bond, (SE_{inv}) is operating in the ring-closing event.

Scheme 3.4. Protonation studies of lepadiformine C intermediate
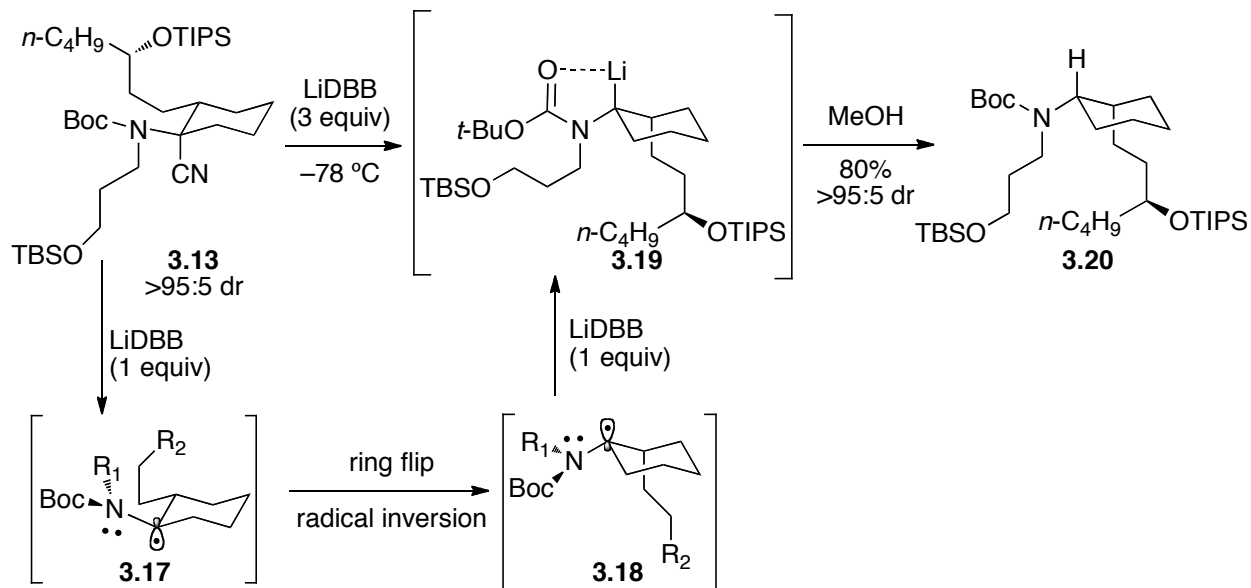
The double inversion mechanism leading to product **3.15** (**Scheme 3.3**) was believed to have been caused by steric interactions.[15] To determine the effect of sterics on the diastereoselectivity of the cyclization, substrate **3.21** (**Scheme 3.5**) was synthesized. Its remote *tert*-butyl group should negate those steric effects. If the same SE_{inv} mechanism was operating, product **3.22** would be produced (**Scheme 3.5**). Instead, equation 1 shows that product **3.23** was formed, showing the mechanism had changed to an electrophilic substitution reaction with retention of stereochemistry, with respect to the C–Li bond (SE_{ret}). To ensure that no radical inversion had occurred, the ratio of alkyllithium species **3.25** was determined by reductively lithiating compound **3.24,** and protonating the active species. The isolated product revealed an increase in the diastereomeric ratio, implying radical interconversion. This result suggested that further study was required to understand when the SE_{ret} or SE_{inv} mechanisms were at work.

Scheme 3.5. Reductive decyanation of **3.21** and **3.24**
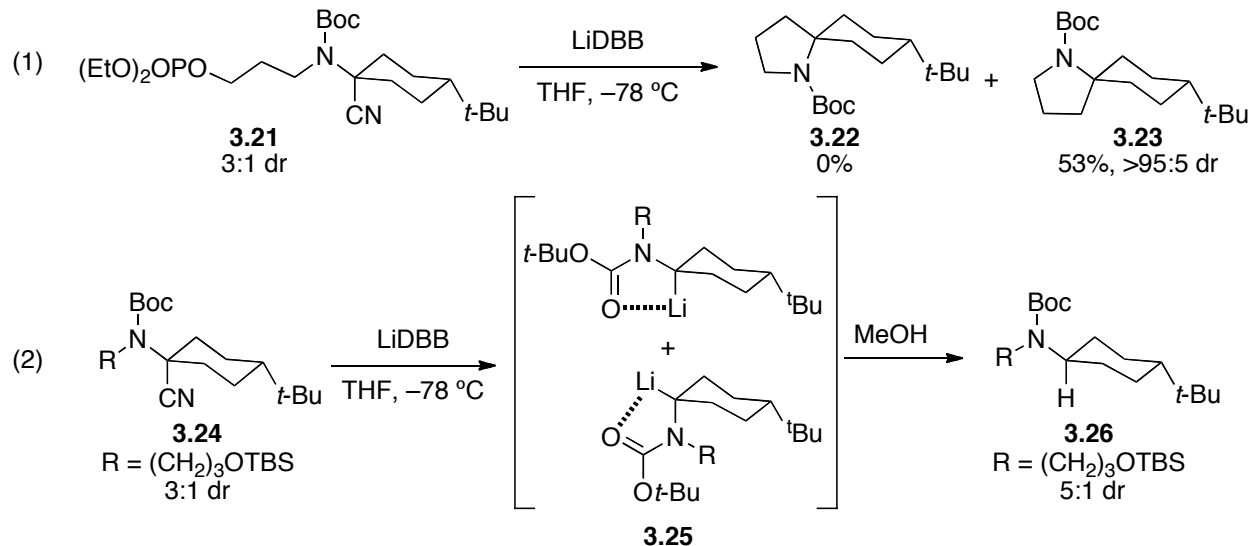
Project Goals

The success of the annulation, activation and reductive cyclization sequence to synthesize the azaspirocycles, provided a reason for generalizing and expanding the methodology. A general outline of this sequence is presented in **Scheme 3.6**. Two areas of interest were identified: 1) examination of the factors influencing the diastereoselectivity from the spirocyclization event, and 2) determination of the functional group tolerance of the established route. Of particular interest was understanding when the SE_{ret} or SE_{inv} mechanism was the major pathway, and if a substrate could react via both mechanisms to give a mixture of spirocyclic diastereomers.[16] To probe these questions and improve this methodology, a collection of spirocycles was planned.

Scheme 3.6. General forward synthesis of spirocycles
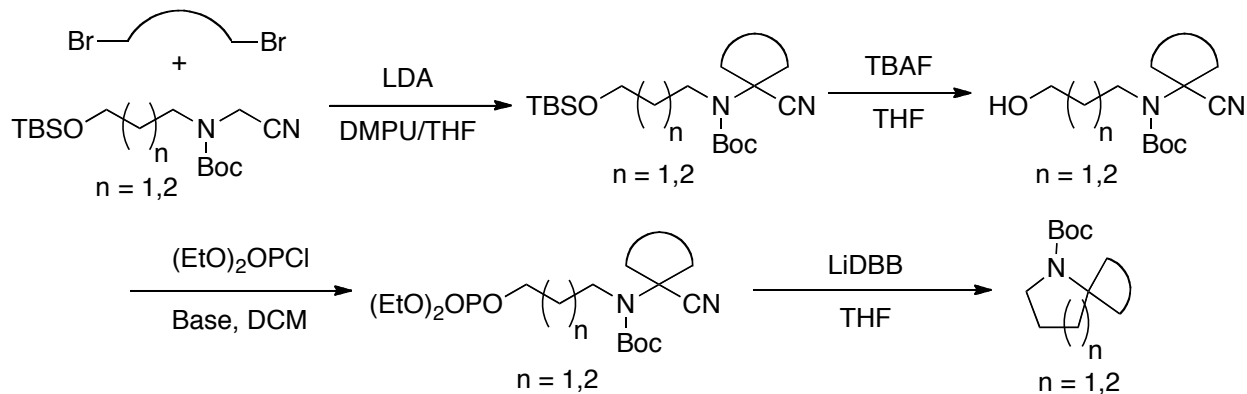
Synthesis of substituted dibromides

To produce phosphate diastereomers for testing reductive lithiation, a series of dibromides were required. Where possible, simple dibromides, such as 1,4-dibromobutane, were purchased; however, four more structurally complex dibromides had to be synthesized. Tetrahydropyran precursor **3.29** was prepared by Williamson ether synthesis with alcohol **3.27** and ethyl bromoacetate yielding **3.28** in 57% yield (**Scheme 3.7**, eq 1).[17] Subsequent reduction to the corresponding diol and bromination gave dibromide **3.29** in 92% yield over two steps. Aromatic dibromide **3.32** was prepared via Knoevenagel condensation of benzaldehyde (**3.30**) with dimethylmalonate (eq 2).[18] Conjugate addition with a second equivalent of dimethylmalonate and double decarboxylation yielded diester **3.31** in poor yield. Reduction of **3.31** to its diol and subsequent bromination afforded the desired dibromides **3.32**.[19] The last two dibromides were prepared via Von Braun degradation (eq 3). Benzoylation of substituted piperidines **3.33** and **3.34** gave respective products **3.35** and **3.36**.[20] Subjecting these substrates to generated PBr$_5$ and destructive distillation afforded the final dibromides **3.37** and **3.38**. With these required dibromides, alkylations onto aminonitrile **3.11** were studied next.

Scheme 3.7. Synthesis of substituted dibromides
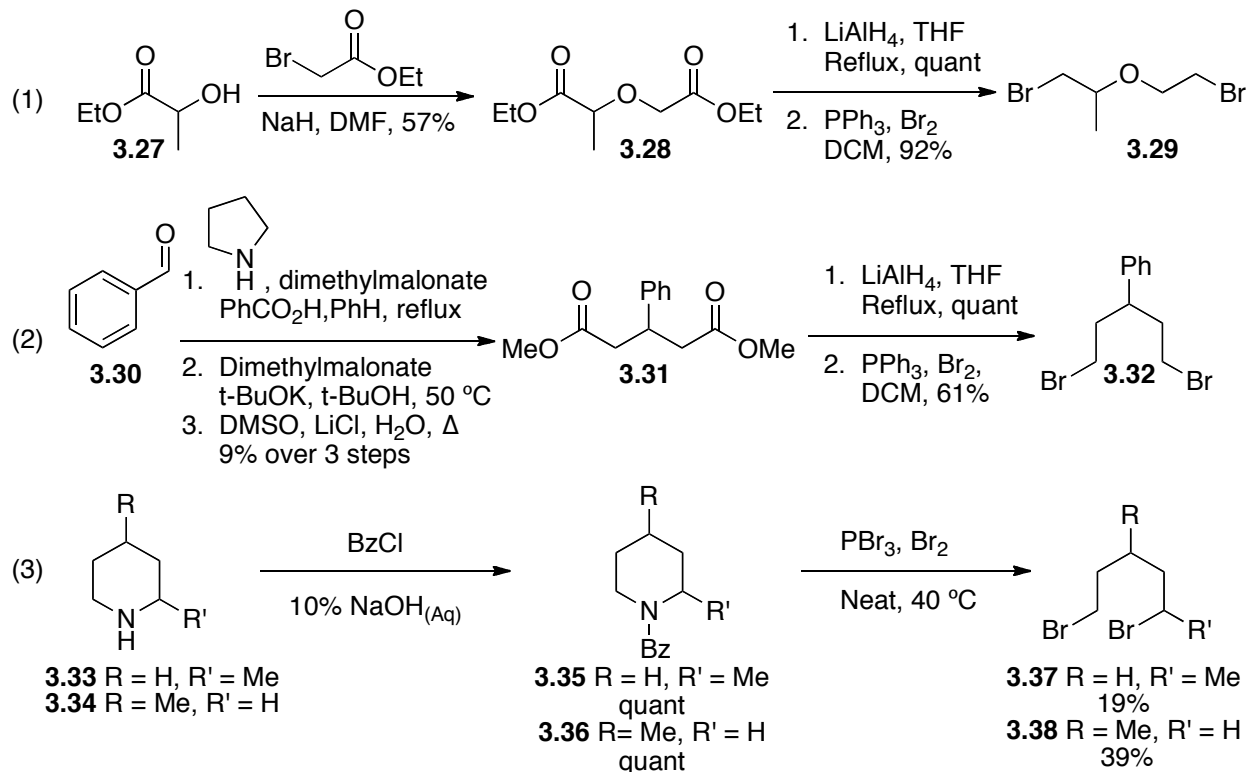
Optimization of double alkylation reaction

Synthesis of the first double-alkylated product **3.39** proved to be more challenging than expected (**Table 3.1**). Initial work to alkylate dibromide **3.29** onto aminonitrile **3.11** used 2.5 equivalents of LDA followed by brief warming to 0 °C. The reaction was then cooled back to –78 °C before another equivalent of LDA was added (entry 1).[21] This led to a yield of <24% as an inseparable mixture of **3.11** and **3.39**. Reaction monitoring by TLC was not possible due to the inability to stain dibromide **3.29**, as well as the identical R_f of aminonitrile **3.11** and product **3.39**. Increasing the reaction temperature to –40 °C and adding 2 equivalents of LDA in the second addition led to a 16% yield of pure **3.39** (entry 2). Reaction molarity was suspected to be the issue. The initial 0.1 M reaction was diluted to 0.05M after the addition of 3.5 equivalents of 0.4 M LDA. Increasing the concentration of

LDA to 1.0 M resulted in an increase in yield of **3.39** to 62% yield with a 1.2:1 dr (entry 3). Running the reaction at –78 °C increased the diastereomeric ratio to 2:1, but again resulted in an inseparable mixture of **3.11** and **3.39**, and a drastically decreased reaction yield (entry 4). Gratifyingly, applying conditions from entry 4 at –40 °C gave **3.39** in 70% yield (entry 5). These optimized conditions were then used for several double alkylation reactions, albeit with mixed results.

Table 3.1. Optimization of double alkylation of **3.11** with **3.29**.

TBSO⌒⌒⌒N(Boc)⌒CN **3.11**   Br⌒⌒O⌒⌒Br **3.29** →(LDA, THF, DMPU, Temp)→ TBSO⌒⌒⌒N(Boc)—C(CN)(tetrahydropyran) **3.39**

Entry	[LDA]	Equiv LDA for 1st, 2nd addition	Temp	Yield	dr[b]
1	0.4	2.5, 1.0	–78 °C	<24%[a]	1.8:1
2	0.5	2.5, 2.0	–40 °C	16%	1.5:1
3	1.0	2.5, 1.0	–40 °C	62%	1.2:1
4	1.0	2.5, 1.75	–78 °C	<16%[c]	2.0:1
5	1.0	2.5, 1.75	–40 °C	70%	1.2:1

[a] Isolated as an inseparable 1:2 mixture of **3.11** : **3.39**. Ratio and yield determined by ^{1}H NMR integrations. [b] Ratio determined by ^{1}H NMR. [c] Isolated as an inseparable 3:1 mixture of **3.11** : **3.39**. Entries 1 and 2 use a 1.0:1.2 ratio of **3.29:3.11**. Entries 3–5 use a 1.2:1.0 ratio of **3.29:3.11**.

The optimized conditions from entry 5 proved to be somewhat unreliable (**Table 3.1**). Reaction yields were hard to reproduce and changed for no apparent reason. Two further changes to the alkylation methodology were made to decrease the variability in reaction yields. First, the mixed aminonitrile and dibromide (1:1.5 equivalents respectively) were weighed into the reaction flask, and dry benzene was added and removed *in vacuo* 3 times. Second, the addition of LDA was changed to 5 equivalents at –

78 °C added over 1 hour with no warming period. These changes provided a reliable method for carrying out future double alkylations.

With this highly optimized alkylation procedure synthesizing substrates to make [4.4] and [4.5] azaspirocycles was begun. All secondary dibromides were found to alkylate with high diastereoselectivity, and products **3.40, 3.43**, and **3.54** were isolated as single diastereomers (**Table 3.2**).[22] Annulated products **3.39, 3.46,** and **3.50**, bearing substation farther away from the nitrile, formed as inseparable mixtures of diastereomers. Not surprisingly, the yields of double alkylation products were higher when using primary rather than secondary dibromides. In all cases, deprotection of the TBS group gave excellent to quantitative yields of the corresponding alcohols. The mixture of diastereomers from alcohols **3.47, 3.51,** and **3.57** were separable and were isolated as pure diastereomers. Subsequent activation of diastereomerically pure alcohols gave the corresponding phosphates. The use of the additive *N*-methylimidazole (NMI) was important to ensure phosphorylation of the alcohol, followed by deprotonation of the resulting oxonium ion. When stronger bases were tested, yields were significantly lower. Presumably, stronger bases generated the alkoxide, which then cyclized into the nearby Boc group. In all cases, the phosphates were made in good to excellent yield. With the reliable 3-step sequence of annulation, deprotection and phosphorylation completed for entries 1–6, the [4.4] and [4.5] spirocycle precursors were available to examine the SE_{ret} and SE_{inv} mechanisms on N-Boc tertiary alkyllithiums.

Table 3.2. Synthesis of diastereomeric spirocycle precursors

Entry	Akylated Nitrile (Yield, dr[a])	Alcohol (Yield)	Major Phosphate (Yield, dr[a]) R = PO(OEt)$_2$	Minor Phosphate (Yield, dr[a]) R = PO(OEt)$_2$
1	**3.40** 64%, >95:5 dr	**3.41** quant	**3.42** 93%	N/A
2	**3.43** 62%, >95:5 dr	**3.44** quant	**3.45** 66%	N/A
3	**3.46** 75%, 2:1 dr	**3.47** 85% (Separated)	**3.48** 74%, >95:5 dr	**3.49** 70%, >95:5 dr
4	**3.50** 78%, 3:1 dr	**3.51** 93% (Separated)	**3.52** 72%, >95:5 dr	**3.53** 62%, >95:5 dr
5	**3.54** 61%, >95:5 dr	**3.55** quant	**3.56** 84%	N/A
6	**3.39** 70%, 1.2:1 dr	**3.57** quant (Separated)	**3.58** 84%, >95:5 dr	**3.59** 74%, >95:5 dr

[a] Ratios determined by ^{1}H NMR.

Reductive lithiation to form [4.5] spirocycles

The nine cyclization precursors were used to examine selectivity for the SE_{ret} and SE_{inv} mechanisms during the spirocyclic ring closure. Reduction of axial nitrile **3.52** gave the cyclized **3.60** in reasonable yield with retention of stereochemistry (**Scheme 3.8**). GCMS analysis showed a dr of 98.2:1.8 for equation 1. Using a 60:40 mixture of nitriles **3.52** and **3.53,** the mixture of diastereomers converged to afford **3.60** with a dr of 98.7:1.3. The 71% yield of **3.60** in entry 2 indicated that the equatorial nitrile must cyclize through what appeared to be an inversion mechanism. To confirm this, pure equatorial nitrile **3.53** was subjected to cyclization conditions, and again yielded spirocycle **3.60** in better yield than the axial nitrile. In all three cases, the stereoselectivity for spirocycle **3.60** was >98:2, showing that the remote stereocenter must have a profound effect on the stereochemical course of the reaction. With this information, attention turned to tetrahydropyrans **3.58** and **3.59** (**Table 3.2**) to see if the methyl group at the 3-position and oxygen substitution would affect the stereoselectivity in a way similar to substrates **3.52** and **3.53** (**Scheme 3.8**).
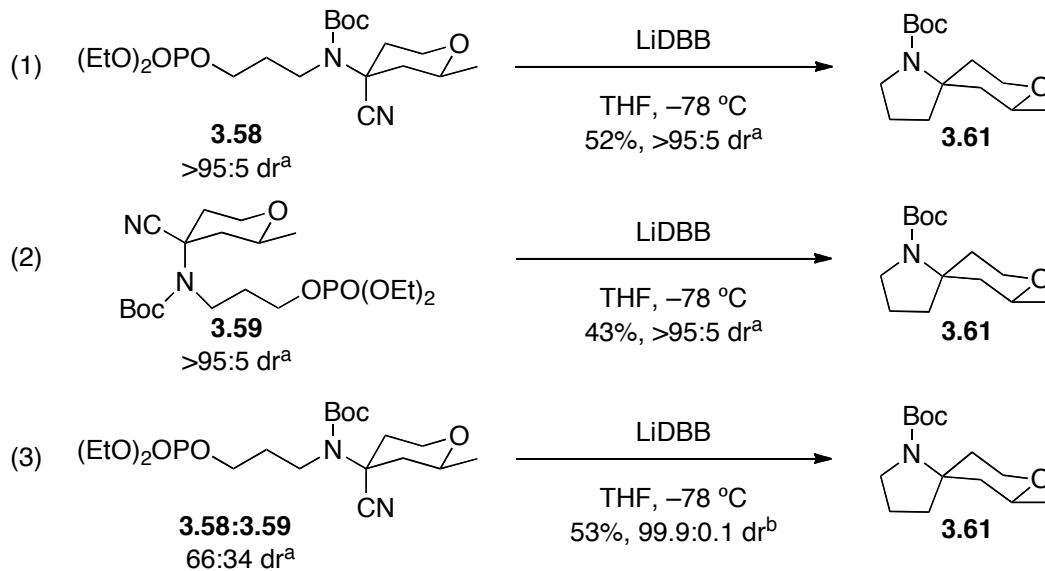
Scheme 3.8. Stereochemical outcome for phenyl containing spirocycle

(1) $(EtO)_2OPO$ ... N(Boc) ... CN ... Ph
3.52
>95:5 dr[a]

LiDBB
THF, −78 °C
51%, 98.2:1.8 dr[b]

Boc–N spirocycle **3.60** Ph

(2) $(EtO)_2OPO$ ... N(Boc) ... CN ... Ph
3.52:3.53
60:40 dr[a]

LiDBB
THF, −78 °C
71%, 98.7:1.3 dr[b]

Boc–N spirocycle **3.60** Ph

(3) NC ... Ph, N(Boc) ... $OPO(OEt)_2$
3.53
>95:5 dr[a]

LiDBB
THF, −78 °C
61%, 98.5:1.5 dr[b]

Boc–N spirocycle **3.60** Ph
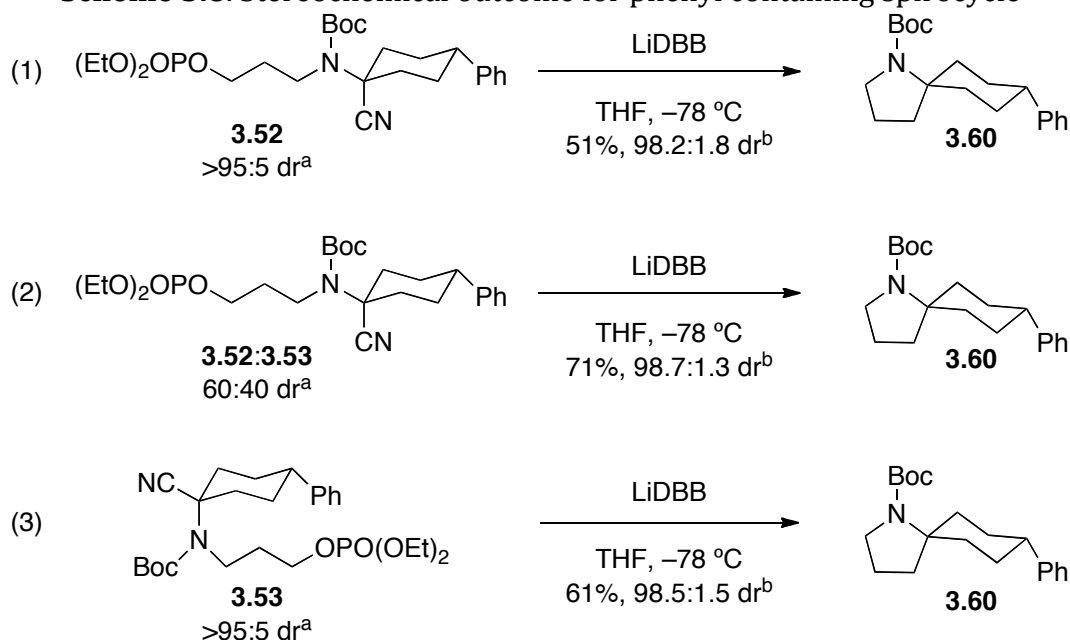
[a] Ratios determined by ^{1}H NMR. [b] Ratios determined by GCMS

Reactions of nitrile diastereomers **3.58** and **3.59** (**Scheme 3.9**) were similar to **Scheme 3.8**. Reacting the axial diastereomer **3.58** with LiDBB gave the equatorially substituted spirocycle **3.61** in good yield with a >95:5 dr (eq 1). Again, retention of stereochemistry was observed. As with equatorial nitrile **3.53** (**Scheme 3.8**), equatorial nitrile **3.59** (**Scheme 3.9**, eq 2) also cyclized with overall inversion of stereochemistry to yield the same spirocycle with equivalent diastereoselectivity as equation 1. Compound **3.59** is shown with an equatorial nitrile. The reasoning behind this is discussed later in this chapter. Using a 2:1 mixture of the nitriles **3.58** and **3.59**, reductive lithiation produced spirocycle **3.61** in 53% yield. GCMS analysis of the product ratio revealed that this major spirocycle was formed with nearly a 1000:1 dr. These surprising results prompted a protonation study to determine if the ratio of alkyllithium intermediates would match.

**Scheme 3.9**. Stereochemical outcome for THP-containing spirocycle

(1) **3.58** >95:5 dr[a] → LiDBB, THF, −78 °C, 52%, >95:5 dr[a] → **3.61**

(2) **3.59** >95:5 dr[a] → LiDBB, THF, −78 °C, 43%, >95:5 dr[a] → **3.61**

(3) **3.58:3.59** 66:34 dr[a] → LiDBB, THF, −78 °C, 53%, 99.9:0.1 dr[b] → **3.61**

[a] Ratios determined by ^{1}H NMR. [b] Ratios determined by GCMS

The mechanism for the stereoselective spirocyclization of nitriles **3.58** and **3.59** to spirocycle **3.61** was thought to be influenced by the mixture of alkyllithiums formed prior to cyclization (**Scheme 3.9**). If a radical isomerization, as seen in compound **3.17** (**Scheme 3.4**), was also at work with nitriles **3.58** and **3.59**, then one predominant alkyllithium species should be produced, leading to one product. To test this, TBS ether **3.39** (**Scheme 3.10**) was reductively lithiated and protonated to yield carbamate **3.63**, which would reveal the ratio of alkyllithium diastereomers **3.62**. This experiment resulted in an enrichment of the ratio of diastereomers from 1.2:1 to 2:1; however, this did not explain the selectivity seen in the cyclization event. Assuming that the increase in the diastereomeric ratio was from radical isomerization, then it would be expected that both nitriles **3.58** and **3.59** (**Scheme 3.9**) would also produce a mixture of radicals and therefore alkyllithiums. One possibility is that only the axial alkyllithium reacts with retention to form the spirocycle, while the equatorial alkyllithium cannot cyclize. Given the

70

highly reactive nature of N-Boc tertiary-alkyllithiums, and their known ability to react through SE_{ret} and SE_{inv}[13] this does not seem likely. While this quenching study showed some radical interconversion, a better explanation was sought.

**Scheme 3.10**. Reductive lithiation and protonation study on **3.39**
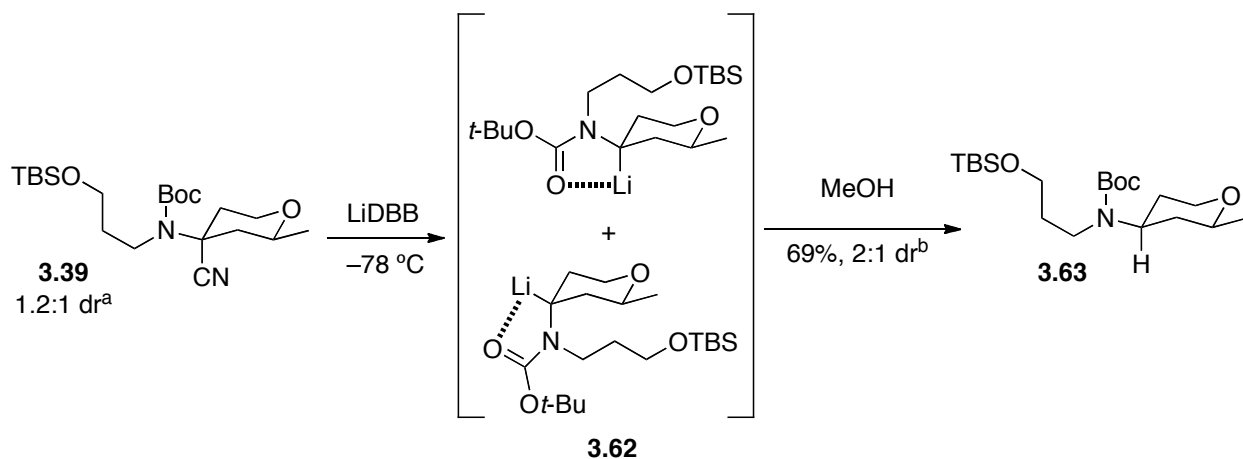
A second and more likely explanation for the diastereoselectivity involves the alkyllithiums dictating whether the mechanism proceeds with retention or inversion. Reacting nitrile **3.58** with one equivalent of LiDBB yielded radical **3.64** (**Scheme 3.11**). Reduction of nitrile **3.59** yielded the epimeric radical **3.66**. The low barrier to inversion allowed radical interconversion between **3.64** and **3.66**.[23] Radical **3.64** was expected to be the predominant species due to its di-equatorial substitution. A second equivalent of LiDBB would produce alkyllithiums **3.65** and **3.67**. These were not expected to interconvert, given their anticipated inversion barrier.[24] Alkyllithium **3.65** should then undergo an SE_{ret} reaction, while alkyllithium **3.67** should react via SE_{inv} with both yielding spirocycle **3.61**. It was hypothesized that the difference in mechanism was the result of the alkyllithium geometry. The reaction of **3.65** leading to **3.61** may allow for electrophile-lithium coordination, leading to the SE_{ret} mechanism, while intermediate **3.67** may lack or

be limited in the electrophile's ability to pre-coordinate to the alkyllithium and therefore reacted via SE_{inv}. The phenyl analogs in **Scheme 3.8** were expected to react through a similar mechanism. A similar hypothesis of inversion or retention products based on lithium-electrophile coordination based was proposed by Gawley[25] and Beak[26] and is detailed in **Figure 1.5**.

Scheme 3.11. Possible explanation of stereochemical outcome of **3.61**
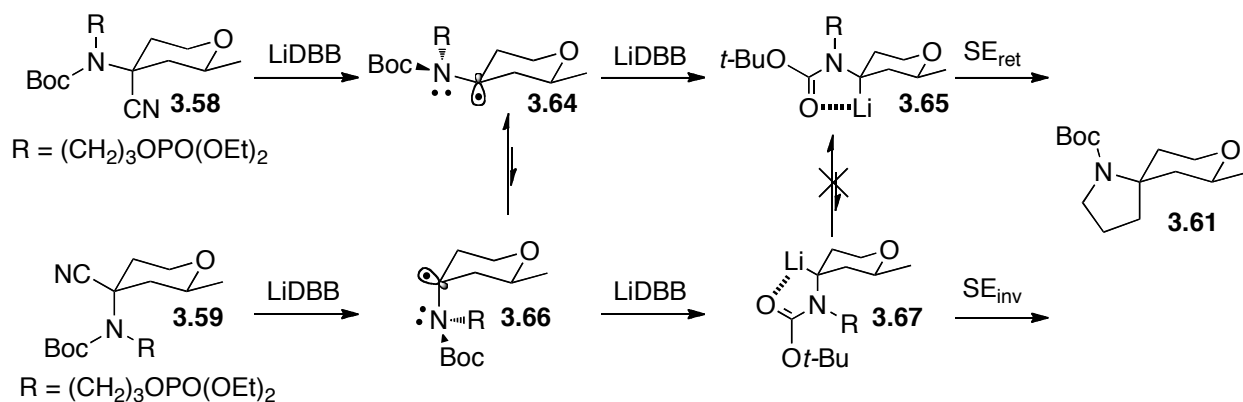
With a plausible explanation for the observed diastereoselectivity, the remaining nitriles **3.42, 3.56** and **3.45** were analyzed (**Table 3.3**). Nitrile **3.42** was reduced and cyclized to yield product **3.68** in good yield with exceptional diastereoselectivity (entry 1). No trace of its spirocyclic diastereomer was detected by GCMS. Since nitrile **3.42** cyclized in close diastereoselectivity to **3.61**, nitrile **3.56** was expected to react with similar diastereoselectivity (entry 2). While the diastereoselectivity for **3.69** was excellent, the 98:2 dr was somewhat disappointing. Reacting a 2:1 ratio of **3.48:3.49** resulted in an outstanding 72% yield of **3.70** with a >95:5 dr by ^{1}H NMR. The importance of the lithium-Boc chelate became a point of interest (**Scheme 3.10, 3.11**). It was decided to intentionally erode the diastereoselectivity by substituting the poorer-chelating potassium. Entry 3 was used as a point of reference for this experiment, and known phosphate **3.45** was reduced to

produce spirocycle **3.71** in reasonable diastereoselectivity. Replacing LiDBB with KDBB, prepared by substituting potassium metal for lithium metal, produced the same spirocycle (entry 5). Surprisingly, the product from entry 5 was isolated in higher yield and higher diastereoselectivity than when made with LiDBB. This suggested that the importance of the lithium-Boc chelate may be inflated.

Table 3.3. Synthesis of [4.5] spirocycles

Entry	Phosphate	Radical Carrier	Spirocycle	Yield and dr
1	**3.42**	LiDBB	**3.68**	60% >99.9:0.1 dr[a]
2	**3.56**	LiDBB	**3.69**	66% 98.0:2.0 dr[a]
3	**3.48:3.49** 2:1 dr[b]	LiDBB	**3.70**	72% >95:5 dr[b]
4	**3.45**	LiDBB	**3.71**	68% 88.0:12.0 dr[a]
5	**3.45**	LiDBB	**3.71**	74% 92.6:7.4 dr[a]

[a] Ratio by GCMS. [b] Ratio by NMR

73

Functional group tolerance of the LiDBB cyclization

The strong reducing nature of LiDBB methodology makes functional group incorporation challenging. It has been well documented that LiDBB will cleave sulfides,[27] halogens,[28] nitriles,[29] epoxides,[30] ketones[31] and other functional groups from their attached carbons, yielding alkyllithiums. This means only radically inert functional groups can be incorporated. The ability to synthesize spirocycles with ketal and nitrogen functional groups would be beneficial to medicinal and academic research. Perry showed that a double alkylation to produce a 7-membered ring gave poor yield.[32] Attempting to form cyclopropanes resulted in decomposition under reductive lithiation conditions, whereas cyclobutane formation resulted in poor diastereoselectivity (3:2 dr). For this reason, the substituted dibromides selected to study functional group tolerance could only form 5 and 6 membered rings when annulated onto aminonitriles. The next step was to synthesize these dibromides for alkylation.

The first dibromides synthesized were the ketal derivatives. Starting with ketone **3.72**, selective bromination gave **3.73** (**Scheme 3.12**, eq. 1).[33] Cyclopropyl ring opening with hydrobromic acid led to dibromide **3.74**.[34] Protection of this ketone under standard conditions led to ketal **3.75**. Synthesis of symmetric dibromide **3.79** started by subjecting ester **3.76** to the Kulinkovich reaction to give cyclopropyl alcohol **3.77** (eq 2).[35] Electrophilic ring opening with NBS gave ketone **3.78**.[36] Although literature precedent showed direct protection of ketone **3.78**, these results could not be reproduced.[37] The inability to protect ketone **3.78** and the tricky Kulinkovich reaction made a different synthetic route to ketal **3.79** appealing. Starting from tricarbonyl **3.80**, a Noyori protection was employed to selectively react with the ketone over the adjacent esters (eq 3).[38] Diester

3.81 was reduced to the corresponding diol, and brominated in outstanding yield to give the desired dibromide **3.79** in 86% yield over 3 steps. This left the protected nitrogen mustard as the last remaining dibromide to synthesize.

Scheme 3.12. Synthesis of protected dibromides
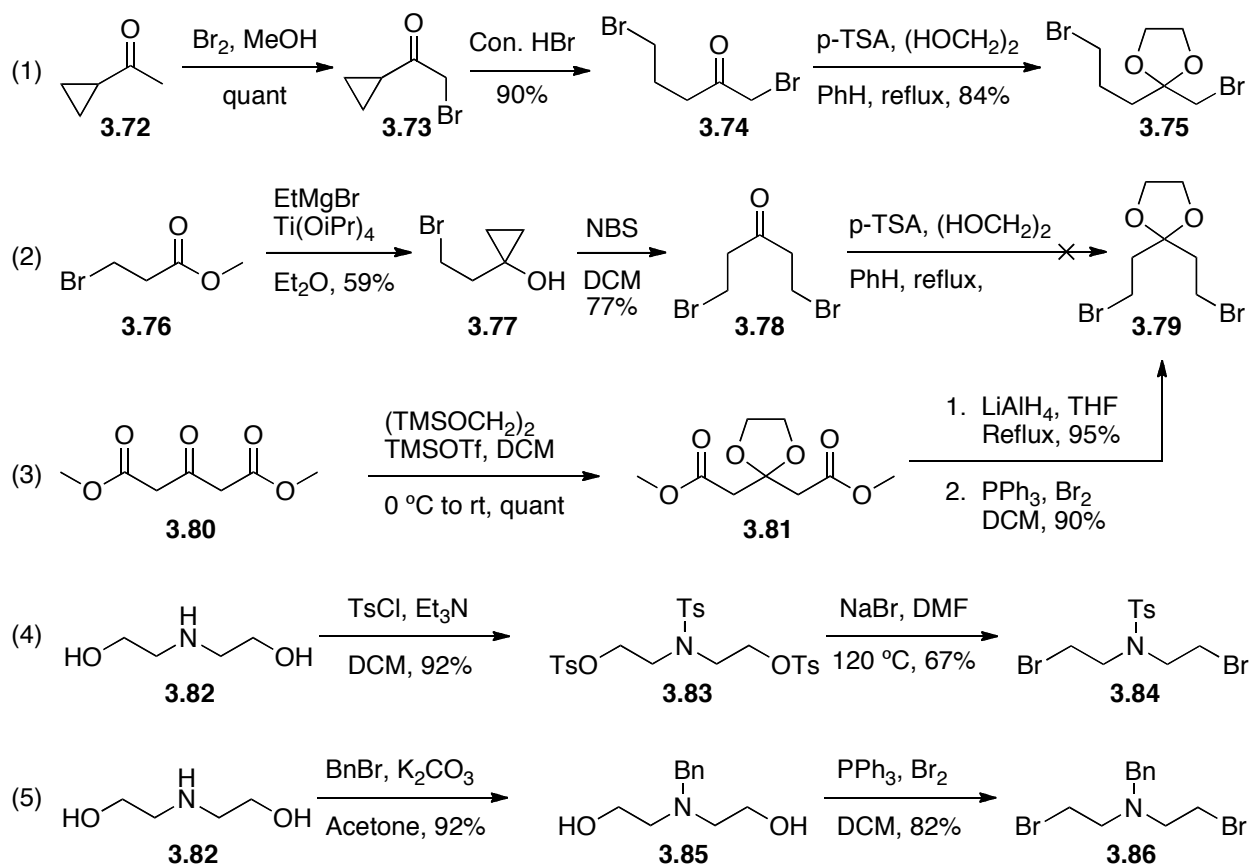
Unpublished research with nitrogens bearing β-leaving groups showed decomposition after only a few hours of storage at –25 °C.[39] A strong electron withdrawing group was needed to deactivate the nitrogen's lone pairs and limit the expected decomposition. Diethanolamine **3.82** was per-tosylated in excellent yield and the tri-tosylate **3.83** was brominated by heating with NaBr in DMF (eq 4).[40] Dibromide **3.84** was immediately reacted with aminonitrile **3.11** but failed to yield any product and so unstable under the strongly basic reaction conditions, that it decomposed before a TLC could be

taken for reaction monitoring. It was hypothesized that the strongly electron withdrawing tosyl group was acidifying the hydrogens alpha to the nitrogen, facilitating decomposition through an elimination pathway. The use of an electron-neutral protecting group was expected to solve this problem. Benzyl protection of aminodiol **3.82**, yielded **3.85** in excellent yield (eq 5). Bromination under standard conditions gave dibromide **3.86**, which was stored frozen in benzene for further use.

**Table 3.4**. Synthesis of achiral/racemic [4.5] spirocycles

Entry	Akylated Nitrile (Yield)	Alcohol (Yield)	Phosphate (Yield)	Spirocycle (Yield)
1	**3.87** 65%	**3.88** quant	**2.32** 89%	**2.33** 67%
2	**3.89** 48%	**3.90** 48%	**3.91** 89%	**3.92** 16%
3	**3.93** 62%	**3.94** 86%	**3.95** 89%	**3.96** 37%
4	**3.97** 57%	**3.98** 95%	**3.99** 61%	**3.100** 62%

Production of spirocycle precursors began with the point-of-reference compound

3.87 (**Table 3.4**). This compound was used to judge the efficiency of the synthesis of the

subsequent spirocycles. Double alkylation of aminonitrile **3.11** with corresponding

dibromides yielded alkylation products **3.87**, **3.89**, **3.93**, and **3.97**. Surprisingly, the nitrogen mustard **3.86** was alkylated in reasonable yield. Unsymmetrical dibromide **3.75** alkylated in slightly lower yield than its symmetric counterpart **3.79**, likely due to steric bulk. Deprotection of each TBS ether proceeded in excellent yield, with the exception of **3.90**. Phosphorylation of these alcohols yielded the cyclization precursors in great to excellent yield, and allowed for testing of the different protecting groups under reductive cyclization conditions.

Reacting nitrile **2.32** with LiDBB produced simple spirocycle **2.33** in 67% yield (**Table 3.4**). The benzyl protected **3.91** was next reacted with LiDBB, giving a disappointing 16% yield. The likely problem was the benzyl protecting group itself. Benzyl-protected oxygens are known to be cleaved by LiDBB[41] and benzyl-protected nitrogens can deprotected with Li/NH$_3$.[42] While cleavage of N-benzyl groups with LiDBB has not been reported, it would appear to take a route similar to that of oxygen. The low yield of product **3.96** was more perplexing. Given the substantially better yield of **3.100**, the problem appeared to be the location of the ketal itself.

Scheme 3.13. Possible decomposition mechanism for **3.95**
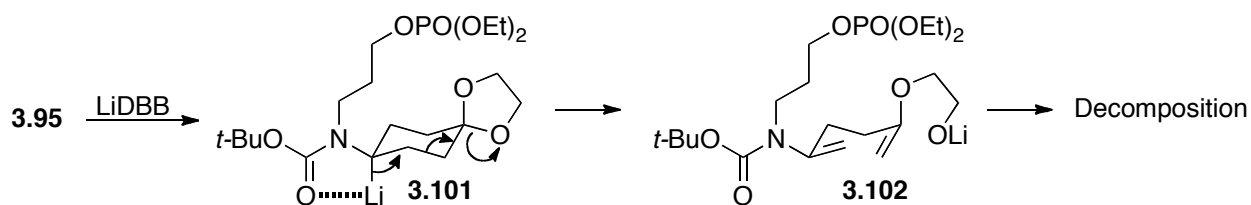
The diminished yield of spirocycle **3.96** was of interest given the much higher yield of similarly substituted spirocycle **3.100**. A decomposition pathway is proposed in **Scheme 3.13**. Reductive lithiation of **3.95** would yield lithiate **3.101**. Elimination of the alkyllithium would lead to alkoxide **3.102**, which could then decompose either under the

reaction conditions or upon work-up.   Attempts to find other products from the reaction work-up revealed nothing informative.

Scheme 3.14. Attempts at selective deprotection of **3.100**

3.103   TFA/DCM   **3.100**   AcOH, THF   **3.104**
   0 °C, 18%   H$_2$O, 65%
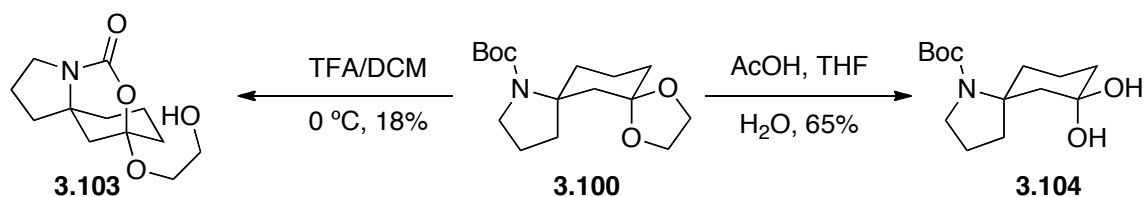
Synthesis of protected spirocycle **3.100** was the most successful of the cyclized products in **Table 3.4**. While the stability of the ketal and Boc protecting groups proved to be robust through the reaction sequence, selective deprotection would be ideal. Removal of the Boc group from spirocycle **3.100** was attempted first (**Scheme 3.14**). Unfortunately, standard TFA/DCM conditions led to the interrupted deprotection product **3.103** in poor 18% yield. The selective removal of the ketal group without cleaving the Boc group was expected to be challenging. A literature search failed to reveal conditions for cleaving a ketal in the presence of a Boc group; however, Babler *et al.* found ketals could be removed with AcOH in THF/H$_2$O. [43] Subjecting spirocycle **3.100** to these conditions led to the surprising isolation of hydrate **3.104**.   Presumably a hydrogen-bonding interaction between the Boc group and an OH of the hydrate stabilized this compound, preventing expulsion of water giving the expected ketone.   This protecting group strategy was deemed unsatisfactory because of the interrupted Boc deprotection and unsatisfactory ketal deprotection

Reductive lithiation to form [5.5] spirocycles

After success of the stereoselective [4.4] and [4.5] spirocycles, attention was turned to the consistently lower yielding [5.5] spirocycles.[14] Using extended aminonitrile[32] **3.105**,

double alkylation yielded annulated products **3.106, 3.110,** and **3.114** with similar dr and yield to their three-carbon shorter analogs (**Table 3.5**). Deprotection of the silyl ethers under standard conditions gave the corresponding alcohols in quantitative yield. Phosphorylation of these alcohols produced the required spirocyclization precursors. As expected, the following spirocyclizations were low yielding in all cases. Phosphate **3.109** was cyclized in a poor 32% yield but with equivalent diastereoselectivity, as compared to **3.60** (**Scheme 3.8**). Compounds **3.113** and **3.117** were isolated with a >95:5 dr (**Table 3.5**). The stereochemical outcome of these nitriles however, is plagued by low yields.

**Table 3.5**. Preparation of [5.5] spirocycles
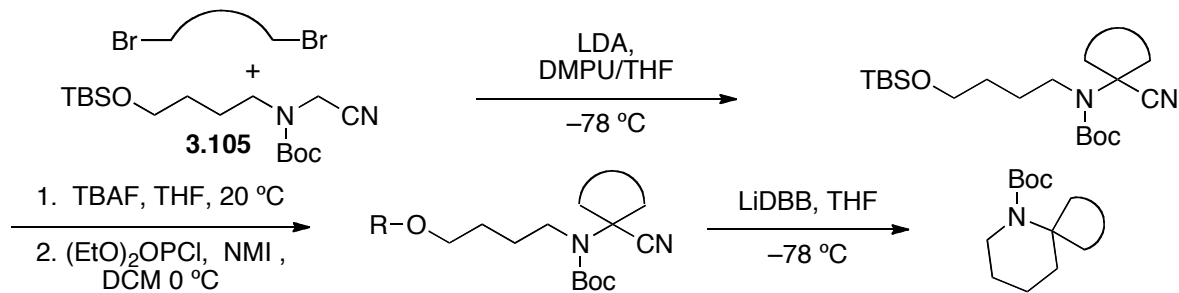
Entry	Akylated Nitrile (Yield, dr)	Alcohol (Yield)	Phosphate (Yield)	Spirocycle (Yield, dr)
1	**3.106** 79%, 3.6:1 dr[a]	**3.107** quant	**3.108** 81%	**3.109** 32%, 98.3:2.7 dr[b]
2	**3.110** 60%, >95:5 dr[a]	**3.111** quant	**3.112** 73%	**3.113** 27%, >95:5 dr[a]
3	**3.114** 72%, 2:1 dr[a]	**3.115** quant	**3.116** 64%	**3.117** 28%, >95:5 dr[a]

[a] Ratios determined by ^{1}H NMR. [b] Ratios determined by GCMS

   Reductive   lithiation   was   superior   at   forming   spiropyrrolidines   than

spiropiperidines. Pyrrolidine containing spirocycles clearly reacted in higher yield

probably due to the shorter carbon chain on the cyclizing ring. In forming spiropiperidines,

the additional carbon between the forming alkyllithium and the tethered phosphate would

lead to additional conformations and entropic cost to bring the two ends together for

cyclization. A consequence of this would be longer reaction times and greater chance for

decomposition. It was thought that running the reaction at higher temperatures could offset the entropic cost and give higher yields.

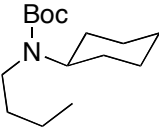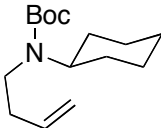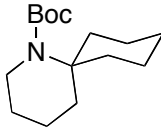**Scheme 3.15**. Simple [5.5] spirocycle synthesis
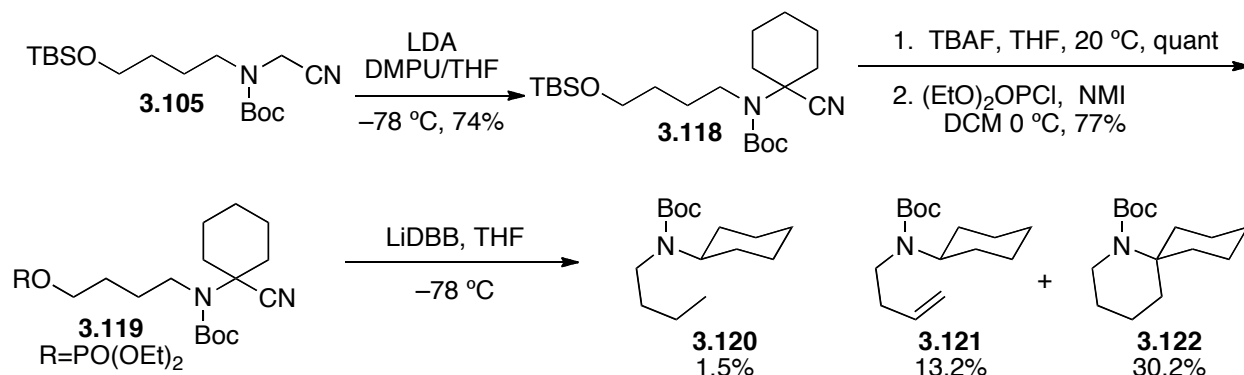
Compounds **3.120–3.122** were isolated as a mixture. The ratios of these products by GCMS were used to determine product yields. Authentic samples are discussed in chapter 4

A simple [5.5] spirocycle was needed to test the effect of increasing reaction temperatures. Aminonitrile **3.105** was alkylated with 1,5 dibromopentane to give annulated product **3.118** (**Scheme 3.15**). Deprotection and phosphorylation proceeded in excellent yield. As expected, reductive lithiation gave a poor 30% yield of spirocycle **3.122**. Two additional products were identified: alkane **3.120** and alkene **3.121**. In all reductive lithiation reactions, a corresponding terminal alkene was observed in 5-10%, usually as an inseparable mixture with the cyclized product.[44] Due to their close proximity, separation of **3.120–3.122** was not attempted. Instead, the mixture of the three compounds was collected and the mass isolated. The sample was analyzed by GCMS.[45] The areas of the three peaks were analyzed as their percent composition of the isolated mixture. These compounds were confirmed with authentic samples prepared in chapter 4. Using this technique, the amounts of the fully reduced **3.120**, elimination product **3.121**, and

spirocycle **3.122** could be quantified as 1.5%, 13.2%, and 30.2% of the reaction mixture respectively. A possible way to improve spirocycle yield was found in Slafer's thesis.[14] He showed that yields of [5.5] spirocycles improved when reductive lithiation was carried out at –30 °C. With this in mind, a temperature study was undertaken to try to increase the desired product yield.

**Table 3.6**. Temperature studies on product distribution from **3.119**

Entry	Temp (°C)	Yield of **3.120** (%)	Yield of **3.121** (%)	Yield of **3.122** (%)
1	–78	1.5	13.2	30.2
2	–40	4.8	10.5	39.5
3	0	2.8	4.1	37.5
4	20	1.6	2.9	36.9

Compounds **3.120–3.122** were isolated as a mixture. The GCMS ratios of these products were used to determine product yields

Entry 1 (**Table 3.6**) shows the original distribution of isolated compounds seen in **Scheme 3.15**. Raising the temperature to –40 °C shifted the product ratio away from **3.120** and **3.121**, and increased the amount of desired spirocycle formed by nearly 10% (**Table 3.6**, entry 2). Intrigued by these results, phosphate **3.119** was reacted at 0 °C (entry 3). While even less of byproducts **3.120** and **3.121** were detected, a slightly lower yield of spirocycle **3.122** was also observed. Increasing the reaction temperature to 20 °C further diminished the amounts of byproducts **3.120** and **3.121**. Spirocycle **3.122** was found in approximately the same yield as the reaction at 0 °C. The poor mass balance implies an unknown decomposition pathway that produces compounds that are too light or reactive to be recovered. Since entry 2 provided the best yield of spirocycle **3.122**, attention was focused on limiting alkene **3.121** at this temperature. Given the high dilution

under which LiDBB reactions are run, this elimination product was most likely from an intramolecular reaction. To try and prevent this, a strategic methyl group was considered as a solution.

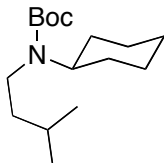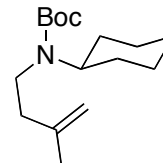**Scheme 3.16**. Synthesis of methyl-substituted aminonitrile **3.123** and spirocycle **3.129**
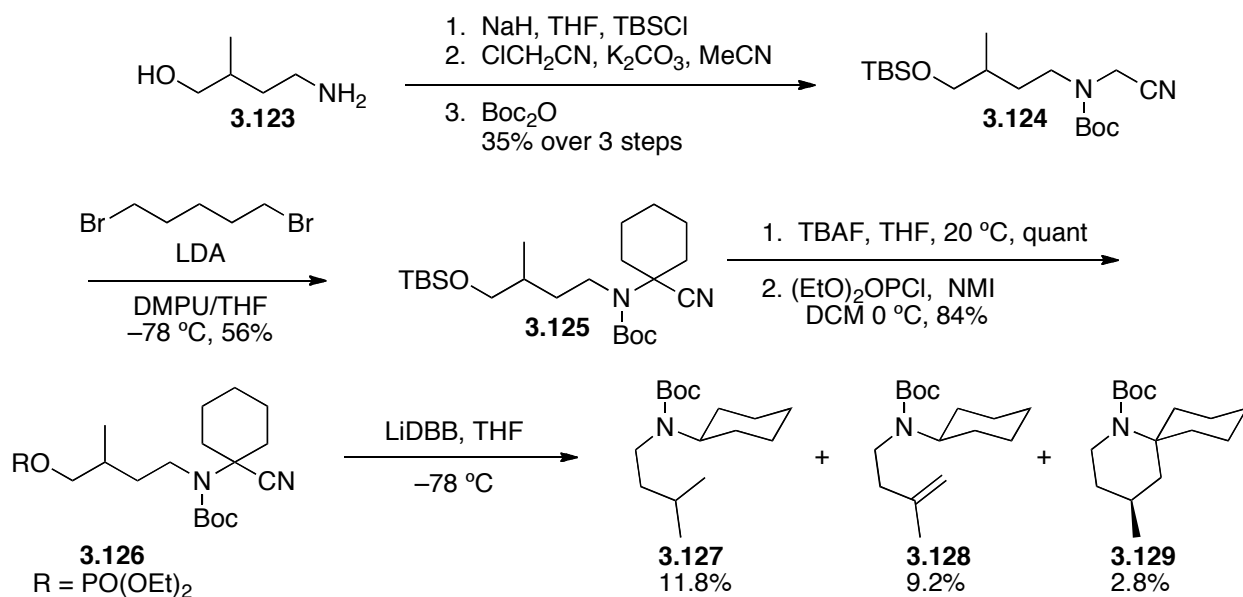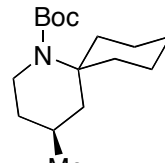

Compounds **3.127–3.129** were isolated as a mixture. The GCMS ratios of these products were used to determine product yields. Compounds **3.127** and **3.128** are assumed to be the structures shown based on their m/z from GCMS and the analogous compounds observed and confirmed in chapter 4

To test adding a methyl group to block elimination, phosphate **3.126** was prepared from aminoalcohol **3.123** (**Scheme 3.16**). A three-step procedure to make aminonitriles **3.11** and **3.105** was used on aminoalcohol **3.122**. Silyl protection of the alcohol and cyanomethylation of the nitrogen followed by Boc protection yielded product **3.124**. Alkylation with 1,5-dibromopentane gave annulated product **3.125**. Deprotection with TBAF and activation of the resultant alcohol as the phosphate ester provided compound **3.126** in excellent yield. Subjecting phosphate **3.126** to LiDBB led to the abysmal yield of 2.8% of spirocycle **3.129**. Whereas formation of alkene **3.128** was slightly suppressed, the

alkane product **3.127** had substantially increased. Reacting phosphate **3.126** at –78 °C showed that suppressing elimination by adding a methyl-group was incorrect. It was hoped that as with phosphate **3.119**, increasing the reaction temperature would change the product distribution and provide more spirocycle **3.129**.

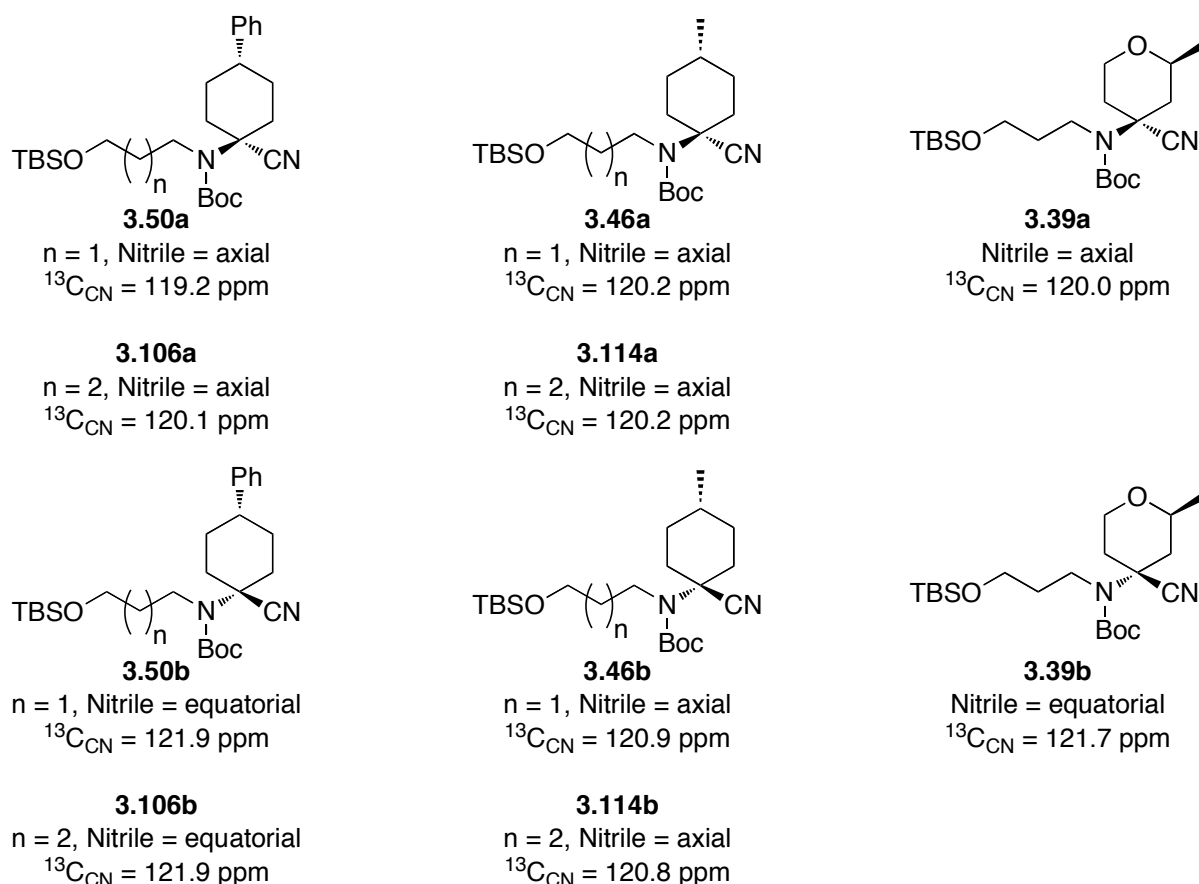**Table 3.7**. Methyl substituted [5.5] spirocycle temperature studies

Entry	Temp (°C)	Yield of **3.127** (%)	Yield of **3.128** (%)	Yield of **3.129** (%)
1	–78	11.8	9.2	2.8
2	–40	4.5	21.5	12.3
3	0	1.6	19.6	18.0
4	20	1.4	11.2	9.7

Compounds **3.127–3.129** were isolated as a mixture. The GCMS ratios of these products were used to determine product yields. Compounds **3.126** and **3.127** are assumed to be the structures shown based on their m/z from GCMS and the analogous compounds observed and confirmed in chapter 4.

The anticipated temperature dependence on spirocycle formation for compound **3.126** was next tested (**Table 3.7**). Entry 1 shows the reaction distribution from **Scheme 3.16**. Increasing the reaction temperature to –40 °C not only substantially increased the yield of spirocycle **3.129**, but also increased the production of elimination product **3.128** (entry 2). The fully reduced product **3.127** was the only compound to be suppressed. Increasing temperatures to 0 °C showed some improvement over entry 2. The non-cryogenic temperatures increased the yield of spirocycle **3.129** to 18%, while slightly lowering the amount of alkene isolated. At 0 °C, alkane product **3.127** was barely detectable. The final temperature increase to 20 °C gave disappointing results. The amounts of all isolated products dropped, with the spirocycle's yield falling to 9.7%. The strategy of methyl incorporation for increasing yields of [5.5] spirocycles was abandoned.

Diagnostic nitrile ^{13}C shifts

**Figure 3.1**. Axial and equatorial Nitrile ^{13}C shifts

3.50a
n = 1, Nitrile = axial
$^{13}C_{CN}$ = 119.2 ppm

3.106a
n = 2, Nitrile = axial
$^{13}C_{CN}$ = 120.1 ppm

3.46a
n = 1, Nitrile = axial
$^{13}C_{CN}$ = 120.2 ppm

3.114a
n = 2, Nitrile = axial
$^{13}C_{CN}$ = 120.2 ppm

3.39a
Nitrile = axial
$^{13}C_{CN}$ = 120.0 ppm

3.50b
n = 1, Nitrile = equatorial
$^{13}C_{CN}$ = 121.9 ppm

3.106b
n = 2, Nitrile = equatorial
$^{13}C_{CN}$ = 121.9 ppm

3.46b
n = 1, Nitrile = axial
$^{13}C_{CN}$ = 120.9 ppm

3.114b
n = 2, Nitrile = axial
$^{13}C_{CN}$ = 120.8 ppm

3.39b
Nitrile = equatorial
$^{13}C_{CN}$ = 121.7 ppm

Numbered structure ending with an "a" denotes the major diastereomer, while the letter "b" denotes the minor diastereomer.

The ^{13}C peak of the nitrile in spirocycle precursors showed a trend based on the nitrile's orientation as axial or equatorial. Compounds **3.50a**, **3.46a**, **3.39a**, **3.106a** and **3.114a** were all assumed to have axial nitriles since this placed the largest groups all equatorial (**Scheme 3.15**). These axial nitriles, fell between 119.2 to 120.2 ppm. For alkylation products **3.50b** and **3.106b**, the larger A-value of the phenyl ring,[46] as well as clean splitting patterns in ^{1}H NMR led to the conclusion of an equatorial nitrile as the one lowest energy conformation. Substrates **3.46b** and **3.114b**, were expected to produce axial

nitriles since this would place the larger N-Boc group equatorial.   A comparison of the axial

(**3.130**) and equatorial (**3.39b**) nitrile conformation revealed an unfavorable 1,3-diaxial

interaction between the axial methyl and nitrile groups in **3.130** (**Scheme 3.17**).   It is,

therefore, reasonable to believe that **3.39b** is the lower energy conformation of the two

considered. The identified equatorial nitriles all fell between 121.7 to 121.9 ppm. A similar

conclusion was reached by Fleming and Wei, who found that cyclohexanecarbonitriles

could have their nitrile assigned as axial or equatorial based on the ^{13}C chemical shift of the

nitrile. [47]   This suggests that ^{13}C NMR can be used on the related cyclic-aminonitrile systems

to assign the nitrile as axial or equatorial.

Scheme 3.17. Explanation of axial N-Boc in **3.39b**
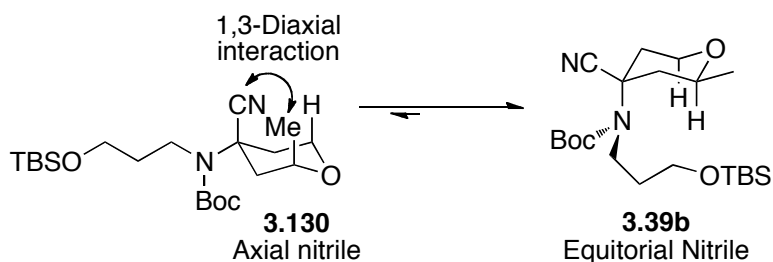
Conclusions

The usefulness of α–aminonitriles in the synthesis of substituted spiropyrrolidines

was examined and found to be highly diastereoselective. From the results of quenching

studies, it was hypothesized that the reaction mechanism was based on whether the

alkyllithium was axial or equatorial. The synthesis of spiropiperidines was explored and

found to cyclize in high diastereoselectivity, but with low yields.   Attempts to increase

yields by raising temperatures were minimally successful.   Further research into

azaspirocycles should give clearer insight into improving this methodology.

General Experimental and Laboratory conditions

All glassware was flame- or oven-dried and cooled under argon unless otherwise stated. All reactions and solutions were conducted under argon unless otherwise stated. All reagents were used as received unless otherwise stated. Toluene (PhMe), tetrahydrofuran (THF), dimethylformamide (DMF), dichloromethane (DCM), and methanol (MeOH) were degassed and dried by filtration through activated alumina under vacuum according to the procedure by Grubbs. [48] 1,3-Dimethyl-3,4,5,6-tetrahydro-2(1H)-pyrimidinone (DMPU), triethylamine (Et$_3$N), diisopropylamine (DIPA), acetonitrile (MeCN), and benzene (PhH) were distilled from CaH$_2$. LDA was titrated against *N*-benzylbenzamide according to the procedure by Duhamel and Plaquevent.[49] All reactions involving LiDBB were conducted with glass stirbars. Thin layer chromatography (TLC) was done on Watman (250 μm) 6 Å glass-backed silica gel plates and visualized using potassium permanganate or Dragondorf. Flash column chromatography (FCC) was performed according to the method by Still, Kahn, and Mitra using Fisher reagent silica gel 60 (230-400 mesh).[50]

Instrumentation

All data collected at ambient temperature unless noted. ^{1}H NMR spectra were taken at 500 MHz, calibrated using residual NMR solvent (CDCl$_3$ at 7.26 ppm), and interpreted on the δ scale. ^{13}C NMR spectra were taken at 125 MHz, calibrated using the NMR solvent (CDCl$_3$ at 77.16 ppm), and interpreted on the δ scale with the following abbreviations: s = singlet, d = doublet, t = triplet, q = quartet, pent = pentet, dd = doublet of doublets, dt = doublet of triplets, td = triplet of doublets, qt = quartet of doublets, tt = triplet of triplets, ddd = doublet of doublet of doublets, dddd = doublet of doublet of doublet of doublets, m =

multiplet, app = apparent, br = broad. IR taken by thin film. All diastereomeric ratios are from ^{1}H NMR unless otherwise stated. High resolution GCMS was run on an Agilent 7890A using a DB-5ms column (30 m by 0.25 mm, 0.25 μm coating) and masses detected with a Waters GCT Premier TOF mass spectrometer using chemical ionization (ammonia) as the detection method. Additional GCMS data were collected on a Thermoquest Trace GC 2000 series using a DB-5ms column (30 m by 0.25 mm, 0.25 μm coating) and masses detected with a ThermoFinnegan TraceMS+ mass spectrometer using electron as the detection method. Samples were prepared in DCM or ethyl acetate (0.1–1 mg /mL loading), mixed with a vortex mixer for 30 seconds and submitted for analysis.

LDA formation

LDA was prepared fresh before each experiment, example procedure:

To a –78 °C solution of DIPA (2.5 mL, 17.9 mmol, 1.15 equiv) in THF (8.2 mL), *n*-BuLi (6.5 mL, 15.6 mmol, 1 equiv) was added dropwise. The solution was allowed to warm to 0 °C in an ice bath, resulting in a ca. 1M solution. This was stirred for 20 minutes prior to use.

LiDBB/KDBB Formation in THF

LiDBB was prepared fresh before each experiment, example procedure:

LiDBB was prepared by adding 4,4'-di-*tert*-butylbiphenyl (DBB, 1.50 g, 5.64 mmol, 1 equiv), to a 50 mL flask, followed by evacuating and flame-drying. Once the DBB was melted, the flask was backfilled with argon and allowed to cool. An ice bath was applied and lithium wire (0.39 g, 56.4 mmol, 10 equiv) was clipped in under a stream of argon. THF (14 mL) was added and the solution turned green, darkening over for 5 hours at 0 °C. This resulted

in a nominal 0.4 M LiDBB solution. The potassium analog of LiDBB was prepared identically except potassium metal was used in place of lithium metal.

Synthesis of Dibromides
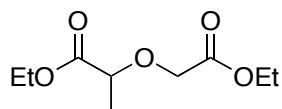
Ethyl 2-(2-ethoxy-2-oxoethoxy)propanoate (3.28) To a 0 °C solution of NaH (3.93 g, 98.1 mmol, 1.13 equiv.) in DMF (38 mL), ethyl lactate (10.0 mL, 87.9 mmol, 1 equiv) was added dropwise over 30 min. After gas evolution slowed, the ice bath was removed and the solution warmed to room temperature for 20 min. The resulting yellow solution was then cooled (0 °C) and ethyl bromoacetate (9.7 mL, 87.9 mmol, 1 equiv) added dropwise over 30 min during which a white precipitate formed. The solution was again warmed to room temperature and the dark orange solution stirred for 2 hours. After quenching with 20 mL water, the organic layer was extracted and aqueous layer washed with ether (3 x 40 mL). The combined organic layers were dried with $MgSO_4$ and concentrated *in vacuo*, giving a yellow oil which was vacuum distilled (pdt at 83–85 °C) to give the diester in 57% yield (10.2 g) as a clear oil.

^{1}H NMR (CDCl$_3$, 500 MHz) δ 4.28 (d, *J*= 16.5 Hz, 1H), 4.25-4.19 (m, 4H), 4.14 (q, *J*= 7.0, 7.0 Hz, 1H), 4.07 (d, *J*= 16.5 Hz, 1H), 1.48 (d, *J*= 7.0 Hz, 3H) 1.29 (app. dt, *J*= 7.3, 3,5 Hz, 6H); ^{13}C NMR (CDCl$_3$, 125 MHz) δ 172.7, 170.1, 75.2, 67.2, 61.2, 61.1, 18.6, 14.4, 14.3; IR (thin film) 2985, 2939, 1751cm^{-1}; HRMS (ESI) calcd for $C_9H_{16}O_5Na$ [M+Na]$^+$ 227.0895, found 227.0890

HO∕∖∕O∕∖OH
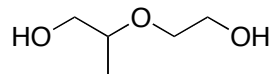
2-(2-hydroxyethoxy)propan-1-ol To a flask in an ice bath charged with LiAlH$_4$ (5.0 g, 150 mmol, 2.2 equiv), THF (128 mL) was added. After gas evolution stopped, ethyl 2-(2-ethoxy-2-oxoethoxy)propanoate (10.5 g, 66 mmol, 1 equiv) was added dropwise. The ice bath was removed and a reflux condenser added. The solution was refluxed for 18 hours, and then allowed to cool to room temperature. Following a Fieser workup, the pH was adjusted to 5 with 2 M HCl. The resulting slurry was filtered and the filtrate dried with MgSO$_4$. Concentration *in vacuo* gave quantitative yield (7.9 g) of the diol as a clear oil.

^{1}H NMR (CDCl$_3$, 500 MHz) δ 3.76-3.73 (m, 2H), 3.72 (app. q. *J*= 4.0 Hz, 1H), 3.65-3.59 (m, 2H), 3.56-3.47 (m, 2H), 2.69 (s, 2H), 1.14 (d, *J*= 6.0 Hz, 3H); ^{13}C NMR (CDCl$_3$, 125 MHz) δ 76.7, 70.2, 66.5, 62.3, 16.2; IR (thin film) 3386, 2935, 3877 cm^{-1}; HRMS (ESI) calcd for C$_5$H$_{12}$O$_3$Na [M+Na]$^+$ 143.0684, found 143.0683

Br∕∖∕O∕∖Br
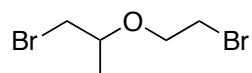
1-bromo-2-(2-bromoethoxy)propane (**3.29**) To a 0 °C solution of triphenylphosphine (18.8 g , 71.6 mmol, 2.5 equiv) in DCM (51 mL), Br$_2$ (3.8 mL, 72.8 mmol, 2.55 equiv) was added dropwise. To this orange solution, a mixture of Et$_3$N (12 mL, 85.9 mmol, 3 equiv) and 2-(2- hydroxyethoxy)propan-1-ol (3.4 g, 29 mmol, 1 equiv) in DCM (9 mL) was added dropwise at 0 °C. The solution was stirred overnight at room temperature. After quenching with Na$_2$S$_2$O$_{3(aq)}$ (180 mL), the reaction was diluted with H$_2$O (180 mL) and the aqueous layer extracted with Et$_2$O (3 x 180 mL). The combined organic layers were dried over MgSO$_4$, filtered and concentrated under vacuum to give a yellow oil. Flash column

chromatography (95:5 pentane/Et$_2$O) gave 1- bromo-2-(2-bromoethoxy) propane as a clear oil in 92% yield (7.9 g).

^{1}H NMR (CDCl$_3$, 500 MHz) δ 3.85-3.79 (m, 2H), 3.71 (sextet, *J*=5.6 Hz, 1H), 3.46 (t, *J*=6.2 Hz, 2H), 3.42 (dd, *J*=5.5, 5 Hz, 1H), 3.35 (dd, *J*=5.5, 5.0 Hz, 1H), 1.31 (d, *J*= 6 Hz, 3H); ^{13}C NMR (CDCl$_3$, 125 MHz) δ 75.9, 69.5, 36.3, 30.6, 19.2; IR (thin film) 2974, 2931, 2897, 2877, 2858 cm^{-1}; HRMS (CI) calcd for C$_5$H$_{14}$Br$_2$ON [M+NH$_4$]$^+$ 261.9442, found 261.9442
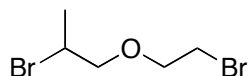
2-bromo-1-(2-bromoethoxy)propane To a 0 °C solution of triphenylphosphine (2.29 g, 8.56 mmol, 2.1 equiv), and KBr (740 mg, 6.11 mmol, 1.5 equiv) in DCM (7.5 mL), Br$_2$ (0.5 mL, 9.58 mmol, 2.35 equiv) was added dropwise. To this orange solution, a mixture of Et$_3$N (1.5 mL, 10.2 mmol, 2.5 equiv) and 1-(2- hydroxyethoxy)propan-2-ol (0.49 g, 4.08 mmol, 1 equiv) in DCM (7 mL) was added dropwise. The solution was stirred overnight at room temperature. After quenching with Na$_2$S$_2$O$_{3(aq)}$ (25 mL), the reaction was diluted with 25 mL Et$_2$O and the aqueous layer extracted 3 x 25 mL Et$_2$O. The combined organic layers were dried over MgSO$_4$, giving a yellow oil. Flash column chromatography (8:1 pentane/Et$_2$O) gave 1-bromo-2-(2-bromoethoxy)propane as a clear oil in 78% yield (811 mg). The analytical data matched those previously reported.[51]
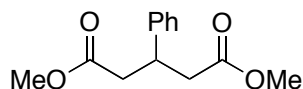

Dimethyl 3-phenylpentanedioate (**3.31**) Prepared from benzaldehyde as described by Leonardi *et al.*[52] The analytical data matched those previously reported.
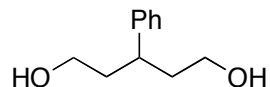
3-phenylpentane-1,5-diol Prepared from dimethyl 3-phenylpentanedioate as described by López-Cortina *et al.*[19] The analytical data matched those previously reported.
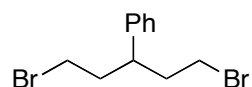

(1,5-dibromopentan-3-yl)benzene (**3.32**) Prepared from dimethyl 3-phenylpentanedioate as described by López-Cortina *et al.*[19] The analytical data matched those previously reported.
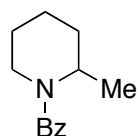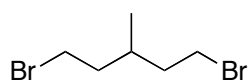

(2-methylpiperidin-1-yl)(phenyl)methanone (**3.35**) Prepared from 2-methylpiperidine as described by Nguyen and Cartledge.[20] The analytical data matched those previously reported.
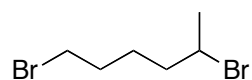

1,5-dibromohexane (**3.37**) Prepared from (2-methylpiperidin-1-yl)(phenyl)methanone as described by Nguyen and Cartledge.[20] The analytical data matched those previously reported.
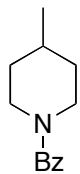
(4-methylpiperidin-1-yl)(phenyl)methanone (**3.36**) Prepared from 4-methylpiperidine as described by Nguyen and Cartledge.[20] The analytical data matched those previously reported.


1,5-dibromo-3-methylpentane (**3.38**) Prepared from (4-methylpiperidin-1-yl)(phenyl)methanone as described by Nguyen and Cartledge.[20] The analytical data matched those previously reported.
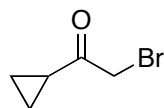

2-bromo-1-cyclopropylethanone (**3.73**) Prepared from cyclopropyl methyl ketone as described by Zhdanko and Nenajdenko.[53] The analytical data matched those previously reported.
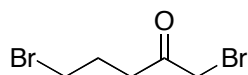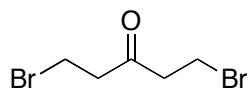

1,5-Dibromopentan-2-one (**3.74**) Prepared from 2-bromo-1-cyclopropylethanone as described by Weidong *et. al.*[54] The analytical data matched those previously reported.
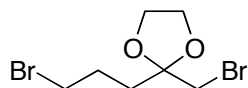
2-(bromomethyl)-2-(3-bromopropyl)-1,3-dioxolane (**3.75**) To a solution of 1,5-dibromopentan-2-one (2.17 g, 8.90 mmol, 1 equiv) in toluene (33mL), ethylene glycol (3.0 mL, 54.3 mmol, 6.1 equiv) and p-TSA (0.182 g, 0.89 mmol, 0.1 equiv) were added. A Dean-Stark trap, reflux condenser and oil bath were added and the reaction mixture heated to reflux for 18 hours. After cooling to RT, the mixture was diluted with H_2O (75 mL), sat. $NaHCO_3$ (12 mL), and DCM (75 mL). The organic layer was separated and the aqueous layer was washed with DCM (3x 30 mL). The combined organic layers were dried over $MgSO_4$, filtered, and concentrated *en vacuo* to give a yellow oil. Purification by FCC (2:3 DCM/hexanes) gave a 84% (2.14 g) yield of a light yellow oil. The spectral data matched those previously reported.[33]
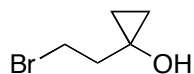
1-(2-bromoethyl)cyclopropanol (**3.77**) Prepared from methyl 3-bromopropionate as described by Denmark and Marcin.[55]   The analytical data matched those previously reported.
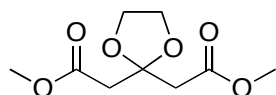

1,5-dibromopentan-3-one (**3.78**) Prepared from 1-(2-bromoethyl)cyclopropanol as described by Denmark and Marcin.[55]   The analytical data matched those previously reported.

TMSO⌒OTMS
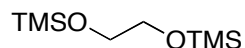
**2,2,7,7-Tetramethyl-3,6-dioxa-2,7-disilaoctane**.

Prepared from ethylene glycol as described by Noyori *et. al.*[38] The analytical data matched those previously reported.


Dimethyl 2,2'-(1,3-dioxolane-2,2-diyl)diacetate. (**3.81**) To a 0 °C solution of dimethyl 3-oxopentanedioate (0.26 mL, 1.80 mmol, 1 equiv) in DCM (33 mL), 2,2,7,7-tetramethyl-3,6-dioxa-2,7-disilaoctane (0.643 g, 3.11 mmol, 1.73 equiv) and TMSOTf (0.2 mL, 1.08 mmol, 0.6 equiv) were added. After stirring for 1 day at 0 °C, the temperature was increased to 15 °C and stirred for 1 additional day. The mixture was quenched with 1.8 mL pyridine and 7 mL sat. NaHCO$_3$. After diluting with 30 mL DCM and 10 mL H$_2$O, the organic layer was removed and the aqueous layer washed (3x 10 mL DCM). Drying with MgSO$_4$ and concentration gave the crude product. Flash column chromatographed (5:2 Hexanes/EtOAc) yielded the monoprotected product in 93% yield (2.14 g) as a light yellow oil. The analytical data matched those previously reported.[56]
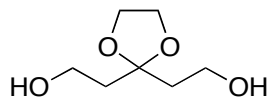
2,2'-(1,3-dioxolane-2,2-diyl)diethanol Prepared from dimethyl 2,2'-(1,3-dioxolane-2,2-diyl)diacetate as described by Davenport and Regan.[57]   The analytical data matched those previously reported.
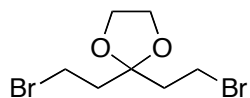
2,2-Bis(2-bromoethyl)-1,3-dioxolane (**3.79**). To a 0 °C solution of PPh$_3$ (358 mg, 1.36 mmol, 2.2 equiv) in DCM (1.1 mL) was added bromine (0.75 mL, 1.45 mmol, 2.35 equiv) dropwise. The resulting orange suspension was left on ice for 25 min, warmed to room temperature over 20 min and then cooled to 0 °C. To that suspension was added a solution of 2-(2-(hydroxymethyl)-1,3-dioxolan-2-yl) ethanol (0.1 g, 0.627 mmol, 1 equiv) and Et$_3$N (0.22 mL, 1.54 mmol, 2.5 equiv) in DCM (0.2 mL) dropwise. After 2 h at 0 °C, the solution was stirred at RT for 2 days. The reaction was quenched with 1 mL of sat. Na$_2$S$_2$O$_3$, and diluted with 2 mL H$_2$O, and 6 mL of diethyl ether. The organic layer was removed and the aqueous layer was extracted with diethyl ether (2 mL x 3). The combined organic layers were dried over MgSO$_4$, filtered, and concentrated *en vacuo* to give a yellow residue. The residue was repeatedly suspended with pentanes and filtered until a yellow solid was obtained. Flash column chromatography (9:1 pentane/ether) gave 158mg (90%) as a white solid. mp = 50–51 °C. The spectral data matched those previously reported.[58]
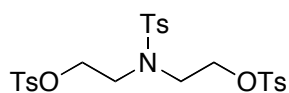

(Tosylazanediyl)bis(ethane-2,1-diyl) bis(4-methylbenzenesulfonate) (**3.83**)

Prepared from diethanolamine as described by Chak and McAuley.[40] The analytical data matched those previously reported.
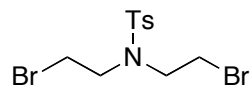
N,N-bis(2-bromoethyl)-4-methylbenzenesulfonamide (**3.84**) Prepared from (Tosylazanediyl)bis(ethane-2,1-diyl) bis(4-methylbenzenesulfonate) as described by Chak and McAuley.[40] The analytical data matched those previously reported.
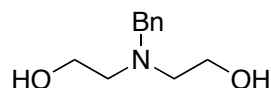
2,2'-(benzylazanediyl)diethanol (**3.85**)

Prepared from diethanolamine as described by Dong *et. al*.[59] The analytical data matched those previously reported.
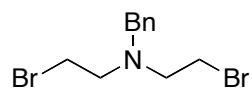
N-benzyl-2-bromo-N-(2-bromoethyl)ethanamine (**3.86**)

Prepared from 2,2'-(benzylazanediyl)diethanol as described by Dong *et. al*.[58] The analytical data matched those previously reported.

Synthesis of Aminonitriles
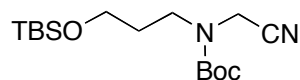
***Tert*-butyl (3-((*tert*-butyldimethylsilyl)oxy)propyl)(cyanomethyl) carbamate** (**3.11**).

To a 0 °C solution of NaH (6.1 g, 151 mmol, 2.3 equiv) in THF (110 mL), 3-aminopropan-1-ol (5 mL, 65.4 mmol, 1 equiv) was added dropwise and stirred for 5 min. The solution was

warmed to room temperature for 20 min, then cooled back down to 0 °C.   TBSCl (12.8 g, 85.0 mmol, 1.3 equiv) was then added. The ice bath was removed and the solution left at room temperature overnight. After quenching with 5 mL H_2O, the solution was diluted with DCM (60 mL), brine (30 mL), H_2O (30 mL).   The organic layer was removed and the aqueous layer extracted with DCM (4 x 50 mL).   The combined organic layers were dried with $MgSO_4$ and concentrated to give 12.4 g of a yellow oil. Quantitative conversion was assumed.

To this crude reaction mixture (12.4 g), a solution of chloroacetonitrile (8.5 mL, 134 mmol, 2 equiv) and potassium carbonate (18.1 g, 130 mmol, 2 equiv) in acetonitrile (150 mL) was added. The solution was refluxed for 10 hours. Following filtration through a 3 cm pad of Celite, the solution was concentrated to give 17.25 g as a yellow oil. Again the reaction was assumed to be quantitative.

To the previous crude reaction mixture, Boc_2O (26.1 g, 119 mmol, 2 equiv) was added and the reaction stirred overnight at room temperature.   The solution was then placed under vacuum to remove *tert*-butanol, giving 37.1 g of a yellow oil. Flash column chromatography (9:1 hexanes/ether to 3:1 hexanes/ether) gave the desired product in 80% yield (17.2 g). The analytical data matched those previously reported.[60]
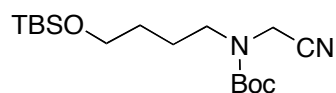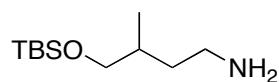

***Tert*-butyl (4-((*tert*-butyldimethylsilyl)oxy)butyl)(cyanomethyl)carbamate** (**3.105**). To a 0 °C solution of NaH (0.98 g, 24.4 mmol, 2.2 equiv) in THF (15 mL), 4-aminobutan-1-ol (1 mL, 11.1 mmol, 1 equiv) was added dropwise and stirred for 5 min. The solution was

warmed to room temperature for 20 min, then cooled back down to 0 °C. TBSCl (2.01 g, 13.3 mmol, 1.2 equiv) was then added. The ice bath was removed and the solution left at room temperature overnight. After quenching with 5 mL H_2O, the solution was diluted DCM (30 mL), brine (30 mL), H_2O (30 mL).   The organic layer was removed and the aqueous layer extracted with DCM (4 x 50 mL).   The combined organic layers were dried with $MgSO_4$ and concentrated to give 2.5 g of a yellow oil. Quantitative conversion was assumed.

To this crude reaction mixture (2.5 g), a solution of chloroacetonitrile (1.7 mL, 22.8 mmol, 2 equiv) and potassium carbonate (3.07 g, 22.8 mmol, 2 equiv) in acetonitrile (21 mL) was added. The solution was refluxed for 10 hours. Following filtration through a 3 cm pad of Celite, the solution was concentrated to give a yellow oil. Again the reaction was assumed to be quantitative.

To the previous crude reaction mixture, Boc_2O (3.6 g, 16.6 mmol, 1.5 equiv) was added and the reaction stirred overnight at room temperature.   The solution was then placed under vacuum to remove *tert*-butanol, giving 3.0 g of a yellow oil. Flash column chromatography (8:1 hexanes/ethyl acetate) gave the desired product in 42% yield (1.35 g). The analytical data matched those previously reported.[59]
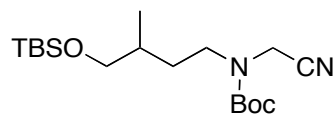

4-((*tert*-butyldimethylsilyl)oxy)-3-methylbutan-1-amine To a 0 °C solution of NaH (0.83 g, 20.6 mmol, 2.2 equiv) in THF (15 mL), 4-amino-2-methylbutan-1-ol (1 mL, 9.39 mmol, 1 equiv) was added dropwise and stirred for 5 min. The solution was warmed to

room temperature for 20 min, then cooled back down to 0 °C.   TBSCl (1.70 g, 11.2 mmol, 1.2 equiv) was then added. The ice bath was removed and the solution left at room temperature overnight. After quenching with 5 mL H_2O, the solution was diluted with DCM (60 mL), brine (30 mL), H_2O (30 mL).   The organic layer was removed and the aqueous layer extracted with DCM (4 x 50 mL).   The combined organic layers were dried with $MgSO_4$ and concentrated to give 2.5 g of a yellow oil. This was taken on crude.   The analytical data matched those previously reported.[61]
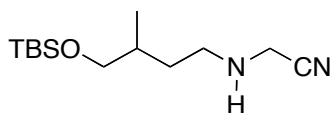
2-((4-((*tert*-butyldimethylsilyl)oxy)-3-methylbutyl)amino)acetonitrile To a solution of 4-((*tert*-butyldimethylsilyl)oxy)-3-methylbutan-1-amine (2.25 g, 10.4 mmol, 1 equiv) in acetonitrile (24 mL), chloroacetonitrile (1.6 mL, 21.2 mmol, 2 equiv) and potassium carbonate (2.86 g, 21.2 mmol, 2 equiv) was added. The solution was refluxed for 10 hours. Following filtration through a 3 cm pad of Celite, the solution was concentrated to give 3.1 g of a yellow oil. This was taken on crude. An analytical sample was purified by flash column chromatography (97:3 DCM/methanol with 1% Et_3N).

^{1}H NMR ($CDCl_3$, 500 MHz) δ 3.50 (s, 1H), 3.47-3.35 (m, 2H), 2.85-2.70 (m, 2H), 1.75-1.59 (m, 2H), 1.31 (dddd, J = 13.2, 8.5, 7.9, 5.5 Hz, 1H), 1.48 (s, 1H), 0.91 (d, J = 3.2 Hz, 3H), 0.89 (s, 9H), 0.04 (s, 6H); ^{13}C NMR ($CDCl_3$, 125 MHz) δ 118.0, 68.2, 47.0, 37.4, 33.9, 33.2, 26.1, 18.4, 16.8, -5.3; IR (thin film) 3334, 2955, 2929, 2887, 2856, 2234 cm^{-1}; HRMS (ESI) calcd for $C_{13}H_{28}N_2OSiNa$ [M+Na]+ 279.1869, found 279.1879

Tert-butyl (4-((_tert_-butyldimethylsilyl)oxy)-3-methylbutyl)(cyanomethyl)carbamate

(**3.124**) To the previous crude reaction mixture (3.0 g), Boc$_2$O (3.2 g, 14.7 mmol, 1.5 equiv) was added and the reaction stirred overnight at room temperature. The solution was then placed under vacuum to remove _tert_-butanol, giving 4.3 g of a yellow oil. Flash column chromatography (9:1 hexanes/ethyl acetate) gave the desired product in 35% yield over 3 steps (1.25 g).

^{1}H NMR (CDCl$_3$, 500 MHz) δ 4.35-3.92 (br m, 2H), 3.43 (td, _J_ = 9.7, 5.7 Hz, 2H), 3.40-3.30 (m, 1H), 1.80-1.65 (m, 1H), 1.64-1.54 (m, 1H) 1.48 (s, 9H), 1.37-1.27 (m, 1H), 0.91 (d, _J_ = 7.0 Hz, 3H), 0.89 (s, 9H), 0.03 (s, 6H); ^{13}C NMR (CDCl$_3$, 125 MHz) δ 154.8, 153.9*, 116.3, 81.5 (br), 68.0, 45.8, 35.5*, 34.9*, 33.5, 31.3 (br) 29.8, 28.3, 26.0, 18.4, 16.6, -5.3, -5.3*; IR (thin film) 2956, 2931, 2282, 1702 cm^{-1};HRMS (ESI) calcd for C$_{18}$H$_{36}$N$_2$O$_3$SiNa [M+Na]$^+$ 379.2393, found 379.2400

Double Alkylation Products

Double Alkylation: General Procedure A:

To a solution of nitrile (1.0 equiv) and dibromide (1.5 equiv) in 1:1 DMPU/THF to make a 0.1 M solution LDA was added (1.0 M, 2.5 equiv) dropwise over 20 min at –78 °C. After 1 h, the solution was slowly warmed to 0 °C over 4 h, then cooled to –78 °C followed by addition of LDA (1 equiv). After 15 min the solution was slowly warmed to 0 °C, quenched with saturated aq. NH$_4$Cl and poured on Et$_2$O. The organic layer was separated and the aqueous layer was extracted with Et$_2$O (3x). The combined organic layers were dried over MgSO$_4$

and concentrated *in vacuo.* Purification by flash column chromatography gave the title compound.

Double Alkylation: General Procedure B:

To a solution of nitrile (1.0 equiv) and dibromide (1.5 equiv) in 1:1 DMPU/THF to make a 0.1 M solution LDA was added (1.0 M, 2.5 equiv) dropwise over 20 min at –40 °C. After 1 h, the solution was slowly warmed to 0 °C over 4 h, then cooled to –40 °C followed by addition of LDA (1 equiv). After 15 min the solution was slowly warmed to 0 °C, quenched with saturated aq. NH_4Cl and poured on Et_2O. The organic layer was separated and the aqueous layer was extracted with Et_2O (3x). The combined organic layers were dried over $MgSO_4$ and concentrated *in vacuo.* Purification by flash column chromatography gave the title compound.

Double Alkylation: General Procedure C:

To a solution of nitrile (1.0 equiv) and dibromide (1.5 equiv) in 1:1 DMPU/THF to make a 0.1 M solution LDA was added (1.0 M, 5 equiv) dropwise over 60 min at –78 °C. The reaction was monitored by TLC until all of the nitrile was consumed. The reaction was slowly warmed to 0 °C, quenched with saturated aq. NH_4Cl and poured on Et_2O. The organic layer was separated and the aqueous layer was extracted with Et_2O (3x). The combined organic layers were dried over $MgSO_4$ and concentrated *in vacuo.* Purification by flash column chromatography gave the title compound.

**Double Alkylation: General Procedure D:**

To a solution of nitrile (1.0 equiv) and dibromide (1.5 equiv) in 1:1 DMPU/THF to make a 0.1 M solution LDA was added (1.0 M, 5 equiv) dropwise over 60 min at 0 °C. The reaction was monitored by TLC until all of the nitrile was consumed.   The reaction was quenched with saturated aq. NH$_4$Cl and poured on Et$_2$O. The organic layer was separated and the aqueous layer was extracted with Et$_2$O (3x). The combined organic layers were dried over MgSO$_4$ and concentrated *in vacuo.* Purification by flash column chromatography gave the title compound.
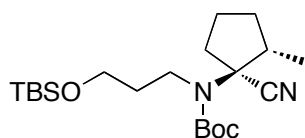
***Tert*-butyl(3-((*tert*-butyldimethylsilyl)oxy)propyl)(1-cyano-2methylcyclopentyl) carbamate (3.40)** Following general procedure A, FCC (7:1 Hexanes/EtOAc) yielded 155 mg (64%, >95:5 dr) as a clear oil. Performed on a 0.61 mmol scale.

^{1}H NMR (CDCl$_3$, 500 MHz) δ 3.69–3.62 (m, 1H), 3.62–3.52 (m, 2H), 3.26 (ddd, *J* = 15.0, 10.0, 5.0 Hz, 1H), 2.61 (q, *J* = 7.5Hz, 1H), 2.58–2.50 (m, 1H), 2.21 (ddd, *J* = 14.5, 9.5, 5.0 Hz, 1H), 1.99–1.90 (m, 1H), 1.90–1.67 (m, 4H), 1.63–1.53 (m, 1H), 1.52 (s, 9H), 1.25 (d, *J* = 6.5, 3H), 0.90 (s, 9H), 0.05 (s, 6H); ^{13}C NMR (CDCl$_3$, 125 MHz) δ 154.9, 120.3, 81.6, 66.4, 60.8, 42.8, 42.1, 38.6, 32.9, 31.7, 28.5, 26.0, 18.3, 17.3, –5.3; IR (thin film) 2955, 2917, 2861, 2231, 1701 cm^{-1}; HRMS (ESI) calcd for C$_{21}$H$_{40}$N$_2$O$_3$SiNa [M+Na]$^+$ 419.2706, found 419.2691
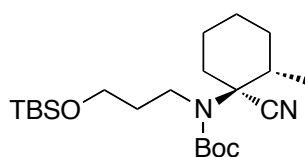
***Tert*-butyl(3-((*tert*-butyldimethylsilyl)oxy)propyl)(1-cyano2methylcyclohexyl)**

carbamate (**3.43**) Following general procedure C, FCC (11:1 hexanes/EtOAc) gave 546 mg

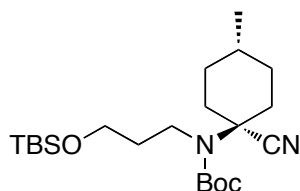(62%, >95:5 dr) as a clear oil. Performed on 2.1 mmol scale.

^{1}H NMR (CDCl$_3$, 500 MHz) δ 3.69–3.50 (m, 2H), 3.51 (app t, *J* = 7.3 Hz, 2H), 2.81 (br s, 1H),

2.42 (br s, 1H), 2.01 (2, 1H), 1.92–1.58 (m, 6H), 1.51–1.37 (m, 10H), 1.27 (app qt, *J* = 13.0,

3.5 Hz, 1H), 1.01 (d, *J* = 6.5 Hz, 3H), 0.90 (s, 9H), 0.05 (s, 6H); ^{13}C NMR (CDCl$_3$, 125 MHz) δ

154.0, 118.0, 80.9, 61.1, 36.4, 33.4, 32.4, 28.5, 26.1, 25.0, 23.9, 18.5, 17.2, -5.2 ;   IR   (thin

film) 2929, 2857, 2238, 1696 cm^{-1};HRMS (ESI) calcd for C$_{22}$H$_{42}$N$_2$O$_3$SiNa [M+Na]$^+$ 433.2863,

found 433.2856

***Tert*-butyl(3-((*tert*-butyldimethylsilyl)oxy)propyl)(1-cyano-4methylcyclohexyl)**

carbamate (**3.46**) Following general procedure C, FCC (14:1 hexanes/EtOAc) gave 1.1 g

(75%, 2.7:1 dr) as a clear oil. Performed on 3.5 mmol scale.

3.46a (major isomer): ^{1}H NMR (CDCl$_3$, 500 MHz) δ 3.59 (t, *J* = 6.0 Hz, 2H), 3.32 (app t, *J* =

7.5 Hz, 2H), 2.39 (d, *J* = 12.5 Hz, 2H), 1.92–1.79 (m, 2H), 1.79–1.65 (m, 3H), 1.65–1.51 (m,

2H), 1.51–1.32 (m, 11H), 0.93 (d, *J* = 6.0 Hz, 3H), 0.87 (s, 9H), 0.02 (s, 6H); ^{13}C NMR (CDCl$_3$,

125 MHz) δ 154.5, 120.2, 81.3, 62.6, 44.2, 34.9, 31.8, 30.1, 29.1, 28.4, 27.3, 26.0, 21.7, 18.3, -

5.3;   IR   (thin   film)   2953,   2928,   2858,   2253,   1698   cm^{-1};   HRMS   (ESI)   calcd   for

C$_{22}$H$_{42}$N$_2$O$_3$SiNa [M+Na]$^+$ 433.2863, found 433.2874
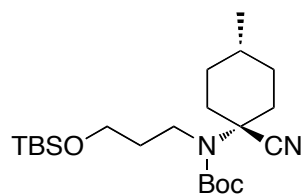
3.46b (minor isomer): ^{1}H NMR (CDCl$_3$, 500 MHz) δ 3.60 (t, *J* = 6.0 Hz, 2H), 3.35 (app t, *J* = 6.5 Hz, 2H), 2.17 (app t, *J* = 11.5 Hz, 2H), 2.09–2.00 (m, 2H), 1.79–1.65 (m, 3H), 1.65–1.51 (m, 2H), 1.51–1.32 (m, 11H), 0.95 (d, *J* = 7.0 Hz, 3H), 0.87 (s, 9H), 0.02 (s, 6H); ^{13}C NMR (CDCl$_3$, 125 MHz) δ 154.8, 120.8, 81.3, 62.7, 57.8, 44.6, 31.6, 30.9, 30.3, 28.4, 27.2, 26.0, 18.8, 18.3, -5.3; IR (thin film) 2953, 2928, 2858, 2253, 1698 cm^{-1}; HRMS (ESI) calcd for C$_{22}$H$_{42}$N$_2$O$_3$SiNa [M+Na]$^+$ 433.2863, found 433.2874
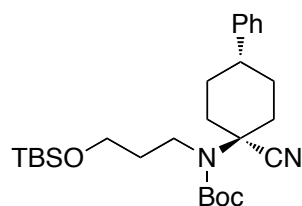

***Tert*-butyl(3-((*tert*-butyldimethylsilyl)oxy)propyl)(1-cyano-4-phenylcyclohexyl) carbamate (3.50)** Following general procedure C, FCC (97:3 Hexanes/EtOAc) yielded 140 mg (78%, 3:1 dr) as a clear oil. Performed on a 2.1 mmol scale. The analytical data matched those previously reported. [62]
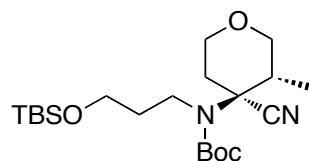

***Tert*-butyl (3-((*tert*-butyldimethylsilyl)oxy)propyl)(4-cyano-3-methyltetrahydro-2*H*-pyran-4-yl)carbamate (3.54)** Following general procedure A, FCC (7:1 Hexanes/EtOAc) yielded 148 mg (61%, >95:5 dr) as a clear oil. Performed on a 0.61 mmol scale.

^{1}H NMR (CDCl$_3$, 500 MHz) δ 3.97 (dd, *J* = 7.5, 4.5 Hz, 1H), 3.83 (dd, *J* = 8.0, 4.3 Hz, 1H), 3.72 (dt, *J* = 11.5, 1.7 Hz, 1H), 3.68–3.51 (m, 3H), 3.40 (t, *J* = 11.5, 1.7 Hz, 2H), 2.86 (br s, 1H), 2.46 (br s, 1H), 2.11 (d, *J* = 13.5 Hz, 1H), 1.88–1.74 (m, 2H), 1.48 (s, 9H), 0.96 (d, *J* = 6.5 Hz, 1H), 0.89 (s, 9H), 0.42 (s, 6H) ;^{13}C NMR (CDCl$_3$, 125 MHz *denotes minor rotamer) δ 154.2, 117.4, 18.6, 70.9, 65.3, 61.0, 44.9, 35.9, 34.6, 33.5, 28.6*, 28.5, 26.0, 18.4, 21.1, –5.3, –5.4*; IR (thin film) 2958, 2931, 2858, 1701 cm-1; HRMS (ESI) calcd for C$_{21}$H$_{40}$N$_2$O$_4$SiNa [M+Na]$^+$ 435.2655, found 435.2649
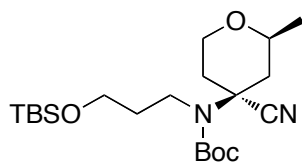

Tert-Butyl (3-((_tert_-butyldimethylsilyl)oxy)propyl)(4-cyano-2-methyltetrahydro-2H-pyran-4-yl)carbamate (**3.39**) Following general procedure A, FCC (10:1 Hexanes/EtOAc) yielded 170 mg (70%, 1.2:1 dr) as a clear oil. Performed on a 0.61 mmol scale.

3.39a (minor isomer): ^{1}H NMR (CDCl$_3$, 500 MHz) δ 3.85 (app d, *J* = 12 Hz, 1H), 3.64–3.55 (m, 4H), 3.53–3.42 (m, 2H), 2.74 (app t, *J* = 16.0 Hz, 2H), 2.09–2.06 (m, 1H), 1.50 (s, 9H), 1.18 (d, *J* = 6.5 Hz, 3H), 0.88 (s, 9H), 0.44 (s, 6H); ^{13}C NMR (CDCl$_3$, 125 MHz *denotes minor rotamer) δ 155.6, 121.7, 82.1, 68.4, 62.6, 60.7, 52.0, 43.2, 41.3, 34.5, 31.4, 28.4, 26.0, 25.8*, 21.3, 18.4, –5.3; IR (thin film) 2954, 2931, 2858, 1705 cm-1; HRMS (ESI) calcd for C$_{21}$H$_{40}$N$_2$O$_4$SiNa [M+Na]$^+$ 435.2655, found 435.2657
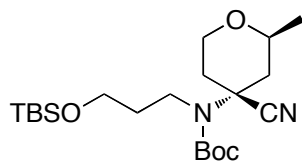
3.39b (major isomer): ^{1}H NMR (CDCl$_3$, 500 MHz) δ 4.02 (dd, *J* = 9.0, 3.5 Hz 1H), 3.86–3.80

(m, 2H), 3.61 (t, J = 5.5Hz, 2H), 3.41 (t, J = 7.8Hz, 2H), 2.48 (d, J = 13.0 Hz, 1H), 2.43 (d, J = 13.0 Hz, 1H), 1.87 (dt, J = 12.5, 4.5 Hz, 1H), 1.74 (pent, J = 6.0 Hz, 2H), 1.55 (app t, J = 11.5 Hz, 1H), 1.50 (s, 9H), 1.24 (d, J = 6.5 Hz, 3H), 0.88 (s, 9H), 0.41 (s, 6H); ^{13}C NMR (CDCl$_3$, 125 MHz *denotes minor rotamer) δ 154.6, 120.0, 81.9, 70.6, 64.5, 60.6, 55.8, 42.1, 41.4, 35.1, 33.4, 28.5, 28.4*, 26.0, 25.8*, 21.5, 18.4, −5.3; IR (thin film) 2954 , 2931, 2858, 1705; HRMS (ESI) calcd for C$_{21}$H$_{40}$N$_2$O$_4$SiNa [M+Na]$^+$ 435.2655, found 435.2657
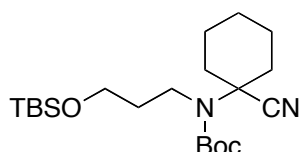
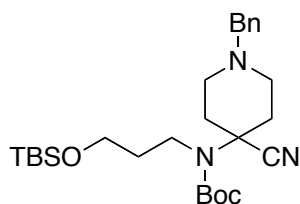**Tert-butyl(3-((tert-butyldimethylsilyl)oxy)propyl)(1-cyanocyclohexyl)carbamate**

(**3.87**) Following general procedure D, FCC (93:7 hexanes/EtOAc) yielded 1.39 g (73%) of a clear oil. Performed on 4.9 mmol scale. The analytical data matched those previously reported. [60]

Tert-butyl(1-benzyl-4-cyanopiperidin-4-yl)(3-((tert-butyldimethylsilyl)oxy)propyl)

carbamate (**3.89**) Following general procedure C, FCC (5:1 Hexanes/EtOAc) yielded 100 mg (48%) as a clear oil. Performed on a 0.43 mmol scale.

^{1}H NMR (CDCl$_3$, 500 MHz) δ 7.36-7.24 (m, 5H), 3.61 (t, J=5.8 Hz, 2H), 3.54 (s, 2H), 3.41 (t, J=7.7 Hz, 2H), 2.91 (d, J=6.2 Hz, 2H), 2.51-2.38 (m, 4H), 1.95 (app dt, J=12.0, 3.5 Hz, 2H),

1.85-1.72 (m, 2H), 1.50, (s, 9H), 0.88 (s, 9H), 0.04 (s, 6H); ^{13}C NMR (CDCl$_3$, 125 MHz) δ

154.7, 138.3, 129.1, 128.4, 127.3, 120.0, 81.8, 62.6, 60.7, 56.3, 50.4, 41.6, 34.9, 33.4, 28.5,

26.0, 18.3, -5.3; IR (thin film) 3061, 3025, 2952, 2930, 2856, 2816, 2235, 1702 cm^{-1}; HRMS

(ESI) calcd for C$_{27}$H$_{45}$N$_3$O$_3$SiNa [M+Na]$^+$ 510.3128, found 510.3138
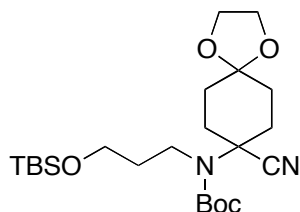
***Tert*-butyl(3-((*tert*-butyldimethylsilyl)oxy)propyl)(8-cyano1,4dioxaspiro[4.5]decan-8-yl) carbamate** (**3.93**) Following general procedure B, FCC (12:1 to 3:1 hexanes/EtOAc)

gave 164 mg (62%) as a clear oil. Performed on 0.62 mmol scale.

^{1}H NMR (CDCl$_3$, 500 MHz) δ 3.99–3.88 (m, 4H), 3.61 (t, J = 6.0 Hz, 2H), 3.42 (app t, J = 7.7

Hz, 2H), 2.49–2.42 (m 2H), 2.10–1.95 (m, 4H), 1.82–1.73 (m, 4H), 1.50 (s, 9H), 0.89 (s, 9H),

0.44 (s, 6H); ^{13}C NMR (CDCl$_3$, 125 MHz) δ 154.7, 119.8, 106.8, 81.7, 64.8, 64.4, 60.8, 56.7,

41.8, 33.5, 32.6, 32.1, 28.5, 26.0, 18.4, –5.3; IR (thin film) 2955, 2886, 2858, 1701 cm^{-1};

HRMS (ESI) calcd for C$_{23}$H$_{42}$N$_2$O$_5$SiNa [M+Na]$^+$ 454.2863, found 454.2760.
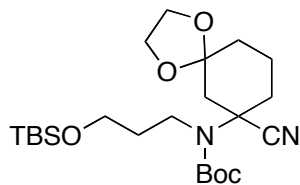
***Tert*-butyl(3-((*tert*-butyldimethylsilyl)oxy)propyl)(7-cyano-1,4dioxaspiro[4.5]decan-7-yl)carbamate** (**3.97**) Following general procedure B, FCC (5:1 hexanes/EtOAc) gave
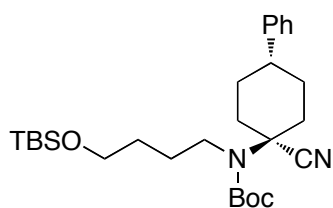
152 mg (57%) as a clear oil. Performed on 0.61 mmol scale.

^{1}H NMR (CDCl$_3$, 500 MHz) δ 4.12–4.05 (m, 1H), 4.05–3.08 (m, 1H), 3.96–3.88 (m, 2H), 3.61

(app dt, J = 5.7, 1.3 Hz, 2H), 3.45 (app t, J = 8.0 Hz, 2H), 2.79 (dt, J = 13.5, 2.3 Hz, 1H), 2.35 (br d, J = 11.5 Hz, 1H), 2.19–1.96 (m, 1H), 1.94–1.85 (m, 2H), 1.81 (d, J = 13.5 Hz, 2H), 1.78–1.70 (m, 2H), 1.57–1.53 (m, 1H), 1.50 (s, 9H), 0.89 (s, 9H), 0.43 (s, 6H); ^{13}C NMR (CDCl$_3$, 125 MHz) δ 154.5, 120.5, 107.3, 81.7, 65.9, 65.1, 64.5, 56.9, 42.2, 42.1, 34.5, 34.5, 33.4, 28.5, 26.0, 20.4, 18.4, –5.3; IR (thin film) 2956, 2884, 2863, 1700 cm^{-1}; HRMS (ESI) calcd for C$_{23}$H$_{42}$N$_2$O$_5$SiNa [M+Na]$^+$ 454.2863, found 454.2765.

Tert-butyl(4-((_tert_-butyldimethylsilyl)oxy)butyl)(1-cyano-4-phenylcyclohexyl) carbamate (3.106) Following general procedure C, FCC (93:7 Hexanes/EtOAc) yielded 376 mg (79%, 3.6:1 dr) as a clear oil. Performed on a 0.98 mmol scale.

3.106a (major isomer): ^{1}H NMR (CDCl$_3$, 500 MHz) δ 7.34-7.29 (m, 2H), 7.26-7.19 (m, 3H), 3.63 (t, J = 6.3 Hz, 2H), 3.40 (t, J=7.8 Hz, 2H), 2.55 (app br d, J=10.0 Hz, 3H), 2.05-1.88 (m, 6H), 1.68-1.61 (m, 2H), 1.52 (s, 9H) 1.51-1.47 (m, 2H), 0.90 (s, 9H). 0.57 (m, 6H); ^{13}C NMR (CDCl$_3$, 125 MHz) δ 154.6, 145.4, 128.7, 127.0, 126.6, 120.1, 81.6, 62.6, 57.8, 44.4, 43.2, 35.1, 31.1, 30.2, 28.5, 27.4, 26.1, 18.4, -5.2; IR (thin film) 3028, 2929, 2860, 2248, 1695 cm^{-1}; HRMS (ESI) calcd for C$_{28}$H$_{46}$N$_2$O$_3$SiNa [M+Na]$^+$ 509.3175, found 509.3169
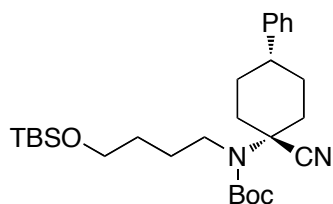
3.106b (minor isomer): ^{1}H NMR (CDCl$_3$, 500 MHz) δ 7.35-7.29 (m, 2H), 7.26-7.18 (m, 3H), 3.60 (t, *J*=6.3 Hz, 2H), 3.40 (br t, *J*=8.0 Hz, 2H) 2.81(tt, *J*=8.5, 4.0 Hz, 1H), 2.59 (br d, *J*=9.0 Hz, 2H), 2.08 (ddd, *J*=13.5, 10.5, 3.0Hz, 2H), 2.04-1.95 (m, 2H), 1.84 (app q, *J*=11.2 Hz, 2H), 1.68-1.62 (m, 2H), 1.51 (s, 9H), 1.50-1.45 (m, 2H), 0.88 (s, 9H), 0.35 (s, 6H); ^{13}C NMR (CDCl$_3$, 125 MHz) δ 155.4, 144.6, 128.7, 126.9, 126.4, 121.9, 81.7, 62.8, 54.2, 45.0, 40.2, 33.9, 30.4, 28.4, 28.2, 26.1, 25.8, 18.4, -5.2; IR (thin film) 3022, 2930, 2854, 2242, 1695 cm^{-1}; HRMS (ESI) calcd for C$_{28}$H$_{46}$N$_2$O$_3$SiNa [M+Na]$^+$ 509.3175, found 509.317
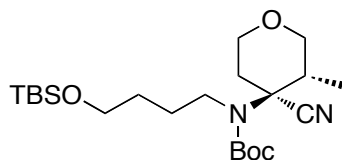
Tert-butyl(4-((_tert_-butyldimethylsilyl)oxy)butyl)(4-cyano-3-methyltetrahydro-2_H_-pyran-4-yl)carbamate (**3.110**) Following general procedure C, FCC (10:1 hexanes/EtOAc) gave 744 mg (60%, >95:5 dr) as a clear oil. Performed on 2.9 mmol scale.

^{1}H NMR (CDCl$_3$, 500 MHz) δ 3.99 (dd, *J* = 12.0, 4.0 Hz, 1H), 3.85 (dd, *J* = 12.0, 4.5 Hz, 1H), 3.74 (td, *J* =12.5, 2.0 Hz, 1H), 3.63 (t, *J* = 6.0 Hz, 2H), 3.56–3.47 (m, 1H), 3.44–3.32 (m, 2H), 2.94 (br s, 1H), 2.57 (br s, 1H), 2.06 (d, *J* = 13.0 Hz, 1H), 1.67 (pent. *J* = 8.5 Hz, 2H), 1.56–1.46 (m, 11H), 0.97 (d, *J* = 7.0 Hz, 3H), 0.90 (s, 9H), 0.05 (s, 6H); ^{13}C NMR (CDCl$_3$, 125 MHz) δ 154.1, 117.4, 71.0, 71.0, 65.3, 62.8, 63.9, 47.7, 35.9, 34.5, 30.3, 28.5, 27.3, 26.1, 18.4, 12.0, -5.2; IR (thin film) 2930, 2856, 1698 cm^{-1}; HRMS (ESI) calcd for C$_{22}$H$_{42}$N$_2$O$_4$SiNa [M+Na]$^+$ 449.2812, found 449.2805
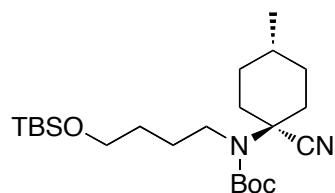
***Tert*-butyl(4-((*tert*-butyldimethylsilyl)oxy)butyl)((1s,4s)-1-cyano-4**

methylcyclohexyl)carbamate (**3.114**) Following general procedure C, FCC (14:1 hexanes/EtOAc) gave 1.1 g (72%, 2:1 dr) as a clear oil. Performed on 3.5 mmol scale.

3.114a (major isomer): ^{1}H NMR (CDCl$_3$, 500 MHz) δ 3.59 (t, J = 6.0 Hz, 2H), 3.32 (app t, J =7.5 Hz, 2H), 2.39, (d, J =12.5 Hz, 2H), 1.92–1.79 (m, 1H), 1.79–1.65 (m, 3H), 1,65–1.51 (m, 2H), 1.51–1.32 (m, 14H), 0.87 (s, 9H), 0.02 (s 6H); ^{13}C NMR (CDCl$_3$, 125 MHz) δ 154.5, 120.2, 81.3, 62.6, 57.8, 44.2, 34.9, 31.8, 30.1, 29.1, 28.4, 27.3, 26.0, 21.7, 18.3, -5.3;   IR (thin film) 2954, 2930, 2233, 1701 cm^{-1}; HRMS (ESI) calcd for C$_{23}$H$_{44}$N$_2$O$_3$SiNa [M+Na$^+$]$^+$ 447.3019, found 447.3028
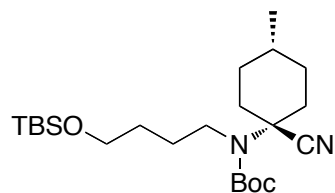
3.114b (minor isomer): ^{1}H NMR (CDCl$_3$, 500 MHz) δ 3.60 (t, J = 6.0 Hz, 2H), 3.35 (app t, J =6.5 Hz, 2H), 2.17, (d, J =11.5 Hz, 2H), 2.09–2.00 (m, 2H), 1.92–1.79 (m, 1H), 1.79–1.65 (m, 3H), 1,65–1.51 (m, 2H), 1.51–1.32 (m, 12H), 0.87 (s, 9H), 0.02 (s 6H); ^{13}C NMR (CDCl$_3$, 125 MHz) δ 154.8, 120.8, 81.3, 62.7, 56.7, 44.6, 31.6, 30.9, 30.3, 28.4, 27.2, 27.0, 26.0, 18.7, 18.3, -5.3; IR (thin film) 2954, 2930, 2233, 1701; HRMS (ESI) calcd for C$_{23}$H$_{44}$N$_2$O$_3$SiNa [M+Na]$^+$ 447.3019, found 447.3028

Tert-butyl(4-((tert-butyldimethylsilyl)oxy)butyl)(1-cyanocyclohexyl)carbamate

(**3.118**) Following general procedure D, FCC (10:1 hexanes/EtOAc) gave 1.39 g (73%) as a clear oil. Performed on 4.6 mmol scale.
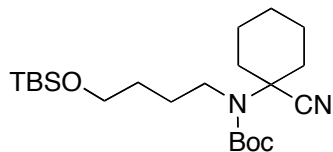
^{1}H NMR (CDCl$_3$, 500 MHz) δ 3.61 (t, J = 6.3 Hz, 2H), 3.35 (app d, J = 7.8 Hz, 2H), 2.40 (d, J =10.0 Hz, 2H), 1.87–1.55 (m, 9H), 1.54–1.37 (m, 11H), 0.89 (s, 9H), 0.05 (s, 6H); ^{13}C NMR (CDCl$_3$, 125 MHz) δ 154.5, 120.2, 81.4, 62.7, 58.0, 44.2, 35.2, 30.2, 28.5, 27.4 26.0, 24.8, 23.5, 18.4, -5.2; IR (thin film) 2933, 2859, 2236, 1700 cm^{-1}; HRMS (ESI) calcd for C$_{22}$H$_{42}$N$_2$O$_3$SiNa [M+Na]$^+$ 433.2863, found 433.2861;
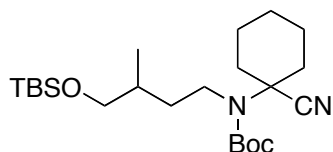
Tert-butyl(4-((tert-butyldimethylsilyl)oxy)-3-methylbutyl)(1-cyanocyclohexyl)

carbamate (**3.125**) Following general procedure D, FCC (15:1 hexanes/EtOAc) gave 0.509 g (56%) as a clear oil. Performed on 2.5 mmol scale.

^{1}H NMR (CDCl$_3$, 500 MHz) δ 3.47-3.35 (m, 3H), 3.31 (ddd, J = 15.0, 11.2, 5.3 Hz, 1H), 2.41 (t, J = 10.8 Hz, 2H), 1.86-1.62 (m, 8H), 1.56 (sext. J = 6.5 Hz, 1H), 1.50 (s, 9H), 1.32 (dddd, J = 12.6, 11.0, 7.7, 5.3 Hz, 1H), 1.23-1.11 (m, 1H), 0.95-0.85 (m, 12H), 0.04 (s, 6H); ^{13}C NMR (CDCl$_3$, 125 MHz) δ 154.4, 121.2, 81.4, 68.0, 57.9, 42.7, 35.2, 35.1, 34.3, 34.2, 28.5, 26.0, 24.8, 23.5, 18.4, 16.7, -5.3; IR (thin film) 2933, 2859, 2235, 1701 cm^{-1}; HRMS (ESI) calcd for C$_{23}$H$_{44}$N$_2$O$_3$SiNa [M+Na]$^+$ 447.3019, found 447.3001

General Procedure for Silyl Deprotection

To neat silyl ether (1 equiv) TBAF was added (1.0 M in THF, 2 equiv). After the reaction was complete by TLC, the solution was diluted with ethyl acetate followed by water. The organic layer was separated and the aqueous layer was extracted with EtOAc (5x). The combined organic layers were dried over MgSO₄, filtered and concentrated *in vacuo* to give a yellow oil. Purification by flash column chromatography gave the title compound.
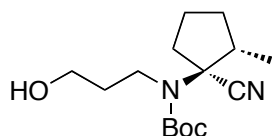
***Tert*-butyl (1-cyano-2-methylcyclopentyl)(3-hydroxypropyl)carbamate** (**3.41**)

Following the general procedure, FCC (2:3 hexanes/EtOAc) yielded 167 mg (quant) as a clear oil. Preformed on a 0.58 mmol scale.

^{1}H NMR (CDCl₃, 500 MHz) δ 4.01 (dd, *J* = 12.5, 5.0 Hz, 1H), 3.86 (dd, *J* = 12.0, 4.5 Hz, 1H), 3.79–3.68 (m, 2H), 3.68–3.52 (m, 3H), 3.40 (t, *J* = 11.5 Hz, 1H), 2.89 (br s,1H), 2.80–2.40 (m, 2H), 2.03 (app d, *J* = 12.0 Hz, 1H), 1.84 (pent., *J* = 12.0 Hz, 2H), 1.52 (s, 9H), 0.98 (t, *J* = 7.0 Hz, 3H); ^{13}C NMR (CDCl₃, 125 MHz) δ 155.0, 117.3, 82.8, 71.0, 65.3, 59.3, 44.2, 36.3, 34.7, 33.2, 28.5, 28.3, 12.0; IR (thin film) 3428, 2972, 2930, 2856, 2239, 1697 cm^{-1}; HRMS (ESI) calcd for $C_{15}H_{26}N_2O_4Na$ [M+Na]⁺ 321.1790 , found 321.1789
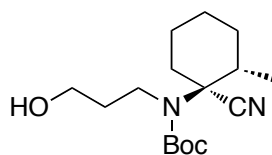
***Tert*-butyl ((1*S*,2*S*)-1-cyano-2-methylcyclohexyl)(3-hydroxypropyl)carbamate** (**3.44**)

Following the general procedure, FCC (2:1 Hexanes/EtOAc with 1% Et₃N) yielded 335 mg

(quantitiative yield) of a clear oil. Performed on a 1.2 mmol scale.

^{1}H NMR (CDCl$_3$, 500 MHz) δ 3.73–3.56 (m, 4H), 2.44 (br s, 1H), 1.97 (s, 1H), 1.91–1.57 (m, 8H), 1.49 (s, 9H), 1.24 (qt, J = 13.0, 4.3 Hz), 1.43 (q, J = 12.5 Hz, 1H), 1.02 (d, , J = 6.5 Hz, 3H); ^{13}C NMR (CDCl$_3$, 125 MHz) δ 155.0, 118.0, 59.3, 36.9, 34.4, 33.1, 32.4, 28.5, 25.0, 23.9, 17.0; IR (thin film) 3449, 2931, 2864, 1694 cm^{-1}; HRMS (ESI) calcd for C$_{16}$H$_{28}$N$_2$O$_3$Na [M+Na]$^+$ 319.1998, found 319.2005

Tert-butyl (1-cyano-4-methylcyclohexyl)(3-hydroxypropyl)carbamate (**3.47**)

Following the general procedure, FCC (3:2 Hexanes/EtOAc with 1% Et$_3$N) yielded 636 mg (85% yield) of a clear oil. Performed on a 2.5 mmol scale. Diastereomers were partially separated; the yield given is for the total mass isolated.

3.47a (major isomer): ^{1}H NMR (CDCl$_3$, 500 MHz) δ 3.62 (t, J = 5.5 Hz, 2H), 3.59 (app t, J = 7.0 Hz, 2H), 2.18–2.05 (m, 4H), 1.97–1.87 (m, 3H), 1.76 (tt, J = 6.5, 5.0 Hz, 2H), 1.52 (s, 9H), 1.51–1.43 (m, 2H), 0.98 (d, J = 7.5 Hz, 3H); ^{13}C NMR (CDCl$_3$, 125 MHz) δ 155.9, 120.5, 82.7, 59.0, 57.3, 44.6, 33.4, 30.8, 29.1, 28.4, 26.7, 18.5; IR (thin film) 3456, 2930, 2870, 2234, 1698 cm^{-1}; HRMS (ESI) calcd for C$_{16}$H$_{28}$N$_2$O$_3$Na [M+Na]$^+$ 319.1998, found 319.1988
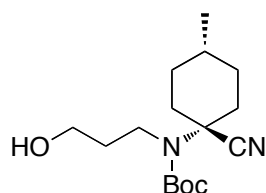
3.47b (minor isomer): ^{1}H NMR (CDCl$_3$, 500 MHz) δ 3.59 (t, J = 5.0 Hz, 2H), 3.55 (t, J = 7.0 Hz, 2H), 2.81 (br s, 1H), 2.41 (br d, J = 13.0 Hz, 2H), 1.83–1.67 (m, 6H), 1.53 (s, 9H), 1.50–1.41 (m, 2H), 0.95 (d, J = 6.0 Hz, 3H); ^{13}C NMR (CDCl$_3$, 125 MHz) δ 155.7, 120.1, 82.8, 58.8, 40.3, 35.2, 33.7, 31.8, 31.6, 28.4, 21.7; IR (thin film) 3459, 2929, 2869, 2235, 1699 cm^{-1}; HRMS (ESI) calcd for C$_{16}$H$_{28}$N$_2$O$_3$Na [M+Na]$^+$ 319.1998, found 319.1996
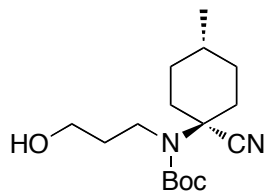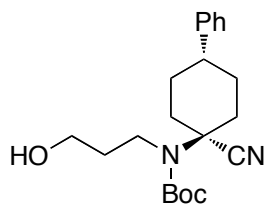

Tert-butyl (1-cyano-4-phenylcyclohexyl)(3-hydroxypropyl)carbamate (**3.51**)
Following the general procedure, FCC (1:1 Hexanes/EtOAc with 1% Et$_3$N) yielded 557 mg (93% yield) of a clear oil. Performed on a 1.7 mmol scale. The analytical data matched those previously reported.[62] Diastereomers were partially separated; the yield given is for the total mass isolated.
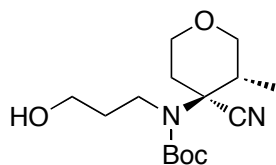
Tert-butyl(4-cyano-3-methyltetrahydro-2H-pyran-4-yl)(3-hydroxypropyl)carbamate (**3.55**) Following the general procedure, FCC (2:3 hexanes/EtOAc) yielded 56 mg (quant) as a clear oil. Preformed on a 0.42 mmol scale

^{1}H NMR (CDCl$_3$, 500 MHz) δ 4.01 (dd, J = 12.5, 5.0 Hz, 1H), 3.86 (dd, J = 12.0, 4.5 Hz, 1H),

3.79–3.68 (m, 2H), 3.68–3.52 (m, 3H), 3.40 (t, J = 11.5 Hz, 1H), 2.89 (br s,1H), 2.80–2.40 (m, 2H), 2.03 (app d, J = 12.0 Hz, 1H), 1.84 (pent., J = 12.0 Hz, 2H), 1.52 (s, 9H), 0.98 (t, J = 7.0 Hz, 3H); ^{13}C NMR (CDCl$_3$, 125 MHz) δ 155.0, 117.3, 82.8, 71.0, 65.3, 59.3, 44.2, 36.3, 34.7, 33.2, 28.5, 28.3, 12.0; IR (thin film) 3428, 2972m 2930, 2856, 2239, 1697 cm^{-1}; HRMS (ESI) calcd for C$_{15}$H$_{26}$N$_2$O$_4$Na [M+Na]$^+$ 321.1790, found 321.1789

Tert-butyl(4-cyano-2-methyltetrahydro-2H-pyran-4-yl)(3-hydroxypropyl)carbamate

(**3.57**) Following the general procedure, FCC (2:3 hexanes/EtOAc) to yield 108 mg (quant) as a clear oil. Preformed on a 0.42 mmol scale.   Diastereomers were partially separated; the yield given is for the total mass isolated.

3.57a (major isomer): ^{1}H NMR (CDCl$_3$, 500 MHz) δ 3.91–3.85 (m, 1H), 3.68–3.56 (m, 5H), 3.56–3.48 (m, 1H), 2.70 (app. t, 2H), 2.12–2.04 (m, 1H), 1.87–1.78 (m, 3H), 1.52 (s, 9H), 1.44 (s, 1H), 1.21 (d, J = 6.0 Hz, 3H); ^{13}C NMR (CDCl$_3$, 125 MHz, *denotes carbon rotamer) δ 156.1, 121.5, 83.0, 68.4, 62.5, 59.4, 51.9, 41.9, 41.4, 34.8, 31.7, 28.5*, 28.4, 21.2; IR (thin film) 3433, 3035, 2978, 2935, 2873, 1697 cm^{-1}; HRMS (ESI) calcd for C$_{15}$H$_{26}$N$_2$O$_4$Na [M+Na]$^+$ 321.1793, found 321.1790
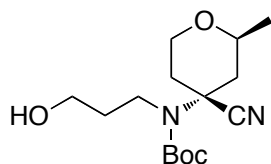
3.57a (major isomer): ^{1}H NMR (CDCl$_3$, 500 MHz) δ 4.07–4.01 (m, 1H), 3.86–3.77 (m, 2H),

3.60 (t, J = 5.8 Hz, 2H), 3.53 (t, J = 6.5 Hz, 2H), 2.41 (app d, J = 13.0 Hz, 1H), 2.37 (app d, J = 13.0 Hz, 1H), 1.94–1.86 (m, 1H), 1.72 (pent, J = 6.0 Hz, 2H), 1.53 (s, 9H), 1.52 (s, 1H), 1.25 (d, J = 6.5 Hz, 3H); ^{13}C NMR (CDCl$_3$, 125 MHz) δ 155.4, 119.7, 83.2, 70.6, 64.4, 58.9, 55.9, 42.1, 41.2, 35.1, 33.5, 28.4, 21.5; IR (thin film) 3433, 3035, 2978, 2935, 2873, 1697 cm^{-1}; HRMS (ESI) calcd for C$_{15}$H$_{26}$N$_2$O$_4$Na [M+Na]$^+$ 321.1793, found 321.1790
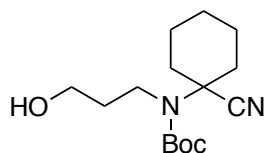
***Tert*-butyl (1-cyanocyclohexyl)(3-hydroxypropyl)carbamate** (**3.88**) Following the general procedure, FCC (1:1 Hexanes/EtOAc with 1% Et$_3$N) yielded 981 mg (quantitative yield) of a clear oil. Performed on a 3.5 mmol scale. The analytical data matched those previously reported.[60]
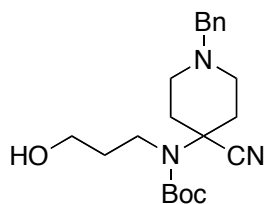
***Tert*-butyl (1-benzyl-4-cyanopiperidin-4-yl)(3-hydroxypropyl)carbamate** (**3.90**) Following the general procedure, FCC (1:3 Hexanes/EtOAc with 1% Et$_3$N) yielded 90 mg (84% yield) of a clear oil. Performed on a 0.29 mmol scale.

^{1}H NMR (CDCl$_3$, 500 MHz) δ 7.35-7.23 (m, 5H), 3.60 (t, J=5.5 Hz, 2H), 3.57-3.50 (m, 4H), 3.07 (br s, 1H), 2.94 (d, J=12.5 Hz, 2H), 2.48-2.35 (m, 4H), 1.96 (dt, J=12.3, 3.3 Hz, 2H), 1.72 (pen, J=5.9 Hz, 2H), 1.53 (s, 9H); ^{13}C NMR (CDCl$_3$, 125 MHz) δ 155.6, 138.0, 129.1, 128.5,

127.4, 119.8, 83.0, 62.5, 58.8, 56.5, 50.3, 40.2, 34.9, 33.5, 28.4; IR (thin film) 3456, 3061, 3027, 2974, 2935, 2877, 2817, 2235, 1698 cm^{-1}; HRMS (ESI) calcd for $C_{21}H_{31}N_3O_3Na$ [M+Na]$^+$ 396.2263, found 396.2256
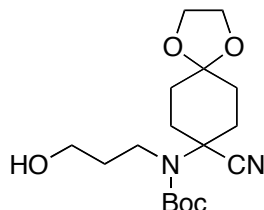
Tert-butyl(8-cyano-1,4-dioxaspiro[4.5]decan-8-yl)(3-hydroxypropyl)carbamate

(**3.94**) Following the general procedure, FCC (2:3 hexanes/EtOAc) gave 86mg (87%) as a clear oil. Performed on a 0.29 mmol scale.

^{1}H NMR (CDCl$_3$, 500 MHz) δ 4.0–3.98 (m, 4H), 3.59 (t, J = 5.5 Hz, 2H), 3.54 (t, J = 6.6 Hz, 2H), 3.00 (br s, 1H), 2.38 (d, J = 11.5 Hz, 2H), 2.12–1.96 (m, 4H), 1.80 (app d, J = 12.0 Hz, 2H), 1.71 (quint, J = 6.0 Hz, 2H), 1.54 (s, 9H); ^{13}C NMR (CDCl$_3$, 125 MHz) δ 155.6, 119.5, 106.6, 83.1, 64.8, 64.5, 58.8, 57.0, 40.4, 33.6, 32.6, 32.1, 28.4; IR (thin film) 3477, 2954, 2875, 2254, 1694 cm^{-1}; HRMS (ESI) calcd for $C_{17}H_{28}N_2O_5Na$ [M+Na]$^+$ 363.1894, found 363.1902.
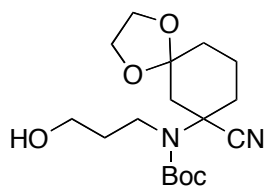
Tert-butyl   (7-cyano-1,4-dioxaspiro[4.5]decan-7-yl)(3-hydroxypropyl)carbamate

(**3.98**) Following the general procedure, FCC (3:2 Hexanes/EtOAc) yielded 118 mg (quantitative yield) of a clear oil. Performed on a 0.35 mmol scale.

^{1}H NMR (CDCl$_3$, 500 MHz) δ 4.0-3.98 (m, 4H), 3.59 (t, J = 5.5 Hz, 2H), 3.54 (t, J = 6.6 Hz, 2H), 3.00 (br s, 1H), 2.38 (d, J = 11.5 Hz, 2H), 2.12–1.96 (m, 4H), 1.80 (app d, J = 12.0 Hz, 2H), 1.71 (quint, J = 6.0 Hz, 2H), 1.54 (s, 9H); ^{13}C NMR (CDCl$_3$, 125 MHz) δ 155.6, 119.5, 106.6, 83.1, 64.8, 64.5, 58.8, 57.0, 40.4, 33.6, 32.6, 32.1, 28.4; IR (thin film) 3477, 2954, 2875, 2254, 1694 cm^{-1}; HRMS (ESI) calcd for C$_{17}$H$_{28}$N$_2$O$_5$Na [M+Na]$^+$ 363.1894, found 363.1902.

Tert-butyl (1-cyano-4-phenylcyclohexyl)(4-hydroxybutyl)carbamate (3.107)

Following the general procedure, FCC (1:2 Hexanes/EtOAc with 1% Et$_3$N) yielded 132 mg (quantitative yield) of a clear oil. Performed on a 0.35 mmol scale. Diastereomers were partially separated; the yield given is for the total mass isolated.

3.107a (major isomer): ^{1}H NMR (CDCl$_3$, 500 MHz) δ 7.34-7.29 (m, 2H), 7.26-7.19 (m, 3H), 3.65 (t, J=6.3 Hz, 2H), 3.41 (app t, J=7.6 Hz, 2H) 2.82 (tt, J=8.5, 4.4 Hz, 1H), 2.57 (app s, 2H), 2.09 (app ddd, J=13.9, 10.3, 2.6Hz, 2H), 2.04-1.97 (m, 2H), 1.92-1.82 (m, 2H), 1.68-1.62 (m, 2H), 1.57-1.49 (m, 11H); ^{13}C NMR (CDCl$_3$, 125 MHz) δ 155.4, 144.5, 128.7, 126.9, 126.5, 121.9, 82.0, 62.4, 44.7, 33.8, 29.9, 28.4, 28.1, 26.0; IR (thin film) 3437, 3057, 2931, 2869, 2234, 1700 cm^{-1}; HRMS (ESI) calcd for C$_{22}$H$_{32}$N$_2$O$_3$Na [M+Na]$^+$ 395.2310 , found 395.2306
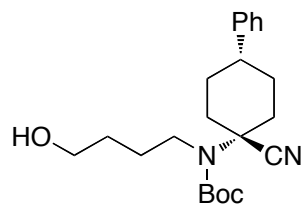
3.107a (minor isomer): ^{1}H NMR (CDCl$_3$, 500 MHz) δ 7.35-7.29 (m, 2H), 7.26-7.19 (m, 2H), 3.69 (t, J=6.3 Hz, 2H), 3.43 (app t, J=7.8 Hz, 2H), 2.61-2.50 (m, 3H), 2.08-1.90 (m, 7H), 1.73-1.63 (m, 2H), 1.61-1.55 (m, 2H), 1.53 (s, 9H); ^{13}C NMR (CDCl$_3$, 125 MHz) δ 154.6, 145.3, 128.3, 127.0, 126.7, 120.0, 81.9, 62.4, 57.9, 44.3, 43.1, 35.2, 31.1, 29.8, 28.5, 27.3; IR (thin film) 3477, 3029, 2979, 2921, 2664, 2231, 1695 cm^{-1}; HRMS (ESI) calcd for C$_{22}$H$_{32}$N$_2$O$_3$Na [M+Na]$^+$ 395.2310, found 395.2311

***Tert*-butyl(4-cyano-3-methyltetrahydro-2H-pyran-4-yl)(4-hydroxybutyl)carbamate**

(**3.111**) Following the general procedure, FCC (1:1 Hexanes/EtOAc with 1% Et$_3$N) yielded 287 mg (85% yield) of a clear oil. Performed on a 1.2 mmol scale.

^{1}H NMR (CDCl$_3$, 500 MHz) δ 4.00 (dd, J = 12.5, 4.5 Hz, 1H), 3.86 (dd, J = 12.0, 4.5 Hz, 1H), 3.74 (td, J = 12.5, 1.5 Hz, 1H), 3.70 (t, J = 6.5 Hz, 2H), 3.60–3.50 (m, 1H), 3.40 (app t, J = 11.5 Hz, 2H), 2.96 (br s, 1H), 2.60 (bs s, 1H), 2.04 (d, J = 13.0 Hz, 1H), 1.76–1.66 (m, 2H), 1.57 (pent. J = 6.5 Hz, 3H), 1.50 (s, 9H), 0.97 (t J = 7.5 Hz, 3H); ^{13}C NMR (CDCl$_3$, 125 MHz) δ 154.1, 117.5, 81.8, 71.1, 65.4, 62.4, 36.0, 34.6, 29.8, 28.5, 26.8, 11.9; IR (thin film) 3431, 2969 2924, 2859, 2238, 1696 cm^{-1}; HRMS (ESI) calcd for C$_{16}$H$_{28}$N$_2$O$_4$Na [M+Na]$^+$ 335.1947, found 335.1960
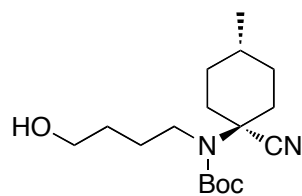
Tert-butyl(1-cyano-4-methylcyclohexyl)(4-hydroxybutyl)carbamate (**3.115**)

Following the general procedure, FCC (3:2 Hexanes/EtOAc with 1% Et$_3$N) yielded 753 mg (quantitative yield) of a clear oil. Performed on a 2.5 mmol scale. Diastereomers were partially separated; the yield given is for the total mass isolated.

3.115a (major isomer): ^{1}H NMR (CDCl$_3$, 500 MHz) δ 3.68 (t, J = 6.0 Hz, 2H), 3.41 (app t, J = 8.0 Hz, 2H), 2.22 (t, J = 11.5 Hz, 2H), 2.11–2.01 (m, 2H), 1.94–1.82 (m, 3H), 1.72–1.60 (m, 3H), 1.60–1.53 (m, 2H), 1.52 (s, 9H), 1.47–1.38 (m, 2H), 0.98 (d, J = 7.0 Hz, 3H); ^{13}C NMR (CDCl$_3$, 125 MHz) δ 155.0, 120.9, 81.7, 62.4, 56.8, 44.5, 31.1, 29.9, 29.2, 28.5, 27.2, 26.7, 18.9; IR (thin film) 3455, 2930, 2868, 2235, 1698 cm^{-1}; HRMS (ESI) calcd for C$_{17}$H$_{30}$N$_2$O$_3$Na [M+Na]$^+$ 333.2154, found 333.2169
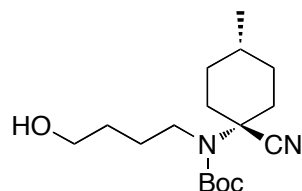
3.115b (major isomer): ^{1}H NMR (CDCl$_3$, 500 MHz) δ 3.66 (t, J = 6.0 Hz, 2H), 3.36 (app t, J = 7.5 Hz, 2H), 2.40 (br d, J = 11.5 Hz, 2H), 1.82–1.69 (m, 6H), 1.57–1.48 (m, 11H), 1.47–1.48 (m, 2H), 0.95 (d, J = 6.0 Hz, 3H); ^{13}C NMR (CDCl$_3$, 125 MHz) δ 154.6, 120.2, 81.8, 62.3, 58.0, 44.1, 35.1, 31.9, 31.6, 29.8, 28.4, 27.4, 27.2, 21.8; IR (thin film) 3465, 2930, 2870, 2234, 1699 cm^{-1}; HRMS (ESI) calcd for C$_{17}$H$_{30}$N$_2$O$_3$Na [M+Na]$^+$ 333.2154, found 333.2145
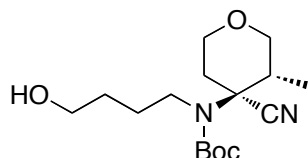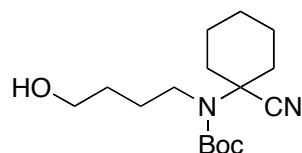
***Tert*-butyl (1-cyanocyclohexyl)(4-hydroxybutyl)carbamate** (**3.119**) Following the general procedure, FCC (1:1 Hexanes/EtOAc with 1% Et$_3$N) yielded 458 mg (quantitative yield) of a clear oil. Performed on a 1.5 mmol scale.

^{1}H NMR (CDCl$_3$, 500 MHz) δ 3.67 (app t, *J* = 6.3 Hz, 2H), 3.38 (t, *J* = 7.8 Hz, 2H), 2.39 (app d, *J* = 8.5 Hz, 2H), 1.88–1.59 (m, 11H), 1.59–1.47 (m, 11H), 1.27–1.12 (m, 1H); ^{13}C NMR (CDCl$_3$, 125 MHz) δ 154.6, 120.2, 81.8, 62.4, 58.1, 44.1, 35.2, 29.8, 28.5, 27.2, 24.8, 23.8; IR (thin film) 3456, 2973, 2937, 2865, 2236, 1697 cm^{-1}; HRMS (ESI) calcd for C$_{16}$H$_{28}$N$_2$O$_3$Na [M+Na]$^+$ 319.1998, found 319.1999
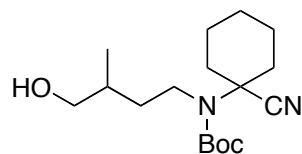
***Tert*-butyl (1-cyanocyclohexyl)(4-hydroxy-3-methylbutyl)carbamate** Following the general procedure, FCC (2:1 Hexanes/EtOAc with 1% Et$_3$N) yielded 430 mg (quantitative yield) of a clear oil. Performed on a 1.4 mmol scale.

^{1}H NMR (CDCl$_3$, 500 MHz) δ 3.55-3.30 (m, 4H), 2.38 (d, *J* = 8.3 Hz), 2.00 (br s, 1H), 1.89-1.57 (m, 9H), 1.46-1.35 (m, 9H), 1.46-1.35 (m, 1H), 1.27-1.11 (m, 1H), 0.97-0.90 (m, 3H); ^{13}C NMR (CDCl$_3$, 125 MHz) δ 154.5, 120.2, 81.7, 67.6, 58.1, 42.4, 35.2, 34.2 33.8, 28.4, 24.7, 23.4, 16.7; IR (thin film) 3468, 2936, 2867, 2237, 1697 cm^{-1}; HRMS (ESI) calcd for C$_{17}$H$_{30}$N$_2$O$_3$Na [M+Na]$^+$ 333.2154, found 333.2144

General Phosphorylation Procedure

To a 0.06 M solution of alcohol (1 equiv) in DCM at 0 °C was added *N*-methylimidazole (6 equiv) followed by diethyl chlorophosphate (5 equiv). After the reaction was complete by TLC, diethylene glycol (8 equiv) was added. After 60 min, a 1:1 solution of saturated NaHCO$_3$ and brine were added and the mixture was diluted with EtOAc. The organic layer was separated and the aqueous layer was extracted with EtOAc (5x). The combined organic layers were washed with brine, dried over MgSO$_4$, filtered and concentrated *in vacuo.* Purification by column chromatography gave the title compound.
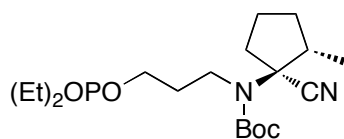
***Tert*-butyl((1-cyano-2-methylcyclopentyl)(3-((diethylphosphoryl)oxy)propyl) carbamate (3.42)** Following the general procedure, FCC (1:1 hexanes/EtOAc) yielded 163 mg (93%) as a clear oil. Preformed on a 0.39 mmol scale.

^{1}H NMR (CDCl$_3$, 500 MHz) δ 4.12 (pent., *J* = 7.3 Hz, 4H), 4.08–4.00 (m, 2H), 3.62 (ddd, *J* = 14.6, 9.5, 6.1 Hz, 1H), 3.31 (ddd, *J* = 14.7, 9.5, 5.9 Hz, 1H), 2.60 (q, *J* = 7.5 Hz, 1H), 2.52 (ddd, *J* = 14.8, 7.6, 7.2 Hz, 1H), 2.20 (ddd, *J* = 13.8, 9.5, 5.9 Hz, 1H), 1.96 (app sext., *J* = 6.7 Hz, 3H), 1.89–1.80 (m, 1H), 1.80–1.70 (m, 1H), 1.58–1.46 (m, 10H), 1.35 (t, *J* = 7.0 Hz, 6H),1.24 (d, *J* = 6.6 Hz, 3H); ^{13}C NMR (CDCl$_3$, 125 MHz) δ 154.7, 120.1, 82.0, 66.7, 65.4 (d, $^2J_{PC}$ = 6.0 Hz), 64.0 (d, $^2J_{PC}$ = 6.0 Hz), 42.6, 42.1, 38.4, 31.6, 30.8 (d, $^3J_{PC}$ = 6.0 Hz), 28.5, 21.4, 17.1, 16.3 (d, $^3J_{PC}$ = 6.0 Hz); 2964, 2908, 2224, 1696 cm^{-1}; HRMS (ESI) calcd for C$_{19}$H$_{35}$N$_2$O$_6$PNa [M+Na]$^+$ 441.2130 , found 441.2112.
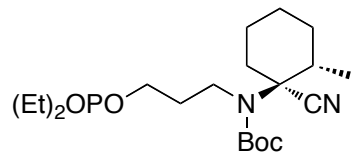
***Tert*-butyl(1-cyano-2-methylcyclohexyl)(3-((diethylphosphoryl)oxy)propyl)**

carbamate (3.45) Following the general procedure, FCC (3:2 Hexanes/EtOAc with 1%

Et$_3$N) yielded 323 mg (66% yield) of a clear oil. Performed on a 0.84 mmol scale.   The

analytical data matched those previously reported.[13]

***Tert*-butyl((1-cyano-4-methylcyclohexyl)(3-((diethylphosphoryl)oxy)propyl)**

carbamate (3.48) Following the general procedure, FCC (1:2 Hexanes/EtOAc with 1%

Et$_3$N) yielded 520 mg (74%) of a clear oil. Performed on a 1.6 mmol scale.

^{1}H NMR (CDCl$_3$, 500 MHz) δ 4.11 (pent, *J* = 7.0 Hz, 4H), 4.04 (q, *J* = 6.5 Hz, 2H), 3.46 (app t, *J*

= 8.0 Hz, 2H), 2.41 (d, *J* = 12.5 Hz, 2H), 1.92 (ddd, *J* = 13.5, 7.0, 6.0 Hz, 2H), 1.78 (d, *J* = 11.5

Hz, 2H), 1.71 t, *J* = 12.5 Hz, 2H), 1.50 (s, 9H), 1.48–1.40 (m, 3H), 1.34 (t, *J* = 6.5 Hz, 6H), 0.95

(d, *J* = 6.0 Hz, 3H); ^{13}C NMR (CDCl$_3$, 125 MHz) δ 154.5, 120.1, 81.9, 65.4 (d, $^2J_{PC}$ = 6.0 Hz),

64.0 (d, $^2J_{PC}$ = 6.0 Hz), 58.0, 41.3, 35.1, 31.8, 31.6, 31.4 (d, $^3J_{PC}$ = 6.4 Hz), 28.4, 21.7, 16.3 (d,

$^3J_{PC}$ = 6.9 Hz); IR (thin film) 2925, 2860, 2235, 1699 cm^{-1}; HRMS (ESI) calcd for

C$_{20}$H$_{37}$N$_2$O$_6$PNa [M+Na]$^+$ 455.2287, found 455.2289

Tert-butyl((1-cyano-4-methylcyclohexyl)(3-((diethylphosphoryl)oxy)propyl)

carbamate (3.49) Following the general procedure, FCC (1:2 Hexanes/EtOAc with 1%

Et₃N) yielded 411 mg (68%) of a clear oil. Performed on a 1.4 mmol scale.

^{1}H NMR (CDCl$_3$, 500 MHz) δ 4.11 (pent, *J* = 8.0 Hz, 4H), 4.06 (q, *J* = 6.0 Hz, 2H), 3.52–3.46

(m, 2H), 2.25–2.15 (m, 2H), 2.09–2.02 (m, 2H), 2.00–1.74 (m, 5H), 1.50 (s, 9H), 1.45–1.38

(m, 2H), 1.34 (td, *J* = 7.0, 1.0 Hz, 6H), 0.97 (d, *J* = 6.0 Hz, 3H); ^{13}C NMR (CDCl$_3$, 125 MHz) δ

154.8, 120.8, 81.9, 65.5 (d, $^2J_{PC}$ = 6.0 Hz), 63.9 (d, $^2J_{PC}$ = 6.0 Hz), 56.9, 41.7, 32.9, 31.1, 30.9

(d, $^3J_{PC}$ = 6.9 Hz), 29.2, 28.4, 27.3, 18.9, 16.3 (d, $^3J_{PC}$ = 6.9 Hz); IR (thin film) 2977, 2930,

2870, 2233, 1700 cm^{-1}; HRMS (ESI) calcd for C$_{20}$H$_{37}$N$_2$O$_6$PNa [M+Na]$^+$ 455.2287, found

455.2289
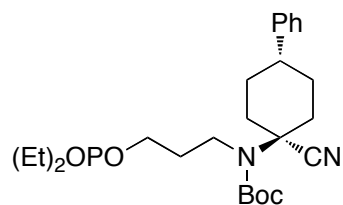
Tert-butyl(1-cyano-4-phenylcyclohexyl)(3-((diethylphosphoryl)oxy)propyl)

carbamate (3.52) Following the general procedure, FCC (1:1 hexanes/EtOAc) yielded 68

mg (72%) as a clear oil. Preformed on a 0.19 mmol scale. The analytical data matched

those previously reported.[62]
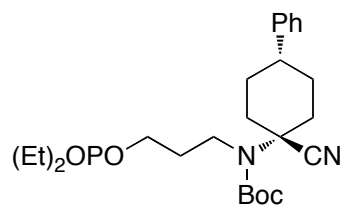
***Tert*-butyl(1-cyano-4-phenylcyclohexyl)(3-((diethylphosphoryl)oxy)propyl)**

carbamate (**3.53**) Following the general procedure, FCC (1:1 hexanes/EtOAc) to yield 15

mg (92%) as a clear oil. Preformed on a 0.042 mmol scale. The analytical data matched
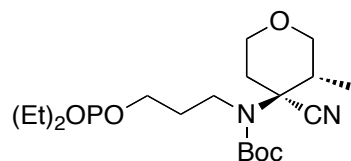
those previously reported.[60]

***Tert*-butyl(4-cyano-3-methyltetrahydro-2H-pyran-4-yl)(3((diethylphosphoryl)oxy)**
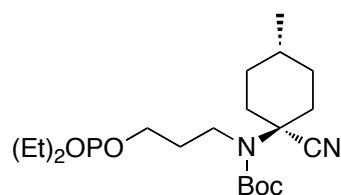
propyl)carbamate (**3.56**) Following the general procedure, FCC (2:3 hexanes/EtOAc)

yielded 231 mg (84%) as a clear oil. Preformed on a 0.63 mmol scale.

^{1}H NMR (CDCl$_3$, 500 MHz) δ 4.12 (pent., J = 7.1 Hz, 4H), 4.10–4.05 (m, 2H), 4.00 (dd, J = 12.3,

4.3 Hz, 1H), 3.84 (dd, J = 11.8, 4.0 Hz, 1H), 3.73 (dt, J = 12.0, 1.7 Hz, 1H), 3.67–3.60 (m, 1H),

3.54–3.42 (m, 1H), 3.39 (t, J = 11.5 Hz, 1H), 2.93 (br s, 1H), 4.00 (br s, 1H), 2.08–1.94 (m,

3H), 1.49 (s, 9H), 1.34 (t, J = 7.0 Hz, 6H), 0.96 (d, J = , 7.0 Hz, 3H); ^{13}C NMR (CDCl$_3$, 125 MHz)

δ 152.9, 117.2, 82.0, 71.0, 65.3 (d, $^2J_{PC}$ = 6.5 Hz), 64.0 (d, $^2J_{PC}$ = 5.5 Hz), 44.8, 36.0, 34.5, 31.2

(d, $^3J_{PC}$ = 6.9 Hz), 28.4, 28.3, 16.3 (d, $^3J_{PC}$ = 6.9 Hz), 11.9; IR (thin film) 2973, 2936, 2219,

1696 cm^{-1}; HRMS (ESI) calcd for C$_{19}$H$_{35}$N$_2$O$_7$PNa [M+Na]$^+$ 457.2079, found 457.2078.
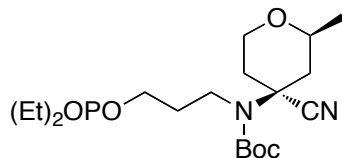
Tert-butyl(4-cyano-2-methyltetrahydro-2H-pyran-4-yl)(3-((diethylphosphoryl)oxy)propyl)carbamate (**3.58**) Following the general procedure, FCC (2:3 hexanes/EtOAc) yielded 47 mg (74%) as a clear oil. Preformed on a 0.15 mmol scale.

^{1}H NMR (CDCl$_3$, 500 MHz) δ 4.10 (pentet, J = 7.4 Hz, 4H), 4.08–4.00 (m, 2H), 3.86 (br d, J = 12.0 Hz, 1H), 3.63–3.40 (m, 4H), 2.68 (t, J = 16.8 Hz, 4H), 1.80 (dd, J = 11.0, 3.0 Hz, 1H), 1.49 (s, 9H), 1.33 (t, J = 7.0 Hz, 6H), 1.20 (t, J = 6.0 Hz, 3H); ^{13}C NMR (CDCl$_3$, 125 MHz) δ 155.3, 121.5, 82.5, 68.3, 65.3 (d, $^2J_{PC}$ = 6.3 Hz), 64.0 (d, $^2J_{PC}$ = 5.0 Hz), 62.4, 52.0, 42.5, 41.3, 29.3 (d, $^3J_{PC}$ = 6.3 Hz), 28.4, 21.2, 16.3 (d, $^3J_{PC}$ = 6.3Hz); IR (thin film) 2978, 2933, 2871, 1704 cm^{-1}; HRMS (ESI) calcd for C$_{19}$H$_{35}$N$_2$O$_7$PNa [M+Na]$^+$ 457.2079, found 457.2082
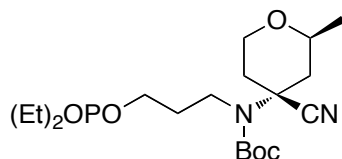
Tert-butyl(4-cyano-2-methyltetrahydro-2H-pyran-4-yl)(3-((diethylphosphoryl)oxy)propyl)carbamate (**3.59**) Following the general procedure, FCC (2:3 hexanes/EtOAc) yielded 65 mg (84%) as a clear oil. Preformed on a 0.15 mmol scale.

^{1}H NMR (CDCl$_3$, 500 MHz) δ 4.09 (pent, J = 7.3 Hz, 4H), 4.05–3.98 (m, 3H), 3.80 (app t, J = 12.0 Hz, 2H), 3.43 (app t, J = 7.8 Hz, 2H), 2.42 (d, J = 13.0 Hz, 1H), 2.36 (d, J = 13.0 Hz, 1H), 1.94–1.81 (m, 3H), 1.53 (app d, J = 11.0 Hz, 1H), 1.48 (s, 9H), 1.32 (t, J = 7.0 Hz, 6H), 1.22 (d, J = 6.0 Hz, 3H); ^{13}C NMR (CDCl$_3$, 125 MHz) δ 154.3, 119.7, 82.3, 70.5, 65.2 (d, $^2J_{PC}$ = 6.3 Hz), 64.3, 64.0 (d, $^2J_{PC}$ = 6.3 Hz), 55.8, 42.0, 41.2, 35.0, 31.2 (d, $^3J_{PC}$ = 6.3 Hz), 28.4, 28.32*, 21.4,

16.3 (d, $^3J_{PC}$ = 6.3Hz); IR (thin film) 2978, 2936,1704; HRMS (ESI) calcd for $C_{19}H_{35}N_2O_7PNa$ [M+Na]$^+$ 457.2079, found 457.2070
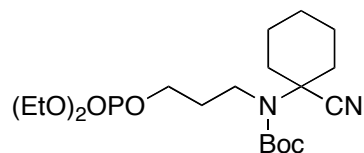
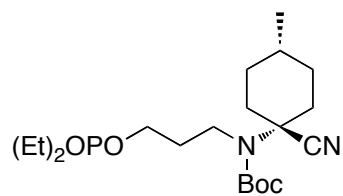***Tert*-butyl (1-cyanocyclohexyl)(3-((diethoxyphosphoryl)oxy)propyl)carbamate** (**2.32**) Following the general procedure, FCC (1:2 Hexanes/EtOAc with 1% Et$_3$N) yielded 760 mg (89%) of a clear oil. Performed on a 2.0 mmol scale. The analytical data matched those previously reported.[60]
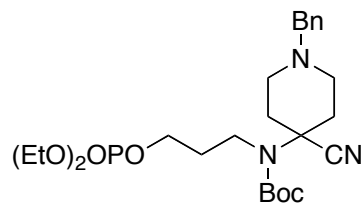

***Tert*-butyl(1-benzyl-4-cyanopiperidin-4-yl)(3-((diethoxyphosphoryl)oxy)propyl)**

carbamate (**3.91**) Following the general procedure, FCC (100% EtOAc with 1% Et$_3$N) yielded 56 mg (82%) of a clear oil. Performed on a 0.098 mmol scale.

^{1}H NMR (CDCl$_3$, 500 MHz) δ 7.35–7.28 (m, 4H), 7.27–7.22 (m, 1H), 4.11 (pent, *J* = 8.0 Hz, 4H), 4.05 (q, *J* = 6.3 Hz, 2H), 3.53 (s, 2H), 3.46 (app t, *J* = 7.5 Hz, 2H), 2.93 (d, *J* = 12.0, 2H), 2.47–2.38 (m, 4H), 1.98–1.88 (m, 4H), 1.51 (s, 9H), 1.33 (td, *J* = 7.5, 1.0 Hz, 6H); ^{13}C NMR (CDCl$_3$, 125 MHz) δ 154.5, 138.1, 129.1, 128.4, 127.3, 119.8, 82.2, 65.4 (d, $^2J_{PC}$ = 6.0 Hz), 63.9 (d, $^2J_{PC}$ = 6.0 Hz), 62.5, 56.4, 50.3, 41.1, 34.9, 31.2, 28.4 (d, $^3J_{PC}$ = 6.9 Hz), 16.3 (d, $^3J_{PC}$ = 6.4

Hz); IR (thin film) 2978, 2977, 2816, 2235, 1700 cm^{-1}; HRMS (ESI) calcd for $C_{25}H_{40}N_3O_6PNa$

[M+Na]$^+$ 532.2552, found 532.2546
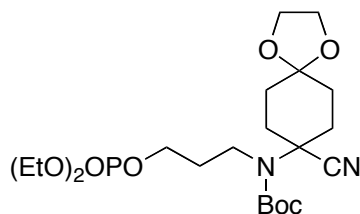
Tert-butyl(8-cyano-1,4-dioxaspiro[4.5]decan-8-yl)(3-((diethoxyphosphoryl)oxy)

propyl)carbamate (**3.95**) Following the general procedure, FCC (2:3 hexanes/EtOAc to

100% EtOAc) yielded 84 mg (89%) as a clear oil. Performed on a 0.20 mmol scale.

^{1}H NMR (CDCl$_3$, 500 MHz) δ 4.12 (quintet, J = 7.3 Hz, 4H), 4.05 (q, J = 12.0 Hz, 2H), 3.99–

3.89 (m, 4H), 3.46 (app t, J = 7.8 Hz, 2H), 2.45–2.39 (m, 2H), 2.09–1.97 (m, 4H), 1.92 (app

quintet, J = 6.5 Hz, 2H), 1.83–1.76 (m, 2H), 1.51 (s, 9H), 1.34 (t, J = 7.0 Hz, 6H); ^{13}C NMR

(CDCl$_3$, 125 MHz) δ 154.5, 119.6, 106.7, 82.2, 65.4 (d, $^2J_{PC}$ = 6.3 Hz), 64.8, 64.5, 64.0 (d, $^2J_{PC}$ =

5.0 Hz), 56.8, 41.4, 32.6, 32.1, 31.3 (d, $^3J_{PC}$ = 6.3 Hz), 28.4, 16.3 (d, $^3J_{PC}$ =6.3Hz); IR (thin

film) 2977, 2937, 2235, 1698 cm^{-1}; HRMS (ESI) calcd for $C_{21}H_{37}N_2O_8PNa$ [M+Na]$^+$ 499.2185,

found 499.2165.
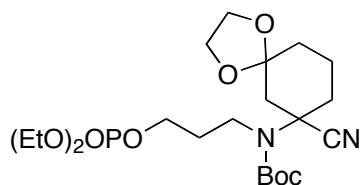
Tert-butyl(7-cyano-1,4-dioxaspiro[4.5]decan-7-yl)(3-((diethoxyphosphoryl)oxy)

propyl)carbamate (**3.99**) Following the general procedure, FCC (2:3 hexanes/EtOAc to

EtOAc) yielded 226 mg (86%) as a clear oil. Preformed on a 0.55 mmol scale.

^{1}H NMR (CDCl$_3$, 500 MHz) δ 4.12 (quint, J = 7.3 Hz, 4H), 4.08–4.00 (m, 4H), 3.96–3.89 (m, 2H), 2.74 (br d, J = 13.4 Hz, 1H), 2.31 (br d, J = 10.8 Hz, 1H), 2.08–1.78 (m, 8H), 1.51 (s, 9H), 1.34 (t, J = 7.1 Hz, 6H); ^{13}C NMR (CDCl$_3$, 125 MHz) δ 154.3, 120.3, 82.5, 65.4 (d, $^2J_{PC}$ = 6.0 Hz), 65.1, 64.5, 64.0 (d, $^2J_{PC}$ = 6.0 Hz), 42.2, 41.8, 34.4 31.2 (d, $^3J_{PC}$ = 6.4 Hz) 29.8, 28.5, 20.4, 16.3 (d, $^3J_{PC}$ = 6.5Hz); IR (thin film) 2978, 2934, 2238, 1699 cm^{-1}; HRMS (ESI) calcd for C$_{21}$H$_{37}$N$_2$O$_8$PNa [M+Na]$^+$ 499.2185, found 499.2165.
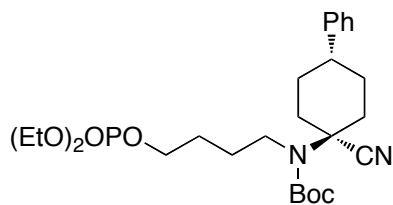
Tert-butyl(1-cyano-4-phenylcyclohexyl)(4-((diethoxyphosphoryl)oxy)butyl) carbamate (**3.108a**) Following the general procedure, FCC (1:1 hexanes/EtOAc with 1% Et$_3$N) yielded 117 mg (81%) as a clear oil. Performed on a 0.28 mmol scale.

3.108a (major isomer): ^{1}H NMR (CDCl$_3$, 500 MHz) δ 7.35-7.29 (m, 2H), 7.26-7.18 (m, 3H), 4.10 (pent, J=7.1 Hz, 4H), 4.02 (q, J=6.6 Hz, 2H), 3.40 (app. t, J=6.8 Hz, 2H), 2.82 (tt, J=8.8, 3.9 Hz, 1H), 2.57 (br s, J=6.6 Hz, 2H), 2.13-2.04 (m, 2H), 2.04-1.96 (m, 2H) 1.85 (app. q, J=10.6 Hz, 2H), 1.75-1.65 (m, 4H), 1.51 (s, 9H), 1.33 (dt, J=7.0, 0.9 Hz, 6H); ^{13}C NMR (CDCl$_3$, 125 MHz) δ 155.3, 144.5, 128.7, 126.9, 126.5, 121.8, 82.0, 67.1 (d, $^2J_{PC}$ = 6.0 Hz), 63.9 (d, $^2J_{PC}$ = 6.0 Hz), 54.3, 44.6, 33.9, 28.4, 28.2, 27.9 (d, $^3J_{PC}$ = 7.0 Hz), 25.8, 16.3 (d, $^3J_{PC}$ = 6.5 Hz); IR (thin film) 3059, 2977, 2932, 2870, 2232, 1701 cm^{-1}; HRMS (ESI) calcd for C$_{26}$H$_{41}$N$_2$O$_6$PNa [M+Na]$^+$ 531.2600, found 531.2596
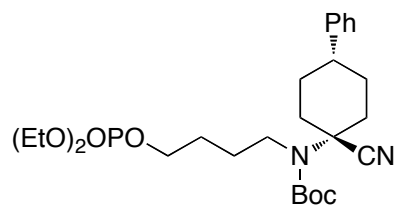
3.108a (minor isomer): ^{1}H NMR (CDCl$_3$, 500 MHz) δ 7.35-7.29 (m, 2H), 7.26-7.19 (m, 3H), 4.12 (pent, *J*=7.3 Hz, 4H), 4.07 (q, *J*=6.0 Hz, 2H), 3.43 (app. t, *J*=7.0 Hz, 2H), 2.61-2.50 (m, 2H), 2.07-1.90 (m, 6H), 1.76-1.68 (m, 3H), 1.53 (s, 9H), 1.35 (t, *J*=7.2 Hz, 6H); ^{13}C NMR (CDCl$_3$, 125 MHz) δ 154.5, 145.3, 128.7, 127.0, 126.7, 120.0, 81.9, 67.1 (d, $^2J_{PC}$ = 6.0 Hz), 63.9 (d, $^2J_{PC}$ = 6.0 Hz), 57.9, 44.1, 43.1, 35.2, 31.1, 28.5, 27.8 (d, $^3J_{PC}$ = 7.0 Hz), 27.1, 16.3 (d, $^3J_{PC}$ = 7.0 Hz); IR (thin film) 3058, 3026, 2977, 2933, 2867, 2233, 1697 cm^{-1}; HRMS (ESI) calcd for C$_{26}$H$_{41}$N$_2$O$_6$PNa [M+Na]$^+$ 531.2600, found 531.2591
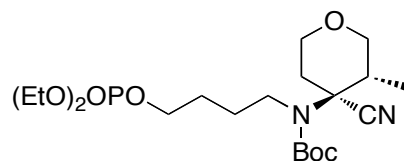
***Tert*-butyl(4-cyano-3-methyltetrahydro-2H-pyran-4-yl)(4((diethoxyphosphoryl)oxy) butyl)carbamate** (**3.112**) Following the general procedure, FCC (1:2 Hexanes/EtOAc with 1% Et$_3$N) yielded 300 mg (73%) of a clear oil. Performed on a 0.92 mmol scale.

^{1}H NMR (CDCl$_3$, 500 MHz) δ 4.11–3.97 (m, 6H), 3.94 (dd, *J* = 12.5, 4.5 Hz, 1H), 3.79 (dd, *J* = 11.5, 4.0 Hz, 1H), 3.67 (tt, *J* = 12.5, 1.5 Hz, 1H), 3.53–3.43 (m, 1H), 3.40–3.27 (m, 2H), 2.90 (br s, 1H), 2.53 (br s, 1H), 1.97 (d, *J* = 13.5, 1H), 1.72–1.60 (m, 4H), 1.44 (s, 9H), 1.29 (t, *J* = 7.0 Hz, 6H), 0.90 (d, *J* = 7.0 Hz, 3H); ^{13}C NMR (CDCl$_3$, 125 MHz) δ 153.8, 117.2, 81.6, 70.9, 67.0 (d, $^2J_{PC}$ = 6.0 Hz), 65.2, 64.0, 63.7 (d, $^2J_{PC}$ = 6.0 Hz), 47.3, 35.8, 34.4, 28.3, 27.7 (d, $^3J_{PC}$ =

6.9 Hz), 26.6, 16.2 (d, $^3J_{PC}$ = 6.9 Hz); IR (thin film) 2976, 2935, 2912, 2858, 2237, 1698 cm^{-1};

HRMS (ESI) calcd for $C_{20}H_{37}N_2O_7PNa$ [M+Na]$^+$ 471.2236, found 471.2233
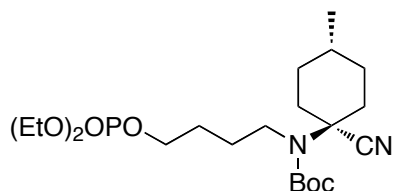
***Tert*-butyl(1-cyano-4-methylcyclohexyl)(4-((diethoxyphosphoryl)oxy)butyl)**

carbamate (**3.116**) Following the general procedure, FCC (1:2 Hexanes/EtOAc with 1%

Et$_3$N) yielded 520 mg (74%) of a clear oil. Performed on a 1.1 mmol scale.

^{1}H NMR (CDCl$_3$, 500 MHz) δ 4.11 (pent, J = 7.5 Hz, 4H), 4.04 (q, J = 6.0 Hz, 2H), 3.37 (app t, J

= 7.5 Hz, 2H), 2.40 (br d, J = 12.5 Hz, 2H), 1.81-1.57 (m, 9H), 1.50 (s, 9H), 1.48-1.39 (m, 2H),

1.34 (t, J = 7.0 Hz, 6H), 1.34 (t, J = 7.0 Hz, 6H), 0.95 (d, J = 6.0 Hz, 3H); ^{13}C NMR (CDCl$_3$, 125

MHz) δ 154.5, 120.2, 81.7, 67.1 (d, $^2J_{PC}$ = 6.0 Hz), 63.9 (d, $^2J_{PC}$ = 6.0 Hz), 58.0, 43.9, 35.1, 31.9,

31.6, 28.4, 27.8 (d, $^3J_{PC}$ = 6.9 Hz), 27.0, 21.8, 16.3 (d, $^3J_{PC}$ = 6.9 Hz); IR (thin film) 2973, 2939,

2234, 1700 cm^{-1}; HRMS (ESI) calcd for $C_{21}H_{39}N_2O_6PNa$ [M+Na]$^+$ 469.2444, found 469.2456
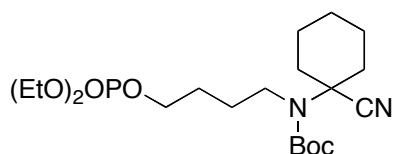
***Tert*-butyl(1-cyanocyclohexyl)(4-((diethoxyphosphoryl)oxy)butyl)carbamate**

(**3.119**) Following the general procedure, FCC (1:2 Hexanes/EtOAc with 1% Et$_3$N) yielded

480 mg (75%) of a clear oil. Performed on a 1.5 mmol scale.

¹H NMR (CDCl₃, 500 MHz) δ 4.11 (pent, *J* = 7.0 Hz, 4H), 4.04 (q, *J* = 6.5 Hz, 2H), 3.36 (app t, *J* = 6.8 Hz, 2H), 2.38 (app d, *J* = 9.5 Hz, 2H), 1.87–1.57 (m, 11H), 1.50 (s, 9H), 1.34 (t, *J* = 7.0 Hz, 6H), 1.24–1.11 (m, 1H); ¹³C NMR (CDCl₃, 125 MHz) δ 154.4, 120.1, 81.7, 67.1 (d, $^2J_{PC}$ = 6.0 Hz), 63.9 (d, $^2J_{PC}$ = 6.0 Hz), 58.2, 43.9, 35.2, 28.4, 27.8 (d, $^3J_{PC}$ = 6.9 Hz), 24.8, 23.5, 16.3 (d, $^3J_{PC}$ = 6.5 Hz); IR (thin film) 2977, 2938, 2234, 1698 cm⁻¹; HRMS (ESI) calcd for C₂₀H₃₇N₂O₆PNa [M+Na]⁺ 455.2287, found 455.2277
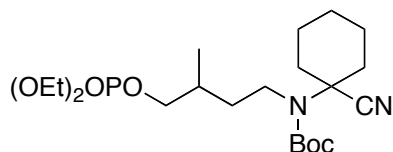
Tert-butyl(1-cyanocyclohexyl)(4-((diethoxyphosphoryl)oxy)-3-methylbutyl) carbamate (**3.126**) Following the general procedure, FCC (1:1 Hexanes/EtOAc with 1% Et₃N) yielded 440 mg (84%) of a clear oil. Performed on a 0.97 mmol scale.

¹H NMR (CDCl₃, 500 MHz) δ 4.10 (pent, *J* = 7.3 Hz, 4H), 3.84 (t, *J* = 6.1 Hz, 2H), 3.47-3.27 (m, 2H), 2.37 (br d, *J* = 10.4 Hz, 2H), 1.85-1.60 (m, 9H), 1.49 (s, 9H), 1.44-1.37 (m, 1H), 1.32 (t, *J* = 7.1 Hz, 6H), 1.32 (t, *J* = 7.1 Hz, 6H), 1.22-1.11 (m, 1H), 0.98 (t, *J* = 6.7 Hz, 3H); ¹³C NMR (CDCl₃, 125 MHz) δ 154.3, 120.1, 81.6, 71.8 (d, $^2J_{PC}$ = 6.0 Hz), 63.8 (d, $^2J_{PC}$ = 6.0 Hz), 58.1, 42.4, 35.1, 33.9, 32.3 (d, $^3J_{PC}$ = 7.4 Hz), 28.4, 24.7, 23.5, 16.4 (d, $^3J_{PC}$ = 6.0 Hz); IR (thin film) 2978, 2937, 2235, 1698 cm⁻¹; HRMS (ESI) calcd for C₂₁H₃₉N₂O₆PNa [M+Na]⁺ 469.2444, found 469.2435

Reductive Lithiation General Procedure

An oven-dried round–bottom flask equipped with a glass stir bar was cooled under vacuum and back filled with argon. The flask was charged with 1,10- phenanthroline (1 crystal),

and a 0.06 M solution of phosphate (1 equiv) in THF. The solution was cooled to –78 °C and

n-BuLi (ca. 2 M solution in hexane) was added until a dark brown color persisted (~2

drops). To that solution at –78 °C was added LiDBB (nominal 0.4 M, 3 equiv) *via* syringe to

produce a solution that remained dark green for ≥20 sec. The mixture was stirred for 1 h,

then quenched with MeOH and saturated aq. NH$_4$Cl. The reaction mixture was diluted with

Et$_2$O, the aqueous layer was separated and extracted with Et$_2$O (3x). The combined organic

layers were washed with brine, dried over MgSO$_4$, and concentrated *in vacuo* to give a light

yellow viscous solid. Purification by flash column chromatography gave the title compound.

In some instances the title compound co-eluted with an elimination product.

This alkene was dihydroxylated by making a solution of the spirocycle/alkene mixture in

1:1 acetone/H$_2$O (0.16 M solution) and adding 1 mol% K$_2$OsO$_4$ and 3 equiv *N*-

methylmorpholine oxide. The solution was heated to 40 °C over night, quenched with

Na$_2$S$_2$O$_3$ and extracted with Et$_2$O (3x). The combined organic layers were dried over MgSO$_4$,

filtered and concentrated *in vacuo* to give a yellow oil. Purification by flash column

chromatography gave the title compound.

The ^{1}H and ^{13}C data for spirocycles contained mixtures of 2 or more rotamers. These were

characterized by normalizing the integrations such that the total number of protons is

equal to the total number of hydrogens expected for a single diastereomer, or by heating to

343 K to coalesce the rotamer signals.
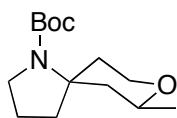
***Tert*-butyl 7-methyl-8-oxa-1-azaspiro[4.5]decane-1-carboxylate** (**3.61**) Following the

general procedure, FCC (3:2 pentane/Et$_2$O) yielded 12 mg (53%) as a clear oil (99.9:0.1 dr by GCMS). Preformed on a 0.08 mmol scale. Stereochemistry assigned by reduction of the *N*–Boc to the *N*-Me derivative; see next section

^{1}H NMR (CDCl$_3$, 500 MHz) δ 3.93 (dd, *J* = 6.5, 5.0 Hz, 1H), 3.52–3.33 (m, 4H), 2.80* (br s, 1H), 2.54 (br s, 1H), 2.27(br s, 1H), 1.95 (br s, 2H), 1.74 (app pentet, *J* = 6.9 Hz, 2H), 1.49 (s, 9H), 1.46* (s, 9H), 1.45 (s, 9H)*, 1.38–1.20 (m, 2H), 1.18 (d, *J* = 6.0 Hz, 3H); ^{13}C NMR (125 MHz, C$_6$D$_6$, 342K) δ 153.6, 78.7, 71.8, 65.8, 62.1, 48.0, 42.6, 36.9, 30.2, 28.8, 22.4, 22.1; IR (thin film) 2971, 2928, 2868, 1693 cm^{-1}; HRMS (ESI) calcd for C$_{14}$H$_{25}$NO$_3$Na [M+Na]$^+$ 278.1732, found 278.1731.
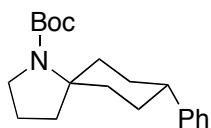
***Tert*-butyl 8-phenyl-1-azaspiro[4.5]decane-1-carboxylate** (**3.60**) Following the general procedure, FCC (9:1 hexanes/EtOAc) to yield 30 mg (73%) as a clear oil (98.2:1.8 dr by GCMS). Preformed on a 0.13 mmol scale. The analytical data matched those previously reported.[62]
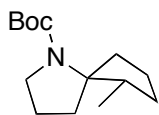
***Tert*-butyl 6-methyl-1-azaspiro[4.4]nonane-1-carboxylate** (**3.68**) Following the general procedure, FCC (14:1 pentane/Et$_2$O) yielded 98 mg (60%) as a clear oil (>99.9:0.1 dr by GCMS). Preformed on a 0.68 mmol scale. Stereochemistry assigned in the next section

^{1}H NMR (CDCl$_3$, 500 MHz) δ 3.58–3.22 (m, 1.9H), 3.04–2.90 (m, 0.52H), 2.75–2.62 (m, 0.43H), 2.46 (q, J = 9.7 Hz, 0.55H), 2.26 (q, J = 9.7 Hz, 0.44H), 2.01–1.84 (m, 1.0H), 1.84–1.60 (m, 4.54H), 1.58–1.29 (m, 11.52), 1.11 (app. pent., J = 10.0 Hz, 0.94H), 0.95 (d, J = 6.6 Hz, 0.33H), 0.84 (br. s, 2.78H); ^{13}C NMR (CDCl$_3$, 125 MHz, *denotes minor rotamer) δ 154.5*, 153.3, 79.2*, 78.5, 72.0, 71.4*, 48.7, 37.9*, 36.1, 34.8, 34.2, 32.8, 31.4*, 31.1, 28.7, 22.3, 21.9*, 20.5*, 20.2, 13.5, 13.4*; IR: 2964, 2871, 1694 cm^{-1}; HRMS (ESI) calcd for C$_{14}$H$_{25}$NO$_2$Na [M+Na]$^+$ 262.1783, found 262.1783.
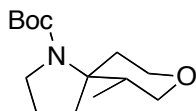
Tert-butyl 6-methyl-8-oxa-1-azaspiro[4.5]decane-1-carboxylate (**3.69**) Following the general procedure, FCC (3:2 pentane/Et$_2$O) yielded 101 mg (53%) as a clear oil (98.0:2.0 dr by GCMS). Preformed on a 1.0 mmol scale. Stereochemistry assigned by reduction to the *n*-Boc derivative; see next section

^{1}H NMR (CDCl$_3$, 500 MHz) δ 3.92 (dd, J = 11.6, 5.1 Hz, 0.82 H), 3.72 (dd, J = 11.2, 3.8 Hz, 0.95H), 3.56 (ddd, J = 8.4, 8.3, 3.4 Hz, 0.42H), 3.47 (app, t J = 10.0 Hz, 1H), 3.39 (q, J = 8.6 Hz, 0.45H), 3.31 (q, J = 8.5 Hz, 0.37H), 3.07 (q, J = 10.4 Hz, 1.1H), 2.87–2.71 (m, 0.73H), 2.51 (dt, J = 12.8, 4.8 Hz, 0.38H), 2.04–1.90 (m, 0.74), 1.90–1.68 (m, 2.52H), 1.62 (app s, 2.83H), 1.53–1.42 (m, 8.0 H), 1.33 (d, J = 12.5 Hz, 0.56H), 1.27 (d, J = 13.5 Hz, 0.79H), 1.16 (d, J = 7.5 Hz, 0.54H), 0.682 (br t, J = 8.3 Hz, 2.2H); ^{13}C NMR (CDCl$_3$, 125 MHz, *denotes minor rotamer) δ 154.4, 153.4*, 79.9*, 78.8, 71.9, 71.7*, 66.4, 66.2*, 65.0*, 64.7, 48.7, 48.4*, 36.5, 36.3*, 35.2*, 34.9, 30.3, 29.4, 28.8*, 28.7*, 28.7, 22.6*, 20.0, 10.6, 10.5*; IR: 2973, 2936, 2219, 1696 cm^{-1}; HRMS (ESI) calcd for C$_{14}$H$_{25}$NO$_3$Na [M+Na]$^+$ 278.1732, found 278.1732
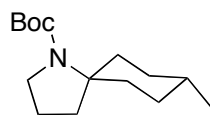
***Tert*-butyl 8-methyl-1-azaspiro[4.5]decane-1-carboxylate** (**3.70**) Following the general

procedure, FCC (5:1 pentane/DCM to 16:1 pentane/Et$_2$O) yielded 25 mg (72%) of a clear

oil. Performed on a 0.19 mmol scale. Stereochemistry assigned by analogy to **3.117**.

^{1}H NMR (CDCl$_3$, 500 MHz) δ 3.41 (app d, *J* = 11.5 Hz, 2H), 2.54 (br s, 1H), 2.31 (br s, 1H),

1.83 (br s, 2H), 1.69 (pent, *J* = 7.0 Hz, 2H), 1.66–1.59 (m, 2H), 1.54–1.39 (m, 9H), 1.37–1.24

(m, 3H), 0.98 (dq, *J* = 13.5, 2.5 Hz, 2H), 0.87 (d, *J* = 6.0 Hz, 3H); ^{13}C NMR (CDCl$_3$, 125 MHz,

denotes minor rotamer) δ 154.6, 153.6, 79.3, 78.5*, 63.9, 63.5*, 48.1, 37.4, 36.3, 34.4,

34.1*, 33.7*, 33.2, 32.1, 31.6*, 29.8*, 28.8, 22.5, 22.0*; IR (thin film) 2950, 2926, 2868, 1701

cm^{-1}; HRMS (ESI) calcd for C$_{15}$H$_{27}$NO$_2$Na [M+Na]$^+$ 276.1939, found 276.1937
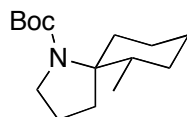
***Tert*-butyl 6-methyl-1-azaspiro[4.5]decane-1-carboxylate** (**3.71**) Following the general

procedure, FCC (5:1 pentane/DCM to 10:1 pentane/Et$_2$O) yielded 40 mg (68%) of a clear

oil. Performed on a 0.23 mmol scale. The analytical data matched those previously
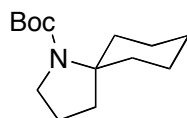
reported.[13]

***Tert*-butyl   1-azaspiro[4.5]decane-1-carboxylate**   (**2.33**)   Following   the   general

procedure, FCC (5:1 pentane/DCM to 15:1 pentane/Et$_2$O) yielded 19 mg (67%) of a clear

oil. Performed on a 0.12 mmol scale. The analytical data matched those previously reported.[60]
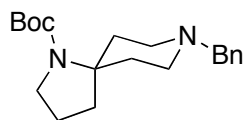
***Tert*-butyl 8-benzyl-1,8-diazaspiro[4.5]decane-1-carboxylate** (**3.92**) Following the general procedure, FCC (5:1 pentane/DCM to 3:2 hexanes/EtOAc) yielded 12 mg (16%) of a clear oil. Performed on a 0.22 mmol scale.

^{1}H NMR (CDCl$_3$, 500 MHz) δ 7.40–7.28 (m, 5H), 4.95 (d, *J* = 15.0 Hz, 0.5H), 4.72 (s, 0.9H), 4.46 (d, *J* = 14.0, 0.5H), 3.37 (ddd, *J* = 11.0, 7.0, 6.0 Hz, 0.6H), 3.71–3.63 (m, 0.5H), 3.54–3.31 (m, 3.2H), 3.19–3.09 (m, 0.5H), 2.91 (td, *J* = 13.5, 5.0 Hz, 0.6H), 2.19–2.02 (m, 1.8H), 2.01 1.79 (m, 2H), 1.61 (s, 1.5H), 1.56–1.36 (m, 9.8H), 1.36–1.24 (m, 0.8H) ^{13}C NMR (CDCl$_3$, 125 MHz, *denotes minor rotamer) δ 157.7*, 157.5, 154.2*, 153.1, 135.8, 135.8*, 129.0, 128.5*, 128.5, 128.2, 128.0*, 81.5, 80.5*, 68.7*, 68.6, 51.3*, 51.3, 48.3*, 48.3, 43.5*, 43.2, 36.0, 34.9*, 32.8, 28.5*, 28.4, 22.8*, 22.3; IR (thin film) 3061, 3027, 2973, 2930, 2870, 2804, 1953, 1688 cm^{-1}; HRMS (ESI) calcd for C$_{20}$H$_{30}$N$_2$O$_2$Na [M+Na]$^+$ 353.2205, found 353.2208
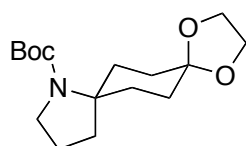
***Tert*-butyl-4-dioxalane-cyclohexylspiropyrrolidine** (**3.96**) Following the general procedure, FCC (2:1 pentane/Et$_2$O) yielded 9 mg (37%) of a white solid. Performed on a 0.081 mmol scale.

^{1}H NMR (CDCl$_3$, 500 MHz) δ 3.92 (s, 4H), 3.45 (app br s, 1H), 3.38 (app br s, 1H), 2.87 (app t, J = 11.9 Hz, 1H), 2.65 (app t, J = 12.0 Hz, 1H) 1.98-1.86 (m, 2H), 1.72 (app quint, J = 6.8 Hz, 4H), 1.60 (dt, J = 13.7, 4.2 Hz, 2H), 1.54-1.40 (m, 9H), 1.35-1.28 (m, 2H); ^{13}C NMR (CDCl$_3$, 125 MHz, *denotes minor rotamer) δ 154.6, 153.2*, 108.2, 79.5, 78.6*, 64.5*, 64.4, 64.2*, 63.0*, 62.7, 48.0, 36.7, 35.7*, 32.8, 31.5, 30.6, 28.7, 22.3*, 21.9; IR (thin film) 2971, 2932, 2874, 1693 cm^{-1}; HRMS (ESI) m / z calcd for C$_{16}$H$_{27}$NO$_4$Na [M+Na]$^+$ 320.1838, found 320.1835; mp = 260 °C (decomp).
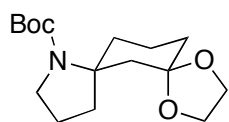
$Tert$-butyl-4-dioxalane-cyclohexylspiropyrrolidine (**3.100**) Following the general procedure, FCC (2:1 pentane/ Et$_2$O) yielded 26 mg (62%) of a clear oil. Performed on a 0.14 mmol scale.

^{1}H NMR (CDCl$_3$, 500 MHz, * denotes minor rotamer) δ 3.88 (app dd, J = 11.5, 5.0 Hz, 4H), 3.46 (app d, J = 7.8 Hz, 2H), 3.38 (app d, J = 8.5 Hz, 2H), 2.81* (d, J = 13.5 Hz, 1H), 2.52* (d, J = 13.5 Hz, 1H), 2.46 (t, J = 12.1 Hz, 2H), 2.21 (app t, J = 10.0 Hz, 2H), 2.16–2.06* (m, 1H), 1.89–1.74 (m, 2H), 1.74–1.61 (m, 4H), 1.56–1.26 (m, 13H); ^{13}C NMR (CDCl$_3$, 125 MHz, * denotes minor rotamer) δ 154.3, 153.5*, 110.0, 109.8*, 79.7*, 78.7, 64.6, 64.5*, 63.8, 48.0, 47.9*, 42.1, 40.8•, 38.2*, 37.2, 34.6*, 34.2, 33.7, 32.4, 28.7, 22.4, 22.0*, 20.7; IR (thin film) 2967, 2873, 1690 cm^{-1}; HRMS (ESI) calcd for C$_{16}$H$_{27}$NO$_4$Na [M+Na]$^+$ 320.1838, found 320.1829.
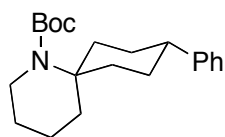
NOESY Correlations
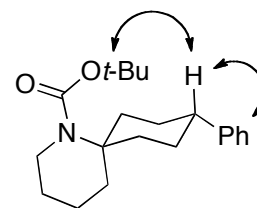
Tert-butyl 9-phenyl-1-azaspiro[5.5]undecane-1-carboxylate (**3.109**) Following the general procedure, FCC (5:1 pentane/DCM to 12:1 pentane/Et$_2$O) yielded 9 mg (32%) of a clear oil. Performed on a 0.086 mmol scale. . Relevant NOSEY correlations shown.

^{1}H NMR (CDCl$_3$, 500 MHz) δ 7.32–7.25 (m, 2H), 7.23–7.14 (m, 3H), 3.51 (t, _J_ = 6.0 Hz, 2H), 2.78 (td, _J_ = 13.0, 6.0 Hz, 2H), 2.63 (tt, _J_ = 12.5, 3.5 Hz, 1H), 1.86 (t, _J_ = 7.0 Hz, 2H), 1.79 (d, _J_ = 13.0 Hz), 1.72 (d, _J_ = 13.0 Hz, 2H), 1.68–1.55 (m, 6H), 1.49 (s, 9H); ^{13}C NMR (CDCl$_3$, 125 MHz) δ 155.6, 147.4, 128.4, 126.9, 126.0, 79.3, 58.2, 43.5, 40.6, 32.1, 30.9, 29.2, 28.8, 22.9, 16.4; IR (thin film) 3058, 3025, 2969, 2928, 2867, 1687 cm^{-1}; HRMS (ESI) calcd for C$_{21}$H$_{31}$NO$_2$Na [M+Na]$^+$ 352.2253, found 352.2254
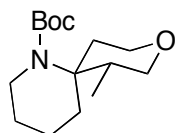
Tert-butyl 7-methyl-9-oxa-1-azaspiro[5.5]undecane-1-carboxylate (**3.113**) Following the general procedure, FCC (5:1 pentane/DCM to 3:2 pentane/Et$_2$O) yielded 16 mg (27%) of a clear oil. Performed on a 0.22 mmol scale. Stereochemistry assigned by analogy to **3.69**

^{1}H NMR (CDCl$_3$, 500 MHz) δ 4.19–3.94 (m, 0.63H), 3.89 (dd, _J_ = 11.0, 4.0 Hz, 0.1H), 3.83 (dd, _J_ = 13.5, 4.5 Hz, 1.02H), 3.72–3.61 (m, 1.46H), 3.65 (dt, _J_ = 11.5, 2.5 Hz, 0.95H), 3.44 (dt, _J_ =

11.5, 2.0 Hz, 0.16H), 3.36–3.20 (m, 0.61H), 2.96 (br s, 0.69H), 2.80 (br s, 0.53H), 2.70 (ddt, J = 13.5, 5.0, 1.0 Hz, 0.23 H), 2.40 (br s, 0.52H), 2.27 (br s, 0.55H), 2.14–2.03 (m, 1.54H), 1.95–1.84 (m, 0.84H), 1.70–1.60 (m, 2.90 H), 1.60–1.49 (m, 1.76), 1.48–1.46 (m, 2.9H), 1.49 (s, 6.07H), 1.38–1.23 (m, 1.23H), 1.90 (d, J = 7.0Hz, 1.95H), 1.04 (d, J = 7.0 Hz, 0.23H), 0.78 (d, J = 7.0 Hz, 0.68H); ^{13}C NMR (CDCl$_3$, 125 MHz, *denotes minor rotamer) δ 155.5, 79.7*, 79.3, 70.4*, 69.8, 65.2*, 64.9, 59.7*, 59.5, 41.5, 41.1*, 35.7, 34.3*, 32.1*, 31.7*, 31.4, 28.8*, 28.7, 25.4, 25.2*, 22.6, 21.5*, 19.7, 15.9*, 13.1*, 10.6; IR (thin film) 2966, 2931, 2854, 1698 cm^{-1}; HRMS (ESI) calcd for C$_{15}$H$_{27}$NO$_3$Na [M+Na]$^+$ 292.1889, found 292.1879
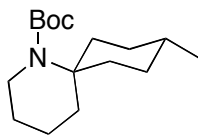
NOESY Correlations
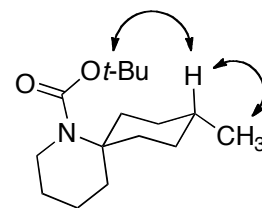
Tert-butyl 9-methyl-1-azaspiro[5.5]undecane-1-carboxylate (**3.117**) Following the general procedure, FCC (5:1 pentane/DCM to 16:1 pentane/Et$_2$O) yielded 25 mg (28%) of a clear oil. Performed on a 0.34 mmol scale. . Relevant NOSEY correlations shown.

^{1}H NMR (CDCl$_3$, 500 MHz) δ 4.38 (t, J = 6.0 Hz, 2H), 2.56 (dt, J = 13.0, 4.0, 2H), 1.73 (t, J = 6.5 Hz, 2H), 1.65–1.51 (m, 7H), 1.49–1.42 (m, 11H), 1.06 (dq, J = 15.0, 5.0 Hz, 2H), 0.87 (d, J = 6.5 Hz, 3H); ^{13}C NMR (CDCl$_3$, 125 MHz) δ 155.8, 79.2, 58.5, 40.5, 32.0, 32.0, 31.9, 29.2, 28.8, 28.7*, 22.9, 22.5, 20.5; IR (thin film) 2929, 2868, 1690 cm^{-1}; HRMS (ESI) calcd for C$_{16}$H$_{29}$NO$_2$Na [M+Na]$^+$ 290.2096, found 290.2086
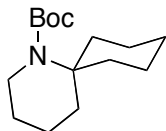
***Tert*-butyl 1-azaspiro[5.5]undecane-1-carboxylate** (**3.122**) Following the general procedure, FCC (5:1 pentane/DCM to 8:1 pentane/Et$_2$O) yielded 26 mg of **3.120**, **3.121**, and **3.122** as yellow oil. GCMS analysis of the mixture showed 2.6 mg (1.5%) of **3.120**, 7.7 mg (9.2%) of **3.121**, and 17.7 mg (30.2%) of **3.122**. Synthesis of products **3.120** and **3.121** detailed in chapter 4. Performed on a 0.23 mmol scale. The analytical data matched those previously reported.[14]
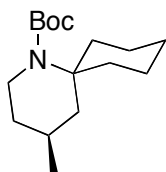
***Tert*-butyl 4-methyl-1-azaspiro[5.5]undecane-1-carboxylate** (**3.129**) Following the general procedure, FCC (5:1 pentane/DCM to 8:1 pentane/Et$_2$O) yielded 11 mg of **3.129**, **3.128**, and **3.129** as yellow oil. GCMS analysis of the mixture showed 5.3 mg (11.8%) of **3.127**, 4.1 mg (9.2%) of **3.128**, and 1 mg (3%) of **3.129**. Products **3.127** and **3.128** are assumed based on side products from the analogous **3.122** Performed on a 0.17 mmol scale.

^{1}H NMR (CDCl$_3$, 500 MHz) δ 3.65 (ddd, *J* = 14.0, 6.0, 4.5 Hz, 1H), 3.33 (ddd, 14.0, 9.0, 4.0 Hz, 1H), 2.83 (ddd, *J* = 13.0, 10.0, 3.5 Hz, 1H), 2.32–2.22 (m, 1H), 1.89 (dd, *J* = 13.5, 3.5 Hz, 1H), 1.83–1.75 (m, 1H), 1.63–1.30 (17H), 1.12–1.02 (m, 2H), 0.91 (d, *J* = 6.5, 3H); ^{13}C NMR

(CDCl$_3$, 125 MHz) δ 156.0, 79.1, 58.8, 41.5, 41.3, 36.9, 33.0, 31.5, 28.7, 25.9, 24.4, 23.1, 22.8, 22.7; IR (thin film) 2925, 2866, 1702 cm^{-1}; HRMS (ESI) calcd for C$_{16}$H$_{29}$NO$_2$Na [M+Na]$^+$ 290.2096, found 290.2092

Deprotection products
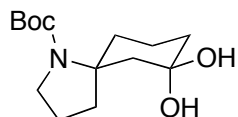
***Tert*-butyl 7,7-dihydroxy-1-azaspiro[4.5]decane-1-carboxylate** (**3.104**) To a solution of spirocycle (0.015 g, 0.050 mmol, 1 equiv) in THF (0.32 mL) were added acetic acid (0.32 mL, 5.6 mmol, 110 equiv) and water (0.12 mL, 6.7 mmol, 132 equiv), and the mixture heated to 65 °C. After 3 hours the reaction was cooled to rt and quenched with 50% sat. NaHCO$_3$ (2 mL) and diluted with EtOAc (3 mL). The organic layer was removed and the aqueous layer extracted with EtOAc (3 x 2 mL). The organic layers were combined, dried with MgSO$_4$ and concentrated. Purification by FCC (2:1 pentane/ether to 100% ether) gave 9 mg (65%) as a clear oil.

^{1}H NMR (C$_6$D$_6$, 500MHz, 342K) δ 3.57–3.50 (m, 4H), 3.45–3.26 (br s, 2H), 2.22 (app dt, *J* = 13.0, 6.9 Hz, 1H), 1.73 (app dt, *J* = 13.1, 6.7 Hz, 1H), 1.70–1.64 (m, 1H), 1.61–1.51 (m, 4H), 1.47 (s, 9H), 1.46–1.40 (m, 2H), 1.29 (app d, *J* = 12.7 Hz, 1H); ^{13}C NMR (C$_6$D$_6$, 125MHz, 342K) δ 153.7, 110.3, 78.6, 64.5, 63.8, 48.1, 35.0, 28.8, 22.5, 21.1**;** IR (thin film) 3349, 2924, 2854, 1693 cm^{-1}; HRMS (ESI) calcd for C$_{14}$H$_{23}$NO$_3$ [M+Na-H$_2$O]$^+$ 276.1576, found 276.1580.
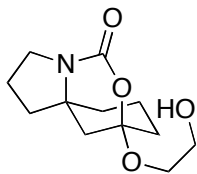
3-(2-hydroxyethoxy)hexahydro-3,6a-methanopyrrolo[1,2-*c*][1,3]oxazocin-1(7*H*)-one

(**3.103**) To a solution of *tert*-butyl-4-dioxalane-cyclohexylspiropyrrolidine (**3.100**, 26 mg, 0.076 mmol, 1 equiv) in DCM (90 μL), TFA (90 μL, 1.1 mmol, 15 equiv) was added. After stirring for 5 hours, the reaction was quenched with a 10% $NaHCO_3$ solution (1 mL), and diluted with DCM (2 mL). The organic layer was extracted and aqueous layer washed with DCM (3 x 2 mL) and the combined organic layers were dried with $MgSO_4$ and concentrated *in vacuo*, giving a yellow oil. Flash column chromatography (94:6 DCM/MeOH with 1% Et_3N) gave 3-(2-hydroxyethoxy)hexahydro-3,6a-methanopyrrolo[1,2-*c*][1,3]oxazocin-1(7*H*)-one in 18% yield (6 mg) as a clear oil.

^1H NMR ($CDCl_3$, 500 MHz) δ 3.85–3.79 (m, 2H), 3.76 (br s, 2H), 3.58–3.46 (m, 2H), 2.21 (app dd, J = 11.5, 2.5 Hz, 1H), 2.01–1.93 (m, 4H), 1.85 (dt, J = 12.5, 2.5 Hz, 1H), 1.81–1.67 (m, 4H), 1.62–1.55 (m, 2H), 1.36–1.27 (m, 1H); ^{13}C NMR ($CDCl_3$, 125 MHz) δ 153.3, 104.6, 63.5, 62.1, 61.2, 46.3, 40.6, 38.6, 35.3, 34.8, 21.6, 19.0; IR (thin film) 3405, 2941, 2883, 1673 cm^{-1}; HRMS (ESI) calcd for $C_{12}H_{19}NO_4Na$ [M+Na]$^+$ 264.1212, found 264.1209

Derivatives for stereochemical analysis

General reduction procedure

To a 0.1 M solution of spirocycle (1 equiv) in THF at 0 °C was added $LiAlH_4$ (7 equiv). The solution was heated to reflux until the reaction was complete by TLC. After a Fieser

workup, the resulting slurry was filtered and dried over MgSO₄, filtered and concentrated *in vacuo* to give the title compound.
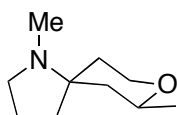
NOESY Correlations
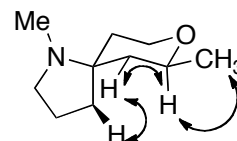
1,7-dimethyl-8-oxa-1-azaspiro[4.5]decane Following the general procedure yielded 25 mg (92%) of a clear oil. Performed on a 0.16 mmol scale. Relevant NOSEY correlations shown.

^{1}H NMR (CDCl₃, 500 MHz) δ 4.42 (s, 1H), 3.79 (dd, *J* = 11.7, 4.8 Hz, 1H), 3.44–3.33 (m, 2H), 2.76–2.63 (m, 2H), 2.25 (s, 3H), 1.73–1.56 (m, 5H), 1.27 (d, *J* = 6.2 Hz, 3H), 1.18 (dt, *J* = 12.6, 2.1 Hz, 1H), 0.96 (dq, *J* = 13.0, 2.0 Hz, 1H); ^{13}C NMR (CDCl₃, 125 MHz) δ 71.7, 65.8, 60.6, 53.3, 40.3, 34.8, 33.6, 31.5, 22.7, 21.5; IR (neat) 2925, 2851, 2780 cm^{-1}; HRMS (ESI) calcd for C₁₀H₂₀NO [M+H] $^+$ 170.1545, found 170.1537.
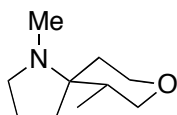
NOESY Correlations
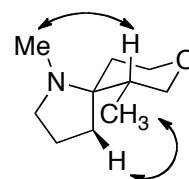
1,6-dimethyl-8-oxa-1-azaspiro[4.5]decane Following the general procedure yielded 20 mg (74%) of a clear oil. Performed on a 0.16 mmol scale. Relevant NOSEY correlations shown.

^{1}H NMR (CDCl₃, 500 MHz) δ 3.96 (app dd, *J* = 11.4, 4.6 Hz, 1H), 3.72 (dd, *J* = 11.2, 4.3 Hz,

1H), 3.46 (dt, J = 12.7, 2.0 Hz, 1H), 3.06 (t, J = 11.4 Hz, 1H), 2.91 (ddd, J = 8.6, 7.1, 4.4 Hz, 1H), 2.60 (q, J = 8.1 Hz, 1H), 2.28 (s, 2H), 1.90 (ddd, J = 11.5, 6.7, 4.4 Hz, 1H), 1.76–1.66 (m, 4H), 1.57 (ddd, J = 9.8, 5.7, 3.6 Hz, 1H), 0.72 (d, J = 6.7 Hz, 3H); ^{13}C NMR (CDCl$_3$, 125 MHz) δ 72.5, 66.4, 62.8, 53.7, 36.2, 33.4, 31.1, 28.2, 22.2, 10.4; IR (neat) 2952, 2846, 2780 cm^{-1}; HRMS (ESI) calcd for C$_{10}$H$_{20}$NO [M+H]$^+$ 170.1545, found 170.1542.
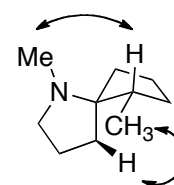
1,6-Dimethyl-1-azaspiro[4.4]nonan-2-one Following the general procedure produced the *n*-methyl derivative, but this proved to be too volatile to be isolated. Oxidation to the amide, following Picot and Lusinchi's procedure,[63] gave a mixture of over oxidized products which were converged by debromination[64] to give 13 mg (34% over 3 steps) as a clear oil. Preformed on a 0.23 mmol scale. Relevant NOSEY correlations shown.

^{1}H NMR (CDCl$_3$, 500 MHz) δ 2.72 (s, 3H), 2.37 (dt, J = 8.9, 6.5 Hz, 2H), 2.07–1.95 (m, 2H), 1.91–1.79 (m, 2H), 1.74–1.63 (m, 1H), 1.47 (ddd, J = 12.3, 7.8, 3.5 Hz, 1H), 1.33–1.22 (m, 1H), 0.85 (d, J = 6.7 Hz, 4H); ^{13}C NMR (CDCl$_3$, 125 MHz) δ 175.3, 71.8, 37.8, 34.3, 30.1, 29.7, 25.7, 24.4, 19.4, 12.0; IR (thin film) 2956, 2873, 1685 cm^{-1}; HRMS (ESI) calcd for C$_{10}$H$_{18}$NO [M+H$^+$]$^+$ 190.12088, found 190.1215

Determination of Alkyllithium Ratio of Reductively Lithiated 3.39
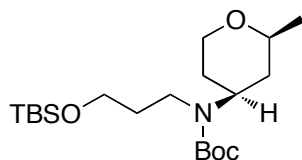
***Tert*-butyl (3-((*tert*-butyldimethylsilyl)oxy)propyl)(2-methyltetrahydro-2H-pyran-4-yl)carbamate** (**3.63**) Following the general procedure for reductive lithiation, FCC (5:1 pentane/DCM to 7:1 hexanes/EtOAc) yielded 43 mg (69%) of a clear oil. Performed on a 0.16 mmol scale. Isolated and characterized as a mixture of diastereomers (2:1) and rotamers.

^{1}H NMR (CDCl$_3$, 500 MHz) δ 4.58–4.18 (m, 0.7H), 4.11 (pent., *J* = 6.5 Hz, 0.3H) 3.81 (dd, *J* = 11.0, 3.0 Hz, 0.7H), 3.50–3.46 (m, 2.5H), 3.17 (app ddd, *J* =12.5, 6.5, 1.0 Hz, 2.9H), 1.89–1.71 (m, 2.3H), 1.71–1.55 (m, 1.3H), 1.55–1.42 (m, 9.6H), 1.40-1.28 (m, 2.8), 1.15–1.06 (m, 3.1H), 1.00–0.91 (m, 9H), 0.09-0.02 (m, 5.9H); ^{13}C NMR (CDCl$_3$, 125 MHz) δ 155.7, 155.6, 79.2, 17.7, 69.3, 67.3, 61.7, 61.6, 60.7, 60.3, 53.2, 48.6, 41.0, 40.8, 39.1, 35.5, 34.7, 32.1, 31.8, 30.5, 28.9, 28.5, 26.5, 22.5, 18.8, 17.3, -4.9; IR (thin film) 2954, 2929, 2856, 1692 cm^{-1}; HRMS (ESI) calcd for C$_{20}$H$_{41}$NO$_4$SiNa [M+Na]$^+$ 410.2703, found 410.2696
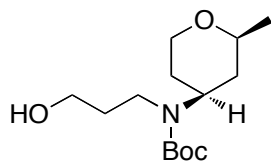
***Tert*-butyl (3-hydroxypropyl)(2-methyltetrahydro-2H-pyran-4-yl)carbamate** Following the general procedure for silyl deprotection, FCC (5:4 hexanes/EtOAc with 1% Et$_3$N) yielded 21 mg (69%) of a clear oil. Performed on a 0.09 mmol scale. Relevant NOSEY correlations shown.

Major isomer: ^{1}H NMR (CDCl$_3$, 500 MHz) δ 4.08–3.72 (m, 2H), 3.58 (br s, 2H), 3.51–3.01 (m, 4H), 1.85–1.53 (m, 6H), 1.52–1.31 (m, 10H), 1.21 (t, J = 6.5 Hz, 3H); ^{13}C NMR (CDCl$_3$, 125 MHz) δ 157.1, 80.6, 73.4, 67.1, 58.6, 54.1, 39.6, 38.7, 33.3, 30.9, 28.6, 22.1; IR (thin film) 2954, 2929, 2856, 1692 cm^{-1}; HRMS (ESI) calcd for C$_{14}$H$_{27}$NO$_4$Na [M+Na] $^+$ 296.1838, found 296.1835
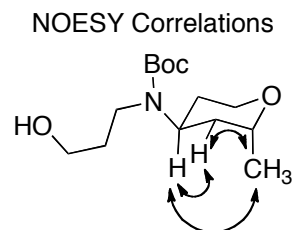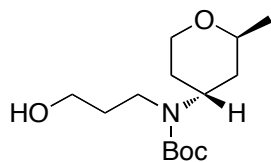
Minor isomer: ^{1}H NMR (CDCl$_3$, 500 MHz) δ 4.35–4.05 (m, 2H), 3.75 (d, J = 6.5 Hz, 2H), 3.59 (br s, 2H), 3.34 (br s, 2H), 1.93 (dt, J = 12.5, 6.0 Hz, 1H), 1.86–1.58 (m, 4H), 1.58–1.38 (m, 10H), 1.37–1.15 (4H); ^{13}C NMR (CDCl$_3$, 125 MHz) δ 156.7, 80.5, 69.2, 60.1, 59.0, 48.7, 39.0, 35.0, 33.5, 31.6, 28.6, 17.8; IR (thin film) 2954, 2929, 2856, 1692 cm^{-1}; HRMS (ESI) calcd for C$_{14}$H$_{27}$NO$_4$Na [M+Na] $^+$ 296.1838, found 296.1835

[1] Smith, L.; Baxendal, I. *Org. Biomol. Chem.* **2015**, *13*, 9907–9933.

[2] Molvi, K.; Haque, N.; Awen, B.; Zameeruddin, H. *World Journal of Pharmacy and Pharmaceutical Sciences* **2014**, *3*, 536–563.

[3] Zheng, Y; Tice, C.; Singh, S. *Bioorg. Med. Chem. Lett.* **2014**, *24***,** 3673–3682.

[4] Rajesh, S.; Perumal, S.; Menendez, J.; Yogeeswari, P.; Sriram, D. *Med. Chem. Commun.* **2011**, *2*, 626–630.

[5] Reviews of spirocycle synthesis: (a) Sannigrahi, M. *Tetrahedron* **1999**, *55*, 9007–9071. (b) Rios, R. *Chem. Soc. Rev.* **2012**, *41*, 1060–1074. (c) Kotha, S.; Deb, A.; Lahiri, K.; Manivannan, E. *Synthesis* **2009**, *2*, 165–193. (d) Trost, B.; Brennan, M.; *Synthesis* **2009**, *18*, 3003–3025.

[6] Specific methodology for spirocycle synthesis: (a) Undheim, K. *Synthesis,* **2015**, *47*, 2497–2522. (b) Castaldi, P.; Troast, D.; Porco Jr., J. *Org. Lett.* **2009**, *11*, 3362–3365. (c) Perry, M.; Morin, M.; Slafer, B.; Rychnovsky, S. *J. Org. Chem.* **2012**, *77*, 3390–3400. (d) Wright, D.; Schulte II, J.; Page, M. *Org. Lett.* **2000**, *2*, 1847–1850. (e) Gharpure, S.; Reddy, R. *Org. Lett.* **2009**, *11*, 2519–2522. (f) Fei, J.; Qian, Q.; Sun, X.; Gu, X.; Zou, C.; Ye, J. *Org. Lett.* **2015**, *17*, 5296–5299. (g) La Cruz, T. E.; Rychnovsky, S. *J. Org. Chem.* **2007**, *72*, 2602–2611. (h) Yang, S-H.; Clark, G.; Caprio, V. *Org. Biomol. Chem.* **2009**, *7*, 2981–2990. (i) Reddy, S.; Reddy, R.; Yaragadda, S.; Reddy, R.; Kumar, R.; Yadav, J.; Sridhar, B. *J. Org. Chem.* **2015**, *80*, 8807–8814. (j)Yang, W.; Sun, X.; Yu, W.; Rai, R.; Deschamps, J.; Mitchell, L.; Jiang, C.; MacKerell Jr., A.; Xue, F. *Org. Lett.* **2015**, *17*, 3070–3073.

[7] Kuramoto, M.; Tong, C.; Yamada, K.; Chiba, T.; Hayashi, Y.; Uemura, D. *Tetrahedron Lett.* **1996**, *37*, 3867–3870.

[8] Koch, A.; Halloran, M.; Haskell, C.; Shah, M.; Polverini, P. *Nature,* **1995**, *376*, 517–519.

[9] Jeon, Y.; Qiao, J.; Li, L.; Thibeault, C.; Hiebert, S.; Wang, T.; Wang, Y.; Lui, Y.; Clark, C.; Wong, H.; Zhu, J.; Wu, D-R.; Sun, D.; Chen, B-C.; Mathur, A.; Chacko, S.; Malley, M.; Chen, X-Q.; Shen, H.; Huang, C.; Schumacher, W.; Bostwick, J.; Stewart, A.; Price, L.; Hua, J.; Li, D.; Levesque, P.; Seiffert, D.; Rehfuss, R.; Wexler, R.; Lam, P. *Bioorg. Med. Chem. Lett.* **2014,** *24*, 1294–1298

[10] Allen, C.; Chow, C.; Caldwell, J.; Westwood, I.; van Montfort, R. *Bioorg. Med. Chem* **2013**, *21*, 5707–5724.

[11] Ribeiro, C.; de Melo, S.; Bonin, M.; Quirion, J.-C.; Husson, H.-P. *Tetrahedron Lett.* **1994**, *35*, 7227–7230.

[12] An example of reductive decyanation on α-aminonitriles with K°, 18-crown-6 and THF was previously known. Zeller, E.; Grierson, D. *Synlett* **1991**, 878–880.

[13] Perry, M.; Morin, M.; Slafer, B.; Wolckenhauer, S.; Rychnovsky, S. *J. Am. Chem. Soc.* **2010**, *132*, 9591–9593.

[14] Slafer, B. Dissertation, University of California-Irvine, **2009**

[15] Leong, J. Dissertation, University of California-Irvine, **2011**

[16] Park, Y.; Boys, M.; Beak, P. *J. Am Chem. Soc.* **1996**, *118*, 3757–3758.

[17] Kelstrup, E. *J. Chem. Soc., Perkin Trans. 1* **1979**, 1029–1036.

[18] Gu, J.; Holland, H. *Syn. Commun. 1998,* 28*,* 3305–3315.

[19] López-Cortina, S.; Medin-Arreguin, A.; Hernandez-Fernández, E.; Bernés, S.; Guerrero-Alvarez, J.; Ordoñez, M.; Fernández-Zertuche, M. *Tetrahedron,* **2010**, *66*, 6188–6194.

[20] Nguyen, B.; Cartledge, F. *J. Org. Chem.* **1986**, *51* 2206–2210.

[21] These conditions were taken from Perry, M.; Morin, M.; Slafer, B.; Wolckenhauer, S.; Rychnovsky, S. *J. Am. Chem. Soc.* **2010**, *132*, 9591–9593.

[22] Ratios by ^{1}H NMR,

[23] Curran, D.; Porter, N.; Giese, B. *Stereochemistry of Radical Reactions Concepts, Guidelines, and Synthetic Applications.*; VHC: Weinheim, Germany, 1996. Pp 5-7

[24] While the stability of tertiary N-Boc amino α–alkyllithiums is not known in the literature, the secondary analogs have been studied: Ashweek, N.; Brandt, P.; Coldham, I.; Dufour, S.; Gawley, R.; Hæffner, F.; Klein R.; Sanchez-Jimenez, G. *J. Am. Chem. Soc.* **2005**, *127*, 449–457

[25] (a) Gawley, R.; Zhang, Q. *J. Org. Chem.* **1995**, *60*, 5763–5769. (b) Gawley, R.; Low, E.; Zhang, Q.; Harris, R. *J. Am. Chem. Soc.* **2000**, *122*, 3344–3350. (c) Faibish, N.; Park, Y.; Lee, S.; Beak, P. *J. Am. Chem. Soc.* **1997**, *119*, 11561–11571.

[26] (a) Kerrick, S.; Beak, P. *J. Am. Chem. Soc.* **1993**, *113*, 9708–9710. (b) Beak, P.; Kerrick, S.; Wu, S.; Chu, J. *J. Am. Chem. Soc.* **1994**, *116*, 3231–3239. (c) Park, Y.; Boys, M.; Beak, P. *J. Am. Chem. Soc.* **1996**, *118*, 3757–3758.

[27] Cohen, T.; Chen, F.; Kulinski, T.; Florio, S.; Capriati, V. *Tetrahedron Lett.* **1995**, *36*, 4459–4462.

[28] (a) Walsh, T. D.; Dabestani, R. *J. Org. Chem.* **1981**, *46*, 1222–1224. (b) Guijarro, D.; Martínez, P.; Yus, M. *Tetrahedron* **2003**, *59*, 1237–1244. (c) Rawson, D.; Meyers, A. *Tetrahedron Lett.* **1991**, *32,* 2095–2098.

[29] Guijarro, D.; Yus, M. *Tetrahedron* **1994**, *50*, 3447–3452.

[30] Cohen, T.; Jeung, I.; Mudryk, B.; Bhupathy, M.; Awad, M. *J. Org. Chem.* **1990**, *55*, 1528–1536.

[31] Guijarro, D.; Mancheño, B.; Tus, M. *Tetrahedron* **1993**, *49*, 1327–1334.

[32] Perry, M. Dissertation, University of California-Irvine, **2011**

[33] Weidong, L.; Huiying, Z.; Guicai, C. Synthetic method of N-alkyl substituted-3-piperidones. CN 200910069437, Feb. 2, 2010.

[34] Schumacher, R.; Tehim, A.; Xie, A. 4'-Amino Cyclic Compounds Having 5-HT6 Receptor Affinity. WO2010/024980A1, March 4, 2010.

[35] Belov, V.; Savchenko, A.; Sokolov, V.; Straub, A.; Meijere, A. *Eur. J. Org. Chem.* **2003**, 551–561.

[36] Schumacher, R.; Tehim, A.; Xie, A. 4'-Amino Cyclic Compounds Having 5-HT6 Receptor Affinity. WO2010/024980A1, March 4, 2010.

[37] Burrell, A.; Coldham, I.; Watson, L.; Oram, L.; Pilgram, C.; Martin, N. *J. Org. Chem.* **2008**, *74*, 2290–2300.

[38] Tsunoda, T.; Suzuku, M.; Noyori, R. *Tetrahedron Lett.* **1980**, *21*, 1357–1358.

[39] Perry, M. Chemistry Department, UCI, Irvine, CA. Personal communication, December 2011.

[40] Chak, B.; McAuley, A. *Can. J. Chem.* **2006**, *84*, 187–195.

[41] Maercker, A. *Angew. Chem., Int. Ed. Engl.* **1987**, *26*, 972–989.

[42] Lubell, W.; Jamison, T.; Rapoport, H. *J. Org. Chem.* **1990**, *55*, 3511–3522.

[43] Babler, J.; Malek, N.; Coghlan, M. *J. Org. Chem.* **1978**, *43,* 1821–1823.

[44] The alkene by-product is removed by oxidation to the diol using OsO_4, NMO, in 1:1 Acetone/H_2O

[45] Greaves, J. University of California Irvine, Irvine, CA. Personal Communication, 2013

[46] Anslyn, E.; Dougherty, D. *Modern Physical Organic Chemistry*.; University Science Books: Sausalito, California, 2006; pp 104–122

[47] Fleming, F.; Wei, G. *J. Org. Chem.* **2009**, *74,* 3551–3553

[48] Pangborn, A.; Giardello, M.; Grubbs, R.; Rosen, R.; Timmers, F. *Organometallics* **1996**, *15*, 1518–1520.

[49] Duhamel, L.; Plaquevent, J. *J. Organomet. Chem.* **1993**, *338*, 1–3.

[50] Still, W.; Khan, M.; Mitra, A. *J. Org. Chem.* **1978**, *43*, 2923–2925.

[51] Sciefer, H.; Beger, J. *J. Prakt. Chemie*, **1983**, *325*, 719–728.

[52] Leonardi, A.; Barlocco, D.; Montesano, F.; Cignarella. G.; Motta, G.; Testa, R.; Poggesi, E.; Seeber, M.; Benedtti, P.; Ganelli, F. *J. Med. Chem.*, **2004**, *47*, 1900–1918.

[53] Zhdanko, A.; Gulevich, A.; Nenajdenko, G. *Tetrahedron*, **2009**, *65*, 4692–4702

[54] Weidong, L.; Zeng, H.; Chen, G. A Process for Preparing N-Substituted-3-Piperidone Derivatives. CN 101638378, Feb 3, 2010

[55] Denmark, S.; Marcin, L. *J. Org. Chem.* **1997**, *62*, 1675–1686

[56] Martínez, A. D. Convertent Approach to the Synthesis of Myriaporone 4 and Derivatives. Ph.D. Dissertation, University of Madrid, Madrid, 2007

[57] Davenport, R.; Regan, A. *Tetrahedron Lett.*, **2009**, *41*, 7619–7622

[58] Gliter, R.; Ramming, M.; Weigl, H.; Wolfart, V.; Irngartinger, H.; Oeser, T. *Liebigs. Ann. Recueil.* **1997**, 1545-1550

[59] Dong, Q.; Rose, M.; Wong, M.; Wong, W-Y.; Gray, H. *Inorg. Chem.* **2011**, *50*, 10213-10224

[60] Perry, M.; Hill, R.; Rychnovsky, S.; *Org. Lett.,* **2013**, *15*, 2226–2229

[61] Chen, C.; MacTaggart, J.; Process for the preparation of trans-3-formylbut-2-enenitrile. U.S. Patent 4,361,702A, Nov 30, 1982

[62] Perry, M.; Hill, R.; Leong, J.; Rychnovsky, S. *Org. Lett.,* **2015**, *17*, 3268–3271

[63] Picot, A.; Lusinchi, X. *Synth. Commun.* **1975**, 109–111.

[64] Park, L.; Keum, G.; Kang, S.; Kim, K.; Kim, Y. *J. Chem. Soc., Perkin Trans. 1.* **2000**, 4462-4463.

Chapter 4

Application of Flow Reactors to LiDBB Methodology

Abstract

A flow reactor approach to reductive lithiation using LiDBB is described herein. Replacement of a thiophenyl alcohol with an epoxide as a β-alkoxy alkyllithium pre-cursor resulted in similar yields of a β-hydroxy ketone. Non-cryogenic flow conditions substantially increased the yield and diastereoselectivity of spiropyrrolidines and a spiropiperidine. The construction and methodology for using LiDBB in flow reactors is described in detail.

Introduction

Batch reactions have long been the standard method for organic synthesis in academic settings. By contrast, industry prefers semi-batch processes, where starting material is added or a product removed from a reactor while the reaction is still proceeding. More than 70% of reactions in industry are semi-batch processes.[1] A third method for synthesis utilizes a flow reactor, in which reagents are constantly pumped through tubing, increasing control over the reaction. The classic example of this is the Haber–Bosch process for generation of ammonia.[2] Industrial scale flow reactors have been used for decades. Their use in academic settings has only recently been utilized. Smaller and modular flow reactors have become available in the last 5-10 years.[3,4] The need for such devices was driven by the desire to perform reactions that would be hazardous or impractical to run in batches.[5,6] Among these three types of set-ups, flow reactors show the most promise for innovation as a disruptive technology in the coming years.

Background

Many research groups have labored to apply technology to flow chemistry, allowing for additional types of reactions and fast reaction monitoring. One of the first areas investigated was how to quickly mix reagents in the reactor.[7,8] While mixing can occur passively by diffusion, the addition of a mixing apparatus leads to a uniform concentration and, therefore, more complete reactions. Several other devices are described in the literature for gasses,[9] slurries[10], immobilized reagents,[11] and inline work-ups.[12] These modular parts are easily installed on existing flow reactor systems. The regulation of back-pressure is possibly the most important of these additions, as it allows high pressure and temperature reactions to occur while material is still flowing through the reactor.[13] Analytical systems have also been adapted for flow conditions. Mass spectrometer,[14] IR/UV-vis,[15] and React IR[16] devices can give instantaneous feedback about reaction yields, allowing for real-time optimization of the reactor. Using the above components in combination has allowed multi-step syntheses of natural products and drugs using several flow reactors connected in series.[17]

Two scales of academic reactors have been reported: microfluidic and minifluidic.[18] A microfluidic reactor is made with 10-500 μm diameter channels.[7] Such systems have better heat transfer and mixing than the minifluidic systems, but are also more susceptible to clogging.[19] Due to their size, microfluidic reactors are best for optimization of reactions rather than preparative scale synthesis. Minifluidic reactors are larger, with diameters of 0.5–several mm and can produce much larger quantities of product than their microfluidic counterpart. While larger tubing results in fewer instances of clogging, the larger tubing also leads to poorer mixing and heat transfer rates. Despite these limitations, both microfluidic and minifluidic reactors are becoming more widespread in organic research.

Flow chemistry's largest advantage over batch reactions is the small volume of reacting compounds within the reactor. As the surface area of the reaction vessel increases in comparison to the volume of reacting solution, the ability to stabilize reaction temperature also increases. This ratio varies greatly among tubing sizes, but ratios of 100–10,000 are reported.[5] By contrast, a round-bottom-flask has a 20:1 ratio. Another consequence of this ratio is that reactions scale better in flow reactors than in batch reactors.[20] Running photochemical reactions in flow reactors also takes advantage of the surface area to volume ratio to boost yields and lower reaction times. Reactions that would be avoided for safety reasons can be conducted in flow reactors since dangerous chemicals can be made and used in situ and are never generated in hazardous quantities.

The fast reaction times and small volumes of the flow reactor allow for extreme conditions to be employed that would be impractical or dangerous under batch conditions. The fluorinating reagent DAST (**4.1**) is known to disproportionate to SF_4 and bis(diethylamine)sulfur difluoride at 90 °C, and can detonate above this temperature (**Scheme 4.1**).[21] Using a flow reactor, fluorination of compound **4.2** was accomplished at 90 °C and residual DAST quenched against $CaCO_3$ and SiO_2 (eq. 1).[22] A back-pressure regulator (BPR) is required to prevent boiling of DCM at 90 °C, while allowing a flow of material through the reactor. Due to the quick reaction times, fluorination occurs before decomposition of DAST. Elemental fluorine has also been used in flow reactors.[23] Azides, another class of potentially explosive compounds, find use under harsh flow reactor conditions. The cycloaddition of **4.4** and **4.5** is accomplished without a catalyst by heating the reagents to 210 °C at nearly 70 barr of pressure (eq 2).[24] Jamison *et al.* have reported a similar synthesis of **4.6** using copper tubing as the catalyst, leading to lower temperature

requirements in flow.[25] Another hazardous reagent, diazomethane, has found use in flow reactors. Equation 3 shows a reactor with a semipermeable poly dimethylsiloxane (PDMS) membrane, which allows for transfer of organic compounds through this divider. [26] Diazomethane is generated in the bottom channel and can pass through the membrane to react with acetic acid in the top channel. In this way, diazomethane is never isolated or generated in large quantities. The two-channel design was devised due to reports of clogging when a single channel approach was tried.[27] Quantitative yields of methyl acetate show proof of concept that can be applied to larger scale syntheses or more complex substrates. These examples show how a flow reactor can increase safely when working with dangerous chemicals.

Buchwald *et al.* have described the design for a self-optimizing flow system.[28] The synthesis of **4.11** was selected since it was known to react with a second equivalent of **4.8** and give the over-arylated product **4.12** (**Scheme 4.2**).[29] A flow reactor was employed to avoid the build up of **4.11** which competes with **4.9** in the cross coupling reaction. One addition made to this system was the use of a valve to redirect some of the solution after leaving the reactor. This allows for a reaction to be analyzed by HPLC to determine the yield. The most significant addition to this flow set-up is the use of a computer to change the flow rates of syringe pumps 1–3. This allows the equivalents and residence time of the reagents to be changed without modifying the set-up. Using the Nelder–Mead Simplex method, the computer was able to optimize conditions without the use of gradient reactions.[30] The computer calculated that a 5:1 ratio of **4.9**:**4.8** with a residence time of 6 minutes gave the best yield at 83%. The flow reactor was also enlarged 50-fold and the

above conditions were found to give nearly identical yields. While such a system is complicated, it opens the door for further automation in organic synthesis.

Scheme 4.1. Flow reactor set-ups for using dangerous reagents
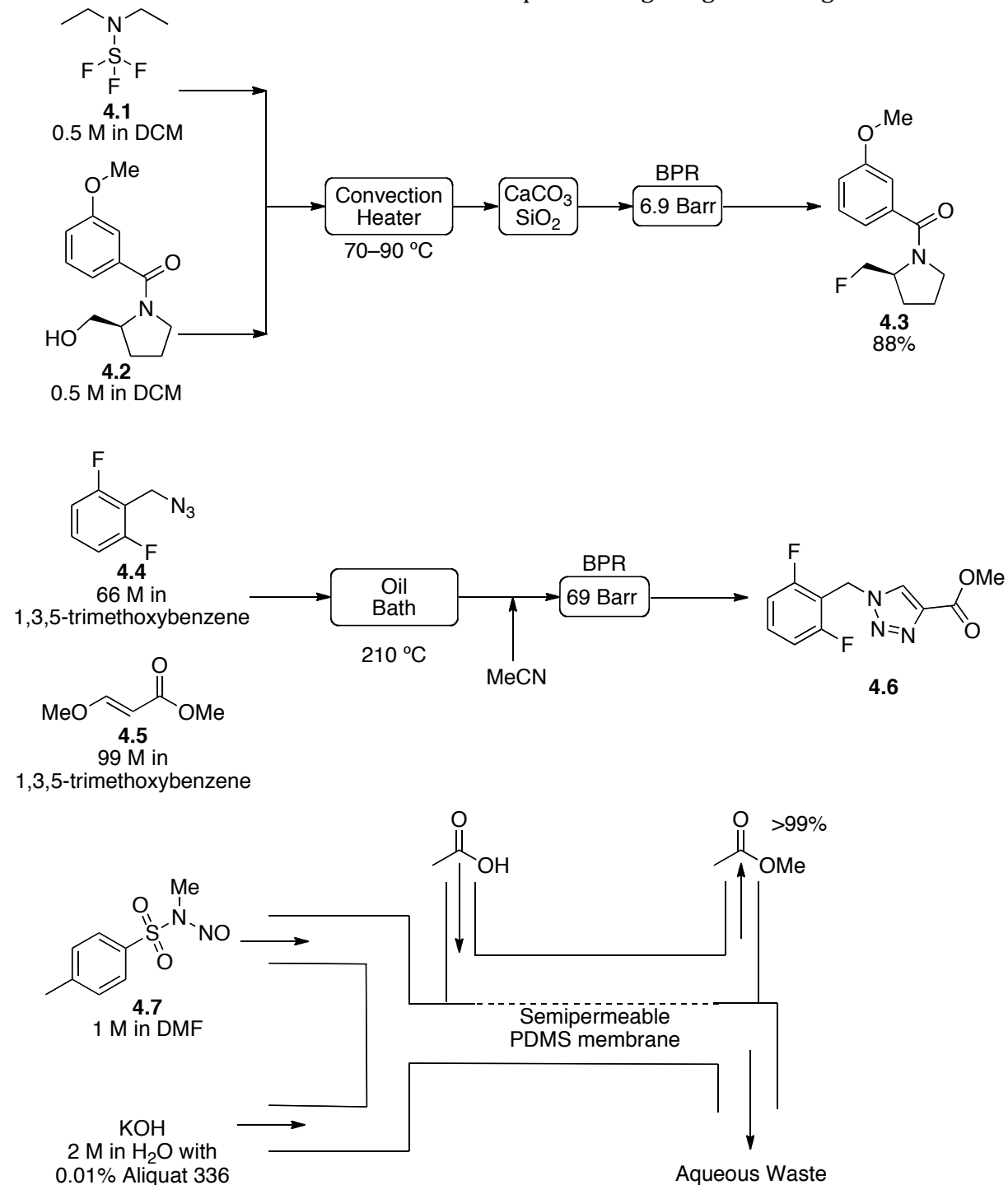
Figure 4.2. Self-optimizing flow reactor
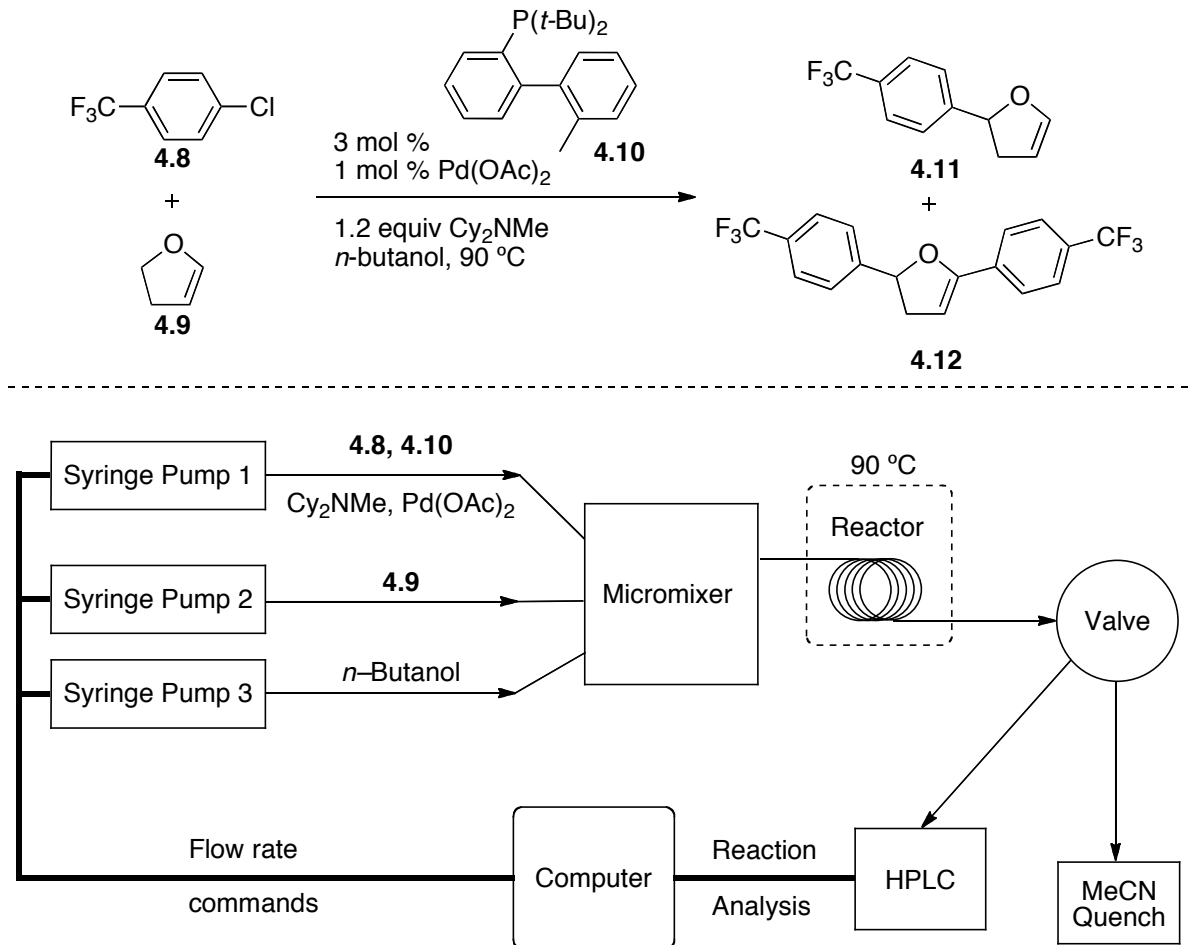
Thin lines denote tubing used for the reactor and modules. Thick lines denote data transfer between the HPLC, computer and syringe pumps

The need for selective lithiation of **4.13** drove research for a flow reactor approach for synthesis of Amitriptyline (**Scheme 4.3, 4.22**).[31] A 1:1 molar mixing of *n*-BuLi and **4.13** in reactor 1 (R$_1$) led to **4.15**, which then undergoes a Wurtz-type coupling, to give **4.16**. The dimerization product then undergoes a second lithium-halogen exchange, providing lithiate **4.17**. At this point, carbon dioxide was introduced using a tube-in-tube system developed by Dr Ley.[32] This system utilizes a semipermeable membrane to deliver gasses, while preventing the addition of bubbles to the flow reactor itself.   The dissolved CO_2 and

4.17 entered reactor 2 (R$_2$) and **4.18** was produced. After flowing through reactor 2, the solution entered the gas remover (GR) and excess CO$_2$ was purged from the system. The solution next enters a back-pressure regulator (BPR) to keep the previous parts of the flow reactor under appropriate pressure. Another equivalent of *n*-BuLi was added and the third reductive lithiation occurs. In reactor 3 (R$_3$), intermediate **4.19** cyclized into the nearby carboxylate and the product **4.14** was isolated in 76% yield. The impressive control over each lithiation step is a consequence of using flow conditions. Attempting to run the reaction in batch required –100 °C reaction conditions and yields varied between 38–55%. A second flow reactor was used to finish the synthesis of Amitriptyline **4.20**.

Scheme 4.3. Preparation of key Amitriptyline intermediate via flow reactors
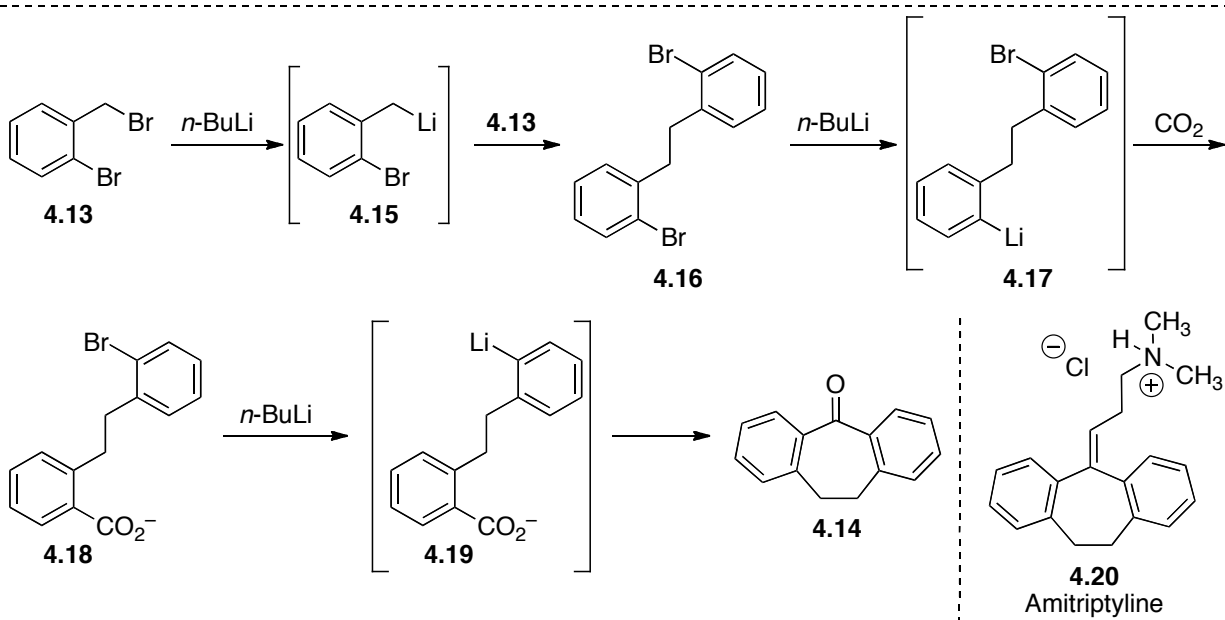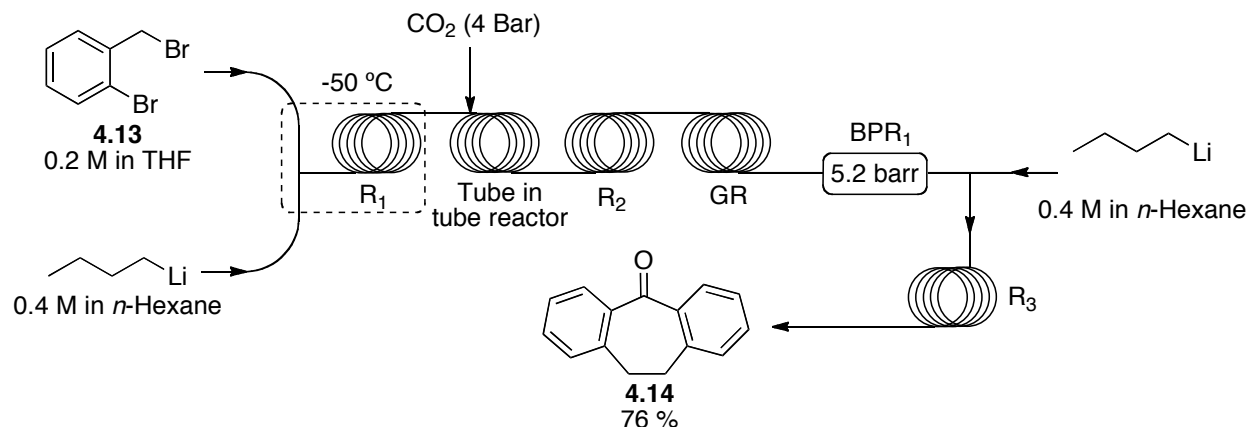
Theory

Designing a flow reactor takes a multitude of variables into consideration. The simple and idealized reactors described herein assume no side products are generated, passive mixing is sufficient and heat generated by the reaction is negligible. With these assumptions, the flow reactor can be described using the mathematical variables and equations defined in **Figure 4.1** and **Table 4.1**. A main consideration for flow reactors is the residence time, or the time it takes for a molecule to enter and exit the reactor. Using

equation 1 (**Table 4.1**), the residence time (R_t) is equal to the reactor length (L_R) divided by the speed of molecule **4.21** through the tube ($\dot{L}$). However, a flow rate is more useful than a linear speed when using syringe pumps. The flow rate through the reactor ($\dot{V}_T$) can be determined by simply multiplying the speed of molecule **4.21** ($\dot{L}$) by the cross-sectional area of the reactor tubing (eq 2). Substituting equation 2 into equation 1 provides equation 3, which details how to set a flow rate through any size reactor and obtain a desired residence time. This equation is sufficient for flow reactors with a single syringe pump. While such a set-up would work for photochemical or thermal reactions, most flow reactor step-up will require two or more syringe pumps delivering reagents to the reactor.

Figure 4.1. Defining reactor design variables
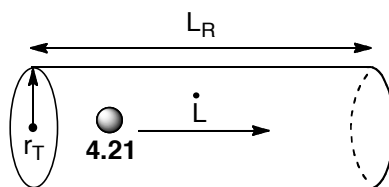
Figure 4.2. Simple schematic of flow reactor with two syringe pumps
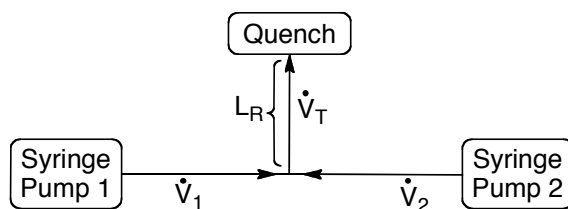
Table 4.1. Equations and definitions for flow reactor theory

1. $R_t = {}^{L_R}/_{\dot{L}}$	$\dot{L}$ = The speed of molecule **4.21** in cm/min. L_R = length of the reactor in cm.
2. $\dot{V}_T = \dot{L} * r_T^2 \pi$	r_T = Radius of the reactor tubing in cm.
3. $R_t = \left({}^{L_R}/_{\dot{V}_T}\right) * (r_T^2 \pi)$	R_t = Minutes the solution takes to move through the reactor; Residence time. $\dot{V}_T$ = Flow rate through the reactor in cm³/min.
4. $\dot{V}_T = \dot{V}_1 + \dot{V}_2$	$\dot{V}_1$ = Flow rate from syringe pump 1 in cm³/min.
	$\dot{V}_2$ = Flow rate from syringe pump 2 in cm³/min.
5. $M_1 * V_1 = M_2 * V_2 * \left({}^{E_1}/_{E_2}\right)$	M_1 = Molarity of solution 1 in mol/liter
	M_2 = Molarity of solution 2 in mol/liter
6. $\left({}^{V_1}/_{V_2}\right) = \left({}^{M_2}/_{M_1}\right)\left({}^{E_1}/_{E_2}\right)$	V_1 = Volume of reactant 1 in cm³.
7. $F_1 = \left({}^{V_1}/_{(V_1 + V_2)}\right)$	V_2 = Volume of reactant 2 in cm³.
8. $F_2 = \left({}^{V_2}/_{(V_1 + V_2)}\right)$	E_1 = Molar equivalents of reactant 1 E_2 = Molar equivalents of reactant 2
9. $\dot{V}_1 = F_1 * \dot{V}_T$	F_1 = Fraction of the instantaneous volume entering the reactor from syringe pump 1
10. $\dot{V}_2 = F_2 * \dot{V}_T$	F_2 = Fraction of the instantaneous volume entering the reactor from syringe pump 2

Equations 4-10 are used to solve for the flow rates from two syringe pumps (**Table 4.1**). To ensure that the reagents from both pumps are combined in the desired stoichiometry, appropriate flow rates for each syringe pump need to be solved for. Equation 4 shows the sum of the flow rates from both syringe pumps are equal to the total

flow rate through the reactor. This is also shown pictorially in **Figure 4.2**. Since solutions of reagents will be used in the reactor, it's best to consider their addition in terms of volumes and molarities. Equation 5 relates the moles of reactants 1 and 2 that are to be mixed in these terms (**Table 4.1**). It also takes into account the stoichiometry (or equivalents of reagents) with the terms E_1 and E_2. The ratio of E_1 / E_2 is required so that units on both sides of the equation are the same. Rearranging this equation yields equation 6. This gives the ratio of two instantaneous volumes (V_1 and V_2) added to the reactor in terms of the two solution molarities (M_1 and M_2) and the molar equivalents of each reagent (E_1 and E_2) needed to give a complete reaction. By solving Equation 6, the ratio of V_1 to V_2 entering the reactor at any point can be determined. Only the ratio of these volumes is important, as will be shown later in the text. The fraction of the total volume entering the reactor, coming from reagents 1 and 2, can be derived via equations 7 and 8. When solved, these become a unitless fraction, or the percent of the total flow rate entering the reactor at any given instant for that reagent. Finally, multiplying these fractions by the total flow rate through the reactor gives the flow rate that must come from that pump to keep the desired ratio of reagents (eq 9,10). After deciding on a residence time for the reaction, appropriate flow rates can now be determined for both syringe pumps.

Scheme 4.4. Example flow reactor set-up
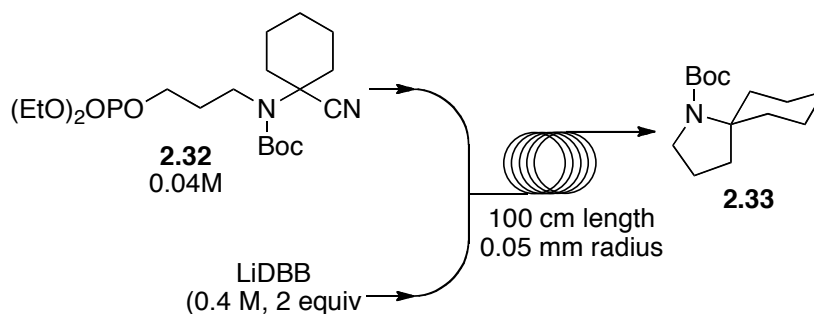
With the number of variables defined as well as the complexity of the above system, an example is provided for clarity. Suppose one wanted to react a 0.04 M solution of phosphate **2.32** with 2 equivalents of 0.4 M LiDBB in a flow reactor for 0.5 minutes (**Scheme 4.4**). This reactor was built from 100 cm of 0.05 cm radius tubing. Using this information, equations 1 and 2 can be solved to find that $\dot{V}_T$ = 1.57 mL/min (**Table 4.1**). Solution 1 is arbitrarily designated the phosphate, making solution 2 the LiDBB. Defining the solutions the other way has no consequence on the mathematical outcome. Since the reaction stoichiometry requires 2 equivalents of LiDBB for 1 equivalent of the phosphate, E_2 is set to 2 and E_1 set to 1. The defined E_1 and E_2, as well as the known molarities of both the phosphate and LiDBB solutions (M_1 and M_2, respectively), are added to equation 6 to show that $\left(V_1 / V_2 \right)$ = 5. Substituting this into equations 7 shows that $F_1 = \left(5V_1 / 6V_1 \right)$. The variable V_1 cancels itself out to reveal that F_1 = 5/6. Applying this and the previously solved $\dot{V}_T$ to equation 9 shows the flow rate of the phosphate in syringe pump 1 ($\dot{V}_1$) must be 1.308 mL/min. Applying the same logic to equations 8 and 10 shows that F_2 = 1/6 and the flow rate $\dot{V}_2$ for the LiDBB solution must be 0.262 mL/min. To simplify optimization of a flow reactor, it was found that using an excel spreadsheet to solve for the flow rate in terms of residence time was exceptionally useful.

Epoxide ring opening in flow

The ability to generate unstable intermediates using a flow reactor led to initial research into the ring opening of epoxides with LiDBB. This work was driven by an unusual finding by Malathong.[33] Using thiophenyl alcohol **4.22**, the dianion **4.23** was formed and added into Weinreb amide **4.24** yielding **4.25** (**Scheme 4.5**). Equation 2 shows that morpholine amide **4.26** is also a viable electrophile for this reaction. However, trying

to directly open epoxide **4.27** with LiDBB led to a substantial loss in yield. Equations 1-3

should all proceed through dilithiate **4.23**; however, using thiophenyl alcohol **4.22** gave a

better yield than epoxide **4.27** for no obvious reason.

Scheme 4.5 Difference in yield of **4.25** based on pre-nucleophile source
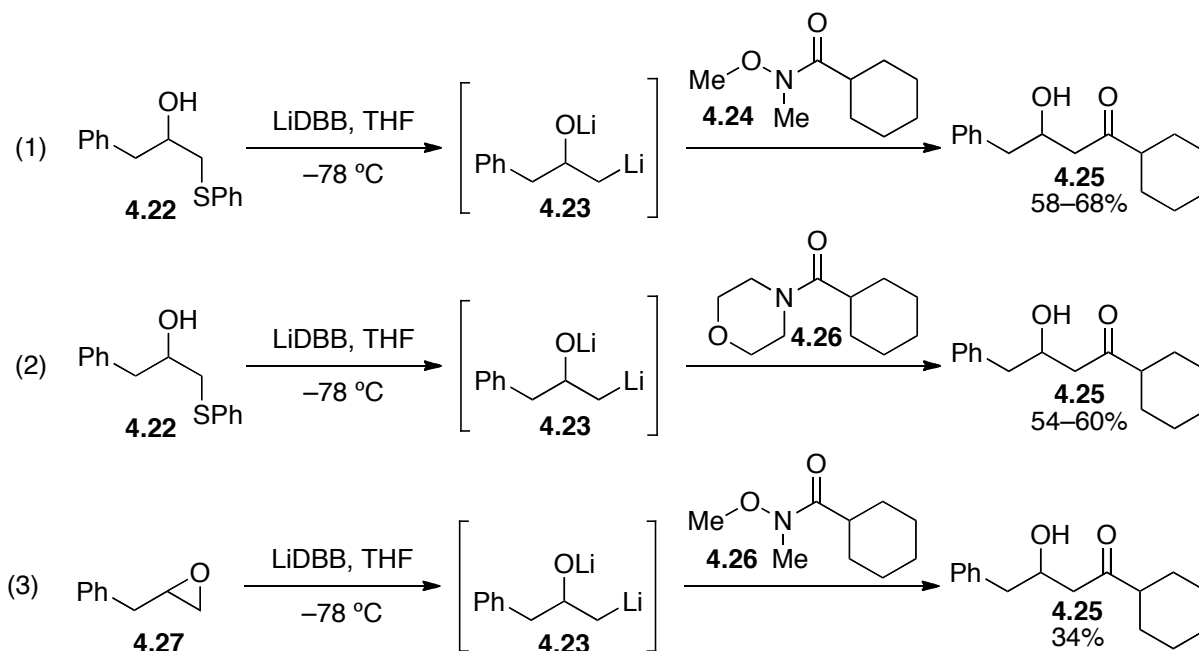
The observed difference in yields, based on the use of a thiophenyl alcohol versus an

epoxide, led to an investigation on why this discrepancy exists and to see if a flow reactor

could be used to increase the overall reaction yield. Using epoxides instead of the

thiophenyl derivate would save time by removing a synthetic step and also avoid using the

foul smelling thiophenol. A literature search revealed publications about β-alkoxy

alkyllithiums. Yus *et al.* have shown dianions like **4.23** were reasonably stable at –78 °C,

but would readily eliminate above this temperature.[34]   Given that LiDBB is at 0 °C when

added to either **4.22** or **4.27** at –78 °C, the solution will warm to an extent (**Scheme 4.5**).

Scheme 4.6 shows the expected decomposition pathway for these substrates to give

alkene **4.28**. It was anticipated that flow reactor conditions would lead to more precise mixing temperatures resulting in a higher overall yield from the epoxide starting material.

Scheme 4.6. Expected elimination pathway for **4.23**
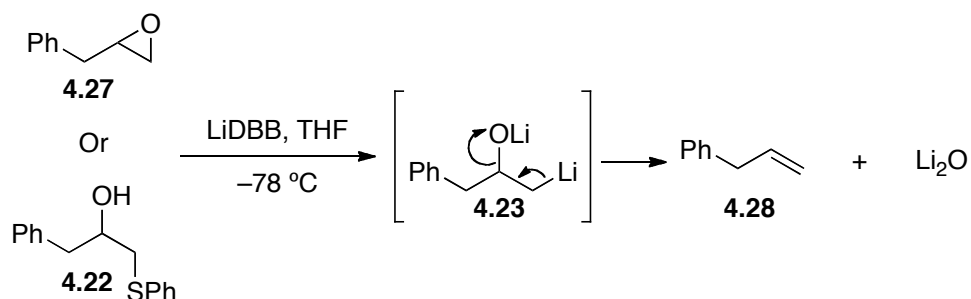
Since reaction temperature was a key variable in high product yield, the ability to precise control of reagent cooling prior to mixing was studied. It was unknown how long the reaction would take in a flow reactor, so the cooling study erred on the side of faster than anticipated flow rates. Initial reactor designs were based on recommendations from a seminar presented by Jamison.[35] Two coils of 0.5 mm diameter perfluoroalkoxy alkane (PFA) tubing were cut such that one had an internal volume of 0.5 mL and the other 1.0 mL. The 0.5 ml coil was immersed in –78 °C bath and connected to a syringe pump. A syringe full of 20 °C THF was attached and the solvent pushed through the tubing with a residence time of 30 seconds. At the end of the coil, a thermocouple measured the exit temperature as –69 °C. This was the temperature that the solution would have entered the reactor. Repeating the test with a 1.0 mL coil resulted in cooling the THF to –75 °C. These numbers were then plugged into Newton's Law of Cooling (**Table 4.2**, eq 1). Assuming an ideal system, this equation would allow for the temperature of the solution to be known for any length of time spent in the cold bath. These conditions were used to calculate the rate of cooling (k) for both lengths of tubing (equation 2 for the 0.5 mL tube and equation 3 for the 1.0 mL tube). Plotting these equations gave **Graph 4.1**. Since mixing at –78 °C was

important to reaction success, the 6 °C difference between the tubing tested was considered to be significant. With an understanding of the time required to cool the solutions prior to reacting, attention was turned to another potential problem: the reactivity of the tubing itself.

Table 4.2. Newton's Law of cooling for flow reactor use

(1) $T(t) = T_b + (T_0 - T_b)e^{-kt}$	$T_n(t)$ = Temperature of the solution in Kelvin, for a reactor volume n, at time t in seconds.
(2) $T_{0.5\,mL}(t) = 195 + (293 - 195)e^{-(0.0796)t}$	T_b = Temperature of the cooling bath in Kelvin.
	T_0 = Initial temperature of the solution in Kelvin.
(3) $T_{1.0\,mL}(t) = 195 + (293 - 195)e^{-(0.116)t}$	k = Rate of cooling in seconds^{-1}.
	t = Time since cooling began in seconds.

Graph 4.1. Expected rates of cooling to –78 °C at 30-second residence time
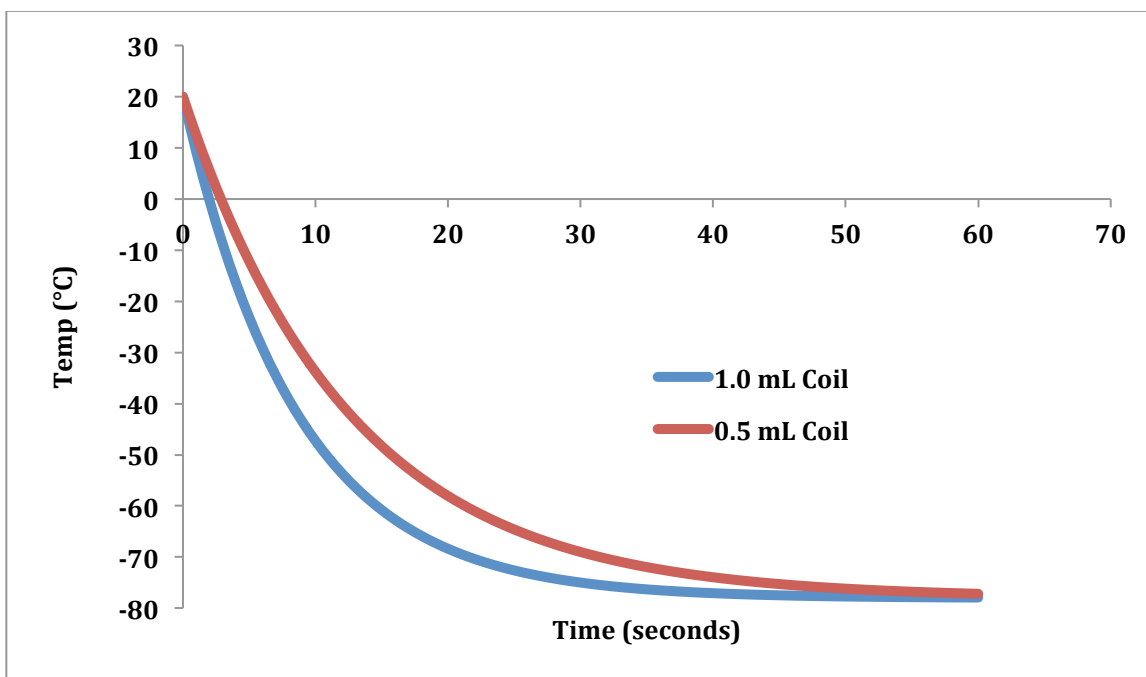
Figure 4.3. Conditioning of flow reactor tubing
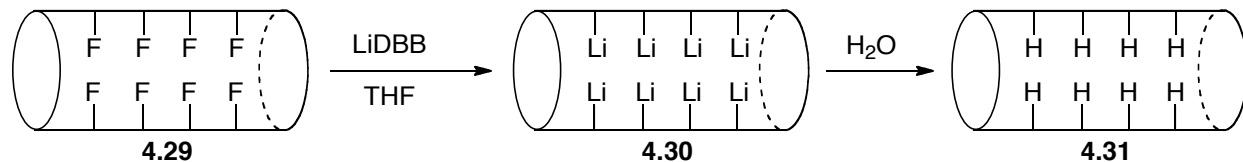
Initial flow reactor studies revealed a potential problem. Common tubing for flow systems is made from polytetrafluoroethylene (PTFE) or PFA and LiDBB is known to react with alkyl fluorides.[36] With reductive lithiation of alkyl fluorides unavoidable, the tubing was deliberately reacted by adding LiDBB and allowing it to react at 20 °C for an hour. It was assumed that only the surface alkyl fluorides (**4.29**) would react to produce the poly-lithiated surface **4.30** (**Figure 4.3**). Flushing the tubing with water was carried out to protonate the tubing, leading to **4.31**. The reasoning for this conditioning was to produce a polyethylene coating inside the tubing. This coating would provide increased chemical resistance, while the remaining perfluoropolymer would still give a more durable reactor than if constructed completely from polyethylene.

Figure 4.4. Schematic of reactor 1
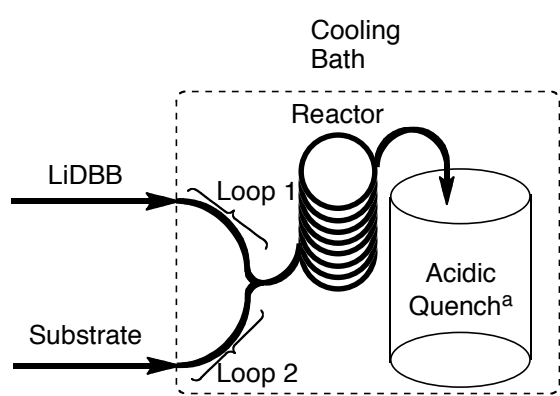
	Diameter (mm)	Length (cm)	Volume (mL)
Reactor	0.5	509	1.0
Loop 1	0.5	509	1.0
Loop 2	0.5	509	1.0

[a] $NH_4Cl_{(aq)}$ used for reactions at 20 °C, while 10 mM HCl in methanol was used for reactions ≤0 °C

Figure 4.4 shows the schematic for the first generation reactor. The system uses syringe pumps to flow a nominal 0.4 M LiDBB solution and a 1:1 molar mixture of **4.27** and **4.26** as a 0.20 M solution. These reagents flow through the previously described 1.0 mL loops and chill to –78 °C before entering and mixing in the reactor. The conditioned reactor was also constructed from 0.5 mm diameter tubing and had an internal volume of 1.0 mL. After the set residence time, the solution exits and is quenched. To ensure the appropriate temperature was being reached, the residence time was set to 2 minutes or 4 times the tested value from **Table 4.2**.

With a flow reactor constructed, ring opening of epoxide **4.27** was briefly tested in batch to find a comparison point for optimizing flow conditions. The morpholine amide **4.26** was selected as the electrophile since LiDBB would cleave the N–O bond present in Weinreb amide **4.24** (**Table 4.3**).[37] Entry 1 used the standard conditions employed by Malathong (See **Table 4.3**).[33] As expected, **4.25** was isolated in a low, 25% yield. Perturbing the concentration of Li⁺ in the system was anticipated to increase reactivity of the formed alkyllithium **4.23**. Enhancing or sequestering lithium was tested by adding LiCl or TMEDA to the reaction mixture (Entries 2-5). Both of these increased the product yield; however, one equivalent of TMEDA gave the highest yield. Allylic alcohol **4.32** was also isolated and attributed to base-induced elimination and ring opening of the epoxide. Based on these results, addition of 1 equivalent of TMEDA was used as a starting point for flow reactor conditions.

Table 4.3. Batch reactions of epoxide ring opening and additives
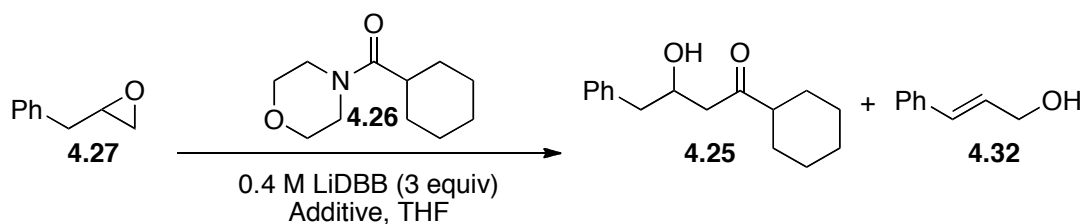
Entry	Additive	Yield of **4.25** (%)	Yield of **4.32**[a] (%)
1	None	25	n/a
2	0.1 equiv LiCl	41	19
3	0.5 equiv LiCl	33	10
4	1 equiv TMEDA	51	24
5	5 equiv TMEDA	33	11

Reactions run with 50 mg of epoxide and 74 mg of amide. Solution was stirred for 18 hours before quenching. [a] Yield by ^{1}H NMR with DMPU as internal standard

Flow reactors can generate reactive intermediates quickly, so it was hoped that faster reaction times at higher temperatures might out compete the observed elimination, and give increased addition into the amide. Entries 1-4 showed a clear drop in the yield of **4.25** as the temperature was increased (**Table 4.4**). Interestingly, there was a minimal loss of yield between –40 °C and 0 °C. One additional by-product, THF derivative **4.33,** was a surprising find, as oxidation should not occur under strong reducing conditions. It was hypothesized that this compound came from a THF radical reacting with molecular oxygen due to the solution quenching open to air. Based on these results, the thiophenyl derivative **4.22** has an advantage over epoxide **4.27,** which is prone to elimination due to benzylic hydrogens adjacent to the epoxide.

Table 4.4. Temperature vs. epoxide ring opening under flow conditions
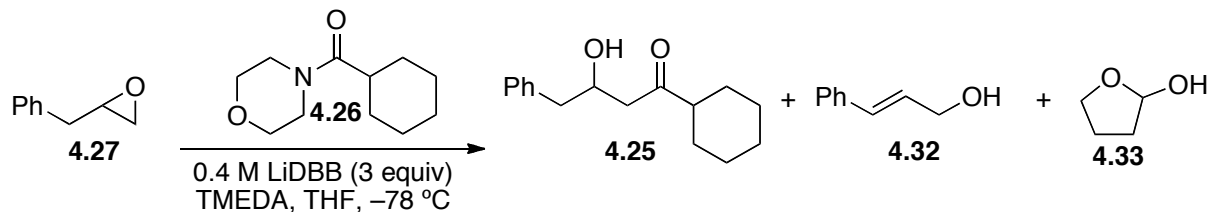
Entry	Temp (°C)	Yield of **4.25** (%)	Yield of **4.26**[a] (%)	mg of **4.33**
1	−78	28	24	0
2	−40	19	23	11
3	0	17	10	12
4	20	0	14	6

Reactions run with 50 mg of epoxide and 74 mg of amide. [a] Yield by ^{1}H NMR with DMPU as internal standard. Residence time of 2 minutes. Flow reactor 1 used

Based on the initial findings of the flow reactor, longer residence times at −78 °C were undertaken next. Increasing the residence time for the reactor to 8 minutes led to a 7% decrease in yield, but with no elimination product **4.32** isolated (**Table 4.5**). Doubling the residence time to 16 minutes gave a substantial boost in yield with no elimination observed. Further increasing the reaction time to 32 minutes gave a 52% yield of **4.25**, with only a small amount of the elimination product. This yield was approximately the same as the batch reaction in **Table 4.3**, entry 4. Therefore, the only improvement that the flow reactor provides is reducing the amount of the elimination product **4.32**.

Table 4.5. Varying residence time for opening epoxides
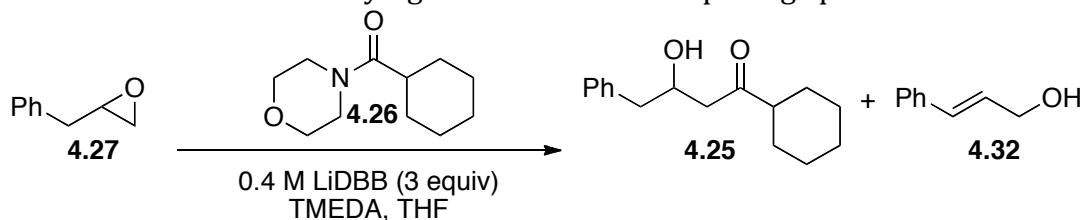
Entry	R_t (Min)	Yield of **4.25** (%)	Yield of **4.32** (%)
1	8	21	0
2	16	47	0
3	32	52	8

Reactions run with 50 mg of epoxide and 74 mg of amide. Flow reactor 1 used

173

The flow reactor approach to ring opening epoxides was somewhat successful. Epoxide **4.27** was a poor substrate for this reaction due to its tendency to eliminate to **4.32** under the reaction conditions (**Table 4.4**). The discrepancy in product yield, based on using a thiophenyl ether or epoxide, appears to be due to this elimination process (**Scheme 4.5**). Nevertheless, flow reactor conditions mixed reagents at –78 °C and gave a slightly higher yield than batch conditions, while limiting the amount of elimination isolated. Further research may find unactivated or sterically hindered epoxides to be more competent pre-nucleophile sources and avoid the need for preparation of the thiophenyl derivatives.

Spirocycles in flow

The successful construction of a flow reactor for reductive lithiation of epoxides led to applying the system to the synthesis of the previously discussed spirocycles (Chapter 3). It was anticipated that using a flow reactor could increase yields by accessing these spirocycles at higher temperatures for shorter reaction times. Additionally, by ensuring the reagents were at –78 °C before mixing, an increase in the diastereoselectivity was expected. For these reasons, the synthesis of [4.5] and [5.5] spirocycles were reevaluated under flow conditions, with assistance from undergraduate Kimberly Hilby.

Before a flow reactor could be tested, authentic samples of suspected side products were prepared. **Scheme 4.7** shows the synthesis of elimination and over-reduction products expected from the reactions in **Tables 4.7** and **4.8**. Starting from cyclohexylamine **4.34**, protection and alkylation with the appropriate bromide led to products **4.36**, **4.37**, and **3.120**, in reasonable to excellent yields (**Scheme 4.7**). In the case of **3.121,** no product was isolated via this route. It was assumed that the bromide **4.40** was prone to elimination

rather than alkylation and a second synthesis was undertaken avoiding the poor carbamate nucleophile. Activation of alcohol **4.38** as the tosylate and alkylation with an excess of **4.34** led to an outstanding yield of the mono-alkylation product. This secondary amine was easily Boc protected under standard conditions to give the last product required. These authentic samples matched the GCMS retention times and splitting patterns previously observed with reaction mixtures of **2.32** and **3.119**.

Scheme 4.7. Preparation of authentic side products **3.120**, **3.121**, **4.36**, **4.37**
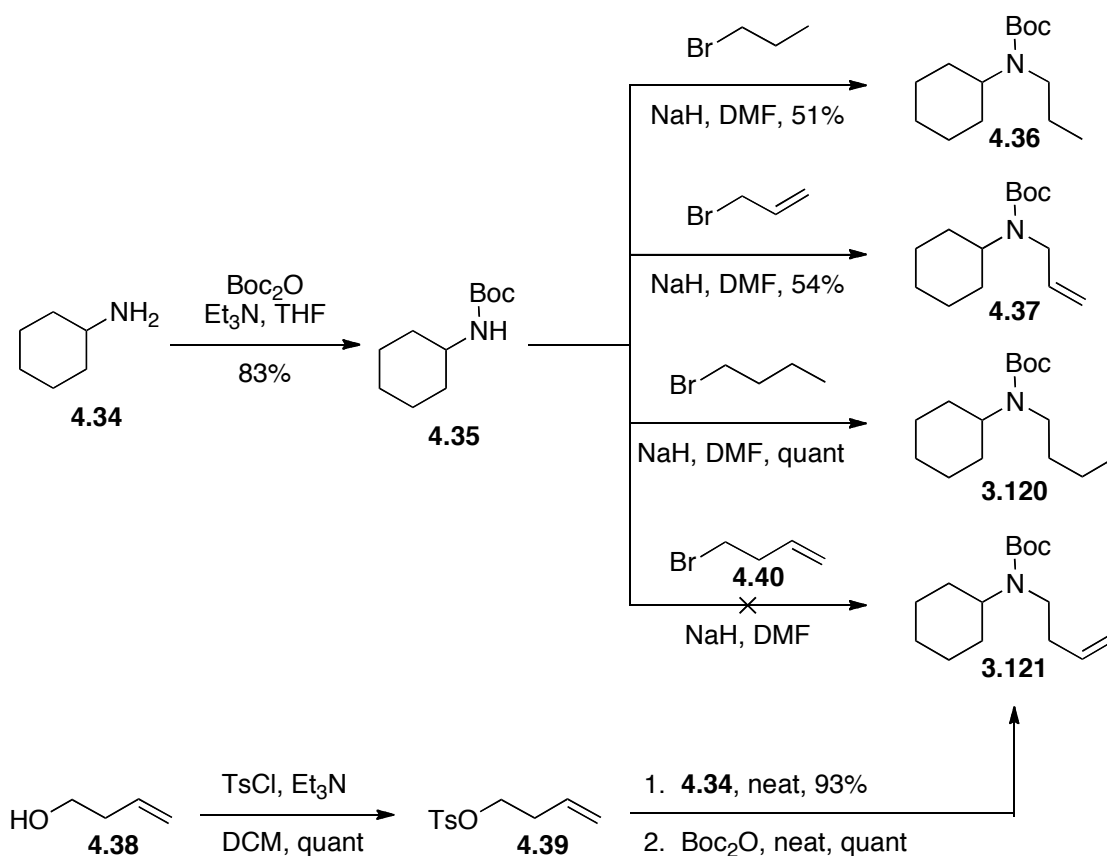
Using the previously described flow reactor (**Figure 4.4**) was complicated by two competing problems. If the reactants were to be cooled in loops 1 and 2 before the reaction, the solution had to remain in the coil for at least 60 seconds in the coil. Additional tubing could be added to reduce this time; however, the design of reactor 1 had restricted the

residence time to ≥30 seconds. Reducing the residence time led to increased reactor

pressure and substantial damage to the syringe pumps. Residence times above 30 seconds

caused a white solid[38] to build up in the reactor itself, leading to clogging and further pump

damage. To address these problems, the loops would need to be removed from the reactor

and a new strategy employed.

Figure 4.5. Schematic of reactor 2

	Diameter (mm)	Length (cm)	Volume (mL)
Reactor	0.5	255	0.5
Loop 1	0.5	15	0.029
Loop 2	0.5	15	0.029
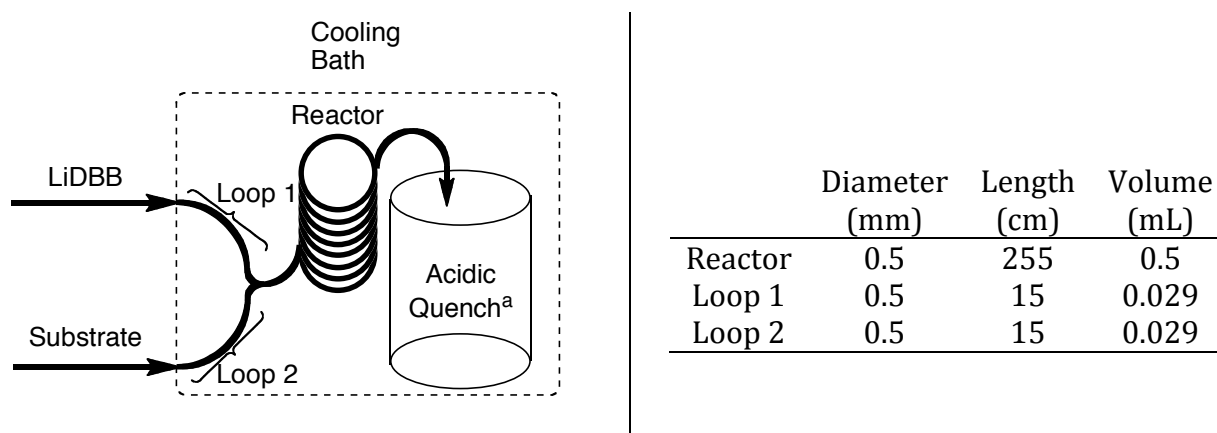
[a] $NH_4Cl_{(aq)}$ used for reactions at 20 °C, while 10 mM HCl in methanol was used for reactions ≤0 °C

A reworking of the system was required to form spirocycles in flow using reactor 1

(**Figure 4.4**). First, the reactor was shortened to reduce the pressure needed to run the

system. Next, loops 1 and 2 were substantially shortened and cooling was approached

differently. Since spirocycles were formed at 20 and 0 °C, reactions run at 20 °C used no

cooling. In contrast, 0 °C reactions used pre-cooled solutions and the reactor was placed in

an ice bath to limit warming. Due to the limitations of the syringe pumps and tubing used,

this reactor was not designed for continuous flow. Instead, the substrate and excess LiDBB

were loaded separately into the syringe pumps and pushed through the reactor until the

phosphate was fully added. After the phosphate addition was complete, both pumps were

stopped and the phosphate syringe was exchanged for one filled with blank THF at the appropriate temperature. The pumps were then restarted. This shutoff and restart took less than 5 seconds. The blank THF was pushed through to ensure all of the material had exited the reactor. While this set-up was not ideal, it was intended as a proof of concept and acceptable for evaluation.

Table 4.6. Effect of residence time on yield of spirocycle **2.33**
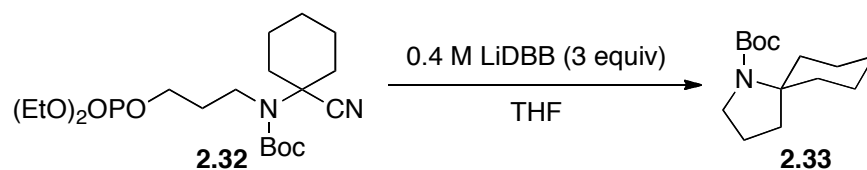
Entry	R_t (Sec)	Temp (°C)	Yield of **2.33** (%)
1	30	0	50
2	15	0	58
3	15	20	69
4	30	20	66
5	7.5	20	68

Reaction run on 50 mg scale (0.04M). Flow reactor 2 used

Based on the studies on forming [5.5] spirocycles (**Table 3.2**), non-cryogenic conditions were known to work. A residence time of 30 seconds was selected for reactor 2 based on attempts to form the spirocycle in reactor 1 (**Figure 4.5**). Using this residence time, the reactor produced spirocycles **2.33** at 0 °C in 50% yield (**Table 4.6**, entry 1). Decreasing the residence time to 15 seconds increased the yield to 58%. The shorted residence time resulted in higher flow rates and likely impacted the rate of mixing in the tubing. Increasing the temperature to 20 °C led to a 69% yield or slightly better than at –78 °C for an hour under batch conditions (**Scheme 3.17**). Increasing the residence time to 30 seconds slightly lowered the yield of **2.33** (entry 4). Since decreasing the residence time gave a better yield between entries 1 and 2, this time was further reduced in entry 5 to see

if the trend would continue. Instead, the spirocycle was isolated in approximately the same

yield as entry 3. From these data, entry 3 was selected as the optimal set of conditions.

Table 4.7. Equivalents of LiDBB to form **2.33** in flow
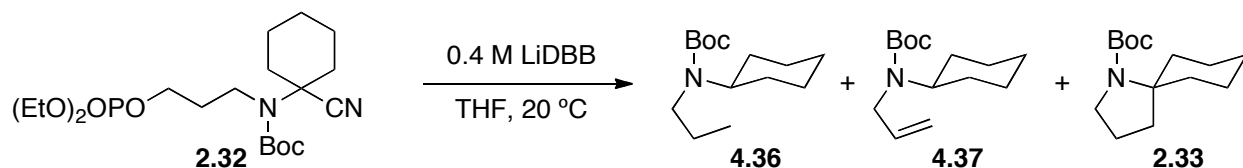
Entry	Equiv LiDBB	Yield of **4.36** (%)	Yield of **4.37** (%)	Yield of **2.33** (%)
1	3	2.0	1.5	66.7
2	4	0.4	1.3	62.1
3	5	0.3	1.1	58.1
4	6	0.4	0.8	60.1

Residence time of 15 seconds. Reaction run on 50 mg scale (0.04M). All yields are from GCMS ratios of the isolated mixture of **4.36**, **4.37**, **2.33**. Flow reactor 2 used

Data showing increasing yield with decreased residence time led to the hypothesis

of incomplete mixing. Industrial and research flow reactors rely on expensive microfluidic

mixing channels to ensure the reagents fully integrate as fast as possible. Given the limited

budget of this reactor, an alternative to this was to increase the equivalents of LiDBB. After

chromatography, **4.36**, **4.37**, and **2.33** were isolated as a mixture and then subjected to

GCMS (**Table 4.7**). From this, a yield for compounds **4.36**, **4.37**, and **2.33** was assigned.

Surprisingly, the yield of spirocycle **2.33** decreased with increasing amounts of LiDBB.

Another intriguing result was the small amount of side-product **4.37**, as batch reactions of

2.32 are known to produce 5-10% of the alkene byproduct.[39] It would appear that the

shorter reaction times can suppress side-product formation. Despite the lower amount of

side-products with higher equivalents of LiDBB, entry 1 gave the best yield of the

spirocycle and 3 equivalents of LiDBB was optimal.

At this point, the flow reactor was again modified based on three undesirable aspects of the reactor 2 design (**Figure 4.5**). Loops 1 and 2 had been shortened to allow for higher flow rates. Since the reactor was not setup for continuous flow conditions, this made it necessary to stop and restart the pumps to ensure all products had exited the reactor. Clogging was still an issue after multiple runs. Lastly the reactor was not able to cool solutions, relying on pre-chilled samples instead. It was decided that larger tubing would solve all of these problems.

Figure 4.6. Schematic of flow reactor 3

	Diameter (mm)	Length (cm)	Volume (mL)
Reactor	1.0	64	0.5
Loop 1	1.6	149	3.0
Loop 2	1.6	248	5.0
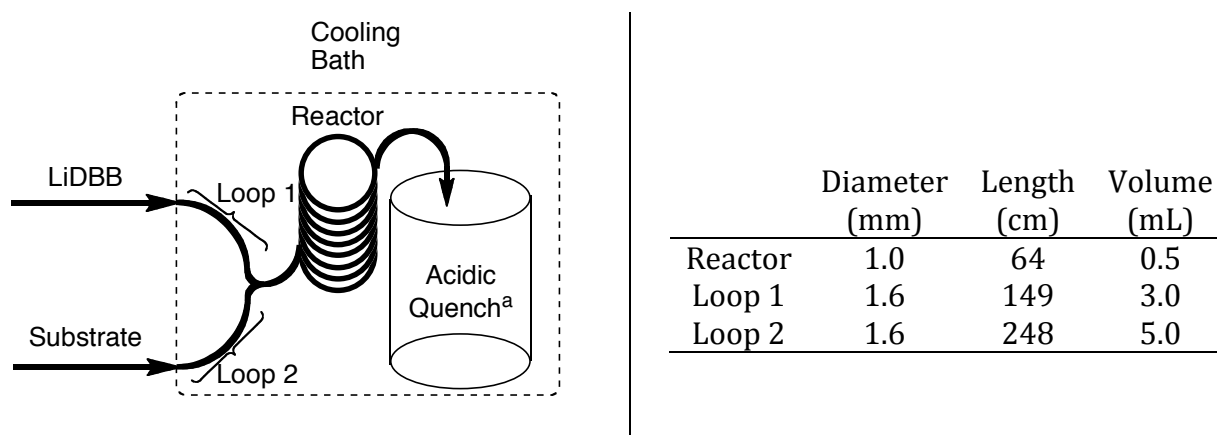
[a] $NH_4Cl_{(aq)}$ used for reactions at 20 °C, while 10 mM HCl in methanol was used for reactions ≤0 °C

Scheme 4.6 details the new reactor design. First, the diameter and length of loops 1 and 2 were increased to allow reagents to be fully loaded into each loop prior to starting the reactor. This allowed for the reagents to be chilled in a cooling bath before reacting. The reagents could be loaded into these coils and there was no longer a need to stop the flow reactor during its run. Instead, a syringe of blank THF was used to push the phosphate through the reactor, while LiDBB was added continually with the other pump. The reactor itself was doubled in diameter to help prevent clogging. Additionally, the connections

between the loops and reactor were changed from compression-fittings to flanged-fittings. This modification removed constriction of the tubing at the union between reactor parts. It was anticipated that these changes would simplify the flow reactor and prevent downtime seen with previous runs.

The improved reactor design was applied to the synthesis of the problematic [5.5] spirocycle **3.122** (**Table 3.2**). As seen in chapter 3, accessing this type of spirocycle with reductive lithiation gave approximately half the yield of its [4.5] counterpart. Since flow reactors can increase yields by employing higher reaction temperatures for shorter durations of time, this strategy was implemented. Entry 1, taken from **Table 3.2**, shows the product distribution from phosphate **3.119** at 0 °C. Applying the optimized flow conditions from **Table 4.7** at 0 °C led to an increase in the yield of the spirocycle but also the other side-products **3.120** and **3.121** (**Table 4.8**). Increasing the temperature to 20 °C unfortunately decreased the amount of spirocycle formed by 4%. Decreasing the residence time to 7.5 seconds yielded best results, with a decrease in the amount of the alkene and alkane side-products formed. Further reducing the residence time had little effect on yield.

Table 4.8. Non-cryogenic flow conditions to form a [5.5] spirocycle
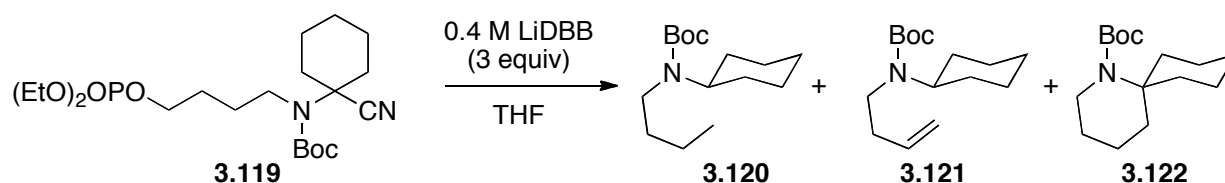
Entry	R_t (Sec)	Temp (°C)	Yield of **3.120** (%)	Yield of **3.121** (%)	Yield of **3.122** (%)
1	n/a[a]	0	2.9	1.6	37.9
2	15	0	4.5	7.4	42.1
3	15	20	6.7	4.1	38.4
4	7.5	20	3.7	2.8	46.1

[a] Batch reaction, 60 min reaction time at –78 °C; See **Table 3.2** for additional trials. Reaction run on 50 mg scale (0.04M). All yields are from GCMS ratios of the isolated mixture of **3.120–3.122**. Flow reactor 3 used

With the success of producing simple spirocycles under flow conditions, attention

was turned to diastereoselective reactions. Reacting phosphate **3.56** in batch was known

to give a 66% yield with a 98.0:2.0 dr (**Scheme 3.13**). Immersing the flow reactor in an

appropriate cooling bath allowed a variety of reaction temperatures to be evaluated. As

expected, diastereoselectivity increased from 72:28 to a single diastereomer as the reaction

temperature was dropped from 20 to –78 °C (**Table 4.9**). Reaction yields peaked at –40 °C;

however, the absence of a second diastereomer in entry 7 made these conditions more

appealing for stereoselective synthesis. Additionally, the conditions of entry 7 gave less

than 0.1% side products.[40] For these reasons, –78 °C was considered the optimal reaction

temperature.

Table 4.9. Temperature dependence on diastereoselectivity of spirocycle **3.69** in flow

Entry	Temp (°C)	Yield (%)	dr[a]
1	20	66	73.6:26.4
2	0	72	74.8:25.2
3	–40	85	90.8:9.2
4	–50	76	92.7:7.3
5	–60	72	94.7:5.3
6	–70	60	99.9:0.1
7	–78	64	>99.9:0.1

Residence time of 7.5 seconds. Reaction run on 50 mg scale (0.04M). [a]Diasteromeric ratio determined by GCMS after reduction of **3.69** to the N–methyl derivative with LiAlH$_4$. Flow reactor 3 used

Figure 4.7. Schematic of flow reactor 4
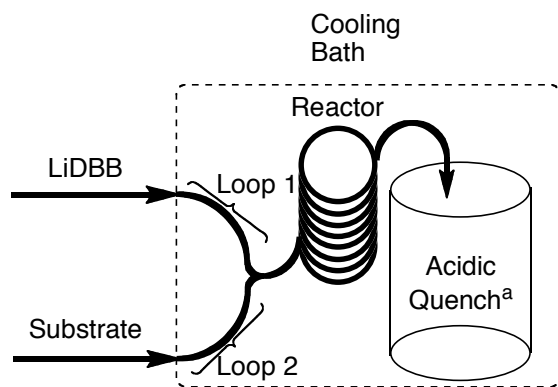
	Diameter (mm)	Length (cm)	Volume (mL)
Reactor	1.0	128	1.0
Loop 1	1.6	149	3.0
Loop 2	1.6	248	5.0

[a] NH$_4$Cl$_{(aq)}$ used for reactions at 20 °C, while 10 mM HCl in methanol was used for reactions ≤0 °C

While flow reactor 3 was a major improvement over reactor 2, the issue of clogging persisted. Higher flow rates seemed to mitigate this problem, so the reactor length was doubled, doubling the flow rate at the same residence time (**Figure 4.7**). Flow reactor 4 was then used to test the affects of solution molarity and equivalents of LiDBB on the cyclization of nitrile **3.119**. All entries in **Table 4.10** were run at 0.02 M solution of **3.119**. Running the reactor at the lower molarity with a 15 second residence time led to a significant drop in yield and more of the alkene side-product (entry 1). Doubling the equivalents of LiDBB significantly increased yield of **3.122** to 53.5% (entry 2). Since increasing flow rates had previously led to higher yields, entry 3 was run at half the residence time of entry 2. However, this led to a 14% drop in yield. The last trial was run with a large excess of LiDBB to see if the lower molarity at higher flow rates was leading to an incomplete mixing. While this did give a good yield of the spirocycle, entry 2 was still the best set of conditions found.

Table 4.10. Low molarity flow conditions to form a [5.5] spirocycle

Entry	R_t (Sec)	Equiv LiDBB	Yield of **3.120** (%)	Yield of **3.121** (%)	Yield of **3.122** (%)
1	15	3	13.1	1.5	31.9
2	15	6	22.8	2.6	53.5
3	7.5	6	8.8	2.3	39.9
4	7.5	12	5.8	1.6	45.7
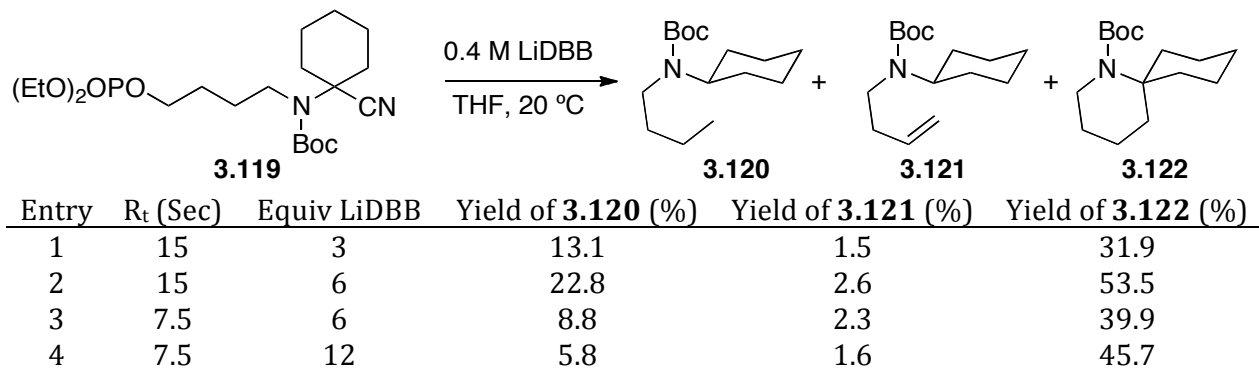
Reaction run on 50 mg scale (0.02M). All yields are from GCMS ratios of the isolated mixture of **3.120–3.122**. Flow reactor 4 used

The increased yields of spirocycle **3.122** at lower molarity and higher equivalents of LiDBB prompted an investigation of the synthesis of [4.5] spirocycle **2.33** under these conditions (**Table 4.11**). Since the reactor had been substantially upgraded, the best conditions from the older reactor were redone, leading to a 59% yield of product **2.33**. Increasing the equivalents of LiDBB increased the yield to 66%. Diluting the phosphate solution to 0.02 M and reacting it with 3 equivalents of LiDBB produced no improvement over entry 2. The last run increased the amount of LiDBB and returned a 7% increase in yield over entry 3. This made entry 4 the best yield for any set of conditions tested to form **2.33**. For entries 1–4, the amount of side products dropped below the ability of GCMS to reliably detect them.

Table 4.11. Low molarity flow conditions to form a [4.5] spirocycle
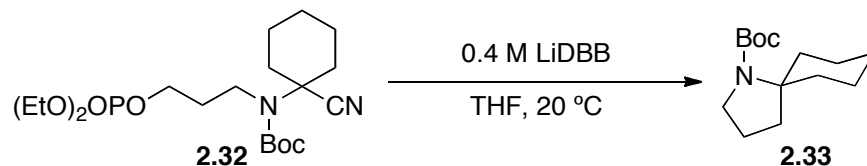
Entry	Phosphate Molarity	Equiv LiDBB	Yield (%)
1	0.04	3	59
2	0.04	6	66
3	0.02	3	65
4	0.02	6	72

Residence time of 15 seconds. Reaction run on 50 mg scale. Compounds **4.38**, and **4.39** were not observed by GCMS. Flow reactor 4 used

The additional reactor length was exceptionally useful in increasing the yields of **3.69**. **Table 4.12** details the results of extending the residence time with the new reactor. The yield of spirocycle **3.69** increased with longer residence times up to 30 seconds (entries 1-3). When this time was doubled to 1 minute, the reaction yield decreased (entry 4). Based on this, entry 3 was considered the best run and these conditions re-run in entry 5. Since the reactor was not designed for continuous flow, five, 50 mg reactions were run and combined to simulate a single long run. This yield was close to that of entry 3. Both the yield and diastereoselectivity of **3.69** were significantly improved using the flow reactor approach.

Table 4.12. Effect of residence time on diastereoselective spirocycle formation
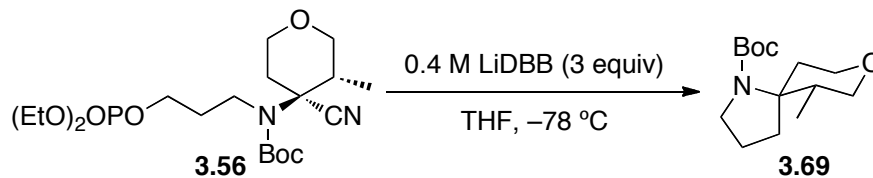
Entry	R_t (Sec)	Yield (%)	dr[a]
1	7.5	75	>99.9:0.1
2	15	79	>99.9:0.1
3	30	86	>99.9:0.1
4	60	67	>99.9:0.1
5	30	83[b]	>99.9:0.1

Reaction run on 50 mg scale (0.04M). Flow reactor 3 used. [a]Diasteromeric ratio determined by GCMS after reduction of **3.69** to the N–methyl derivative with LiAlH$_4$. [b]Run with five, 50 mg reactions

The ability to increase yields using a flow reactor approach to synthesis prompted inquiry into reaction time. Batch reactions to form spirocycles with LiDBB were run for an hour before quenching. In the flow reactor, 30 seconds or less gave the best yields, even at –78 °C. To see if this was due to changing the reaction mode from batch to flow, flow reactor conditions were applied to batch conditions (**Table 4.13**). Entry 1 was run under standard batch conditions and gave a great 67% yield. To ensure that reagents were mixed quickly and at the correct temperature, solutions of excess LiDBB and phosphate **2.32** were chilled to the desired temperature, and the phosphate was added to the LiDBB solution over ~2 seconds. After 30 seconds, the reaction was quenched with NH$_4$Cl$_{(Aq)}$. Entries 2–4 show that increasing reaction temperatures did increase yields up to 0 °C. Entry 4 gave a 20% better yield over entry 1 from **Table 4.6**. Repeating the batch conditions at 20 °C (Entry 5) led to a 7% drop in yield. The data indicate that forming spirocycles at 0 °C over 30 seconds was as viable as 60 minutes at –78 °C.

Table 4.13. Mimicking flow reactions of **2.32** in batch
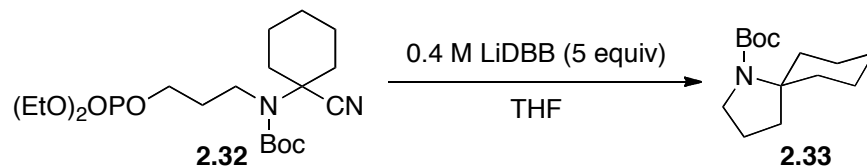
Entry	Time	Temp (°C)	Yield (%)
1	60 min	−78	67
2	30 sec	−78	56
3	30 sec	−40	68
4	30 sec	0	70
5	30 sec	20	63

All reactions run on 50 mg scale

The lower quantities of side products observed under flow conditions prompted a short study to see if these compounds came from the phosphate material or decomposition of the spirocycle itself. Given that THF can be ring-opened by LiDBB (Chapter 2), it was possible that side-products **4.36** and **4.37** were from a similar pathway (**Table 4.14**). To test this, two solutions of spirocycle **2.33** were subjected to standard LiDBB conditions for an hour. Entry 1 failed to produce the observed side products; however, 12% of the spirocycle was not recovered. While spirocycles **2.33** does not appear to decompose to **4.36** and **4.37**, the missing 12% of spirocycle **2.33** suggests an unknown decomposition pathway. Repeating the same conditions at 0 °C led to decomposition of 92% of the spirocycle. Again, none of the usual by-products was observed. The loss of nearly all of the starting material shows that long reaction times can negatively impact the yield of spirocycles. This may help explain why the yields of spirocycles formed in flow reactors are higher than under batch conditions.

Table 4.14. Spirocycle **2.33** stability to LiDBB

Entry	Temp (°C)	Yield of **4.36** (%)[a]	Yield of **4.37** (%)[a]	Recovered **2.33** (%)
1	−78	0	0	88
2	0	0	0	8

[a] By GCMS. Reactions run on 40 mg scale

Conclusions

A flow reactor approach to reductive lithiation with LiDBB was found to be successful as an alternative to batch conditions. Epoxide **4.27** could be reductively ring opened and added to a morpholine amide in equivalent yield, and required only 3% of the time required for the batch process. Use of a flow reactor also was found to limit byproducts observed in batch conditions. Simple [4.5] and [5.5] spirocycles could be formed in improved yield and at non-cryogenic temperatures as compared to their batch preparation. The yield of spiropyrrolidine **2.33** increased from 66% to 72%, while spiropiperidine **3.122** increased from 37% to 53%. Flow conditions improved the already high diastereoselectivity observed with **3.69**. Lastly, a simple [4.5] spirocycle was crafted in batch with excellent yield at 0 °C in 30 seconds, rather than the usual 1 hour at −78 °C. Based on these results, future research could improve the yield and stereoselectivity of spirocycles through the use of flow reactors.

General Experimental and Laboratory conditions

All glassware was flame- or oven-dried and cooled under argon unless otherwise stated.

All reactions and solutions were conducted under argon unless otherwise stated. All

reagents were used as received unless otherwise stated.   Tetrahydrofuran (THF),

dimethylformamide (DMF) and dichloromethane (DCM) were degassed and dried by

filtration through activated alumina under vacuum according to the procedure by Grubbs.[41]

Tetramethylethylenediamine (TMEDA), and triethylamine (Et_3N) were distilled from CaH_2..

All reactions involving LiDBB were conducted with glass stirbars.   Thin layer

chromatography (TLC) was done on Watman (250 μm) 6 Å glass-backed silica gel plates

and visualized using potassium permanganate or Dragondorf.   Flash column

chromatography (FCC) was performed according to the method by Still, Kahn, and Mitra

using Fisher reagent silica gel 60 (230-400 mesh).[42]

Instrumentation

All data collected at ambient temperature unless noted. ^{1}H NMR spectra were taken at 500

MHz, calibrated using residual NMR solvent ($CDCl_3$ at 7.26 ppm), and interpreted on the δ

scale. ^{13}C NMR spectra were taken at 125 MHz, calibrated using the NMR solvent ($CDCl_3$ at

77.16 ppm), and interpreted on the δ scale with the following abbreviations: s= singlet, d=

doublet, t = triplet, q= quartet, dt= doublet of triplets, dd= doublet of doublets, m=

multiplet, app= apparent, br= broad.   IR taken by thin film. High resolution GCMS was run

on an Agilent 7890A using a DB-5ms column (30 m by 0.25 mm, 0.25 μm coating) and

masses detected with a Waters GCT Premier TOF mass spectrometer using chemical

ionization (ammonia) as the detection method. Additional GCMS data were collected on a Thermoquest Trace GC 2000 series using a DB-5ms column (30 m by 0.25 mm, 0.25 μm coating) and masses detected with a ThermoFinnegan TraceMS+ mass spectrometer using electron as the detection method. Samples were prepared in DCM or ethyl acetate (0.1–1 mg /mL loading), mixed with a vortex mixer for 30 seconds and submitted for analysis.

LiDBB Formation in THF

LiDBB was prepared fresh before each experiment, example procedure:

LiDBB was prepared by adding 4,4'-di-*tert*-butylbiphenyl (DBB, 1.50 g, 5.64 mmol, 1 equiv), to a 50 mL flask, followed by evacuating and flame-drying. Once the DBB was melted, the flask was backfilled with argon and allowed to cool. An ice bath was applied and lithium wire (0.39 g, 56.4 mmol, 10 equiv) was clipped in under a stream of argon. THF (14 mL) was added and the solution turned green, darkening over for 5 hours at 0 °C. This resulted in a nominal 0.4 M LiDBB solution.

Reactor Tube Conditioning

To perfluoroalkoxy alkane (PFA) or polytetrafluoroethylene (PTFE) tubing fitted with syringes at both ends, LiDBB (ca. 0.4 M) was added at 20 °C until the tube was filled with the dark-green solution. After reacting for one hour, the LiDBB was removed and the tube was flushed with water.

Testing of Flow Reactor Cooling Loops

PFA tubing (0.5 mL, 0.5 mm ID x 255 cm) was coiled to produce a ca. 6 cm diameter ring. A 12 mL syringe filled with 20 °C THF was attached to one end of the tubing and the syringe placed in a syringe pump. The rest of the coil was placed in a dry ice/acetone bath such that the other end of the tubing pointed up with ca. 2 cm of the tubing above the liquid of the cooling bath. A thermocouple was placed perpendicular to this end of the tubing such that any THF exiting the tubing ran down the length of the thermocouple. The system was covered in aluminum foil and the syringe pump set to a flow-rate of 1.000 ml/min (30 sec residence time). The pump was turned on and the thermocouple monitored until a constant temperature was observed for 1 minute (–69 °C). This process was repeated with a 1.0 mL (0.5 mm ID x 509) piece of tubing (2.00 mL/min flow rate), giving a temperature of –75 °C.

Flow Reactor Tubing Dimensions

Flow Reactor #	Component	Diameter (mm)	Length (cm)	Volume (mL)
	Reactor	0.5	509	1.0
1	Loop 1	0.5	509	1.0
	Loop 2	0.5	509	1.0
	Reactor	0.5	255	0.5
2	Loop 1	0.5	15	0.029
	Loop 2	0.5	15	0.029
	Reactor	1.0	64	0.5
3	Loop 1	1.6	149	3.0
	Loop 2	1.6	248	5.0
	Reactor	1.0	128	1.0
4	Loop 1	1.6	149	3.0
	Loop 2	1.6	248	5.0

Flow Reactor 1 was built from PFA tubing (see table above) and was connected with a 0.50 mm ID Y-connector made from polyether ether ketone (PEEK). Syringe to tubing connections used 1/16"-28 female to male luer adaptor (PEEK) and 1/16"-28 male nuts (PEEK).

Flow Reactor 2 was built from PFA tubing (see table above) and was connected with a 0.50 mm ID Y-connector made from PEEK. Syringe to tubing connections used 1/16"-28 female to male luer adaptor (PEEK) and 1/16"-28 male nuts (PEEK).

Flow Reactor 3 was built from PTFE tubing (see table above) and was connected with a 0.50 mm ID Y-connector made from PEEK. Syringe to tubing connections used ¼"-28 female to male luer adaptor (PEEK) and ¼"-28 male nuts (PEEK). The reactor was 500μL, flanged tubing from Rheodyne.

Flow Reactor 4 was built from PTFE tubing (see table above) and was connected with a 0.50 mm ID Y-connector made from PEEK. Syringe to tubing connections used ¼"-28 female to male luer adaptor (PEEK) and ¼"-28 male nuts (PEEK). The reactor was built from two, 500μL flanged pieces of tubing from Rheodyne connected in series.
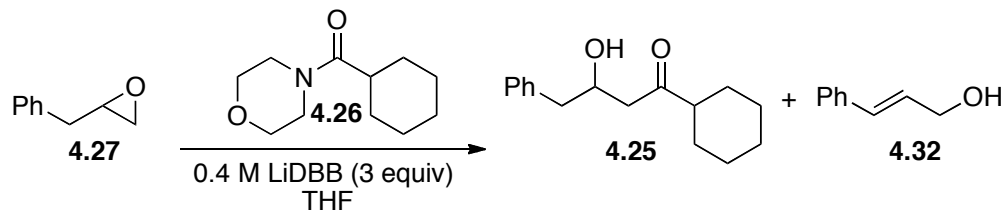
All reactors were tested for leaks by filling the reactor with H_2O, attaching syringes to the 3 coils and applying pressure.

Batch reactions with ring-opened epoxides

Reactions in **Table 4.3** were run identically with the exception of the additive used. The best yielding procedure is presented below:

To a –78 °C solution of **4.27** (50 mg, 0.37 mmol, 1 equiv) in THF (1.5 mL), TMEDA (6μL, 0.37 mmol, 1 equiv) was added. LiDBB (2.8 mL, 1.12mmol, 3 equiv) was added over 20 seconds down the side of the flask. After 15 min, a solution of **4.26** (74 mg, 0.37 mmol, 1 equiv) in THF (0.5 mL) was added over 10 seconds down the side of the flask. The solution was allowed to stir at –78 °C for 18 hours. The reaction was quenched with a $NH_4Cl_{(aq)}$ solution (2 mL), and diluted with Et_2O (10 mL). The organic layer was extracted and aqueous layer washed with Et_2O (3 x 5 mL) and the combined organic layers were dried with $MgSO_4$ and concentrated *in vacuo*, giving a yellow oil. Flash column chromatography (60:30:5:5 Hexanes/DCM/Et_2O/Ethyl acetate) gave 1-cyclohexyl-3-hydroxy-4-phenylbutan-1-one (**4.25**) in 51% yield (47 mg) as a clear oil. (E)-3-phenylprop-2-en-1-ol (**4.32**) was also isolated, but as an inseparable mixture. DMPU was used as internal standard to determine a 24% yield (12 mg). The analytical data of both products matched those previously reported.[33,43]

General Procedure for Epoxide Ring Opening Using Flow Reactor 1
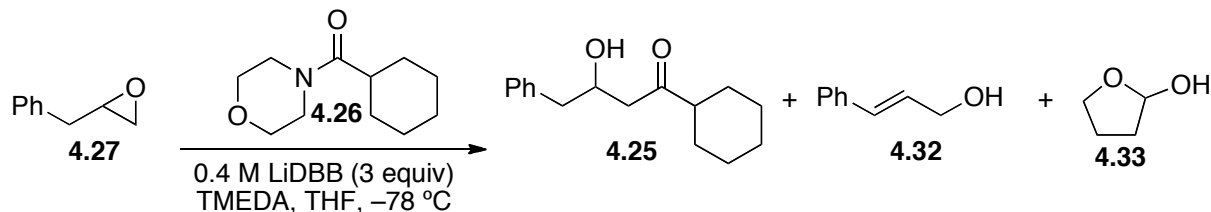
Flow reactor 1 was immersed in an appropriate cooling bath as shown in **Figure 4.4** and the reactor filled with dry THF. A solution of **4.26** (74 mg, 0.37 mmol, 1 equiv), **4.27** (50 mg, 0.37 mmol, 1 equiv), and TMEDA (6 μL, 0.37 mmol, 1 equiv) in THF (2.0 mL) was added to a 3 mL syringe, attached to loop 1, and placed in the syringe pump. At the reactor exit was a vial with 3 mL of 10 mM methanolic HCl if the reaction temperature was ≤ 0 °C or 3 mL of $NH_4Cl_{(aq)}$ if the reaction temperature was at 20 °C.   A second syringe was filled with 10 mL of nominal 0.4 M LiDBB and attached to loop 2. LiDBB was pushed through the flow reactor until the exiting solution was dark-green (ca. 2.5 mL). Both syringe pumps were turned on and monitored until the epoxide/amide solution was fully added. In ≤ 5 seconds, the syringe pumps were turned off, the syringe previously containing the epoxide/amide solution was exchanged for a 6 mL syringe of dry THF, and the pumps turned back on. After the blank THF was fully added, the run was considered complete. The reaction was diluted with 10 mL Et₂O and the aqueous layer extracted 3 x 10 mL Et₂O. The combined organic layers were dried over MgSO₄, giving a yellow oil. Flash column chromatography (60:30:5:5 Hexanes/DCM/Et₂O/Ethyl acetate to 100% Et₂O) gave 1-cyclohexyl-3-hydroxy-4-phenylbutan-1-one (**4.25**), (E)-3-phenylprop-2-en-1-ol (**4.32**) and **4.33**. The analytical data of both products matched those previously reported.[33,43]

Optimization of flow reactor for generation and useage of β-alkoxy alkyllithium
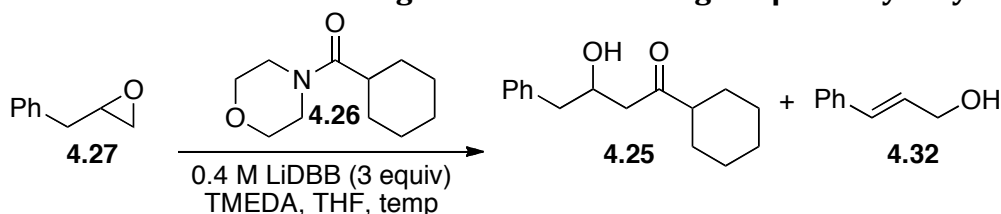
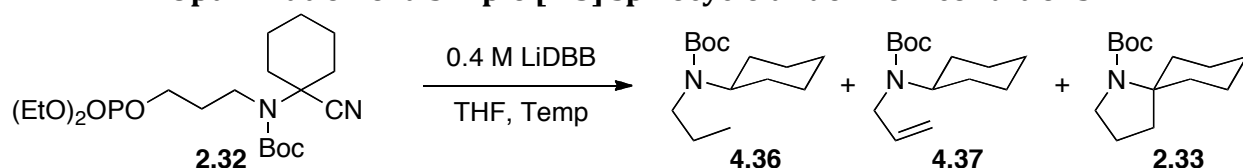| Entry	LiDBB Pump (mL/min)	Epoxide/amide Pump (mL/min)	Residence Time (min)	Temp (°C)	Yield of **4.25** (%)	Yield of **4.32** (%)
1	0.290	0.210	2	−78	28	24 [a]
2	0.290	0.210	2	−40	19	23 [a]
3	0.290	0.210	2	0	17	10 [a]
4	0.290	0.210	2	20	0	14 [a]
5	0.073	0.052	8	−78	21	0
6	0.036	0.026	16	−78	47	0
7	0.018	0.013	32	−78	52	8

All reactions used flow reactor 1. Entries 1–4 are from **Table 4.4** and entries 5–7 are from **Table 4.5**; the best conditions are highlighted in blue. All reactions run with 50 mg (0.37 mmol, 1 equiv) of **4.27**, 74 mg (0.37 mmol, 1 equiv) of **4.26** and 6 μL (0.37 mmol, 1 equiv) of TMEDA. [a] Yield by ^{1}H NMR with DMPU as the internal standard.

General Procedure for reductive cyclization under Flow conditions with Reactor 2

Flow reactor 2 was immersed in an appropriate cooling bath as shown in **Figure 4.5** and the reactor filled with dry THF. A solution of **2.32** (50 mg, 0.12 mmol, 1 equiv) in THF (3.0 mL) was added to a 3 mL syringe, attached to loop 1, and placed in the syringe pump. At the reactor exit was a vial with 3 mL of 10 mM methanolic HCl if the reaction temperature was ≤ 0 °C or 3 mL of $NH_4Cl_{(aq)}$ if the reaction temperature was at 20 °C. A second syringe was filled with 10 mL of nominal 0.4 M LiDBB and attached to loop 2. LiDBB was pushed through the flow reactor until the exiting solution was dark-green (ca. 2.5 mL). Both syringe pumps were turned on and monitored until the phosphate solution was fully added. In ≤ 5 seconds, the syringe pumps were turned off, the syringe previously containing the phosphate solution was exchanged for a 6 mL syringe of dry THF, and the pumps turned back on. After the blank THF was fully added, the run was considered

complete. The reaction was diluted with 10 mL Et$_2$O and the aqueous layer extracted 3 x

10 mL Et$_2$O. The combined organic layers were dried over MgSO$_4$, giving a yellow oil. Flash

column chromatography (5:1 pentane/DCM to 8:1 pentane/Et$_2$O) gave a mixture of **4.36**,

4.37, and **2.33**. Similar ionization was expected with GCMS,[44] therefore the areas from

GCMS were used without calibration to determine the yield of each compound.

Optimization of a simple [4.5] spirocycle under flow conditions

Entry	LiDBB Pump (mL/min)	Phosphate Pump (mL/min)	Residence Time (sec)	Equiv LiDBB	Temp (°C)	Yield of **4.36** (%)	Yield of **4.37** (%)	Yield of **2.33** (%)
1	0.230	0.770	30	3	0	n/a	n/a	50
2	0.460	1.540	15	3	0	n/a	n/a	58
3	0.460	1.540	15	3	20	n/a	n/a	69
4	0.230	0.770	30	3	20	n/a	n/a	66
5	0.919	3.079	7.5	3	20	n/a	n/a	68
6	0.460	1.540	15	3	20	2.0[a]	1.5[a]	66.7[a]
7	0.569	1.430	15	4	20	0.4[a]	1.3[a]	62.1[a]
8	0.664	1.335	15	5	20	0.3[a]	1.1[a]	58.1[a]
9	0.747	1.252	15	6	20	0.4[a]	0.8[a]	60.1[a]

All reactions used flow reactor 2. Entries 1–5 are from **Table 4.6** and entries 6–9 are from **Table 4.7**; the best conditions are highlighted in blue. All reactions run with 50 mg (0.16 mmol, 1 equiv) of **2.32.** [a] Yields are from GCMS ratios of the isolated mixture of **4.36**, **4.37**, and **2.33**

General Procedure for reductive cyclization under Flow conditions (Reactors 3 & 4)

Flow reactor 3 was immersed in an appropriate cooling bath as shown in **Figure 4.5** and

the reactor filled with dry THF. A solution of phosphate (0.16 mmol, 1 equiv) in THF (3.0

mL) was added into loop 2. At the reactor exit was a vial with 3 mL of 10 mM methanolic

HCl if the reaction temperature was ≤ 0 °C or 3 mL of NH$_4$Cl$_{(aq)}$ if the reaction temperature

was at 20 °C. A second syringe was filled with 10 mL of nominal 0.4 M LiDBB and attached

to loop 1. LiDBB was pushed through the flow reactor until the exiting solution was dark-green (ca. 2.5 mL). Both syringe pumps were turned on. After the blank THF was fully added, the run was considered complete. The reaction was diluted with 10 mL Et$_2$O and the aqueous layer extracted 3 x 10 mL Et$_2$O. The combined organic layers were dried over MgSO$_4$, giving a yellow oil. Flash column chromatography gave either a mixture of products (analyzed by GCMS) or a single product (analyzed by [1]NMR).

Optimization of a simple [5.5] spirocycle under flow conditions
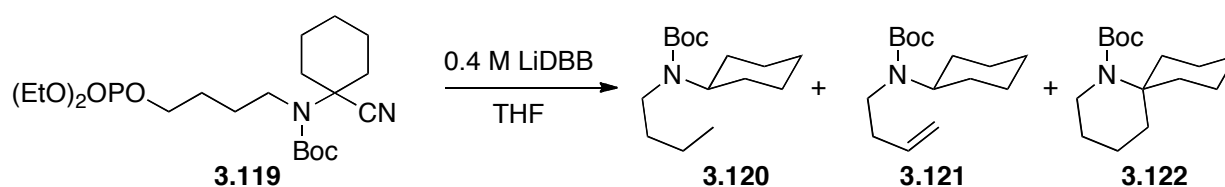
Entry	LiDBB Pump (mL/min)	Phosphate Pump (mL/min)	Residence Time (sec)	Equiv LiDBB	Temp (°C)	Yield of **3.120** (%)	Yield of **3.121** (%)	Yield of **3.122** (%)
1	0.230	0.770	30	3	0	4.5 [a]	7.4 [a]	42.1 [a]
2	0.460	1.540	15	3	0	6.7 [a]	4.1 [a]	38.4 [a]
3	0.460	1.540	15	3	20	3.7 [a]	2.8 [a]	46.1 [a]

All reactions used flow reactor 3. Entries 1–3 are from **Table 4.8**; the best conditions are highlighted in blue. All reactions run with 50 mg (0.16 mmol, 1 equiv) of **3.119.** Phosphate concentration was 0.04 M. [a] All yields are from GCMS ratios of the isolated mixture of **3.120**, **3.121**, and **3.122**

Optimization of a [4.5] spirocycle under flow conditions

3.56 → 3.69

0.4 M LiDBB (3 equiv), THF, temp
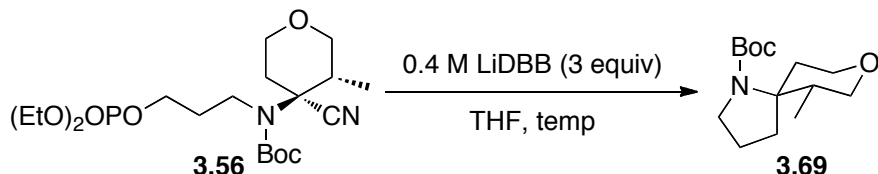
Entry	LiDBB Pump (mL/min)	Phosphate Pump (mL/min)	Residence Time (sec)	Temp (°C)	Yield of 3.69 (%)	dr[a]
1	0.924	3.097	7.5	20	66	72:28
2	0.924	3.097	7.5	0	72	75:25
3	0.924	3.097	7.5	−40	85	90:10
4	0.924	3.097	7.5	−50	76	93:7
5	0.924	3.097	7.5	−60	72	95:5
6	0.924	3.097	7.5	−70	60	99.9:0.1
7	0.924	3.097	7.5	−78	64	>99.9:0.1

All reactions used flow reactor 3. Entries 1–7 are from **Table 4.9**; the best conditions are highlighted in blue. All reactions run with 50 mg (0.16 mmol, 1 equiv) of **3.56.** [a]Diasteromeric ratio determined by GCMS after reduction of **3.69** to the N–methyl derivative with LiAlH$_4$

Optimization of a simple [5.5] spirocycle under flow conditions
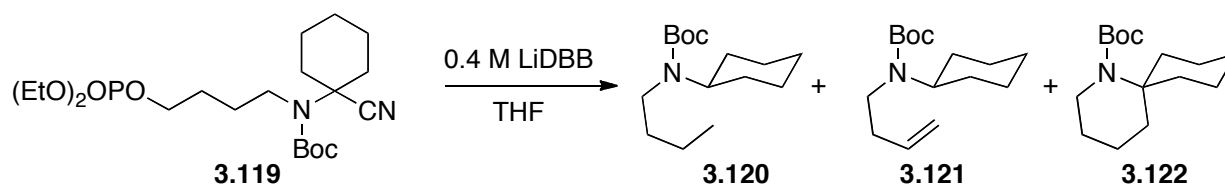
3.119 → 3.120 + 3.121 + 3.122

0.4 M LiDBB, THF

Entry	LiDBB Pump (mL/min)	Phosphate Pump (mL/min)	Residence Time (sec)	Equiv LiDBB	Temp (°C)	Yield of 3.120 (%)	Yield of 3.121 (%)	Yield of 3.122 (%)
1	0.462	1.549	30	3	20	13.1[a]	1.5[a]	31.9[a]
2	3.005	5.037	7.5	6	20	22.8[a]	2.6[a]	53.5[a]
3	1.503	1.519	15	6	20	8.8[a]	2.3[a]	39.5[a]
4	2.188	1.833	15	12	20	5.8[a]	1.6[a]	45.7[a]

All reactions used flow reactor 4. Entries 1–4 are from **Table 4.10**; the best conditions are highlighted in blue. All reactions run with 50 mg (0.16 mmol, 1 equiv) of **3.119.** Phosphate concentration was 0.02 M. [a] All yields are from GCMS ratios of the isolated mixture of **3.120**, **3.121**, and **3.122**
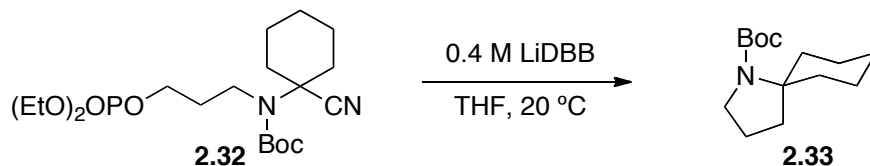
Optimization of a simple [4.5] spirocycle under flow conditions

Entry	LiDBB Pump (mL/min)	Phosphate Pump (mL/min)	Residence Time (sec)	Equiv LiDBB	[Phosphate] (Mol/L)	Yield of 2.33 (%)
1	0.924	3.097	15	3	0.04	59
2	1.503	2.519	15	6	0.04	66
3	0.522	3.499	15	3	0.02	65
4	0.924	3.097	15	6	0.02	72

All reactions used flow reactor 4. All entries are from **Table 4.11**; the best conditions are highlighted in blue. All reactions run with 50 mg (0.16 mmol, 1 equiv) of **2.32.**

Optimization of a [4.5] spirocycle under flow conditions
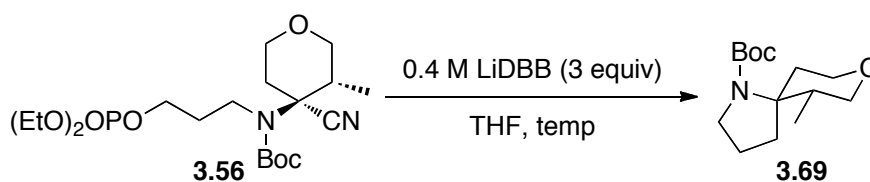
Entry	LiDBB Pump (mL/min)	Phosphate Pump (mL/min)	Residence Time (sec)	Temp (°C)	Yield of 3.69 (%)	dr[a]
1	1.848	6.194	7.5	−78	79	>99.9:0.1
2	0.924	3.097	15	−78	79	>99.9:0.1
3	0.462	1.549	30	−78	86	>99.9:0.1
4	0.231	0.774	60	−78	67	>99.9:0.1
5[b]	0.462	1.549	30	−78	83	>99.9:0.1

All reactions used flow reactor 4. Entries 1–7 are from **Table 4.12** and entries 8–10 are from **Table 4.12**; the best conditions are highlighted in blue. All reactions run with 50 mg (0.16 mmol, 1 equiv) of **3.56.** [a]Diasteromeric ratio determined by GCMS after reduction of **3.69** to the N−methyl derivative with LiAlH₄. [b]Run with five, 50 mg reactions

30 sec Batch Reactions of Spirocycle

To a −78 °C solution of LiDBB (1.5 mL, 0.60 mmol, 5 equiv), **2.32** (50 mg, 0.12 mmol, 1 equiv) in THF (4.2 mL) at −78 °C was added. After stirring for 30 sec, the reaction was quenched with a NH₄Cl$_{(aq)}$ solution (2 mL), and diluted with Et₂O (10 mL). The organic layer was extracted and aqueous layer washed with Et₂O (3 x 5 mL) and the combined

organic layers were dried with MgSO$_4$ and concentrated *in vacuo*, giving a yellow oil. Flash column chromatography (5:1 Hexanes/DCM to 7:1 pentane/Et$_2$O) gave tert-butyl 1-azaspiro[4.5]decane-1-carboxylate (**2.33**) in 56% yield (16 mg) as a clear oil. The analytical data matched those previously reported.[45] The above procedure was repeated with both solutions at –40 °C (68% yield, 19mg), 0 °C (70% yield, 20 mg), and 20 °C (63% yield, 18 mg).

Spirocycle Stability Test

To a –78 °C solution of LiDBB (1.3 mL, 0.51 mmol, 3 equiv), **2.33** (40 mg, 0.17 mmol, 1 equiv) in THF (4.2 mL) was added. After stirring for one hour, the reaction was quenched with a NH$_4$Cl$_{(aq)}$ solution (2 mL), and diluted with Et$_2$O (10 mL). The organic layer was extracted and aqueous layer washed with Et$_2$O (3 x 5 mL) and the combined organic layers were dried with MgSO$_4$ and concentrated *in vacuo*, giving a yellow oil. Flash column chromatography (5:1 Hexanes/DCM to 7:1 pentane/Et$_2$O) gave tert-butyl 1-azaspiro[4.5]decane-1-carboxylate (**2.33**) in 88% recovered yield (35 mg) as a clear oil. The analytical data matched those previously reported.[45]

Repeating the procedure at 0 °C, tert-butyl 1-azaspiro[4.5]decane-1-carboxylate (**2.33**) was recovered in 8% yield (3 mg) as a clear oil.
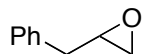

2-benzyloxirane (**4.27**) Prepared from allylbenzene as described by Vi.[33] The analytical data matched those previously reported.
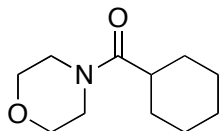
Cyclohexyl(morpholino)methanone (**4.26**) Prepared from cyclohexanecarbonyl chloride

as described by Vi.[33] The analytical data matched those previously reported.
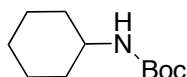
Tert-butyl cyclohexylcarbamate (**4.35**) Prepared from cyclohexylamine as described by

Millet and Baudion.[46]   The analytical data matched those previously reported.
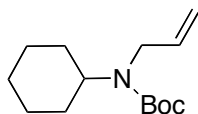
Tert-butyl   allyl(cyclohexyl)carbamate   (4.37)   Prepared   from   tert-butyl

cyclohexylcarbamate as described by Millet and Baudion.[46] The analytical data matched

those previously reported.
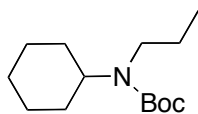
Tert-butyl cyclohexyl(propyl)carbamate (**4.36**) To a 0 °C solution of tert-butyl

cyclohexylcarbamate (150 mg, 0.76 mmol, 1 equiv) in DMF (3.1 mL), NaH (45 mg, 1.14

mmol, 1.5 equiv) was added. After stirring for 1.5 hours at 20 °C, bromopropane (0.10 mL,

1.14 mmol, 1.5 equiv) was added and stirred for 18 hours. The reaction was quenched with

a $NH_4Cl_{(aq)}$ solution (10 mL), and diluted with Et_2O (10 mL).   The organic layer was

extracted and aqueous layer washed with Et$_2$O (3 x 5 mL) and the combined organic layers were dried with MgSO$_4$ and concentrated *in vacuo*, giving a yellow oil. Flash column chromatography (19:1 Hexanes/EtOAc) gave *tert*-butyl cyclohexyl(propyl)carbamate in 51% yield (99 mg) as a clear oil.

^{1}H NMR (CDCl$_3$, 500 MHz) δ 3.98–3.38 (m, 1H), 2.97 (br s, 2H), 1.76 (d, *J* = 9.5 Hz, 2H), 1.70 (app d, *J* = 9.5 Hz, 2H), 1.62 (*d, J* = 13.0 Hz, 1H), 1.54–1.25 (m, 15H), 1.06 (qt, *J* = 13.0, 3.5 Hz, 1H), 0.85 (t, *J* = 7.0 Hz, 3H); ^{13}C NMR (CDCl$_3$, 125 MHz) δ 155.7, 79.0, 55.0, 44.9, 31.4, 28.6, 26.2, 25.8, 24.1, 11.6; IR (thin film) 2965, 2929, 2855, 1686 cm^{-1}; HRMS (ESI) calcd for C$_{14}$H$_{27}$O$_2$NNa [M+Na]$^+$ 264.1939, found 264.1943
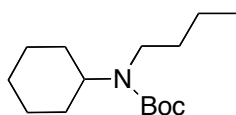
***Tert*-butyl butyl(cyclohexyl)carbamate** (**3.120**) To a 0 °C solution of tert-butyl cyclohexylcarbamate (150 mg, 0.76 mmol, 1 equiv) in DMF (3.1 mL), NaH (45 mg, 1.14 mmol, 1.5 equiv) was added. After stirring for 1.5 hours at 20 °C, bromobutane (0.12 mL, 1.14 mmol, 1.5 equiv) was added and stirred for 18 hours. The reaction was quenched with a NH$_4$Cl$_{(aq)}$ solution (10 mL), and diluted with Et$_2$O (10 mL). The organic layer was extracted and aqueous layer washed with Et$_2$O (3 x 5 mL) and the combined organic layers were dried with MgSO$_4$ and concentrated *in vacuo*, giving a yellow oil. Flash column chromatography (19:1 Hexanes/EtOAc) gave tert-butyl butyl(cyclohexyl)carbamate in quantitative yield (193 mg) as a clear oil.

^{1}H NMR (CDCl$_3$, 500 MHz) δ 3.97–3.38 (m, 1H), 3.01 (br s, 2H), 1.77 (d, *J* = 10.0 Hz, 2H), 1.70 (app d, *J* = 9.5 Hz, 2H), 1.62 (*d, J* = 13.0 Hz, 1H), 1.54–1.16 (m, 17H), 1.06 (qt, *J* = 13.0, 3.5 Hz, 1H), 0.85 (t, *J* = 7.0 Hz, 3H); ^{13}C NMR (CDCl$_3$, 125 MHz) δ 155.7, 79.0, 55.0, 42.9, 31.4,

29.8, 28.7, 26.2, 25.8, 20.5, 14.1; IR (thin film) 2927, 2855, 1688 cm^{-1}; HRMS(ESI) calcd for

$C_{15}H_{29}O_2NNa$ [M+Na]$^+$ 278.2096, found 278.2093
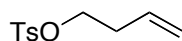
But-3-en-1-yl 4-methylbenzenesulfonate (**4.39**)

To a solution of *p*-toluenesulfonyl chloride (533 mg, 2.80 mmol, 1.2 equiv) in DCM (3.4 mL),

Et$_3$N (0.39 mL, 2.80 mmol, 1.2 equiv) and 3-buten-1-ol (0.2 mL, 2.33 mmol, 1 equiv) were

added. After stirring for 18 hours the reaction was quenched with a NaHCO$_{3(aq)}$ solution

(10 mL), and diluted with DCM (10 mL). The organic layer was extracted and aqueous

layer washed with DCM (3 x 5 mL) and the combined organic layers washed with brine (10

mL). The organic layer was dried with MgSO$_4$ and concentrated *in vacuo*, giving but-3-en-

1-yl 4-methylbenzenesulfonate in quantitative yield (521 mg) as a clear oil. The analytical

data matched those previously reported.[47]
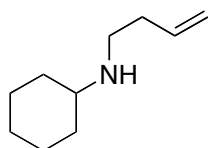
N-(but-3-en-1-yl)cyclohexanamine But-3-en-1-yl 4-methylbenzenesulfonate (492 mg,

2.2 mmol, 1 equiv) and cyclohexylamine (0.77 mL, 6.74 mmol, 3.1 equiv) were heated neat

at 60 °C for 18 hours. The reaction was quenched with a 6 N NaOH$_{(aq)}$ solution (6 mL), and

diluted with DCM (13 mL). The organic layer was extracted and aqueous layer washed

with DCM (5 x 10 mL) and the organic layer dried with MgSO$_4$ and concentrated *in vacuo*.

Flash column chromatography (95:5 DCM/MeOH with 1% Et$_3$N) gave N-(but-3-en-1-

yl)cyclohexanamine in 93% yield (310 mg) as a clear oil. The analytical data matched those previously reported.[48]
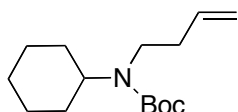
***Tert*-butyl but-3-en-1-yl(cyclohexyl)carbamate** (**3.121**) N-(but-3-en-1-yl)cyclohexanamine (100 mg, 0.65 mmol, 1 equiv) and Boc anhydride (250 mg, 0.98 mmol, 1.5 equiv) were stirred neat for 18 hours. The crude reaction was subjected to flash column chromatography (20:1 Hexanes/ethyl acetate) giving tert-butyl but-3-en-1-yl(cyclohexyl)carbamate in quantitative yield (165 mg) as a clear oil.

^{1}H NMR (CDCl$_3$, 500 MHz) δ 5.81–5.70 (m, 1H), 5.05 (d, *J* = 16.0 Hz, 1H), 5.00 (d, *J* = 10.0 Hz, 1H), 4.00–3.42 (m, 1H), 3.09 (br s, 2H), 2.25 (dt, *J* = 8.0, 7.0 Hz, 2H), 1.83–1.71 (m, 3H), 1.62 (*d, J* = 13.0 Hz, 1H), 1.54–1.23 (m, 15H), 1.07 (qt, *J* = 13.0, 3.8 Hz, 1H); ^{13}C NMR (CDCl$_3$, 125 MHz) δ 155.6, 136.0, 116.1, 79.2, 55.0, 42.6, 35.5, 31.4, 28.6, 28.0, 26.1, 25.7; IR (thin film) 3077, 2974, 2930, 2855, 1694 cm^{-1}; HRMS (ESI) calcd for C$_{15}$H$_{27}$O$_2$NNa [M+Na]$^+$ 276.1939, found 276.1947

[1]Roberge, D. *Org. Process Res. Dev.* **2004**, *8,* 1049–1053.

[2] Ammonia. *Ullmann's Encyclopedia of Industrial Chemistry*, 5th ed. [Online]; Wiley & Sons, Posted Oct. 15, 2011. http://onlinelibrary.wiley.com/doi/10.1002/14356007.a02_143. pub3/pdf (accessed Jan 1, 2016).

[3] Gorsek, A.; Glavic, P. *Chem. Eng. Res. Des.* **1997**, *75* , 709–717.

[4] McQuade, T.; Seeberger, P. *J. Org. Chem.* **2013***, 78*, 6384–6389.

[5] Hartman, R.; McMullen, J.; Jensen, K. *Angew. Chem. Int. Ed.* **2011**, *50*, 7502–7519.

[6] Hessel. V. *Chem. Eng. Technol.* **2009,** *32*, 1655–1681.

[7] Jensen, K. *Chem. Eng. Sci.* **2001**, *56*, 293–303.

[8] (a) Hessel V.; Löwe, H.; Schönfeld, F. *Chem. Eng. Sci.* **2005**, *60*, 2479–2501. (b) Stone, H.; Stroock, A.; Ajdari, A. *Annu. Rev. Fluid Mech.* **2004**, *36*, 381–411. (c) Nguyen, N.; Wu, Z. *J. Micromech. Microeng*. **2005**, *15*, R1 – R16.

[9] Polyzos, A.; O'Brien, M.; Petersen, T.; Idale, R.; Ley, S. *Angew. Chem.* **2011**, *123*, 1222–1225.

[10] Browne, D.; Deadman, B.; Ashe, R.; Baxendale, I.; Ley, S. *Org. Process Res. Dev.* **2011**, *15*, 693–967.

[11] Ley, S.; Schucht, O.; Thomas, A.; Murray, P. *J. Chem. Soc., Perkin Trans. 1* **1999**, 1251–1252.

[12] (a) Heider, P.; Born, S.; Bask, S.; Benyahia, B.; Lakerveld, R.; Zhang, H.; Hogan, R.; Buchbinder, L.; Wolfe, A.; Mascia, S.; Evens, J.; Jamison, T.; Jensen, K. *Org. Process Res. Dev.* **2014**, *18*, 402–409. (b) Delville, M.; Koch, K.; Hest, J.; Rutjes, F. *Org. Biomol. Chem.* **2015**, *13*, 1634–1638. (c) Baxendale, I.; Braatz, R.; Hodnett, B.; Jensen, K.; Johnson, M.; Sharratt, P.; Sherlock, J-P.; Florence, A. *J. Pharm. Sci.* **2015**, *104*, 781–791.

[13] Deadman, B.; Browne, D.; Baxendale, I.; Ley, S. *Chem. Eng. Technol.* **2015**, *38*, 259–264.

[14] Browne, D.; Wright, S.; Deadman, B.; Dunnage, S.; Baxendale, I.; Turner, R.; Ley, S. *Rapid Commun. Mass Spectrom.* **2012***, 26*, 1999–2000.

[15] Lange, H.; Carter, C.; Hopkin, M.; Burke, A.; Goode, J.; Baxendale, I.; Ley, S. *Chem. Sci.* **2011***, 2*, 765–769.

[16] Carter, C.; Baxendale, I.; O'Brien, M.; Pavey, J.; Ley, S. *Org. Biomol. Chem.* **2009**, *7*, 4594–4597.

[17] (a) Hopkin, M.; Baxendale, I.; Ley, S. *Org. Biomol. Chem.* **2013**, *11*, 1822–1839. (b) Baxendale, I.; Griffiths-Jones, C.; Ley, S.; Tranmer, G. *Synlett* **2006**, *3*, 427–430. (c) Baxendale, I.; Deeley, J.; Griffiths-Jones, C.; Ley, S.; Saaby, S.; Tranmer, G. *Chem. Commun.* **2006**, 2566–2568. (d) Riva, E.; Rencurosi, A.; Gagliardi, S.; Passarella, D.; Martinelli, M. *Chem. –Eur. J.* **2011,** *17***,** 6221–6226. (e) Snead, D.; Jamison, T. *Angew. Chem. Int. Ed* **2015***, 54,* 983–987.

[18] *Handbook of Micro Reactors*; Hessel, V.; Schouten, J.; Renken, A.; Wang, Y.; Yoshida, J.-I., Ed.; Wiley-VCH, Weinheim, 2009.

[19] Wegner, J.; Ceylan, S.; Kirschning, A *Chem. Commun.,* **2011**, *47*, 4583–4592.

[20] de Mas, N.; Günther, A.; Kraus, T.; Schmidt, M.; Jensen, K. *Ind. Eng. Chem. Res.* **2005**, *44*, 8997–9013.

[21] L'Heureux, A.; Beaulieu, F.; Bennett, C.; Bill, D.; Clayton, S.; LaFlamme, F.; Mirmehrabi, M.; Tadayon, S.; Tovell, D.; Couturier, M. *J. Org. Chem.* **2010**, *75*, 3401–3411.

[22] Baumann, M.; Baxendale, I.; Martin, L.; Ley, S. *Tetrahedron* **2009***, 65,* 6611–6625.

[23] Breen, J.; Sandford, G.; Yufit, D.; Howard, K.; Fray, J.; Patel, B. *Beilstein J. Org. Chem*. **2011**, *7*, 1048–1052.

[24]Borukhova, S.; Noël, T.; Metten, B.; de Vos, E.; Hessel, V. *ChemSusChem* **2013**, *6*, 2220–2225.

[25] Zhang, P.; Russel, M.; Jamison, T. *Org. Process Res. Dev.* **2014**, *18*, 1567–1570.

[26] Maurya, R.; Park, C.; Lee, J.; Kim, D-P. *Angew. Chem.* **2011**, *123*, 6074–6077.

[27] Struempel M.; Ondruschka, B.; Daute, R.; Stark, A. *Green Chem.* **2007**, *10*, 41–43.

[28] McMuillen, J.; Stone, M.; Buchwald, S.; Jensen, K. *Angew. Chem.* **2010**, *122*, 7230–7234

[29]Littke, A.; Fu, G.; *J. Am. Chem. Soc.* **2001**, *123*, 6989–7000.

[30] (a) Nelder, J.; Mead, R. *Comput. J.* **1965***, 7*, 308–313. (b) Deming, S.; Morgan, S. *Anal. Chem.* **1973***, 45*, 1170–1181

[31] Kupracz, L.; Kirschning, A. *Adv. Synth. Catal.* **2013**, *355*, 3375–3080.

[32] Polyzos, A.; O'Brien, M.; Petersen, T.; Baxendale, R.; Ley, S. *Angew. Chem. Int. Ed.* **2011**, *50*, 1190–1193.

[33] Malathong, V. PhD. Dissertation, University of California, Irvine, 2010.

[34] Burluenga, J.; Florez, J.; Yus, M. *J. Chem. Soc., Perkin Trans. 1* **1983**, 3019–3026.

[35] Jamison, T. Continuous Flow Multi-Step Synthesis. Presented at an organic chemistry seminar, Irvine, CA, 2013.

[36] Guijarro, D.; Martínez, P.; Yus, M. *Tetrahedron* **2003**, *59*, 1237–1244.

[37] Weinreb amides can be used with LiDBB methodology if no extra LiDBB is present in the solution. Once the reaction changes from green to red, no LiDBB is present in the reaction and the Weinreb amide can be added without cleaving the N–O bond. Tay G. PhD. Dissertation, University of California, Irvine, 2015.

[38] This solid is likely $(EtO)_2(O)POLi$, however this was not determined.

[39] As observed by ^{1}H NMR.

[40] As seen by GCMS

[41] Pangborn, A.; Giardello, M.; Grubbs, R.; Rosen, R.; Timmers, F. *Organometallics* **1996**, *15*, 1518–1520.

[42] Still, W.; Khan, M.; Mitra, A. *J. Org. Chem.* **1978**, *43*, 2923–2925.

[43] Shaikh, N.; Junge, K.; Beller, M. *Org. Lett.* **2007**, *9*, 5429–5432.

[44] Greaves, J. University of California Irvine, Irvine, CA. Personal Communication, 2013

[45] Perry, M.; Hill, R.; Rychnovsky, S. *Org. Lett.* **2013**, *15*, 2226–2229

[46] Millet, A.; Baudion, O. *Org. Lett.* **2014**, *16*, 3998–4000.

[47] Falb, E.; Nudelman, A.; Gottlieb, H.; Hassner, A. *Eur. J. Org. Chem.* **2000**, 645–655.

[48] Déry, M.; Assouvie, K.; Heinrich, N.; Rajotte, I.; Lefebure, L.–P.; Legault, M.–A.; Spino, C. *Org. Lett.* **2015**, *17*, 1312–1315.